CRANFIELD UNIVERSITY

María Erans Moreno

ENHANCED SORBENTS FOR THE CALCIUM LOOPING CYCLE AND EFFECTS OF HIGH OXYGEN CONCENTRATIONS IN THE CALCINER

SCHOOL OF WATER, ENERGY AND ENVIRONMENT
PhD in Energy

PhD
Academic Year: 2017 - 2018

Supervisor: Prof Edward J Anthony, Prof Vasilije Manovic
May 2017

CRANFIELD UNIVERSITY

SCHOOL OF WATER, ENERGY AND ENVIRONMENT
PhD in Energy

PhD

Academic Year 2017 - 2018

María Erans Moreno

ENHANCED SORBENTS FOR THE CALCIUM LOOPING CYCLE AND EFFECTS OF HIGH OXYGEN CONCENTRATIONS IN THE CALCINER

Supervisor: Prof Edward J Anthony, Prof Vasilije Manovic
May 2017

This thesis is submitted in partial fulfilment of the requirements for the degree of PhD

ABSTRACT

Increasing CO_2 emissions from the energy and industrial sectors are a worldwide concern due to the effects that these emissions have on the global climate. Carbon capture and storage has been identified as one of a portfolio of technologies that would mitigate the effects of global warming in the upcoming decades.

Calcium looping is a second generation carbon capture technology aimed at reducing the CO_2 emissions from the power and industrial sectors. This thesis assesses the improvement of the calcium looping cycle for CO_2 capture through enhanced sorbent production and testing at lab-, bench- and pilot-scale, and a new operational mode with high oxygen concentrations in the calciner through experimental campaigns in Cranfield's 25 kW_{th} pilot unit.

Novel biomass-templated sorbents were produced using the pelletisation technique and tested at different conditions in a thermogravimetric analyser (TGA) and a bench-scale plant comprising a bubbling fluidised bed (BFB) reactor. Moreover, the effects of sorbent poisoning by SO_2, and the influence of steam were studied in order to explore the effects of real flue gas on this type of material. In addition to the chemical performance, the mechanical strength, i.e. resistance to fragmentation of these materials was tested.

In additon, two different kinds of enhanced materials were produced and tested at pilot-scale. Namely, calcium aluminate pellets and HBr-doped limestone were used in experimental campaigns in Cranfield's 25 kW_{th} pilot plant comprising a CFB carbonator and a BFB calciner. The suitability of these materials for Ca looping was assessed and operation challenges were identified in order to provide a basis for synthetic sorbent testing at a larger scale.

Lastly, a new operational mode was tested, which is aimed at reducing the heat provided to the calciner through high oxygen concentration combustion of a hydrocarbon (in this case natural gas) in the calciner. This approach reduces or even eliminates the recirculated CO_2 stream in the calciner. In consequence, this results in a lower capital (reduced size of the calciner) and operational cost

(less oxygen and less fuel use). Several pilot plant campaigns were performed using limestone as solid sorbent in order to prove this concept, which was successfully verified for concentrations of up to 100% vol oxygen in the inlet to the calciner.

Keywords: Carbon capture, high temperature solid looping, enhanced CaO-based materials, pilot plant testing, CO_2 capture performance, fragmentation

DECLARATION

I declare that no portion of the work referred to in the thesis has been submitted in support of an application for another degree or qualification of this or any other university or another institute of learning.

The four journal papers contained in this submission were published by Elsevier, Royal Society of Chemistry and the Journal of Visualized Experiments that allow reusing and reproducing the entire published material in an unchanged form in the PhD Thesis.

Elsevier[i]

"Theses and dissertations which contain embedded PJAs [Published Journal Article] as part of the formal submission can be posted publicly by the awarding institution with DOI links back to the formal publications on ScienceDirect."

American Chemical Society[ii]

"Reuse/Republication of the Entire Work in Theses or Collections: Authors may reuse all or part of the Submitted, Accepted or Published Work in a thesis or dissertation that the author writes and is required to submit to satisfy the criteria of degree-granting institutions. Such reuse is permitted subject to the ACS' "Ethical Guidelines to Publication of Chemical Research"; the author should secure written confirmation (via letter or email) from the respective ACS journal editor(s) to avoid potential conflicts with journal prior publication*/embargo policies. Appropriate citation of the Published Work must be made**. If the thesis or dissertation to be published is in electronic format, a direct link to the Published Work must also be included using the ACS Articles on Request author-directed link."

Royal Society of Chemistry[iii]

You do not need to request permission to reuse your own figures, diagrams, etc, that were originally published in a Royal Society of Chemistry publication. However, permission should be requested for use of the whole article or chapter except if reusing it in a thesis. If you are including an article or book chapter

published by us in your thesis please ensure that your co-authors are aware of this.

[i]Elsevier (2017), Article sharing, Elsevier B.V., available online: www.elsevier.com/about/company-information/policies/sharing (last accessed: 09/04/2017)

[ii]ACS (2017), Permissions/RightsLinks -Permission Requests and Credit Lines, American Chemical Society Publications, available online: http://pubs.acs.org/page/copyright/permissions_otherpub.html (last accessed: 09/04/2017)

[iii] Royal Society of Chemistry (2017), available online: http://www.rsc.org/journals-books-databases/journal-authors-reviewers/licences-copyright-permissions/ (last accessed: 09/04/2017)

“To my beloved parents, José Luis and Mari Cruz”

“*Religion is a culture of faith; science is a culture of doubt.”*

-Richard Feynman
Nobel Prize in Physics, 1965

“No amount of experimentation can ever prove me right; a single experiment can prove me wrong.”

-Albert Einstein
Nobel Prize in Physics, 1921

ACKNOWLEDGEMENTS

I would like to express my gratitude to Prof Ben Anthony for giving me the opportunity to carry out this research project.

Also, I would like to thank Prof Vasilije Manovic for all he has done for me since before I started this PhD and during these three years. Thank you for your advice, your guidance and your time. I am extremely grateful for the interest you took on my research.

I am immensely grateful to Dr Lunbo Duan and particularly to Dr Michal Jeremias for the scientific discussions and all the work we have done together during these past years. It has been a pleasure working with you both.

I would like to give credit to my German friends and co-workers, especially to Dr Heiko Dieter, Dr Theodor Beisheim, Mr Andreas Gredinger and Mr Matthias Hornberger, thank you for your help and for welcoming me into your institute and the German culture for three months. Also, big thanks to my Italian collaborators, Dr Osvalda Senneca, Dr Antonio Coppola, Prof Fabrizio Scala, Mr Luciano Cortese and particularly to my dear friend Francesca Cerciello thank you for taking me on and treating me like another family member, I miss you.

I would like to show immense appreciation to my best friend and biggest supporter María Martínez, my time in Cranfield would have been very different without you. Big thanks also to my friends, in Villarrobledo and Cranfield.

I am indebted to the technical team in building 43a: Peter, Euan, Howard, and Martin. Howard, thank you for your patience and your help; Martin, this research project would have not been the same without you, thank you for teaching me so many things, including the correct use of sarcasm, during this time. I can safely say we all miss you here and I hope retirement treats you well.

Also, I would like to show gratitude towards the staff and students of the CCCS group and building 40, past and present, for all the help and support throughout this PhD.

To my parents, José Luis and Mari Cruz, thank you again for everything, I love you both. To my brother Luis and my sister-in-law Lourdes for the comfort they have given me during the course of this research. Big thanks to my niece, Marta, and my nephew, David, for making me laugh every day. Likewise, thanks to my grandmother Carola and my aunty Natividad for teaching me so much about life and hard work.

LIST OF PUBLICATIONS

-Published:

Erans, M., Beisheim, T., Manovic, V., Jeremias, M., Patchigolla, K., Dieter, H., Duan, L. and Anthony, E.J., 2016. Effect of SO_2 and steam on CO_2 capture performance of biomass-templated calcium aluminate pellets. Faraday Discussions, 192, pp.97-111.

Erans, M., Manovic, V. and Anthony, E.J., 2016. Calcium looping sorbents for CO_2 capture. Applied Energy, 180, pp.722-742.

Erans, M., Cerciello, F., Coppola, A., Senneca, O., Scala, F., Manovic, V. and Anthony, E.J., 2017. Fragmentation of biomass-templated CaO-based pellets. Fuel, 187, pp.388-397.

Erans, M., Jeremias, M., Manovic, V. and Anthony, E.J., 2017. Operation of a 25 kW_{th} calcium looping pilot-plant with high oxygen concentrations in the calciner (accepted by the Journal of Visualized Experiments).

-Drafts:

Erans, M., Jeremias, M., Manovic, V., and Anthony, E.J., 2017. Pilot testing of enhanced sorbents for Calcium looping.

-These publications are peripheral to the work presented in this thesis and can be found in the Appendices:

Duan, L., Yu, Z., Erans, M., Li, Y., Manovic, V. and Anthony, E.J., 2016. Attrition Study of Cement-Supported Biomass-Activated Calcium Sorbents for CO_2 Capture. Industrial & Engineering Chemistry Research, 55(35), pp.9476-9484.

Duan, L., Su, C., Erans, M., Li, Y., Anthony, E.J. and Chen, H., 2016. CO_2 capture performance using biomass-templated cement-supported limestone pellets. Industrial & Engineering Chemistry Research, 55(39), pp.10294-10300.

TABLE OF CONTENTS

LIST OF FIGURES

LIST OF TABLES

LIST OF EQUATIONS

LIST OF ABBREVIATIONS

2DS	2 Degree Scenario
ALD	Atomic Layer Deposition
ASU	Air Separation Unit
BFB	Bubbling Fluidised Bed
CaL	Calcium looping
CCS	Carbon Capture and Storage
CFB	Circulating Fluidised Bed
CLC	Chemical Looping Combustion
EC	European Commission
FB	Fluidised Bed
GHG	Greenhouse Gases
HTSL	High Temperature Solid Looping
ICP-OES	Inductively Coupled Plasma Optical Emission Spectroscopy
ID	Internal Diameter
IGCC	Integrated Gasification Combined Cycle
IPCC	Intergovernmental Panel on Climate Change
LWR	Long-wave Radiation
MEA	Monoethanolamine
NG	Natural Gas
PA	Pyroligneous Acid
PCC	Precipitated Calcium Carbonate
PHSR	Pressurised Heated Strip Reactor
PSD	Particle Size Distribution
R&D	Research & Development
SI	International System of Units

SATS	Self- Assembly Template Synthesis
SEM	Scanning Electron Microscope
SWR	Short-wave Radiation
TEA	Triethanolamine
XRD	X-Ray Diffraction

1 INTRODUCTION

1.1 Background and motivation

According to the Intergovernmental Panel on Climate Change [1], the global system is exhibiting unambiguous proof of warming; many of these alterations are unique over decades to millennia. Some examples of the consequences of climate change are: the higher average air and ocean temperatures, the augmented sea level and the decline in the quantities of terrestrial snow and ice. These changes have not only been experienced in natural systems, but are also increasingly affecting human activities.

The land and ocean temperatures and global average sea level are shown in Figure 1-1, which illustrates the extraordinary growth of the temperatures as well as the sea level over the past decades, as a consequence of climate change.

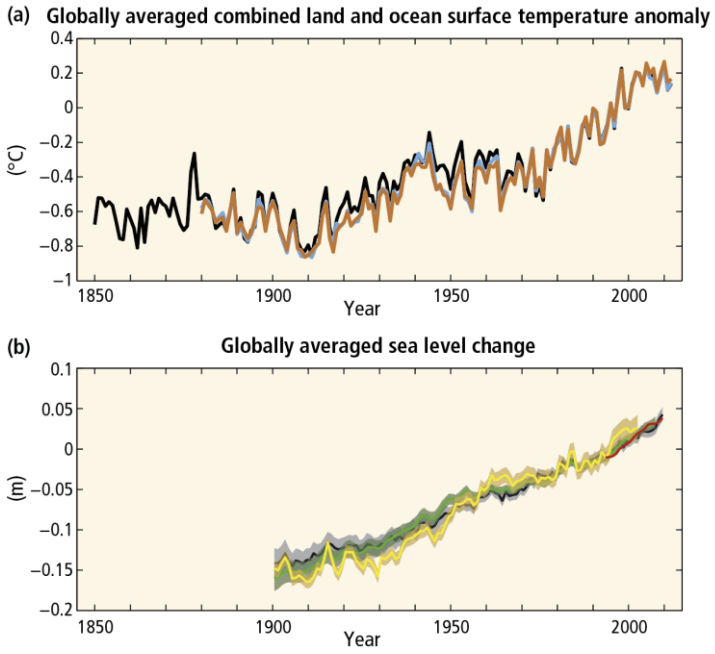

Figure 1-1: (a) Annually and globally averaged combined land and ocean surface temperature relative to the average over the period 1850-2012 (b) Annually and globally averaged sea level change relative to the average over the period 1900-2012 (colours indicate different data sets) [1]

These increases are attributed to the rising concentrations of greenhouse gases due to the widespread use of fossil fuels. Carbon dioxide is the gas that makes the largest contribution [2]; global CO_2 concentrations have increased from 280 ppm_v in the pre-industrial era to more than 400 ppm_v for the first time in May 2013 [3, 4] and to 403.95 ppm_v in January 2017 [5].

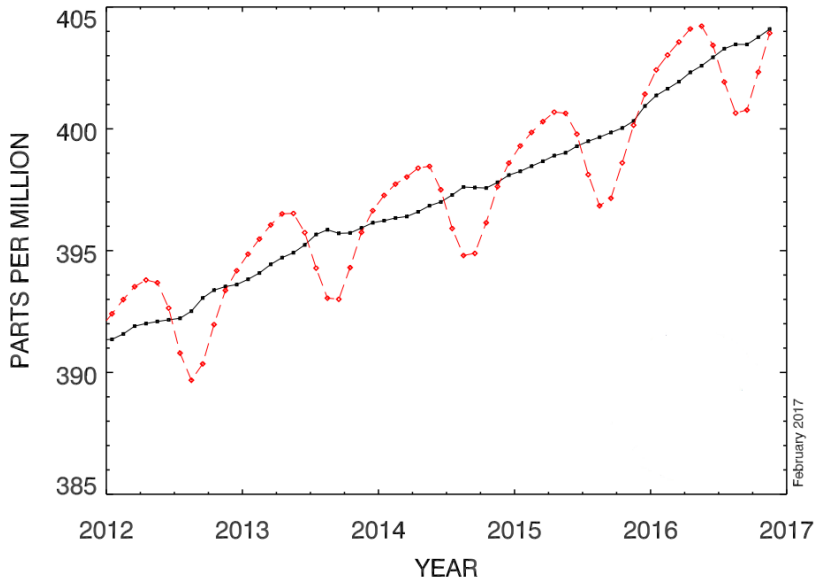

Figure 1-2: Recent Global monthly mean CO_2 concentration over the past five years (the red line represents the monthly average, whilst the black line represents the monthly trend) [5]

Mitigation measures are necessary in order to restrict the increasing concentration of greenhouse gases, specifically for CO_2 to the level of 450 ppm_v to avoid excessive climate change consequences. The current predicted trend is that the energy demand will increase by 34% between 2014 and 2035 [6]. As a result, it is reasonable to expect that fossil fuels will play an important role in the short- to medium-term due to the slow deployment of low-carbon and renewable technologies that can take up to 30 years to become the dominant sources of thermal energy [7].

It is essential for fossil fuel-fired power plants to be decarbonised if the CO_2 concentration is to be limited to the aforementioned level. Carbon capture and storage could provide a mitigation option for CO_2 emission from the power generation and industrial sectors, which are particularly carbon intensive. These

technologies can offer a short- to medium-term solution while the infrastructure, policies, markets and distribution networks are deployed for the widespread introduction of low carbon technologies [7]. According to the European Commission (EC), emissions in the developed countries should be reduced by 30% in 2020 and by 60-80 % in 2050 in order to reach the goal of the two degree scenario (2DS) [8]. The EC has also stated that these aims cannot be accomplished without the implementation of CCS, and suggests that CCS should account for 13 % of the cumulative CO_2 reductions, compared to 30% for renewable energy technologies [9, 10]. According to these data, the rapid deployment of the CCS technologies is of vital importance.

There are several challenges associated with CCS technologies, including the financial cost and the energy penalty associated with the whole chain. Currently, the technology that is closest to the market is post-combustion solvent scrubbing, with solvents such as monoethanolamide (MEA) [11]. Nevertheless, there are some challenges associated with this technology, namely, solvent poisoning (by SO_2 or O_2 [12-14]), solvent degradation and high solvent cost [15]. Another technology that is reasonably close to the market is oxy-fuel combustion; in this system fuel is burnt in a mixture of O_2 and CO_2, where a portion of the outlet gas is recycled to the combustion chamber in order to control the flame temperature. Unfortunately, this process requires an air separation unit (ASU) in order to provide the large quantities of O_2 demanded.

The challenges mentioned here have motivated researchers to explore other CO_2 capture technologies, such as membrane separation or high temperature solid looping cycles. The work presented in this thesis is focused on calcium looping, which utilises two reactors wherein the reversible carbonation/calcination reaction between CaO and CO_2 operates. The advantages of this process are:

-The production of high-grade heat from the carbonation reaction, which can be used to run an additional steam cycle;

-The use of CaO, which is a cheap, environmentally friendly and widely available material;

-The synergy with the cement industry, as the spent sorbent can be used in the kiln as a source of CaO, potentially decarbonising both industries;

-This process can be applied in post-combustion or pre-combustion scenarios for CO_2 capture; and

-Fluidised–bed reactors are a mature technology.

Taking into account all the advantages mentioned above, calcium looping can result in efficiency penalty reduction and economic savings when compared to the other technologies, such as amine scrubbing or oxy-fuel combustion [16]. The main part of the research in this area is focused on sorbent deactivation and how to mitigate this reactivity decay over increasing number of cycles. Several methods and techniques have been developed to enhance natural materials, to produce new synthetic materials and to reactivate spent sorbent. Another crucial line of research is the scale-up of this technology going from TGA and lab-scale experiments to pilot- and demonstration-scale units in order to prove the concept completely before commercialisation.

1.2 Aims and objectives

The aim of this PhD is to contribute towards the body of knowledge of calcium looping for CO_2 capture focusing on scaling-up and improvement of solid sorbents as well as the effects of high oxygen concentrations in the calciner in the overall process through experimental work. In consequence, there are two linked aims taking part in this PhD project:

Aim 1: Demonstrate the capture performance and fragmentation resistance of enhanced sorbents at TGA and lab-scale.

Objective 1a *Conduct a detailed review of the developments in sorbent production for the calcium looping cycle.*

Objective 1b *Demonstrate the scalability of the pelletisation and doping techniques for particle production.*

Objective 1c *Assess the CO_2 performance of biomass-templated pellets using flour as a cheap biomass source through TGA experiment and bench scale experimental campaigns.*

Objective 1d *Assess the effect of SO_2 and steam on the capture performance of the biomass-templated sorbents.*

Objective 1e *Evaluate the fragmentation behaviour of the produced materials as a measure of their mechanical stability.*

Aim 2: Study the effects of high oxygen concentrations in the calciner and the performance of enhanced sorbents in Cranfield's 25 kW_{th} calcium looping pilot plant.

Objective 2a *Assess the effect of high oxygen concentrations in the calciner in the 25 kW_{th} pilot plant with limestone.*

Objective 2b *Test enhanced sorbents in the 25 KW_{th} pilot plant under high oxygen concentrations.*

1.3 Novelty and linkage of project outputs

In order to reach the objectives established for this research project, a number of contributions have been made to the scientific body of knowledge. These have been reported in four published journal publications and an unpublished manuscript; the linkage among them is presented in Figure 1-3.

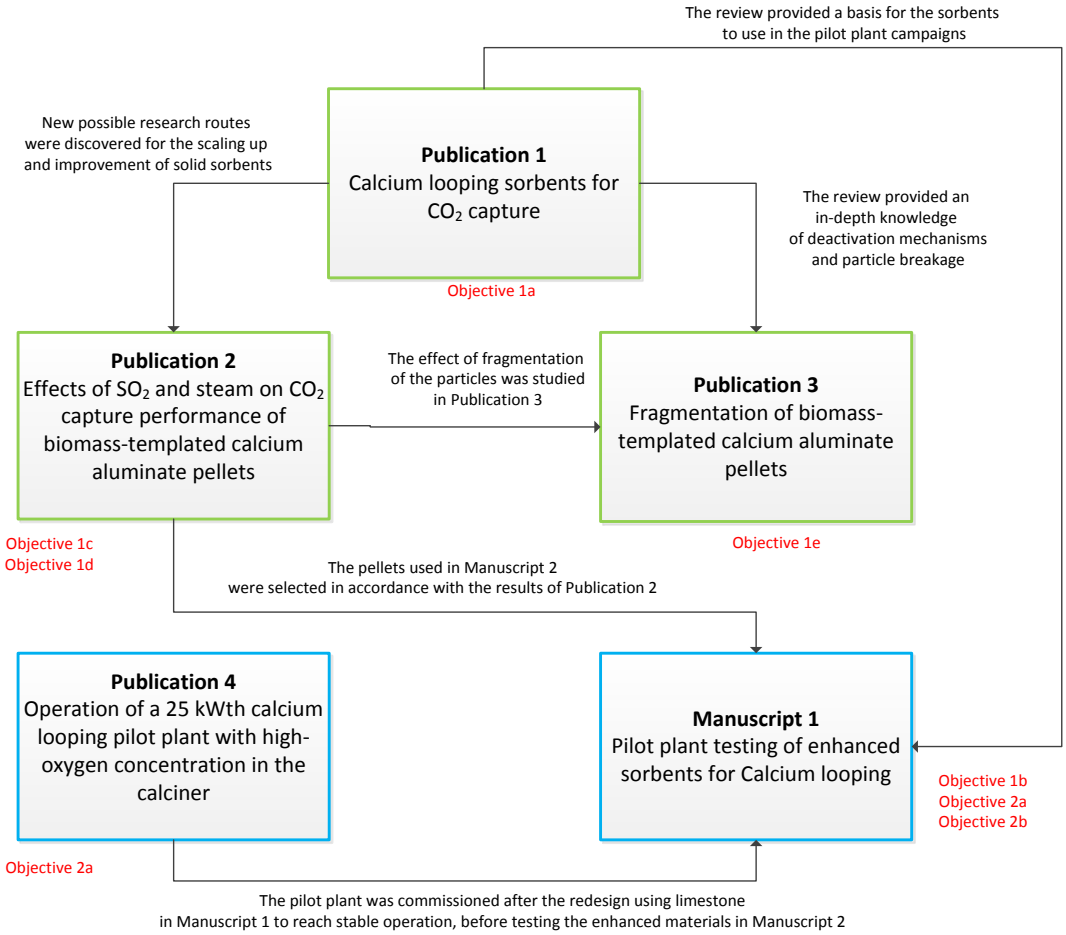

Figure 1-3: Interconnections of the project outputs and manuscripts presented in this thesis

As a basis for this thesis, an extensive literature review on sorbent performance was undertaken in the form of Publication 1 [17]. This publication explored the deactivation mechanisms for calcium looping sorbents, modifications of natural sorbents for enhanced performance, and the types of synthetic materials that have been recently researched. After the literature review, promising and viable solutions were identified for the production of CaO-based, improved solid materials for CO_2 capture. The results of the CO_2 capture performance experiments and the experiments on the fragmentation of the synthetic sorbents prepared can be found in Publications 2 and 3 [18, 19]. The effects of SO_2 and steam on capture performance can also be found in Publication 2. These publications are highly linked since they study almost the same materials but in

two different aspects: the reactivity and the mechanical stability of the manufactured particles.

Moreover, the results from Publications 2 and 3 led to the use of calcium aluminate pellets in the section 7.3.3 of Manuscript 1, since these showed the most promising results with regards to both reactivity and mechanical stability. Publication 4 describes the efforts to develop an operating procedure that was used for the experiments presented in Manuscript 1. In other words, these manuscripts are also highly connected as the experimental procedure used during all of the pilot plant campaigns was developed using limestone in the experiments described in Publication 4 [20].

1.4 Outline of PhD Thesis

The structure of this doctoral thesis with a brief description of the content of each chapter is detailed below:

- **Chapter 1** the background and motivation of this research project are detailed in this chapter, as well as the aims and objectives and an overview of the novelty and how the publications are linked with the aims and objectives.
- **Chapter 2** a general literature review is presented in this chapter with a focus on carbon capture and storage as a chain and more specifically on calcium looping as a post-combustion technology for CO_2 capture.
- **Chapter 3** an in-depth literature review is presented in this chapter describing the developments in calcium looping sorbents. Namely, it discusses natural sorbents, enhanced sorbents, synthetic sorbents and re-activation techniques, giving recommendations for future research.
- **Chapter 4** presents the methodology and results on CO_2 capture performance of four different types of synthetic materials in a thermogravimetric analyser (TGA) and a bench-scale fluidised-bed reactor. It also discusses the effects that SO_2 and steam have on the overall performance of these solid sorbents.

- **Chapter 5** describes the methodology and results with regard to particle fragmentation of three synthetic materials as well as an in-depth particle characterisation section.
- **Chapter 6** offers insights to the operational experience gained through several experimental campaigns in the 25 kW_{th} calcium looping pilot plant operated with high oxygen concentration in the calciner.
- **Chapter 7** details the results from the experimental campaigns of Cranfield's 25 kW_{th} reactor configuration when using enhanced sorbents for CO_2 capture.
- **Chapter 8** presents a general discussion of all the work done through the course of this research linking all the chapters together.
- **Chapter 9** deals with concluding remarks, contributions to existing knowledge and recommendations for future research based on the outcomes detailed in this thesis.

1.5 References

[1] IPCC, 2014. Climate Change 2014: Synthesis Report. Contribution of Working Groups I, II and III to the Fifth Assessment Report of the Intergovernmental Panel on Climate Change. Cambridge University Press, Cambridge, UK and New York, NY, USA.

[2] IPCC, 2007. Climate Change 2007: Synthesis Report. Contribution of Working Groups I, II and III to the Fourth Assessment Report of the Intergovernmental Panel on Climate Change, C.W. Team, K.P. Pachauri, and A. Reisinger, Editors. 2007: Geneva, Switzerland.

[3] IEA, 2013. Redrawing the energy-climate map. World energy outlook special report. IEA Publications, Paris, France.

[4] Olivier, J.G.J., Janssens-Maenhout, G., Muntean, M., Peters, J.A.H.W., 2013. Trends in global CO_2 emissions: 2013 Report. PBL Netherlands Environmental Assessment Agency, Hague, Netherlands.

[5] Dlugokencky, E., Tans, P., 2017. Recent global CO_2 [WWW Document]. NOAA/ESRL. URL www.esrl.noaa.gov/gmd/ccgg/trends/global.html).

[6] BP Energy Outlook 2016. (Available at https://www.bp.com/content/dam/bp/pdf/energy-economics/energy-outlook-2016/bp-energy-outlook-2016.pdf (Accessed 22 February 2017).

[7] Kramer, G.J., Haigh, M., 2009. No quick switch to low-carbon energy. Nature 462 (December), 3–4.

[8] Communication from the Commission to the Council, the European Parliament, the European Economic and Social Committee and the Committee of the Regions - Limiting global climate change to 2 degrees Celsius - The way ahead for 2020 and beyond. 2007, Commission of the European Communities: Brussels.

[9] IEA, 2015. Carbon capture and storage: The solution for deep emissions reductions. IEA Publications, Paris, France.

[10] IEA, 2015. Energy technology perspectives 2015: Executive summary. IEA Publications, Paris, France.

[11] MacDowell, N., Florin, N., Buchard, A., Hallett, J., Galindo, A., Jackson, G., Adjiman, C.S., Williams, C.K., Shah, N., Fennell, P., 2010. An overview of CO_2 capture technologies. Energy & Environmental Science, 3(11), pp. 1645-1669.

[12] Chi, S. and Rochelle, G., Oxidative degradation of monoethanolamine, in First International Conference on CO_2 Sequestration. 2001: Washington, DC, US.

[13] Goff, G.S. and Rochelle, G.T., 2004. Monoethanolamine Degradation: O_2 Mass Transfer Effects under CO_2 Capture Conditions. Industrial & Engineering Chemistry Research, 43, pp. 6400-6408.

[14] Supap, T., Idem, R., Tontiwachwuthikul, P., Saiwan, C., 2006. Analysis of monoethanolamine and its oxidative degradation products during CO_2 absorption from flue gases: A comparative study of GC-MS, HPLC-RID, and

CE-DAD analytical techniques and possible optimum combinations. Industrial & Engineering Chemistry Research, 45(8), pp. 2437-2451.

[15] Aaron, D. and Tsouris, C., 2005. Separation of CO_2 from flue gas: A review. Separation Science and Technology, 40(1-3), pp. 321-348.

[16] Hanak, D. P., Biliyok, C., Anthony, E. J., & Manovic, V., 2015. Modelling and comparison of calcium looping and chemical solvent scrubbing retrofits for CO_2 capture from coal-fired power plant, International Journal of Greenhouse Gas Control, 42, pp. 226-236.

[17] Erans, M, Manovic, V., Anthony, E.J., 2016. Calcium looping sorbents for CO_2 capture. Applied Energy, 180, pp. 722-742.

[18] Erans, M., Beisheim, T., Manovic, V., Jeremias, M., Patchigolla, K., Dieter, H., Duan, L., Anthony, E.J., 2016. Effect of SO_2 and steam on CO_2 capture performance of biomass-templated calcium aluminate pellets. Faraday Discussions, 192, pp. 97-111.

[19] Erans, M., Cerciello, F., Coppola, A., Senneca, O., Scala, F., Manovic, V., Anthony, E.J., 2017. Fragmentation of biomass-templated CaO-based pellets. Fuel, 187, pp. 388-397.

[20] Erans, M., Jeremias, M., Manovic, V. and Anthony, E.J., 2017. Operation of a 25 kW_{th} calcium looping pilot-plant with high oxygen concentrations in the calciner (accepted by the Journal of Visualized Experiments).

2 GENERAL LITERATURE REVIEW

2.1 Climate change and greenhouse gas emission

The IPCC refers to climate change as an alteration in the state of the climate; this variation can be recognised by changes in the variability and/or mean of climatic properties (e.g. average temperature, rain fall and weather patterns, among others). Additionally, these alternations need to persist for a long period of time, usually decades or longer, to be considered as climate change [1].

To understand how global warming works, an understanding of Earth's radiation balance is necessary. Radiation coming, primarily from the Sun, enters the atmosphere, mostly as visible light. Since the Earth's temperature has been relatively stable for centuries, the solar radiation entering the atmosphere should balance the outgoing radiation. As represented in Figure 2-1, around half of the incoming shortwave radiation (SWR) is absorbed by the Earth's surface, about 30% is reflected back to space and 20% is absorbed by the atmosphere [2]. The longwave radiation (LWR) emitted by the Earth's surface (albedo) is mainly absorbed by greenhouse gases and clouds, both of which emit infrared radiation in all directions. The LWR emitted to the Earth's surface, by the clouds and greenhouse gases, heats the lower layers of the atmosphere, causing what we call the greenhouse gas effect. Therefore, if there is an increased concentration of these gases in the atmosphere, they will emit more LWR, consequently increasing the heat received by the Earth's surface.

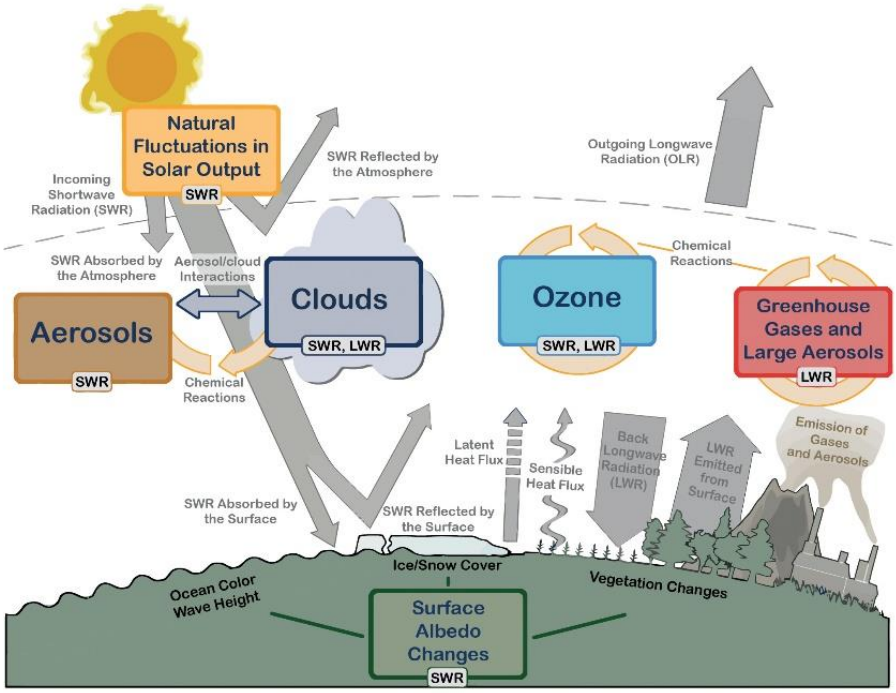

Figure 2-1: Main drivers of climate change. The radiative balance between incoming solar shortwave radiation (SWR) and outgoing longwave radiation (OLR) [2]

It is now accepted that the effects of anthropogenic global warming are the result of an increase in greenhouse gas (GHG) emissions produced primarily from fossil fuel combustion. Figure 2-2 shows the rise in the concentration of carbon dioxide (CO_2), methane (CH_4) and nitrous oxide (N_2O) since 1750 (40%, 150% and 200% increase, respectively), with the increase in the concentration of CO_2 being the most rapid of the decade with 2 ppm/year since 2011 [3, 4]. However, not all of these gases have the same greenhouse potential, with N_2O and CH_4 having 265 and 28 times greater warming potential than CO_2, respectively. Nonetheless, as can be seen in Figure 2-2, they are only present at ppb-level in the atmosphere compared with the ppm-level CO_2 concentrations. Moreover, the concentration of these gases has not increased at the same rate. A representation of this rate can be seen in Figure 2-3.

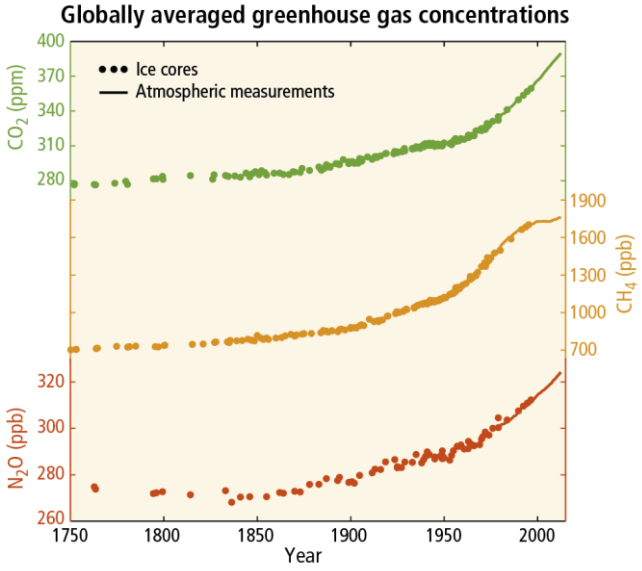

Figure 2-2: Observed changes in atmospheric greenhouse gas concentrations (CO_2, CH_4, N_2O) [3]

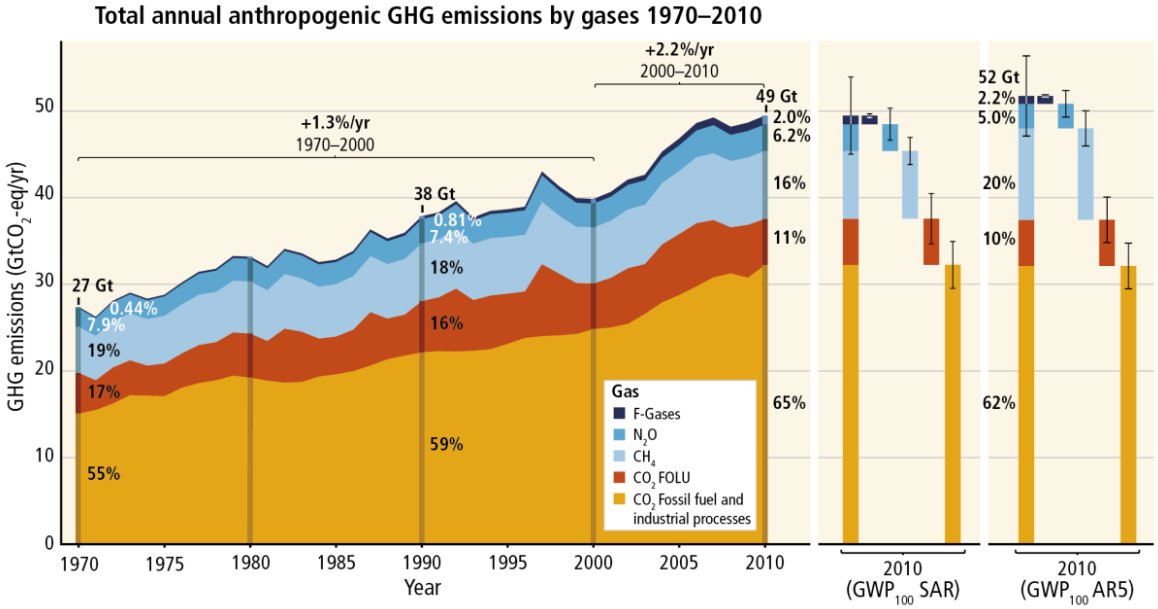

Figure 2-3: Global anthropogenic GHG emissions by gases from 1970-2010 [5]

According to Figure 2-3, carbon dioxide is the most emitted greenhouse gas and contributes about 76% of the total emissions. Economic and population growth are the main drivers for the increase of CO_2 emissions over time. However, it should be noted that population growth between 2000 and 2010 has

remained the same when compared to the previous three decades, whilst the impact of economic growth has increased considerably.

The effects of CO_2 on global warming were first discussed by Tyndall in 1859 [6]. Furthermore, Arrhenius did the first calculations on the repercussions of carbon dioxide emissions on global warming in 1896 [7], and he noticed that the changes of atmospheric CO_2 concentration may cause long-term variations in the climate system.

Climate change caused by anthropogenic emissions will have other environmental implications; these implications are given the name of climate change indicators. These include sea level increases, which will cause inland inundation of areas close to sea level. Another indicator is ocean acidification as a result of the increased concentration of CO_2 in sea water, which poses great risk to ocean ecosystems due to changes in nutrients and food chains. The last indicator is the ice melting, especially in the Artic, sea ice has been thinning and its volume has reduced [8, 9], which contributes to the increase in sea level as well. These effects combined with extreme weather may lead to floods, desertification and drought, which will result in crop failure, low water supplies, human migration, spreading of diseases and extinction of vulnerable species. All of this will result in greater population in the areas that are fit for human inhabitation, which will raise the stress on the resources and lead to potential human conflicts.

In conclusion, mitigation options to limit the effects of climate change are needed. It is important to note that most of the CO_2 emissions come from the power generation sector and the industrial sector [10]. Figure 2-4 shows the global electricity generation prediction by source. It can be seen that the total share of fossil fuel generation falls from 68% in 2012 to 55% in 2040, whilst the electricity generation increases over three-quarters between 2012 and 2040. Coal’s share drops from 41% to 31% during this period, oil’s share also decreases from 5% to 1%. However, the share of natural gas is the only one among all fossil fuels that sees an increment from 22% in 2012 to 38% in 2040. Nuclear remains almost stable with a small boost of 1% during this period, in

contrast, the share of all the renewable energy sources increases to more than double, attaining around one-third of the global electricity generation in 2040. All of this growth comes from non-hydro sources, with wind power accounting for more of half of this boost.

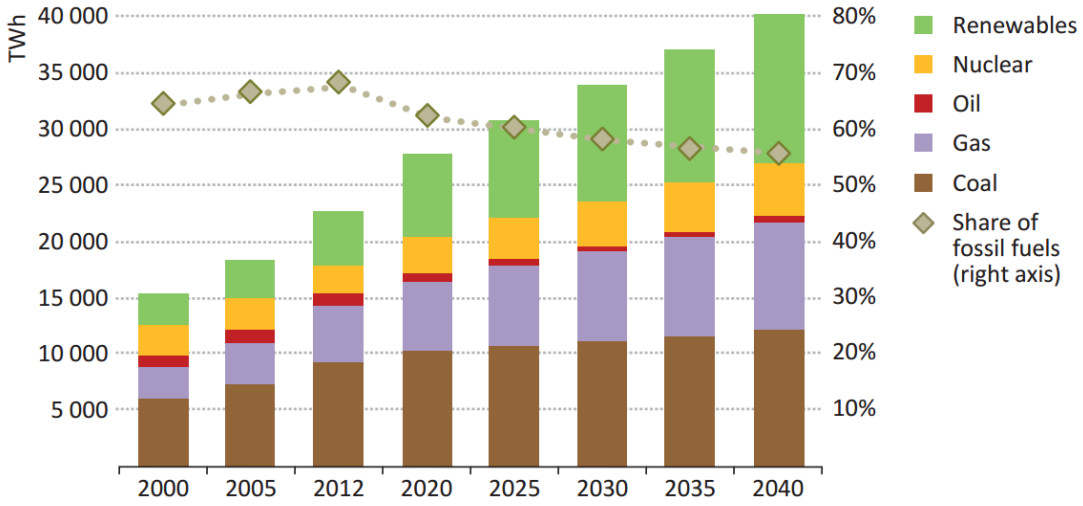

Figure 2-4: World electricity generation by source [11]

It is important to highlight that a portfolio of low-carbon technologies needs to be deployed in order to decarbonise the energy sector. It should be noted that more than a third of the greenhouse gases emissions in 2010 came from the power sector [12]; therefore, its decarbonisation can make a significant contribution towards achieving the 2DS emission reduction targets. However, it must also be remembered that the industrial sector accounts for one fifth of the global CO_2 emissions [13], and its decarbonisation is equally important in order to meet the specific targets agreed by governments.

2.2 Carbon capture and storage

Carbon capture and storage (CCS) involves a chain of processes designed to reduce the CO_2 emissions from large sources of combustion and other chemical reactions, e.g. large-scale power plants and industrial sources. The chain comprises the CO_2 capture, compression, transport, storage and/or utilisation and monitoring. These processes can be seen in Figure 2-5.

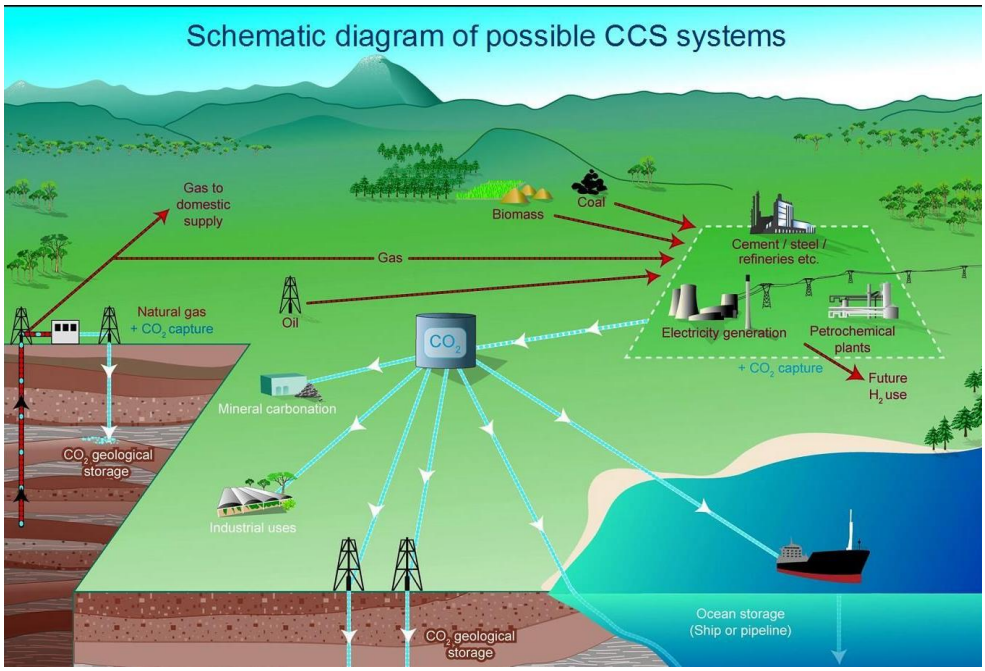

Figure 2-5: Schematic diagram of possible CCS systems showing the sources for which CCS might be relevant, transport of CO_2 and storage options [14]

Plants with integrated CCS systems need between 10-40% more energy to operate the CCS proceses. Most of this energy is used in the CO_2 capture and compression stages. This increases CO_2 production, which can be seen in Figure 2-6, and the net result of adding the CCS system is that the CO_2 emissions drop 80-90% (CO_2 avoided) when compared with a reference plant [14].

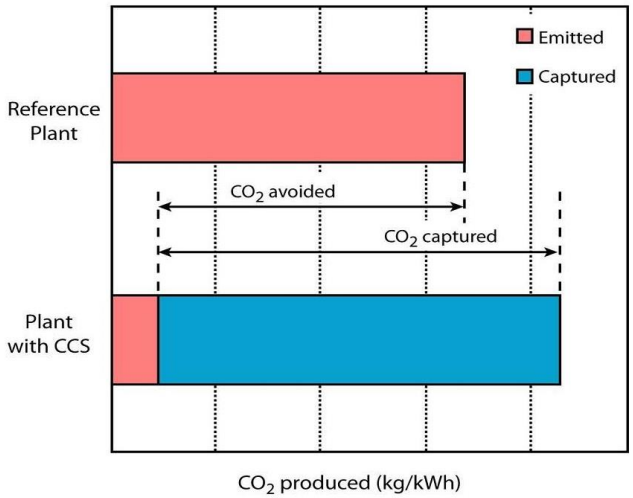

Figure 2-6: CO_2 emitted, captured and avoided [14]

2.2.1 CO_2 capture technologies

There are three paths for CO_2 capture in the power generation systems as can be seen in Figure 2-7. These are: post-combustion, pre-combustion and oxy-fuel combustion, which are detailed below.

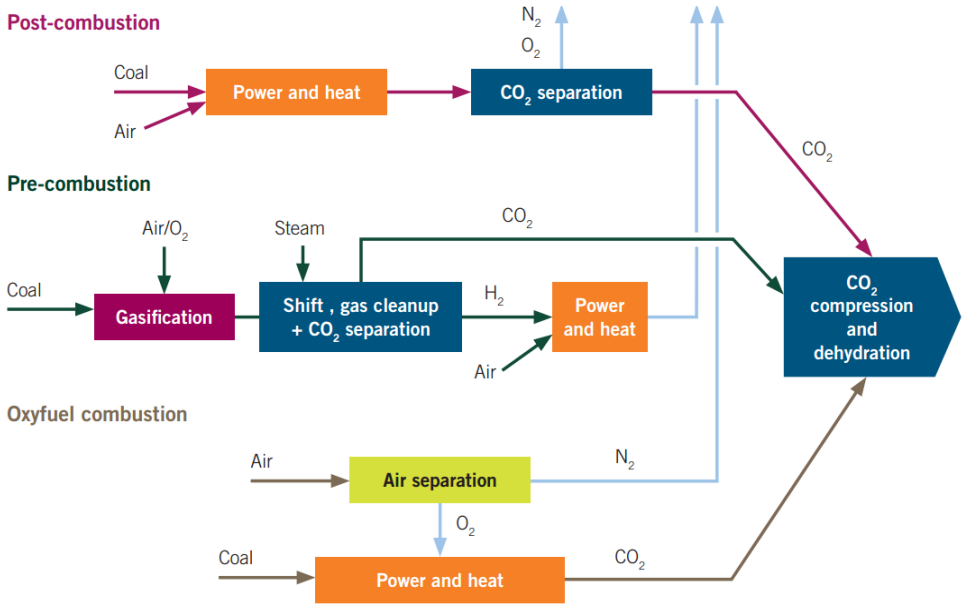

Figure 2-7: Schematic of CO_2 capture processes for power generation [15]

2.2.1.1 Post-combustion CO_2 capture

In these processes, flue gas is treated in order to capture CO_2 after the combustion takes places. The flue gas generally contains 3-15% CO_2 (depending on the fuel used), as well as steam, nitrogen, SO_x, NO_x and particulates. These post-combustion CO_2 capture technologies can be retrofitted to existing plants, i.e. the CO_2 capture processes can be placed downstream of the flue gas treatment of an already built power generation unit [16]. There are various technologies that can be deployed in such systems including: chemical or physical absorption, membrane separation or adsorption.

The main disadvantage of these processes is the energy penalty associated with the low CO_2 partial pressure in the flue gas (~0.1 MPa) after combustion [14, 17]. On the other hand, it is important to highlight that these capture methods can be retrofitted to existing units, which even if it means pre-investing

in modifications for existing units, it will be cheaper than having to build new units to implement carbon capture technologies[18].

2.2.1.2 Pre-combustion CO_2 capture

For the pre-combustion approach, the fuel is partially oxidised in order to produce a syngas containing mainly CO and H_2, and then, the fuel is decarbonised before the combustion process occurs. This technology is suitable for being retrofitted in IGCC (Integrated Gasification Combined Cycle) units and is also appropriate for natural gas reforming plants. Once syngas is obtained, it enters a water-gas shift reactor where steam reacts with the CO in a catalytic chamber producing the mixture containing CO_2 (typically between 15-60% [14]) and H_2. After the catalytic reactor, the CO_2 can be separated from the H_2 by means of absorption, adsorption or membrane separation.

This approach has the potential to be the most economically viable of all the capture options [19, 20], and the efficiency penalties of this process have been calculated to be half of those for a post-combustion process. The H_2 produced in these plants can be used as a carbon-free fuel for production of heat and electricity. However, it is important to note that this capture path incurs energy penalties separation of oxygen needed for the gasification process [21].

2.2.1.3 Oxy-fuel combustion

In an oxy-fuel combustion unit the fuel is combusted in an oxygen-rich atmosphere to produce a flue gas comprising mainly CO_2 (80-98 %, depending on the fuel and system used [22]) and H_2O, owing to the absence of nitrogen from air. Furthermore, this means that emmision of NO_x is tipically lower when compared with combustion in air.

The combustion temperature can be excessively high if the fuel is burnt in pure oxygen; therefore, a portion of the flue gas is recycled into the combustion chamber in order to moderate the flame temperature [22]. The oxygen used in this process is usually produced by cryogenic separation of air; however, this process has a high energy penalty [23, 24]. Thus, new air separation techniques are being investigated such as membrane separation and chemical

looping processes [14, 25]. However, even accounting for energy penalties associated with oxygen production, oxy-fuel combustion is characterised with similar costs and efficiencies to those of post-combustion capture [26, 27].

2.2.1.4 Industrial processes

It is vital to highlight that industrial processes account for one-fifth of the global CO_2 emissions (Figure 2-8); hence, their decarbonisation is crucial to meet the 2DS target. Also, it should be noted that the options to control emissions from the industrial sector are limited, with CCS being the only suitable possibility for large sources of industrial CO_2.

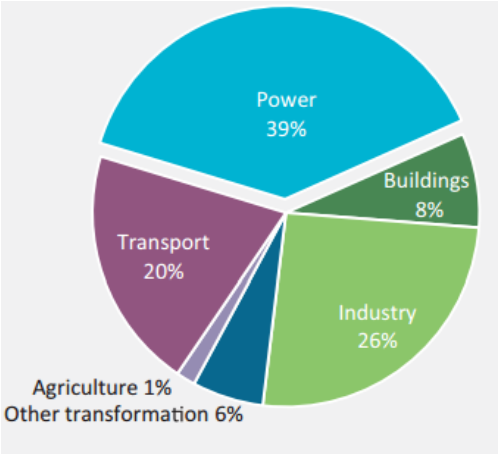

Figure 2-8: CO_2 emissions by sector [28]

Within the industrial sector, the cement industry is the second main CO_2 emitting sector with a total emission of 2 $GtCO_2$ per year in 2007 [29]. For this sector, post-combustion capture is deemed as a viable decarbonisation route due to the moderately high CO_2 concentrations in the flue gas (15-30%$_{vol}$), as it can be retrofitted to current cement plants [30]. Oxy-fuel combustion in cement kilns has also been suggested as a suitable option [30]. Finally, there is a synergy between the cement industry and calcium looping; the spent sorbent from the capture process can be used as a feadstock in the cement kiln as is explained further in Chapter 2.3.2.3 [31].

The iron and steel industry is one of the most energy-intensive sectors in the world. In 2007, this sector alone accounted for 20% of the total industrial energy

consumption [32]. Two approaches can be used in this sector: the first path involves pure oxygen being injected in the blast furnace, whilst the flue gas is being recycled at the top instead of air; and the second path is pre-combustion where the fuel is decarbonised before it enters the blast furnace, the resulting hydrogen could be used to reduce the iron ore. A predicted capture efficiency of 90-95% could be achieved [14].

2.2.2 CO_2 transport

There are four methods for CO_2 transport; namely: pipelines, ships, trains and trucks. The means of transport is subjected to the volume of transported gas and the distance [16]. CO_2 is typically transported in supercritical phase [16], its phase diagram can be found in Figure 2-9, where the critical point can be seen at 31.1°C and 73.9 bar.

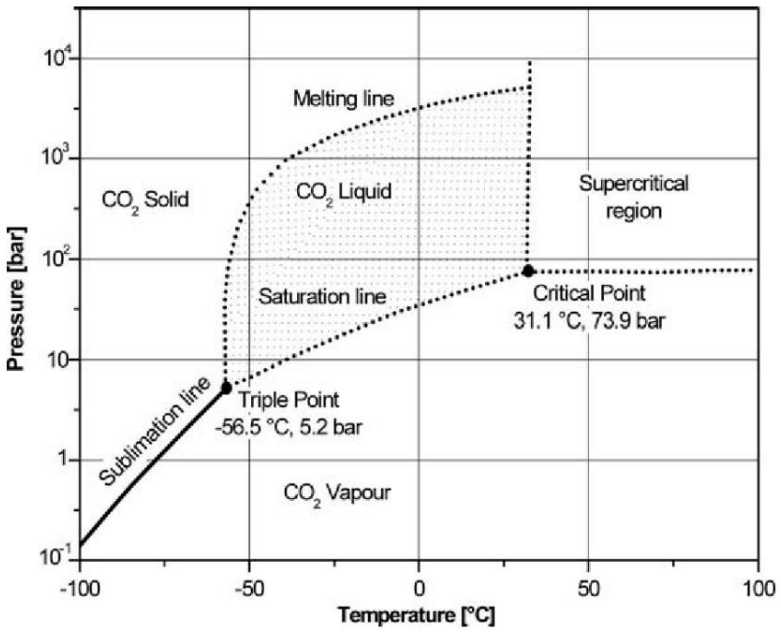

Figure 2-9: Carbon dioxide phase diagram [27]

Pipeline and ships are considered to be the most viable options [33]. The pipeline transportation is prefered, however, ships are feasible when the CO_2 volume is small or the distance is excessively long (1000-1500 km).

For pipeline transportation, the CO_2 is kept at ambient temperature at a pressure in the range of 85-150 bar [16]. Corrosion and hydrate formation are

serious issues when dealing with pipeline transportation. Purity specifications are even stricter for CO_2 transportation by ships, and free water is a key concern as it can freeze. Therefore, a purity of CO_2 of 99.7% is required to avoid this phenomenon [34]. It is important to highlight that these impurities do not only affect the CO_2 transport, but also the injection and storage in two different manners: by modifying thermo-physical properties [35, 36] or by altering the chemical properties of the CO_2 affecting material corrosion and interactions rocks in the sstorage reservoir [36, 37].

2.2.3 CO_2 storage

CO_2 storage is the last step in the CCS chain, and it is imperative that safe storage is assured in order to minise the risk of leakage and other risks to the environment and population's health [17, 38]. There are numerous approaches for CO_2 storage, such as geological storage, which is considered as the most viable option, ocean storage and mineral carbonation [16, 39]. It is important to note that CO_2 storage sites should be sensibly selected. Some of the requirements for CO_2 storage sites are: suitable porosity, permeability and thickness of the reservoir rocks, good sealing capability of the cap rock and stable geological environment [40]. Storage sites mainly involve three types of geological formations: depleted oil and gas reservoirs, unmineable coal beds and saline aquifers. An illustration of the different storage methods in geological formations can be found in Figure 2-10.

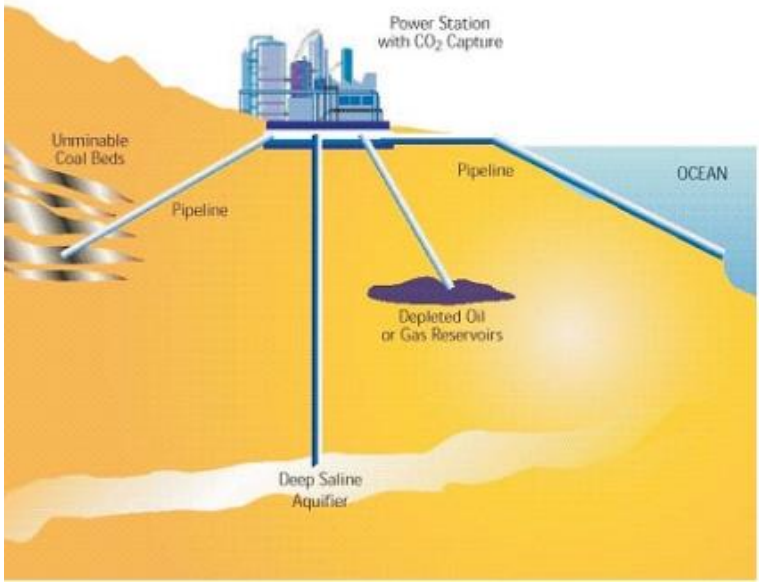

Figure 2-10: A schematic of CO_2 geological storage

CO_2 can be injected into depleted oil and/or gas reservoirs in order to increase the pressure, consequently extracting residual oil and gas, whilst the CO_2 remains in the reservoir perpetually. These technologies are mature with several studies on migration simulation [41, 42], geochemical modelling [43, 44] and risk assessment [45]. Another path is to inject CO_2 into deep beds of coal in order to extract methane trapped in the porous structure of coal seams. The CO_2 is then stored in the space formed by the removal of the trapped methane. Nevertheless, there are some challenges associated with this technique such as issues related to storage capacity, storage integrity, safety and physical and chemical processes [46]. Another geological storage option is saline aquifers, which can be found extensively at sites both onshore and offshore; these aquifers are typically 700-1000 m below ground level [47]. It has been estimated that these geological formations have significant storage potential [14], although they have no commercial use. Crucial parameters for storage in deep saline aquifers include: CO_2 phase behaviour, CO_2-water-rock interaction, and CO_2 trapping mechanisms [16].

A different possibility is mineral carbonation, which is defined as an accelerated form of weathering of natural silicate rock. Here, a metal oxide reacts with CO_2

to form insoluble carbonates and heat. This reaction can take place below (in situ) or above (ex situ) the surface. When the reaction takes place below the ground (in situ), it involves the injection of CO_2 into reservoirs in order to promote the reaction between the CO_2 and the minerals [48]. For ex situ processes, the material needs to be extracted and ground to the micron level for the reaction to occur [14].

Another approach would be to inject CO_2 into the ocean at depths greater than 3 km; here the ocean pressure would ensure that the CO_2 is liquefied and remains at the bottom of the ocean owing to its higher density when compared to sea water at that depth [49, 50]. Oceans are the biggest natural CO_2 sink, and it has been estimated that oceans take carbon at a rate of 1.7 Gt annually, which is larger than the amount of CO_2 sequestered by all terrestrial vegetation [51]. For this reason, ocean storage could be a suitable potential sink for large amounts of anthropogenic CO_2. However, there are some issues associated with this method. Namely, injecting large amounts of CO_2 into the oceans may lead to ocean acidification, affecting the marine ecosystems [52].

2.3 High temperature solid loopings (HTSL)

These technologies are based on the use of high-temperature solids to transfer CO_2, in the case of calcium looping (CaL), or O_2, in the case of chemical looping combustion (CLC), between two interconnected fluidised-bed reactors. There is a clear advantage of HTSL processes when compared to oxy-fuel combustion. Namely, there is no requirement for an ASU, for CLC, and the ASU required for CaL is about a third the size of that for a typical oxy-fired combustion unit [53].

One of the most highlighted aspects of HSTL is the need for a suitable solid material that circulates between the reactors. These solid materials are known as oxygen carriers for CLC, and sorbents for CaL. The physical characteristics of these solid materials are alike for both processes since both are used in fluidized bed systems; however, the chemistry is different. These materials should be environmentally benign, suitable for the reverse reactions occuring over multiple cycles, and they should have sufficient carrying capacity for O_2 (CLC) and CO_2 (CaL). Moreover, these solids should be cheap in order to make

the process economically feasible, and mechanically strong and not prone to agglomeration, especially if they are to be used in fluidized bed systems.

2.3.1 Chemical looping combustion

This concept was first proposed by Lewis and Gilliland [54], where they presented a copper-based cyclic process in order to produce a pure CO_2 stream. Subsequently, it was suggested as a CO_2 capture technology by Ishida and Jin [55], who noted a potential to decrease the exergy losses associated with combustion processes. An illustration of the CLC process is provided in Figure 2-11. The solid material (oxygen carrier) is oxidised in the presence of air in the air reactor following Equation (2-1). The solids are then transferred to the fuel reactor, where they are reduced by the fuel, providing the required oxygen for the combustion; this reaction is shown in Equation (2-2). CO_2 and steam leave the fuel reactor, then, the water is condensed and a highly pure CO_2 stream is left ready for compression and storage [56]. The oxygen carrier in reduced form is transferred back to the air reactor, where the cycle starts again. The oxygen carrier oxidation is and exothermic reaction; the reduction, can be endothermic or exothermic depending on the oxygen carrier and the fuel used [57].

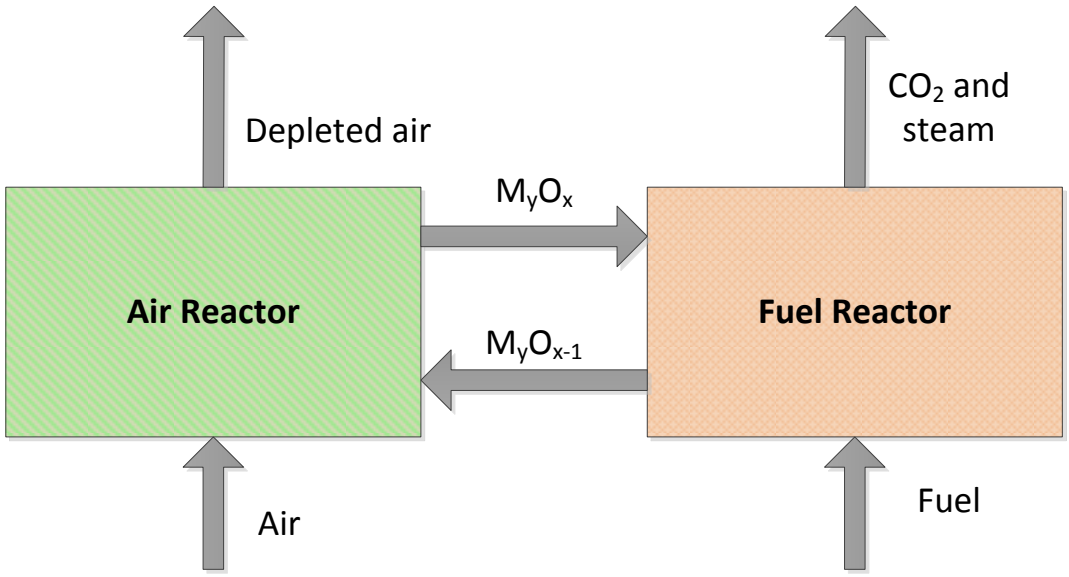

Figure 2-11: Typical example of a CLC scheme

$$M_yO_{x-1} + Air \rightarrow M_yO_x \quad \textbf{(2-1)}$$

$$(2n+m)M_yO_x + C_nH_{2m} = (2n+m)M_yO_{x-1} + mH_2O + nCO_2 \quad \textbf{(2-2)}$$

One of the advantages of this process is the fact that it can be utilised with different types of fuels: gases, liquids and solids; while most of the research efforts is currently on gaseous fuels usage, increasingly, research is being directed towards the use of CLC for solid fuels [58].

2.3.2 Calcium looping

2.3.2.1 Introduction

Calcium looping, as a post-combustion CO_2 capture technology, was first proposed by Shimizu et al. [53]. It is based on the reversible carbonation/calcination reaction of lime-based sorbents as it can be seen in Equation (2-3).

$$CaO + CO_2 \leftrightarrow CaCO_3 \qquad \Delta H_{25℃} = -178.2\ kJ/mol \quad \textbf{(2-3)}$$

The flue gas from the power plant enters the carbonator, where the CO_2 reacts with the CaO, typically at 650 °C, to form $CaCO_3$, which is an exothermic reaction. The saturated sorbent is then transferred to the calciner, where it releases CO_2 at high temperature in an endothermic process, called calcination. The system usually comprises two circulating fluidised beds (CFB), but there are other configurations, such as a CFB and a BFB. In the most widely used configuration, oxygen is fed in the calciner to burn fuel in order to provide heat for the endothermic calcination reaction. Therefore, an air separation unit (ASU) is required to produce oxygen, but this ASU need only be one third of the size of an oxy-fired coal power unit [53]. A schematic of a representative CaL system is shown in Figure 2-12.

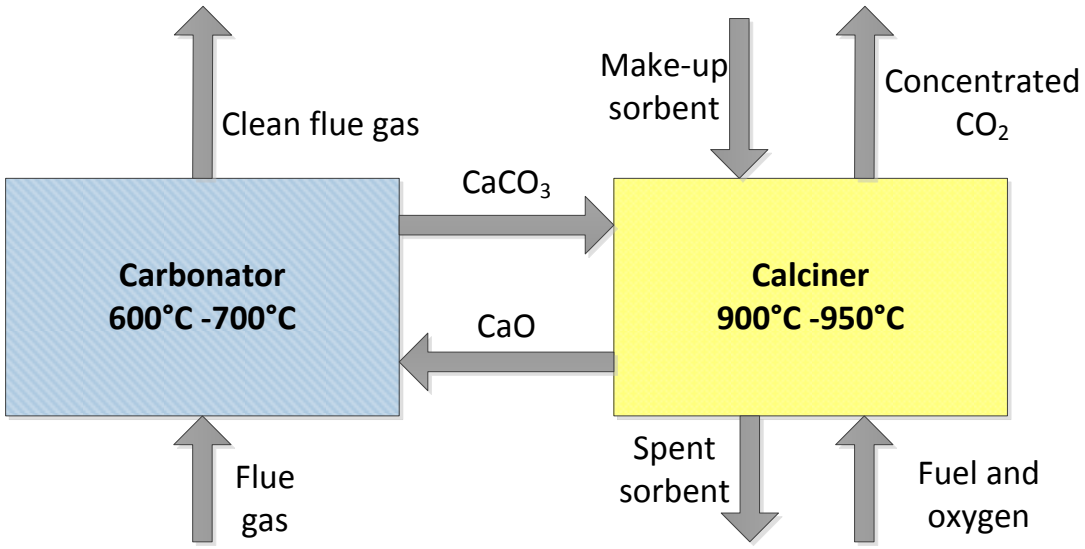

Figure 2-12: An illustration of a typical CaL system

Another significant benefit of this process is that it utilises technologies that have been demonstrated at large-scale, namely, fluidised beds. Large units of up to 460MWe for both atmospheric and pressurised operation are available [53, 59].

In Figure 2-13, the temperature vs. equilibrium vapour pressure of CO_2 in the $CaO/CO_2/CaCO_3$ system is shown. Above the line, carbonation takes place and in the conditions below the line is where the calcination reaction occurs. The equation of Baker [60] (Equation (2-4) in SI units) was developed using experimental data for temperatures above 1170 K and CO_2 pressures above 1.01 bar, therefore, it correlates the data for these conditions extremely well, but it should be noted that there are deviations at lower temperatures and lower CO_2 partial pressures.

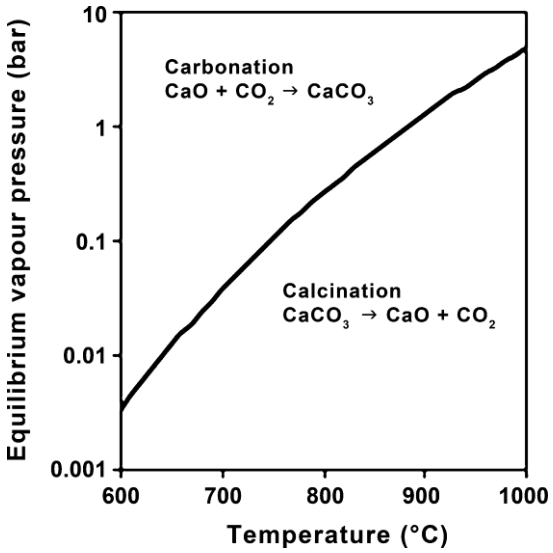

Figure 2-13: Equilibrium vapour pressure of CO_2 vs temperature [61]

$$lnp_e = 27.827 - \frac{19129.4}{T} \quad \textbf{(2-4)}$$

A key challenge for the CaL is sorbent degradation with increasing number of cycles. Natural limestone has a residual capacity of around 8-10%, this degradation during carbonation/calcination cycles is due to the sintering process that a particle undergoes mainly under calcination conditions. There are several routes to reduce this degradation, from enhancing the properties of natural sorbents to producing new synthetic sorbents, as well as reactivation for spent sorbent, and these are all potentially important to ensure the process is as economically viable as possible.

2.3.2.2 Pilot-plant testing of CaL

Another important challenge is the scale-up of the plants from bench/lab scale to pilot/demonstration scale. Currently, there are several plants demonstrating the calcium looping cycle at pilot and demonstration scale, and these include:

- Darmstadt University of Technology (Germany)

The 1 MW_{th} facility comprises two interconnected refractory-lined CFB reactors. The carbonator is 8.66 m tall with 0.59 m ID, operating at temperatures around 650°C, with internal cooling to control the temperature. The calciner is 11.35 m high and 0.4 m ID, and it operates at temperatures below 1000°C. It is important

to highlight the fact that the limestone is fed into the carbonator, where is heated by the exothermic reaction, this configuration is meant to reduce fuel and oxygen consumption in the calciner [62]. A schematic of the plant is given in Figure 2-14. This unit was operated successfully for 400 h. The capture efficiencies achieved during these tests were of up to 90%, close to the equilibrium limits at these temperatures.

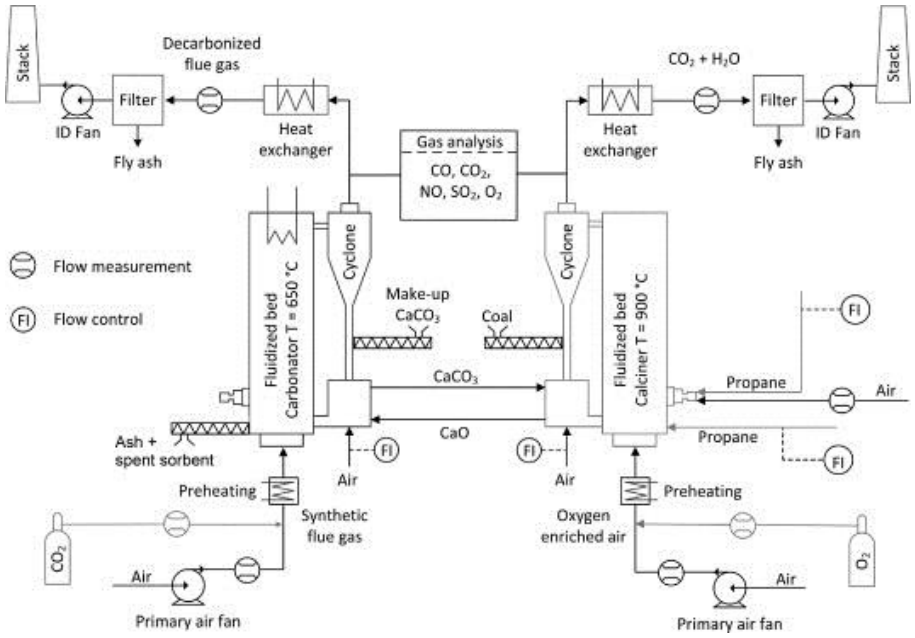

Figure 2-14: Experimental set up of the 1 MW_{th} facility [62]

- Institut für Feuerungs- und Kraftwerkstechnik (IFK (Germany))

The IFK has developed a 200 kW_{th} unit in order to investigate the suitability of CaL at larger scale. A diagram of this unit and its configurations is presented in Figure 2-15. The plant comprises two CFBs, however, the carbonator can be used in a fast-fluidisation regime or in a turbulent regime. The calciner always operates in a fast-fluidisation regime and is 10 m high and 0.21 m ID, and it operates at temperatures ranging from 875 to 930°C. There are two reactors that can serve as the carbonator, when operating in the fast fluidisation regime, it is 10 m tall and 0.23 m ID with operating temperatures of around 650°C [63]; however, when operating as a turbulent bed it is 6 m tall and 0.33 m ID, with operating temperatures of 650-730°C [64]. Successful operation was proven for

more than 600 h, where the facility reached up to 90% capture efficiency in the carbonator [65]. A diagram of this unit can be seen in Figure 2-15.

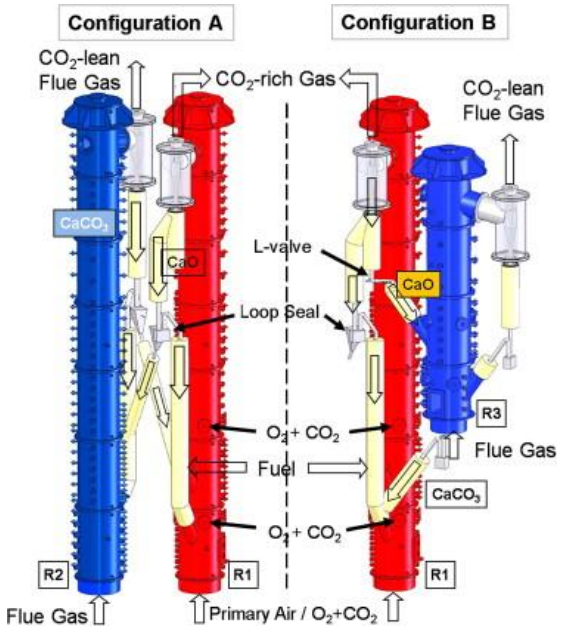

Figure 2-15: Diagram of the 200 kW_{th} unit with its two possible configurations [66]

- Industrial Technology Research Institute (Taiwan)

Here, a 1.9 MW_{th} plant consists of a BFB carbonator operating in a range of 600-700°C.The calciner is a moving bed, i.e. a rotary kiln, and it operates at temperatures ranging from 800 to 900°C [67]. The CO_2 capture level is between 80-95%. One crucial aspect of this design is the uniform temperature distribution in the calciner due to the configuration, which results in a higher usable length that can be used for calcination. A photo illustrating the construction of this plant can be seen in Figure 2-16.

Figure 2-16: Construction of 1.9 MW_{th} CaL plant [67]

- Instituto Nacional Del Carbón, Consejo Nacional de Investigaciones Científicas (INCAR-CSIC (Spain))

This 1.7 MW_{th} pilot was developed comprising two interconnected circulating fluidised beds, operated usually with gas velocities of 3-5 m/s for the circulation to occur in a proper manner [68]. The carbonator is 15 m high and has an ID of 0.75 m, and it operates in a range of temperatures varying form 600-715°C, the calciner is the same height but 0.65 m ID, and it operates at 820-950°C. Here, the calciner is fed with coal with a choice of oxy- or air-firing. The sorbent is transported from one reactor to the other by double bubbling fluidised loop seals, which allows control of the solid inventory in both fluidised beds. This unit was operated for more than 380 h with a capture efficiency in the range of 40-95% [69]. It was reported that CO_2 capture in the carbonator was close to the equilibrium, if the solid inventory was properly controlled [70]. A schematic of this unit is shown in Figure 2-17.

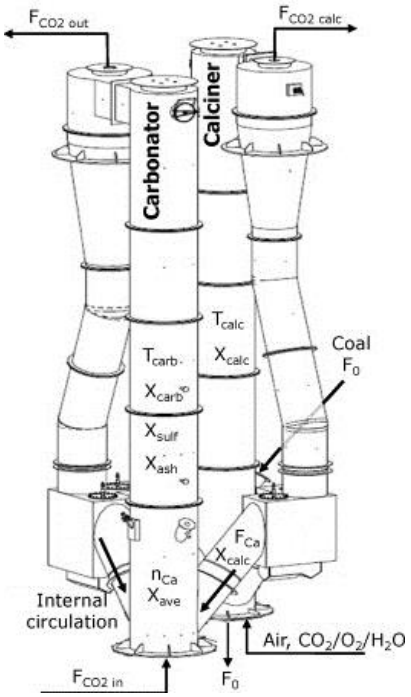

Figure 2-17: Schematic of La Pereda pilot plant (INCAR-CSIS) [69]

-Canmet Energy Technology Centre (Canada)

The 75 kW_{th} unit comprises a carbonator that can be operated under moving or bubbling bed conditions and a CFB calciner. The carbonator and calciner of this plant can be used in several heights: 2-5 m with 0.1 m ID for the carbonator, which operates at temperatures in the range of 580 to 720°C .The calciner, on the other hand, is 4.5-5 m tall with 0.1 m ID and operates at 850-950°C depending on the application [71]. This plant was operated continuously for more than 50 h. Some of the results showed CO_2 capture level of up to 97% during the first cycles [72]. An illustration of this unit can be found in Figure 2-18.

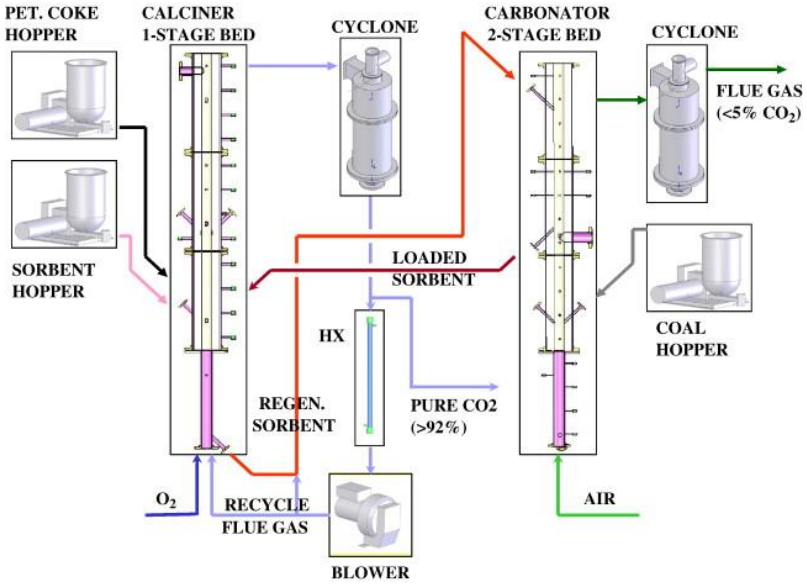

Figure 2-18: Schematic of the Canmet 75 kW_{th} CaL unit [72]

- Cranfield University (UK)

The 25 kW_{th} unit developed by Cranfield University comprises a CFB carbonator, which is 4.3 m tall and 0.1 m ID, and a BFB calciner, which is 1.2 m high and 0.165 m ID. The carbonator and the calciner are electrically heated in order to reach and maintain the desired temperatures [73]. The solids are transferred from one reactor to the other via loop seals [74]. The fresh sorbent is fed to the calciner. This plant has undergone modifications as part of this work, which can be found in Appendix C. The commissioning process of the modified unit can be found in Appendix D. Besides, new results on experimental campaigns using the modified plant can be found in Chapter 6 and Chapter 7. A schematic of the modified plant can be found in Figure 2-19.

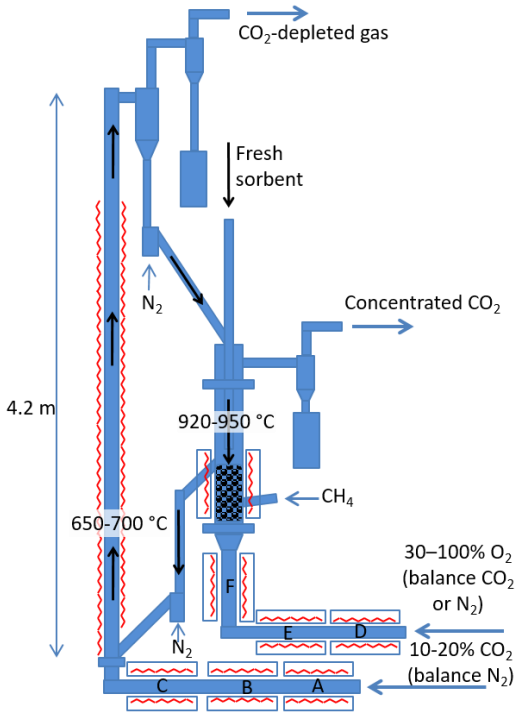

Figure 2-19: Schematic of the modified Cranfield 25 kW_{th} plant

2.3.2.3 Calcium looping applied to the cement industry

A crucial benefit of CaL systems over the competing technologies is that the spent material purged from the calciner can be used as a feedstock in the cement industry. In other words, this would allow to decarbonise both, the power and the cement units. It is well known that cement production is a particularly energy-intensive process, with around 5% of the global anthropogenic CO_2 emissions resulting from cement manufacture [75], and between 0.6 and 1 kg of CO_2 produced per kg of cement [76], with most of the energy consumption used to drive the endothermic calcination reaction in the kiln [77].

The core component of cement is CaO, obtained from calcining natural limestone or chalk. This material is ground and mixed with other ingredients such as sand, clay, bauxite or iron ore, among others. This mixture is heated and calcined, before heating further to 1400-1600 °C [76]; these high temperatures partly sinter the components and react to form clinker. The clinker is then cooled, ground and mixed with other ingredients to form what is known as cement.

Several studies have explored the possibility of using CaL spent sorbent in a cement plant. It was found that cement produced from spent sorbent had lower percentage of the alite (Ca_3SiO_5) phase than in normal Portland cement [78]. It was suggested that this was due to the addition of fuel in the calciner causing interactions between the ash and the CaL sorbent. Another study found that cement with similar properties to commercial cement could be produced from spent sorbent [79].

2.4 References

[1] United Nations, 1998. Kyoto Protocol to the United Nations Framework Convention on Climate Change, Kyoto, Japan.

[2] IPCC, 2013. Climate change 2013. The physical science basic. Working group I contribution to the fifth assessment report of the Intergovernmental Panel on Climate Change. Cambridge University Press, Cambridge, UK and New York, NY, USA.

[3] IPCC, 2014. Climate Change 2014: Synthesis Report. Contribution of Working Groups I, II and III to the Fifth Assessment Report of the Intergovernmental Panel on Climate Change. Cambridge University Press, Cambridge, UK and New York, NY, USA.

[4] IEA, 2015. CO_2 emissions from fuel combustion - highlights. IEA Publications, Paris, France.

[5] IPCC, 2014. Climate Change 2014: Mitigation of Climate Change, Contribution of Working Group III to the Fifth Assessment Report of the Intergovernmental Panel on Climate Change. Cambridge University Press, Cambridge, UK and New York, NY, USA.

[6] Tyndall, J., 1859. Note on the transmission of heat through gaseous bodies. Proceedings of the Royal Society of London, 10, pp. 37-39.

[7] Arrhenius, S., 1896. On the influence of carbonic acid in the air upon the temperature of the ground. The London, Edinburgh, and Dublin Philosophical Magazine and Journal of Science, 41(251), pp. 237-276.

[8] Haas, C., Pfaffling, A., Hendricks, S., Rabenstein, L., Etienne, J. L., Rigor, I., 2008. Reduced ice thickness in Arctic Transpolar Drift favors rapid ice retreat. Geophysical Research Letters, 35(17).

[9] Kwok, R., Cunningham, G. F., Wensnahan, M., Rigor, I., Zwally, H. J., Yi, D., 2009. Thinning and volume loss of the Arctic Ocean sea ice cover: 2003–2008. Journal of Geophysical Research: Oceans, 114(C7).

[10] IEA, 2010. Energy Technology Perspectives: Scenarios & Strategies To 2050. IEA Publications, Paris, France.

[11] IEA, 2014. World Energy Outlook. IEA Publications, Paris, France.

[12] UNEP, 2012. The Emissions Gap Report 2012. United Nations Environment Programme (UNEP), Nairobi.

[13] IEA, 2012. Energy Technology Perspectives: Pathways to a Clean Energy System. IEA Publications, Paris, France.

[14] IPCC, 2005: IPCC Special Report on Carbon Dioxide Capture and Storage. Prepared by Working Group III of the Intergovernmental Panel on Climate Change [Metz, B., Davidson, O., de Coninck, H. C., Loos, M., and Meyer, L. A. (eds.)]. Cambridge University Press, Cambridge, United Kingdom and New York, NY, USA.

[15] GCCSI, 2012. The global status of CCS: 2012. Global CCS Institute, Canberra, Australia.

[16] Leung, D.Y.C., Caramanna, G., Maroto-Valer, M.M., 2014. An overview of current status of carbon dioxide capture and storage technologies. Reneweable and Sustainable Energy Reviews, 39, pp. 426-443.

[17] Spliethoff, H., 2010. Power generation from solid fuels. Springer Science & Business Media.

[18] Irons, R., Sekkapan, G., Panesar, R., Gibbins, J., Lucquiaud, M., 2007. CO_2 Capture Ready Plants. IEA Greenhouse Gas Programme, IEA, UK.

[19] Gibbins, J., 2006. Making New Power Plants 'Capture Ready'. 9th International CO_2 Capture Network, 16 June 2006, Offices of E2, Copenhagen, Denmark, UK.

[20] Ramkumar, S., Fan, L.S., 2010. Calcium Looping Process (CLP) for Enhanced Noncatalytic Hydrogen Production with Integrated Carbon Dioxide Capture. Energy & Fuels, 24, pp. 4408-4418.

[21] Hester, R.E., Harrison, R.M., 2010. Carbon Capture: Sequestration and Storage. Vol. 29. Royal Society of Chemistry.

[22] Kenarsari, S.D., Yang, D., Jiang, G., Zhang, S., Wang, J., Russell, A.G., Wei, Q., Fan, M., 2013. Review of recent advances in carbon dioxide separation and capture. RSC Advances, 3, pp. 22739–22773.

[23] Romeo, L.M., Abanades, J.C., Escosa, J.M., Paño, J., Giménez, A., Sánchez Biezma, A., Ballesteros, J.C., 2008. Oxyfuel carbonation/calcination cycle for low cost CO_2 capture in existing power plants. Energy Conversion Management, 49, pp. 2809–2814.

[24] Ströhle, J., Lasheras, A., Galloy, A., Epple, B., 2009. Simulation of the carbonate looping process for post-combustion CO_2 capture from a coal fired power plant. Chemical Engineering & Technology, 32(3), pp. 435–442.

[25] Herzog, H., Golomb, D., 2004. Carbon capture and storage from fossil fuel use. Encyclopedia of Energy, 1, pp. 1–11.

[26] Yang, H., Xu, Z., Fan, M., Gupta, R., Slimane, R. B., Bland, A. E., Wright, I., 2008. Progress in carbon dioxide separation and capture: A review. Journal of Environmental Sciences, 20(1), pp. 14-27.

[27] Gibbins, J., Chalmers, H., 2008. Carbon capture and storage. Energy Policy, 36(12), pp. 4317-4322.

[28] IEA, 2014. Energy technology Perspectives: Harnessing Electricity’s Potential. IEA Publications, Paris, France.

[29] ENCI, 2008. Werkbezoek CDA Jongerenafdeling. Maastricht, the Netherlands.

[30] IEA GHG, 2008. CO_2 capture in the cement industry. Cheltenham, UK: International Energy Agency Greenhouse Gas R&D Programme.

[31] Rodríguez, N., Alonso, M., Grasa, G., Abanades, J.C., 2008. Process for capturing CO_2 arising from the calcination of the $CaCO_3$ used in cement manufacture. Environmental Science & Technology, 42, pp. 6980-6984.

[32] IEA, 2007. Tracking industrial energy efficiency and CO_2 emissions. IEA Publications, Paris, France.

[33] Svensson, R., Odenberger, M., Johnsson, F., Strömberg, L., 2004. Transportation systems for CO_2 - Application to carbon capture and storage. Energy Conversion and Management, 45, pp. 2343–2353.

[34] Maroto-Valer, M.M., ed., 2010. Developments and Innovation in Carbon Dioxide (CO_2) Capture and Storage Technology: Carbon Dioxide (CO_2) Storage and Utilisation. Elsevier.

[35] Chapoy, A., Nazeri, M., Kapateh, M., Burgass, R., Coquelet, C., Tohidi, B., 2013. Effect of impurities on thermophysical properties and phase behaviour of a CO_2-rich system in CCS. International Journal of Greenhouse Gas Control, 19, pp. 92–100.

[36] Løvseth, S.W., Stang, H.G.J., Westman, S.F., Snustad, I., Austegard, A., 2014. Experimental investigations of impurity impact on CO_2 mixture phase equilibria. Energy Procedia, 63, pp. 2589–2595.

[37] Talman, S., 2015. Subsurface geochemical fate and effects of impurities contained in a CO_2 stream injected into a deep saline aquifer: what is known. International Journal of Greenhouse Gas Control, 40, pp. 267–291.

[38] Miller, B.G., 2011. Clean Coal Engineering Technology. Elsevier.

[39] Van Der Zwaan, B., Smekens, K., 2009. CO_2 capture and storage with leakage in an energy-climate model. Environmental Modelling & Assessment, 14, pp. 135–148.

[40] Solomon, S., Carpenter, M., Flach, T.A., 2008. Intermediate storage of carbon dioxide in geological formations: a technical perspective. International Journal of Greenhouse Gas Control, 2(4), pp. 502–10.

[41] Vidiuk, K., Cunha, L.B., 2007. A simulation study of effects of operational procedures in CO_2 flooding projects for EOR and sequestration. Proceedings of the Canadian international petroleum conference, 12–14 June 2007, Calgary, Alberta, Canada.

[42] Chiaramonte, L., Zoback, M., Friedmann, J., Stamp, V., Zahm, C., 2011. Fracture characterization and fluid flow simulation with geomechanical constraints for a CO_2–EOR and sequestration project Teapot Dome Oil Field, Wyoming, USA. Energy Procedia, 4, pp. 3973–3980.

[43] Preston, C., Moneab, M., Jazrawib, W., Brown, K., Whittakerd, S., White, D., Law, D., Chalaturnyk, R., Rostron, B., 2005. IEA GHG Weyburn CO_2 monitoring and storage project. Fuel Processing Technology, 86(14), pp. 1547–1568.

[44] Cantucci, B., Montegrossi, G., Vaselli, O., Tassi, F., Quattrocchi, F., Perkins, E.H., 2009. Geochemical modeling of CO_2 storage in deep reservoirs: the Weyburn Project (Canada) case study. Chemical Geology, 265(1), pp. 181–197.

[45] Klusman, R.W., 2003. Evaluation of leakage potential from a carbon dioxide EOR/ sequestration project. Energy Conversion and Management, 44(12), pp. 1921–1940.

[46] White, C.M., Strazisar, B.R., Granite, E.J., Hoffman, J.S., Pennline, H.W., 2003. Separation and capture of CO_2 from large stationary sources and sequestration in geological formations—coalbeds and deep saline aquifers. Journal of the Air & Waste Management Association, 53(6), pp. 645–715.

[47] Singh, N., 2008. Deep saline aquifiers for sequestration of carbon dioxide. In: International geological congress, August 2008, Oslo, Norway.

[48] Sipilä, J., Teir, S., Zevenhoven, R., 2008. Carbon dioxide sequestration by mineral carbonation: Literature review update, 2005–2007. Åbo Akademi Rep. VT, 1.

[49] House, K.Z., Schrag, D.P., Harvey, C.F., Lackner, K.S., 2006. Permanent carbon dioxide storage in deep-sea sediments. Proceedings of the National Academy of Sciences, 103(33), pp. 12291–12295.

[50] Bachu, S., 2000. Sequestration of CO_2 in geological media: criteria and approach for site selection in response to climate change. Energy Conversion and Management, 41(9), pp. 953–970.

[51] Yamasaki, A., 2003. An overview of CO_2 mitigation options for global warming – emphasizing CO_2 sequestration options. Journal of Chemical Engineering of Japan, 36(4), pp. 361–375.

[52] Seibel, B.A., Walsh, P.J., 2001. Potential impacts of CO_2 injection on deep-sea biota. Science, 294(5541), pp. 319–320.

[53] Shimizu, T., Hirama, T., Hosoda, H., Kitano, K., Inagaki, M., Tejima, K., 1999. A twin fluid-bed reactor for removal of CO_2 from combustion processes. Chemical Engineering Research and Design, 77(1), pp. 62-68.

[54] Lewis, W.K., Gilliland, E.R., 1954. Production of Pure Carbon Dioxide. U.S. Patent 2,665,972, issued January 12, 1954.

[55] Ishida, M., Jin, H., 1994. A new advanced power-generation system using chemical-looping combustion. Energy, 19(4), pp. 415–422.

[56] Lyngfelt, A., Leckner, B., Mattisson, T., 2001. A fluidized-bed combustion process with inherent CO_2 separation; application of chemical-looping combustion. Chemical Engineering Science, 56(10), pp. 3101–3113.

[57] Jerndal, E., Mattisson, T., Lyngfelt, A., 2006. Thermal analysis of chemical-looping combustion. Chemical Engineering Research and Design, 84(9), pp. 795–806.

[58] Adánez, J., Abad, A., García-Labiano, F., Gayán, P., Luis, F., 2012. Progress in chemical-looping combustion and reforming technologies. Progress in Energy and Combustion Science, 38(2), pp. 215–282.

[59] Everett, G., 1953. Gasification of carbonaceous solid fuels. U.S. Patent 2,654,661, issued October 6, 1953.

[60] Baker, E.H., 1962. 87. The CaO-CO_2 system in the pressure range 1-300 atm. Journal of the Chemical Society, pp. 464-470.

[61] Mcbride, B.J., Zehe, M.J., Gordon, S., 2002. NASA Glenn Coefficients for Calculating Thermodynamic Properties of Individual Species. Cleveland, OH, USA.

[62] Ströhle, J., Junk, M., Kremer, J., Galloy, A., Epple, B., 2014. Carbonate looping experiments in a 1 MW_{th} pilot plant and model validation. Fuel, 127, pp. 13–22.

[63] Dieter, H., Bidwe, A. R., Varela-Duelli, G., Charitos, A., Hawthorne, C., Scheffknecht, G., 2014. Development of the calcium looping CO_2 capture technology from lab to pilot scale at IFK, University of Stuttgart. Fuel, 127, pp. 23-37.

[64] Hawthorne, C., Dieter, H., Bidwe, A., Schuster, A., Scheffknecht, G., Unterberger, S., Käß, M., 2011. CO_2 capture with CaO in a 200 kW_{th} dual fluidized bed pilot plant. Energy Procedia, 4, pp. 441-448.

[65] Dieter, H., Hawthorne, C., Zieba, M., Scheffknecht, G., 2013. Progress in calcium looping post combustion CO_2 capture: successful pilot scale demonstration. Energy Procedia, 37, pp. 48-56.

[66] Dieter, H., Hawthorne, C., Bidwe, A. R., Zieba, M., Scheffknecht, G., 2012. The 200 kW_{th} dual fluidized bed calcium looping pilot plant for efficient CO_2

capture: plant operating experiences and results. In 21st International Conference on Fluidized Bed Combustion, Naples, Italy, June.

[67] Chang, M.H., Huang, C.M., Liu, W.H., Chen, W.C., Cheng, J.Y., Chen, W., Wen, T.W., Ouyang, S., Shen, C.H., Hsu, H.W., 2013. Design and Experimental Investigation of Calcium Looping Process for 3-kW_{th} and 1.9-MW_{th} Facilities. Chemical Engineering & Technology, 36(9), pp. 1525-1532.

[68] Sánchez-Biezma, A., Ballesteros, J.C., Diaz, L., De Zárraga, E., Álvarez, F.J., López, J., Arias, B., Grasa, G., Abanades, J.C., 2011. Postcombustion CO_2 capture with CaO. Status of the technology and next steps towards large scale demonstration. Energy Procedia, 4, pp. 852-859.

[69] Arias, B., Diego, M.E., Abanades, J.C., Lorenzo, M., Diaz, L., Martínez, D., Alvarez, J. and Sánchez-Biezma, A., 2013. Demonstration of steady state CO_2 capture in a 1.7 MW_{th} calcium looping pilot. International Journal of Greenhouse Gas Control, 18, pp. 237-245.

[70] Sánchez-Biezma, A., Paniagua, J., Diaz, L., Lorenzo, M., Alvarez, J., Martínez, D., Arias, B., Diego, M.E., Abanades, J.C., 2013. Testing postcombustion CO_2 capture with CaO in a 1.7 MW_{th} pilot facility. Energy Procedia, 37, pp. 1-8.

[71] Hughes, R.W., Lu, D.Y., Anthony, E.J., Macchi, A., 2005. Design, process simulation and construction of an atmospheric dual fluidized bed combustion system for in situ CO_2 capture using high-temperature sorbents. Fuel Processing Technology, 86(14), pp. 1523-1531.

[72] Lu, D.Y., Hughes, R.W., Anthony, E.J., 2008. Ca-based sorbent looping combustion for CO_2 capture in pilot-scale dual fluidized beds. Fuel Processing Technology, 89(12), pp. 1386-1395.

[73] Cotton, A., Finney, K.N., Patchigolla, K., Eatwell-Hall, R.E.A., Oakey, J.E., Swithenbank, J., Sharifi, V., 2014. Quantification of trace element emissions from low-carbon emission energy sources: (I) Ca-looping cycle for post-

combustion CO_2 capture and (II) fixed bed, air blown down-draft gasifier. Chemical Engineering Science, 107, pp. 13-29.

[74] A. M. Cotton, 2013. Engineering scale-up and environmental effects of the calcium looping cycle for post-combustion CO_2 capture, PhD thesis, Cranfield University, Cranfield, UK.

[75] IEA, 2009. Cement technology roadmap. IEA Publications, Paris, France.

[76] Imbabi, M.S., Carrigan, C. and McKenna, S., 2012. Trends and developments in green cement and concrete technology. International Journal of Sustainable Built Environment, 1(2), pp. 194-216.

[77] Alsop, P.A., Chen, H. and Tseng, H., 2007. Cement plant operations handbook: for dry process plants. Tradeship.

[78] Dean, C.C., Dugwell, D. and Fennell, P.S., 2011. Investigation into potential synergy between power generation, cement manufacture and CO_2 abatement using the calcium looping cycle. Energy & Environmental Science, 4(6), pp. 2050-2053.

[79] Telesca, A., Calabrese, D., Marroccoli, M., Tomasulo, M., Valenti, G.L., Duelli, G. and Montagnaro, F., 2014. Spent limestone sorbent from calcium looping cycle as a raw material for the cement industry. Fuel, 118, pp. 202-205.

3 CALCIUM LOOPING SORBENTS FOR CO_2 CAPTURE

María Erans, Vasilije Manovic and Edward J Anthony

Combustion and CCS Centre, Cranfield University, Bedford, Bedfordshire, United Kingdom

Submitted 10th May 2016, Accepted 16th July 2016

Published in Applied Energy, 2016, 180, 722-742

DOI: 10.1016/j.apenergy.2016.07.074

Statement of contributions of joint authorship

María Erans conducted the literature review and wrote this manuscript. Vasilije Manovic and Edward J Anthony proof-read and critically commented on the manuscript before its submission to Applied Energy.

Abstract

Calcium looping (CaL) is a promising technology for the decarbonation of power generation and carbon-intensive (cement, lime and steel) industries. Although CaL has been extensively researched, some issues need to be addressed before deployment of this technology at commercial scale. One of the important challenges for CaL is decay of sorbent reactivity during capture/regeneration cycles. Numerous techniques have been explored to enhance natural sorbent performance, to create new synthetic sorbents, and to re-activate and re-use deactivated material. This review provides a critical analysis of natural and synthetic sorbents developed for use in CaL. Special attention is given to the suitability of modified materials for utilisation in fluidised-bed systems. Namely, besides requirements for a practical adsorption capacity, a mechanically strong material, resistant to attrition, is required for the fluidised bed CaL operating conditions. However, the main advantage of CaL is that it employs a widely available and inexpensive sorbent. Hence, a compromise must be made between improving the sorbent performance and increasing its cost, which means a relatively practical, scalable, and inexpensive method to enhance

sorbent performance, should be found. This is often neglected when developing new materials focusing only on very high adsorption capacity.

Keywords: CO_2 capture; Calcium looping; Sorbent; Limestone; Synthetic sorbent; Sorbent modification method

Highlights:

• The extensive literature on Ca looping sorbents and their properties has been reviewed.

• Currently, there is a lack of experiments on doped sorbents in realistic systems.

• Most complex methods of sorbent modification appear to be prohibitively expensive for CCS applications.

• A major challenge of all sorbent modification processes is their scalability.

3.1 Introduction

The CO_2 concentration in the atmosphere has risen from 280 ppmv in 1750 to 400 ppmv in 2015 which is the highest level in the past 650,000 years [1]. According to the Intergovernmental Panel on Climate Change (IPCC) [2] and [3], this increase in CO_2 concentration is the main cause for an increase of 0.74 ± 0.18 °C in global temperature; it is also a probable reason for a rise of 0.1 to 0.2 m in sea level over the past century. The energy market still depends heavily on relatively cheap fossil fuels, which, added to the expected increase of 37% in energy demand by 2040 [4], means that fossil fuels will continue to be used during this century and possibly beyond. Hence, it is necessary to find mitigation options for CO_2 emissions.

Carbon capture and storage (CCS) is a potential mitigation option, which consists of capturing the carbon dioxide present in a stream in order to transport it and store it in a safe location [5] and [6]. A diverse range of CCS technologies has been investigated and a number of demonstration projects have been started or planned [7], although currently the dominant CO_2 mitigation strategies are pre-combustion, oxy-fuel and post-combustion techniques [8].

The CCS technology that is closest to the market is post-combustion amine scrubbing, with solvents such as monoethanolamine (MEA) [9]. There are some problems associated with this process such as solvent degradation, cost, and the corrosive nature of the solvent [10-16]. Another technology that is close to the market is oxy-fuel combustion, where fuel is burned in a mixture of O_2 and recycled CO_2, but the drawback of this technology is the energy required to run the air separation unit (ASU) to produce the oxygen needed for combustion [17]. However, significantly the first large-scale deployment of CCS, an amine-based technology started its operation in October 2014 at SaskPower's Boundary Dam Power Station (Canada) with a lignite-fired boiler [18]. Nonetheless, the relatively slow deployment of CCS technologies, is mainly caused by their associated economic penalties [19, 20], and the lack of supportive government policies [21, 22]. Therefore, these are drivers that have triggered the development of alternative CCS technologies such as second- and

third-generation carbon capture technologies aiming at lower economic and efficiency penalties.

One viable solution arising from this development is calcium looping (CaL), which is based on the reversible carbonation of lime. This second-generation technology [23] is attracting a vast amount of R&D resources with numerous demonstration projects throughout the world [24].

This work reviews the CaL process in general, taking into account its challenges, mainly sorbent reactivity decay and attrition in fluidised bed (FB) reactors. Then, it examines current research in the area of sorbent testing and modification starting with natural sorbents (limestone) and naturally-derived sorbents (dolomite among others) and discusses their properties over extended numbers of cycles. As the reactivity of these sorbents suffers from a drastic decrease while in continuous operation, enhancement options, such as hydration, are also discussed along with more complex methods that have been proposed to produce sintering- and attrition-resistant sorbents with an emphasis on preparation methods. Finally, reactivation of “spent” sorbent and its re-use are also discussed. The main objective of this study is to provide recommendations for economically viable sorbent modifications and treatments of different types of sorbents and their suitability for utilisation in commercial-scale equipment.

3.2 Process description

CaL was first proposed as a post-combustion carbon capture technology by Shimizu et al. in 1999 [25]. The schematic diagram of CaL application for post-combustion CO_2 capture is shown in Figure 3-1.

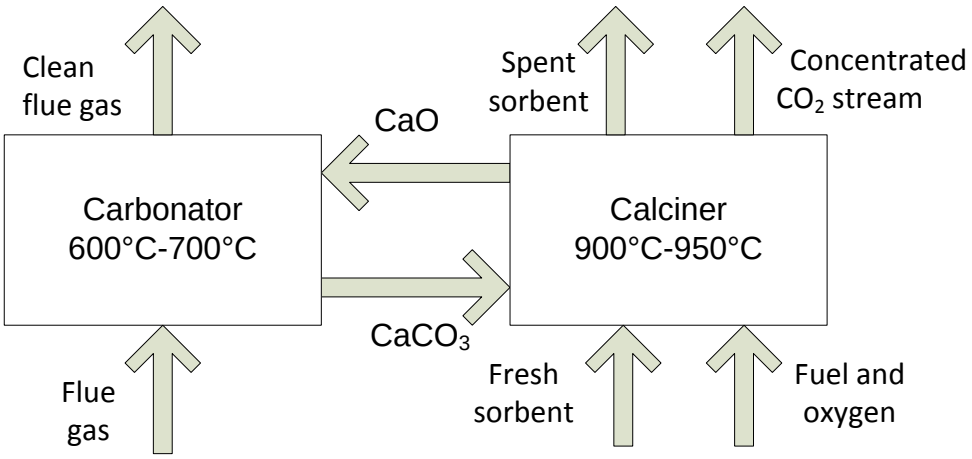

Figure 3-1: Schematic diagram of calcium looping process for post-combustion CO_2 capture

In this process the solid sorbent cycles between two interconnected FBs. The flue gas enters the carbonator where a CaO-based material reacts with the CO_2 present, resulting in formation of $CaCO_3$ (saturated sorbent). This carbonation reaction occurs at a fairly rapid rate between 580 and 700 °C [25-27], which is suitable for practical operation, given a trade-off between reaction kinetics and the equilibrium driving forces [28, 29]. This reaction has two stages: (i) an initial, relatively fast stage, controlled by the chemical reaction kinetics, followed by (ii) a much slower stage, which is limited by the diffusion of the reactants through the formed $CaCO_3$ product layer, which is postulated to have reached a critical level when it attains a thickness of around 50 nm [30]. The two-stage mechanism for the carbonation reaction is shown in Figure 3-2, which gives the sorbent conversion as a function of reaction time obtained in a thermogravimetric analyser (TGA) [31]. Where X_N is the CaO molar conversion in each cycle, X_K is the molar conversion under fast reaction regime and X_D the molar conversion under diffusion-controlled regime.

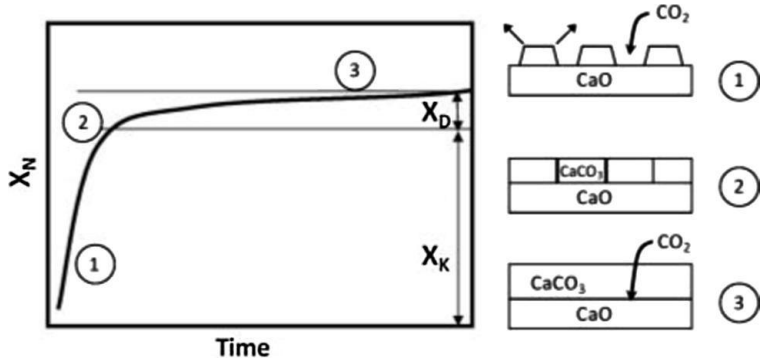

Figure 3-2: Schematic illustration of sorbent conversion during carbonation [31]

It is important to define the “maximum” carbonation conversion of any sorbent as the moles of CO_2 that react in the period of fast reaction, rather than compared to the stoichiometry of complete CaO to $CaCO_3$ conversion [32]. Subsequently, the CO_2-saturated sorbent is transferred to the calciner, in which sorbent is regenerated at high temperatures and the concentrated CO_2 stream is produced. This calcination reaction is typically performed at temperatures above 900 °C due to the chemical equilibrium and (practical) reaction rate requirements, while maintaining sintering at a reasonably low level [33]. Since calcination is an endothermic reaction, heat needs to be supplied, which is typically achieved by burning a fuel in this chamber using pure O_2 in order to obtain a highly concentrated CO_2 stream at the end of the process [25, 34]. Finally, the regenerated sorbent is transferred to the carbonator to start the cycle again.

This technology has various advantages when compared to other carbon capture options such as amine scrubbing:

- Relatively low efficiency penalty, from 7% to 8% [35, 36] with the capture step responsible only for 2–3% primarily due to oxygen requirement [37].
- Use of limestone, a widely available, inexpensive [38] and environmentally benign sorbent [20].
- The cost of CO_2 avoided has been calculated to be \$29–50/t-CO_2, which accounts for around 50% less than for amine scrubbing [39-43].

One of the major challenges of this technology is the relatively fast sorbent reactivity decay resulting in a residual activity of 8–10% after about 20 or 30

cycles, due to sintering during calcination [32]. This phenomenon has attracted research aimed at improving the performance of natural sorbents, and synthesising sorbents with enhanced properties.

3.3 Reactivity decay over cycles

It is common knowledge that the decay in activity of CaO-based sorbents is inevitable. The main causes for this decrease of reactivity are sintering and attrition. These phenomena are described in depth in this section with the mechanisms and theories that explain particle behaviour during cycling.

3.3.1 Sintering

Sintering is the change in pore shape, pore shrinkage and grain growth that particles of CaO endure while heating. This phenomenon increases at higher partial pressures of steam and CO_2, and also with impurities [44]. It has been discovered that the sintering that contributes to the reactivity decay occurs mainly during the calcination of such particles [45]. However, some of the decay is connected to closure of small pores upon carbonation that do not reopen subsequently [46]. The deactivation rate escalates when increasing temperature in the calcination step and lower reactivity is associated with higher temperatures [47].

There have been several studies that have proven the bimodal pore size distribution created upon calcination [30, 45]. During calcination, small pores are formed due to the CO_2 release; however, larger pores are not only present in the initial material but are also formed caused by sintering, which driven by the minimization of surface energy, changes smaller pores to larger pores.

It has also been noted in several studies [48-50] that increasing carbonation time results in a sorbent with higher reactivity towards CO_2. The effect of this longer carbonation has been investigated by Álvarez and Abanades [30]. They suggested that although the larger pores were accessible through pores with smaller openings, they were closed at the surface. Presumably, if the slow carbonation solid diffusion reaction occurs for longer periods, the solid bulk enlarges in order to fill the larger pores in a more substantial way. This leads to

a higher CaO reactivity in the next calcination. On the other hand, this longer carbonation step may be impractical when talking about industrial operation.

A schematic way of understanding this sintering phenomenon is shown in Figure 3-3 [51]. In this diagram the course of several calcination/carbonation cycles is shown. In the first calcination, a highly porous and reactive CaO is produced. The first carbonation is not complete due to pore blocking; some of these pores do not open in the following calcination. This pattern is repeated until a substantially less reactive sorbent is recovered after a high number of cycles.

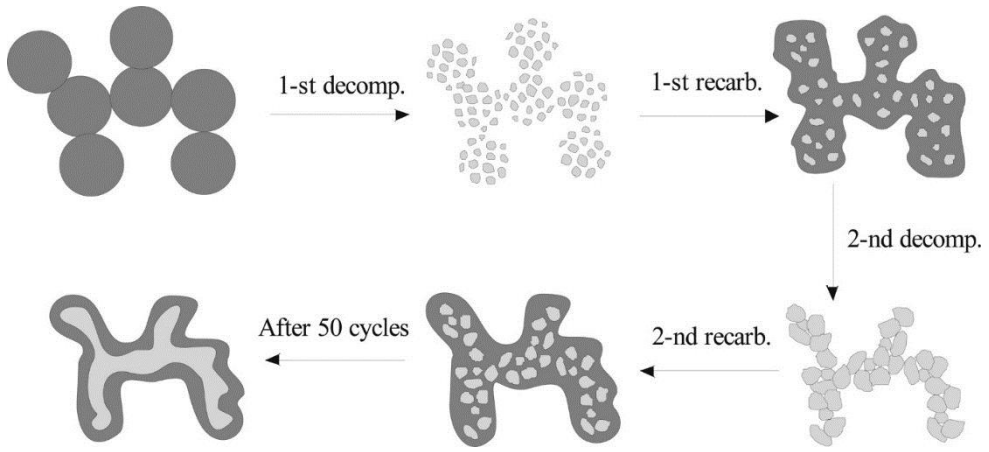

Figure 3-3: Transformation of the lime-based sorbent structure during carbonation/calcination ($CaCO_3$ phase is dark grey, CaO phase is light grey) [51]

3.3.2 Attrition

The mechanisms for fragmentation/attrition are as follows: primary fragmentation, takes place when the sorbent is introduced into the reactor. It is mainly caused by thermal stresses and overpressures due to CO_2 release as part of the calcination reaction. Secondary fragmentation, which is caused by mechanical stresses from impacts between the particle and the reactor; and attrition by abrasion which is also due to mechanical stresses but generates finer fragments than secondary fragmentation [52].

Interestingly, it is believed that the attrition rate is higher during the first cycles and then subsequently decreases [53, 54]. Nonetheless, attrition becomes a more significant problem when dealing with pilot-scale FBs. In one study, 30%

of the initial limestone was recovered in the cyclone after 3 cycles (<0.1 mm) and 60% after 25 cycles, whilst the initial particle size was 0.4–0.8 mm [29].

Attrition is highly dependent on the experimental set-up. Namely, it depends on the gas velocities, size and configuration of the plant. This phenomenon becomes even more important when exploring new sorbents. In the authors' view, there should be a shift in research from only studying reactivity decay caused by sintering to a complete analysis of any new synthetic material including attrition investigations.

3.4 Natural material-based sorbent

The use of natural materials ground to a particle size distribution, suitable for FB operation, is the easiest and cheapest way of obtaining a solid CO_2 carrier due to its availability and possible re-use for the cement industry [55]. Reactivity decay is caused mainly by sintering, which decreases the specific surface area with increasing cycle number resulting in a loss of capacity. Other causes of deactivation include poisoning of the material through sulphation/sulphidation reactions and ash fouling [20, 56]. This can be reduced by boosting the Ca to C ratio in the carbonator or increasing the purge flow of spent sorbent in order to get more fresh sorbent into the reactor [57].

3.4.1 Limestone

The reversible carbonation of lime is shown in the following reaction:

$$CaO + CO_2 \leftrightarrow CaCO_3 \qquad \Delta H_{25°C} = -178.2\ kJ/mol \qquad \textbf{(3-1)}$$

Most of the investigations performed on natural limestone reactivity for CO_2 capture in calcination/carbonation cycles were executed using either a TGA, or less frequently a bubbling FB [50, 58], where the sorbent stays in the same reactor as opposed to being transported between two reactors. Although these tests are suitable for sorbent screening purposes, the results are less useful for numerous reasons; for example, they neglect particle attrition during solid circulation as well as phenomena such as reactions with sulphur or ash components.

In general, studies on the reactivity of natural limestone show qualitatively the same decay over a number of cycles. Grasa and Abanades [59] tested different types of limestone from different locations (Blanca from Spain, Cadomin and Havelock from Canada, Piasek from Poland and Gotland from Sweden) and a dolomite (approx. 50% MgCO3) using a TGA. The results presented in Figure 3-4 show that the decay in carbonation capacity after a number of cycles is a common feature in all types of limestone and for all process conditions. Further investigations with TGAs showed that residual limestone conversion converges to a value of X_r = 0.07–0.08 [34, 60, 61].

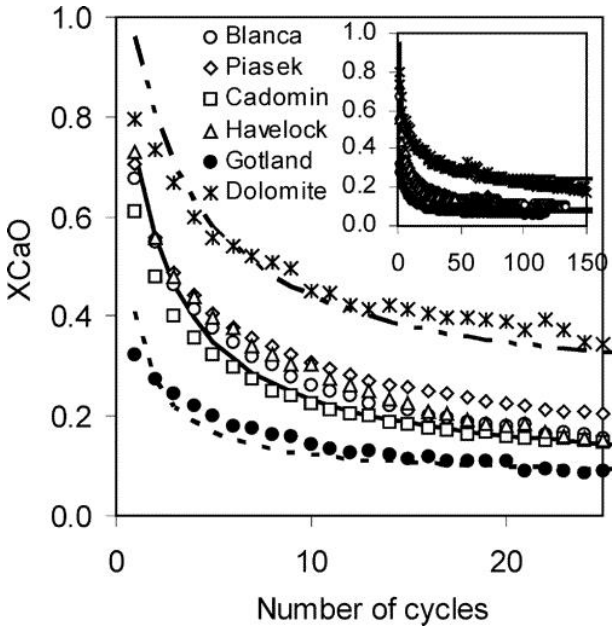

Figure 3-4: Conversion vs. number of cycles for experiments carried out with different types of limestone. Particle size 0.4–0.6 mm. Calcination temperature 850 °C, 10 min; carbonation temperature 650 °C, 10 min; pCO_2 of 0.01 MPa [59]

The attrition mechanisms of limestone under FB CO_2 capture conditions are complex [62]. Chen et al. [63] explored the most important factors that contribute to attrition in the carbonation reaction and concluded that they are (from most to least important): carbonation temperature; carbonator superficial gas velocity; exposure time; and pressure. For calcination, the key attrition parameter is temperature, with attrition rate increasing with higher temperatures. It was also noted that CO_2 release in this reaction had a more important role than thermal stress. Jia et al. [58] studied attrition in a small pilot-

scale circulating FB reactor and concluded that even with the limited number of limestone samples tested the results varied considerably with the type of limestone used. Another important finding was that elutriation of fines is more pronounced during the first few carbonation/calcination cycles and then decreases over cycles [52].

Arguably, the first demonstration of CO_2 capture in a FB reactor using limestone-derived sorbent at the pilot plant scale was performed by Lu et al. [29] using a 75 kW_{th} dual FB reactor. The authors found that the capture efficiency dropped from 90% in the first cycle to 72% after 25 cycles, which they attributed to sintering. Figure 3-5 shows how the micro-porosity of the sample decreased while the macro-porosity increased when the sorbent was subjected to capture/regeneration cycles. As a result of attrition, 50% of the original sorbent was recovered in the cyclones as fines. Finally, the authors concluded that attrition, sulphation and process optimisation needed further investigation in order to understand their influence on the process. Larger and more realistic pilot plant tests have been performed subsequently; these experiments include 1800 h in the 1.7 MW_{th} unit at CSIC (Spain) [64] with 170 h of stable operation and CO_2 capture close to the equilibrium at a given temperature [65]. Similarly, in Darmstadt University of Technology a 1 MWth plant ran during different testing campaigns demonstrating constant CO_2 capture in the carbonator of approximately 85% when maintaining 660 °C in the carbonator [66]. In IFK (Stuttgart), a 200 kW_{th} plant has run for over 600 h with a capture level above 90% [67].

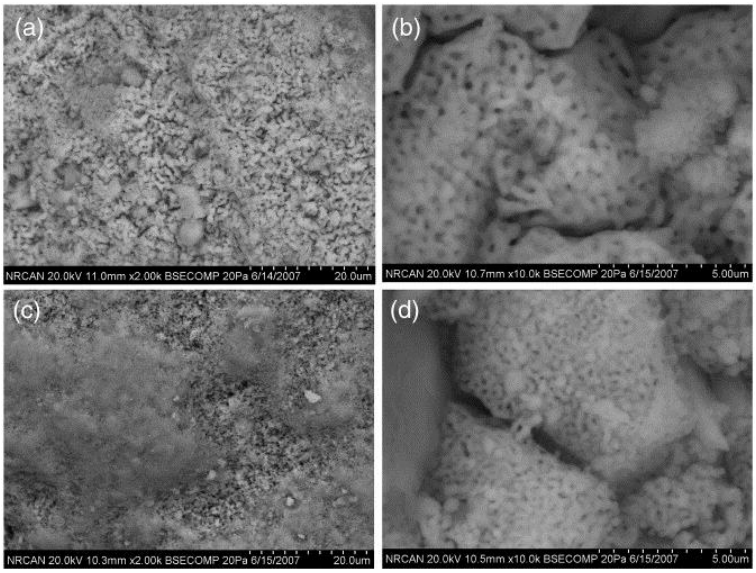

Figure 3-5: SEM of surface area of samples from carbonator: (a and b) after 3 cycles and (c and d) after 25 cycles [29]

Manovic and Anthony [68] performed a parametric study of CO_2 capture using limestone-based sorbents. The parameters included sorbent particle size, impurities, limestone type, temperature, CO_2 concentration, carbonation/calcination duration and heating rate. It was found that increasing the carbonation temperatures had a negative outcome on long-term sorbent reactivity. The effect of particle size on CO_2 carrying capacity was negligible and the differences encountered were likely due to differences in the content of impurities in different particle size samples. It was also discovered that prolonged carbonation time has a negative impact on sorbent reactivity accelerating its decay. Manovic et al. [69] carried out further investigations on the effect of calcination conditions. This work concluded that high temperatures and CO_2 partial pressures that would be encountered in real systems had a negative effect on the sorbent carrying capacity, which is due to the change in the particle morphology caused by sintering.

3.4.2 Dolomite

Dolomite ($CaMg(CO_3)_2$), which contains about 20% MgO and 30% CaO [70], is another naturally occurring material that can be used as a sorbent for CaL technology, although it is less common than limestone. MgO does not undergo

carbonation under typical CaL conditions [71] and, therefore, the stoichiometric capture capacity of calcined dolomite is just 0.46 compared to 0.79 for lime.

Although dolomite shows a lower initial CO_2 uptake, it exhibits a higher residual activity (after 20–30 cycles). The reasons for this are that the porosity of the sorbent is preserved by the unreacted MgO and less sintering occurs due to its higher melting point. Valverde, Sanchez-Jimenez and Perez-Maqueda [72] have shown this better performance of dolomite in a TGA under realistic sorbent regeneration conditions (70% vol CO_2 and 950 °C).

Itskos et al. [73] performed a study in a TGA and concluded that the effect of sulphation on CO_2 capture activity for dolomite was not significantly different than for limestone.

3.4.3 Other natural materials

Deshpande and Yuh [74] studied the use of animal products as a CaL sorbent. They tested five different materials: egg shells (chicken, duck and ostrich) and sea shells (oyster and clam). The samples were treated with acetic acid and crushed. The study concluded that using these materials in CaL cycles is cost-effective, but it is unlikely that these residues can be produced in the quantities needed for the commercial deployment of CaL. Moreover, they exhibited higher capacity after water hydration techniques were employed for regeneration of spent sorbent. The results for the initial CO_2 capture activity can be seen in Table 3-1.

Table 3-1: Waste animal initial CO_2 capture capacity (%) [75]

Sorbent source (type of shell)	Initial CO_2 capture capacity (wt %)
Chicken egg	60
Ostrich egg	45
Duck egg	61
Oyster shell	34
Clam shell	21

Sacia et al. [75] investigated pre-treatments using solutions of 1 and 2 M acetic acid and regeneration using pure water, 0.5 M, 2 M, 5 M, 50%, and glacial acetic acid, with regenerations performed every 5 cycles. The natural material used in this work was oyster shells. The authors concluded that the pre-treated samples behaved better in a TGA (from around 30% conversion in the 5th cycle in untreated shells to 50% conversion in the best case, 1 M acetic acid for 15 min). Moreover, the regeneration of the natural material was also successful, especially with 2 M acetic acid. It was also suggested that acetic acid regenerations tend to renew the initial porosity of the sorbent.

Chicken eggshells and mussel shells have been compared to limestone in a study performed by Ives et al. [76]. It was found that the CO_2 uptake of the eggshells and mussel shells was very similar to that of the limestone investigated (Purbeck) over 50 cycles. Therefore, there was no clear advantage of using these natural sorbents rather than limestone from the reactivity point of view. Shan et al. [77] have also examined eggshells mixed with bauxite tailings (BT) to see how the latter impacted the ability to capture CO_2. They found that the addition of BT was beneficial to the process with a carbonation conversion of 55% after 40 cycles.

There is a clear advantage in the use of limestone and other natural materials, namely their low price, availability and direct use with minimal processing. However, one of the most important aspects and justifications for limestone use is that it is a highly researched material for SO_2 and CO_2 capture. On the other hand, the decay in reactivity during the capture cycles and attrition associated with limestones require make up of fresh material, which results in reduction in the efficiency of the process and economic penalties. Also, the use of waste materials as a natural source of Ca-based sorbents (marine shells and other animal-derived materials) provides a good example of re-use of those materials which otherwise would require disposal and be subject to related costs. However, the availability and performance of these sorbents in cyclic FB operation need to be further investigated, especially taking into account that the particles are of irregular shape, which enhances their attrition.

3.5 Enhancement of natural sorbents

Although limestone is the cheapest material for the CaL process, its challenges with reactivity decay and attrition have led researchers to modify it to improve its properties whilst maintaining a low cost. These techniques represent a midpoint between the use of natural materials and utilisation of complex techniques for synthesis of sorbents and such solutions are expected to be generally less costly than the production of new sorbents.

3.5.1 Calcium hydroxide

Calcium hydroxide can be used as a sorbent for the CaL process. However, this material is extremely fragile. Wu et al. [78] performed a study in which they showed that calcium hydroxide has higher sorption capacity, with the maximum CO_2 uptake at 650 °C. They showed that the reason for the improved properties of the sorbent is the formation of cracks during the hydration of the material, which results in higher pore surface area and volume. This increased the conversion of CaO by 52% by the 20^{th} cycle [79].

Although the morphological properties of calcium hydroxide-derived lime are more favourable than that of calcium carbonate-derived CaO, the hydrated material is typically soft and not suitable for direct utilisation in FB reactors. Therefore, some type of granulation, extrusion or other treatment would be required, before its final use under realistic CaL conditions. This step would increase the final price of the sorbent.

3.5.2 Doping

Researchers have also attempted to decrease the reactivity decay over the cycles through doping of the material to avoid or postpone the sintering.

Salvador et al. [50] investigated the addition of sodium chloride (NaCl) and sodium carbonate (Na_2CO_3) using wet impregnation. The addition of NaCl improved the capture capacity, maintaining it at 40% of overall capacity over 13 cycles due to positive changes in the pore structure. However, the addition of Na_2CO_3 had no apparent effect on capture capacity. Both of these tests were

performed using a TGA. When the doped sorbents were tested in FB conditions, the sorption capacity of both decreased as a result of pore blocking. These dopants were also studied using a wet impregnation technique by Fennell et al. [46], which consists of pouring a solution of known and very low molarity onto the sorbent. Then the mixture is stirred, sealed, decanted and dried. The samples were later tested in a small, hot FB with dilution by sand addition to reduce temperature rises due to the exothermic carbonation reaction. It appears that doping with small quantities of Na_2CO_3 showed a small improvement in the carrying capacity. However, a higher dopant quantity in the solution (more than 0.1 M) had a detrimental effect and decreased the carrying capacity of the limestone sorbent [46].

Other tests with KCl and K_2CO_3 using wet impregnation were performed using two types of limestone (Havelock and Imeco) [80]. González et al. [80] concluded that doping with lower solution concentration (0.05 M) improved the performance of both types of limestone. They also suggested that doping with KCl reduced attrition of limestone due to the crystallisation of the dopant in cracks in the particles. Al-Jeboori et al. [81] performed experiments with other inorganic salts ($MgCl_2$, $CaCl_2$ and $Mg(NO_3)_2$) and the Grignard reagent (isopropyl-magnesium chloride) [82]. All of these dopants produced some improvement as shown in Figure 3-6, which is in agreement with the results discussed above [46, 80]. In summary, samples doped with lower molarity solutions showed an increase and those with higher ones showed a reduction in the carrying capacity.

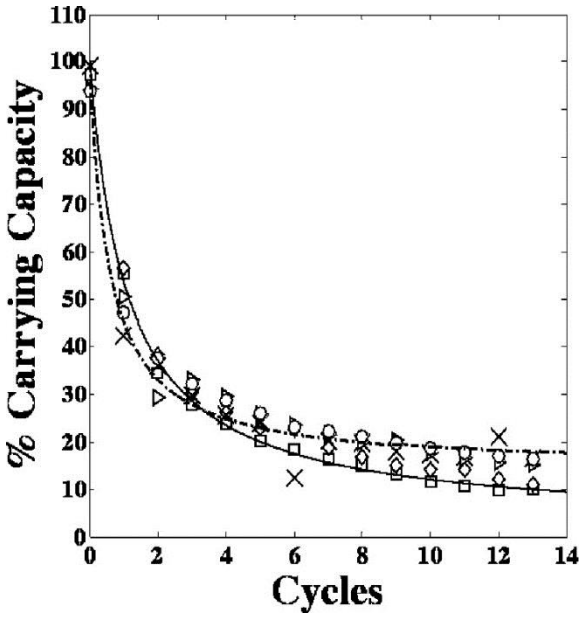

Figure 3-6: Carrying capacity (normalised) for Havelock limestone, plotted against the number of cycles: (—□—) un-doped, (--◇--) 0.159 mol% $Mg(NO_3)_2$, (--×--) 0.165 mol% $MgCl_2$, (▷) 0.138 mol% $CaCl_2$, (O) 0.15 mol% Grignard reagent [82]

Manganese salts ($Mn(NO_3)_2$ and $MnCO_3$) also improve the cyclic carbonation conversion. In a study using wet impregnation, tests in a fixed-bed reactor and a TGA showed a residual carbonation conversion of $Mn(NO_3)_2$- and $MnCO_3$-doped sorbents of 0.27 and 0.24, respectively, after 100 cycles. Sun et al. [83] also showed that the sorbent retained an improved pore structure, pore volume and pore size. $Mn(NO_3)_2$-doped $CaCO_3$ achieves the highest cyclic carbonation conversions when the Mn/Ca molar ratio is 1/100 and the optimum molar ratio of Mn/Ca for $MnCO_3$-doped $CaCO_3$ is 1.5/100.

Another suitable doping material is attapulgite ($Mg_5Si_8O_{20}(HO)_2(OH_2)_4 \cdot 4H_2O$). The microstructure of the modified particle was improved by the formation of Ca_2SiO_4, Al_2O_3 and $Ca_3Al_{10}O_{18}$; these compounds were distributed in the material, enhancing the resistance to sintering during multiple cycles [84]. In this work a technique of dry mixing followed by hydration was applied. The results showed that the hydration method exhibited 128% higher CO_2 capture performance than undoped limestone.

Manovic et al. [85] investigated doping of pellets (calcium oxide and calcium aluminate cement) with $CaBr_2$ in the presence of steam during carbonation and calcination; natural limestone was used as a material for comparison, and both sorbents were tested in a TGA. The findings showed improved performance for both pellets and limestone when doped with low quantities of bromide of 0.2 mol%. The most improved parameter was the conversion rate during the diffusion-controlled stage of carbonation. This type of dopant has been tested in other studies in conjunction with steam addition. Al-Jeboori et al. [81] and Gonzalez et al. [86] concluded that the effects of doping and steam addition were effectively additive, at least at the levels tested.

Other types of dopants such as HCl, HNO_3 and HI have been tested with the quantitative wet impregnation method, and all the halogen dopants exhibited an increase in carrying capacity with Havelock doped with HCl and HBr from 0.135 to 0.259 mol% and HNO_3 from 0.102 to 0.205 mol%, and Longcliffe doped with HCl and HBr from 0.102 to 0.189 mol% and HI from 0.15 to 0.245 mol% [81]. The carrying capacity of Havelock (Canadian) limestone treated with these reagents is shown in Figure 3-7.

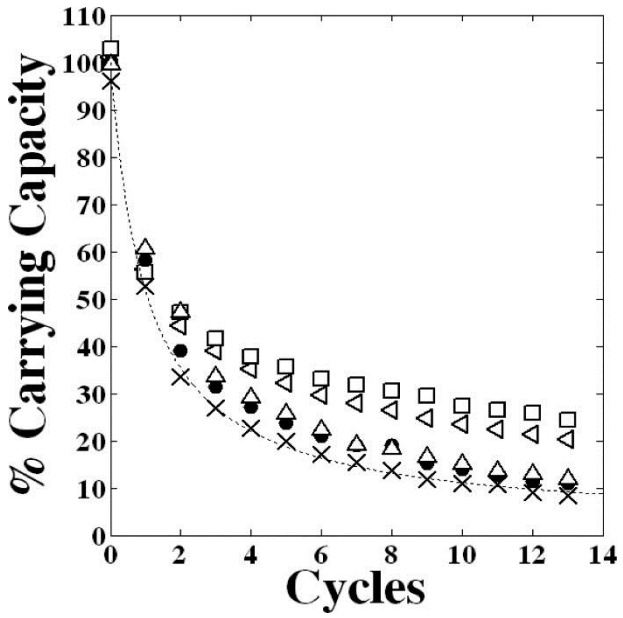

Figure 3-7: Carrying capacity (normalised) for Havelock limestone, plotted against the number of cycles: (×) undoped, (□) 0.167 mol% HBr, (sideways open triangle) 0.167 mol% HCl, (Δ) 0.164 mol% HNO_3, (●) 0.167 mol% HI [81]

These results encouraged research into the use of other group 1A elements in calcined limestone, such as Li, K, Rb and Cs. The capture performance of alkali metal-doped CaO has been linked to the electro-positivity of the material [87]. The material doped with 20% Cs for instance had higher sorption in the first cycle than the other materials.

Some metal-based dopants have been further investigated, such as γ-Al_2O_3, SiO_2 sands and MgO. Sun et al. [88] also examined other dopants including TiO_2 and ZrO_2. These materials were tested in a TGA and did not exhibit very promising results.

Doping has been used as an enhancement technique due to the positive effects that some dopants have on the pore structure, pore volume and pore size (see Table 3-2). While this approach is not excessively complex, the cost of the dopants must be taken into account when assessing their economic feasibility. Also, scale-up of the impregnation techniques is a challenge that has to be resolved before their use at pilot plant- or demonstration-scale due to the large amount of sorbent that would need treatment. One especially promising approach is doping with sea water, due to its availability and low cost. This path would make doping a highly promising enhancement technique.

Table 3-2: Summary table of doping

Dopant	Method	Main findings	References
NaCl and Na_2CO_3	Quantitative wet impregnation	NaCl improved the sorbent by 0.15 in relative CO_2 capture capacity ($gCO_2/g_{sorbent}$) when compared to limestone in TGA after 13 cycles; Na_2CO_3 had no apparent effect. Doping with lower molarity is beneficial	[50]
NaCl and Na_2CO_3	Wet impregnation	Na_2CO_3 in small quantities had a positive effect increasing the carrying capacity by 0.14 $gCO_2/g_{sorbent}$ after 20 cycles. Lower molarity beneficial	[46]
KCl and K_2CO_3	Wet impregnation	KCl improved attrition resistance and reactivity by 0.15 $gCO_2/g_{sorbent}$ after 15 cycles when compared to limestone. Lower molarity beneficial	[80]
$MgCl_2$, $CaCl_2$ and $Mg(NO_3)_2$	Wet impregnation	All dopants showed an improvement of around 10% after 14 cycles in carrying capacity when lower	[82]

		molarity solutions were used	
$Mn(NO_3)_2$ and $MnCO_3$	Wet impregnation	Observed an optimal Mn to Ca ratio, improved capture capacity by 69% when compared to undoped limestone after 100 cycles	[83]
Attapulgite	Dry mixing and hydration	Hydration showed much better performance (128% increase when compared to limestone after 20 cycles) than natural limestone	[84]
$CaBr_2$	Quantitative wet impregnation	Steam addition and doping have additive positive effects on the sorbent going from 22 $gCO_2/100g_{sorbent}$ to 31 $gCO_2/100g_{sorbent}$ after 11 cycles	[81,85,86]
Halogen dopants	Quantitative wet impregnation	All of them showed improvement in capacity, especially 0.167% mol HBr which went from 10% carrying capacity of undoped limestone to 25% in the doped sorbent after 14 cycles	[81]
Group 1A elements	Wet impregnation	The performance has been linked to electropositivity with a sorption capacity of 50 wt%CO_2/wt%sorbent after 35 min	[87]
Other metal-based materials	Wet impregnation	Al_2O_3 showed promising results from 0.2 CaO conversion to $CaCO_3$ of 0.4 when a ratio of 1:1 CaO to Al_2O_3 after 15 cycles	[88]

3.5.3 Thermal pre-treatment

There have been several studies that demonstrated that thermal pre-treatment was a valid method to improve the conversion of CaO in long series of cycles [89-91]. A theory to explain this behaviour was proposed by Lysikov et al. [51]. This was based on the formation of a skeleton of interconnected CaO caused by repeated carbonation/calcination cycles; the skeleton acts as an outer reactive CaO layer and stabilises the sorption capacity. Manovic and Anthony [89] followed this work testing samples in a TGA up to very high temperatures (up to 1300 °C) under a nitrogen atmosphere. These tests demonstrated that particles were highly sintered and carbonation occurred only on the surface of the solid particle. The model suggests that the pre-treatment results in the formation of an internal skeleton, which protects the integrity of the particle. When sorbents are preheated, after the $CaCO_3$ decomposes, ion diffusion continues, stabilises the skeleton, but the porous structure in the hard skeleton

is able to maintain significant carbonation. This model is depicted schematically in Figure 3-8.

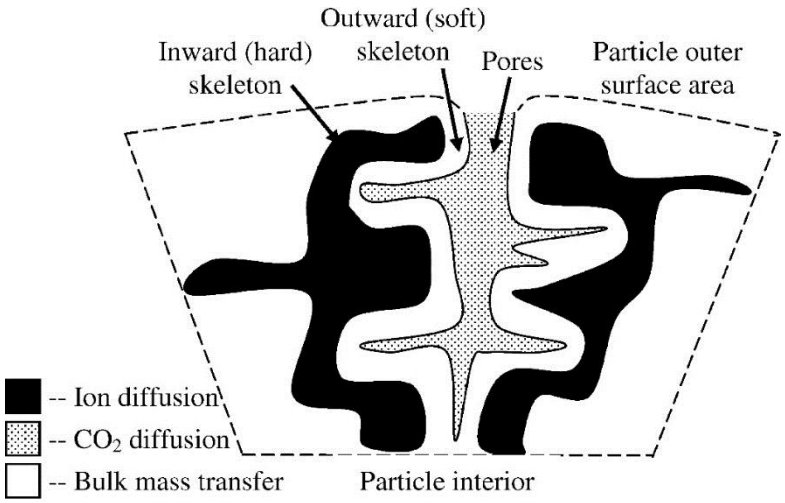

Figure 3-8: Schematic representation of proposed pore-skeleton model [89]

In the early cycles only the less reactive hard skeleton exists, but conversion increases as the soft skeleton develops. These studies showed that even if the pre-treated limestone exhibited lower initial sorption capacity, this capacity is augmented over many cycles owing to the softening of the hard skeleton. A drawback of this enhancement technique is that although the reactivity was increased, attrition of the particles rose substantially [92].

Thermal pre-treatment has not been successful in all types of limestone [91] and it is believed that it only works on certain varieties of the natural material. It is probable that different types of limestone require different conditions for the pre-treatment due to differences in impurity composition and internal structure [60].

With regard to synthetic materials, a study of precipitated calcium carbonate (PCC) in a slurry bubbling FB used an extra thermal pre-treatment stage for these particles [93].

There are clear advantages to this treatment; it is straightforward and inexpensive (see Table 3-3). However, it should be noted that it would require extra energy to heat up the amount of material needed before its final use. This

can result in a decrease of the power output of the power plant. Therefore, any heat integration technique used would require additional heat exchange systems.

Table 3-3: Summary table for thermal pre-treatment

Type of material	Temperature	Main findings	Reference
Kelly Rock, Cadomin, Graymont and Havelock limestone	1100°C	A model with skeleton changes is proposed to explain the reactivation of particles after pre-treatment in long series of cycles, the improvement was of 25% in carbonation conversion of untreated Kelly rock to the 24 h sample treated to 900°C after 30 cycles	[89]
Microna 3 (US limestone) and coarser limestone	1100°C	Material heated for 5 h was found to be more stable than that heated for 2 h with an increase of capacity ($mmolCO_2/g_{sorbent}$) from 7 to 7.4, which is more stable than the material calcined at 900°C after 80 cycles	[90]
La Blanca and Kelly Rock	1000-1200°C	No improvement in La Blanca possibly due to composition (high purity). Not all limestone types are suitable for thermal pre-treatment	[91]
Monodisperse carbonate particles (precipitated $CaCO_3$ with calcium nitrate and ammonium carbonate)	1100°C and 1300°C	Samples treated at 1100°C are not strong enough to resist sintering under test conditions, but samples treated at 1300°C had a stable carrying capacity of 12% after 200 cycles	[51]
Limestone and dolomite	1000°C	Pre-treatment resulted in benefit in terms of reactivity (improved by about 0.05 in CaO utilization efficiency after 1000 cycles) properties but attrition resistance and mechanical properties were decreased substantially	[92]

3.5.4 Chemical treatment

This refers to the treatment of limestone with a chemical agent in order to achieve superior properties. However, the effect on the sorbent may ultimately produce physical changes in the sorbent morphology.

Limestone treated with acetic acid results in a modified sorbent with a high capture capacity [70, 94]. Natural limestone treated with a 50% acetic acid solution was tested in two FB reactors; the modified sorbent showed better sintering performance and also more favourable pore area and volume [70].

Ridha et al. [95] used calcium aluminate pellets as a base material; the treated synthetic material also exhibited improvement in performance. Treating dolomites with acetic acid has also been studied because of the high sintering resistance of the base material; industrial waste acid from acetate production has been proposed for this treatment in order to reduce costs [70].

Other materials besides acetic acid have been proposed as modifying agents for limestone. Ethanol-water solutions have been discussed, and were previously studied for enhancing SO_2 capture, which resulted in increased porosity of the treated material as a side benefit [96]. This particular treatment gave improved capture capacity, which was increased as the ethanol concentration was raised [97]. However, the high price of ethanol is a drawback for this treatment and further studies need to be done to assess the potential of the procedure.

Propionic acid has been studied for sorbent chemical pre-treatment. In a small molar ratio (4:1 CaO to propionic acid), the modified sorbent exhibited a capture capacity of 0.24 after 100 cycles, approximately four times the capacity of natural limestone [98].

Pyroligneous acid (PA) has also been investigated [99], and it produces a primary phase of calcium acetate hydrate in the modified sorbent. PA-treated limestone displayed a higher carbonation rate than natural limestone as well as improved porosity. Figure 3-9 shows the effect of such a treatment (here CD10 is the sample treated with PA and CD is the untreated limestone).

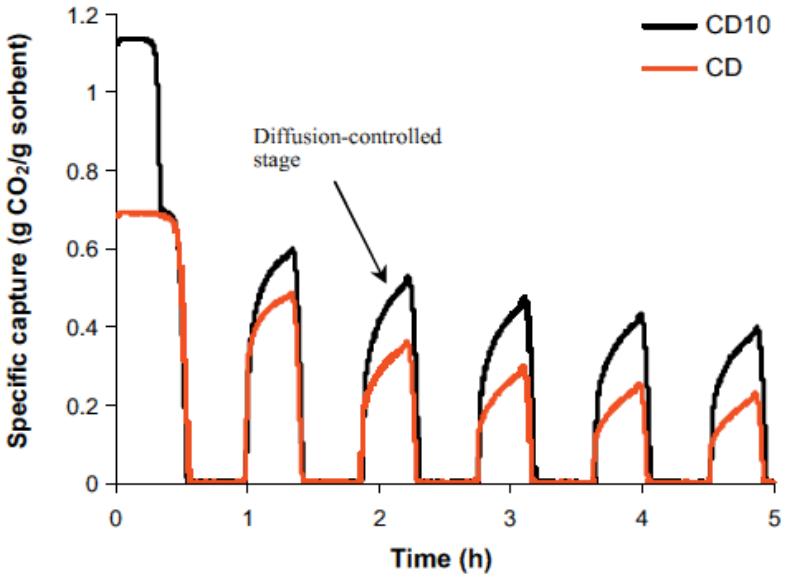

Figure 3-9: Carbon capture profile as a function of time. Calcination at 850 °C in N_2 for 5 min and carbonation at 650 °C in 15% CO_2 for 20 min [100]

Formic acid has also been studied, showing results in line with those exhibited above with higher capture capacity [100]. In addition, Ridha et al. [101] carried out a study of various acid treatments, which showed that the reactivity over cycles was enhanced albeit that the activity was found to decline in a similar manner to that for natural-based sorbents.

Although this treatment presents reactivity benefits such as increased pore volume and pore surface area, it has two drawbacks: the cost and availability of the acid; and the marginal increase in CO_2 uptake. It should also be noted that the final benefit of this procedure depends heavily on limestone type and origin, and the acid used (see Table 3-4). Moreover, this technique would increase the cost of the overall process significantly, which diverges from the main goal of trying to keep the capture costs low. It is expected that treated sorbent would react rapidly with SO_2, which would result in sorbent poisoning and would negate the higher reactivity achieved by this treatment.

Table 3-4: Summary of acid pre-treatment

Acid used for treatment	Material treated	Reactor	Conditions	Main findings	References
Acetic acid	Limestone	Twin fixed-bed reactor	Calcination 920-1100°C in 80% CO_2 20% O_2 (%vol) Carbonation 550-750°C in 15% CO_2	Treated sorbent had higher carbonation levels (0.4 carbonation conversion compared to less than 0.1 for untreated material after 20 cycles), better carbonation kinetics and delayed degradation	[94]
Acetic acid	Limestone	Twin fixed-bed reactor	Calcination 920-1100°C in 80% CO_2 20% O_2 (%vol) Carbonation 550-750°C in 15% CO_2	Treated sorbent had higher resistance to sintering due to smaller grain size and better pore structure with a conversion of the original limestone of 0.15 after 20 cycles and of the modified sorbent of 0.5 after 20 cycles	[70]
Acetic acid	Kaolin-derived $Al(OH)_3$ pellets	TGA	Calcination 920°C in pure CO_2 or 850°C in pure N_2 Carbonation 650-700°C in 15% CO_2	Pellets with acetified lime showed better performance than untreated pellets and limestone and also had higher porosity but poorer CO_2 capture in the presence of SO_2 (from 18% of the treated sample to 29.2 % of natural limestone after 5 cycles)	[95]
Acid waste from acetate production	Dolomite	Twin fixed-bed reactor	Calcination 850-1100°C in 80% CO_2 20% O_2 (%vol) Carbonation 550-750°C in 15% CO_2	Higher carbonation conversion than unmodified sorbent (from 0.2 to 0.45 after 20 cycles), improved sintering behaviour at	[70]

				high temperature, higher surface area	
Ethanol-water solution	Lime (Calcined limestone)	Twin fixed-bed reactor	Calcination 920°C in 80% CO_2 20% O_2 (%vol) Carbonation 550-750°C in 15% CO_2	Carbonation conversion of modified sorbent twice as high as lime from 0.25 in the untreated sample to 0.51 in the ethanol treated sample after 15 cycles. Higher ethanol concentration in the solution enhanced resistance to sintering	[97]
Propionic acid	Lime (Calcined limestone)	Dual fixed-bed reactor	Calcination 850-950°C in 100% N_2 (%vol) Carbonation 650-700°C in 15% CO_2	Modified limestone had faster carbonation rates and higher carbonation conversion (from 0.31 for the treated sample after 100 cycles to 0.08 for the untreated sample after 100 cycles) under realistic conditions. Modified sorbent was more resistant to sintering	[98]
PA	Limestone	TGA	Calcination 850-1000°C in 100% N_2 (%vol) Carbonation 600-700°C in 15% CO_2	Main component of the modified limestone was calcium acetate hydrate. Modified limestone had higher carbonation conversion (from 0.078 after 103 cycles for the untreated sample to 0.33 for the treated sample) and better pore structure	[99]
Formic acid	Lime (Calcined limestone)	TGA	Calcination 850°C in 100% N_2 (%vol) Carbonation 650°C in 15% CO_2	Sorbent morphology was insensitive to acid solution concentration. Liquid solution performed better , it captured 67.4 % more CO_2 than the natural material after 20 cycles	[100]

Organic acids (acetic, vinegar, formic and oxalic acid)	Limestone	TGA	Calcination 850°C in 100% N_2 (%vol) Carbonation 650°C in 15% CO_2	The best organic acid treatment was with oxalic acid with 0.25 $gCO_2/g_{sorbent}$ when compared to 0.13 $gCO_2/g_{sorbent}$ of limestone after 20 cycles, but all of these treated sorbents exhibited better CO_2 uptake than untreated limestone	[101]

3.6 Synthetic sorbents

In this section, new methods for producing synthetic sorbents will be discussed and their suitability for scale up, FB operation and cost will be assessed.

3.6.1 Sorbents from organic-acid precursors

Several complex procedures have been developed to synthesise new sorbents using acid treatments; these sorbents often have alumina (Al_2O_3) or other similar material as a support. The process comprises an active component integrated with an inert support diluted in an acid solution [102, 103].

Citric acid can be used for producing this type of material, for example. Aluminium nitrate is dissolved in citric acid and calcium carbonate is added. The mixture is then stirred, aged, dried, crushed, sieved, and heated in a four-step activation procedure to obtain the Ca-Al_2O_3 based sorbent [102]. The heating procedure appears to favour the formation of the porous structure in synthetic sorbents due to the mild conditions employed. The results of this study by Zhang et al. [102] revealed high sintering resistance due to the formation of $Ca_3Al_2O_6$ and also an increased capture capacity as shown in Figure 3-10.

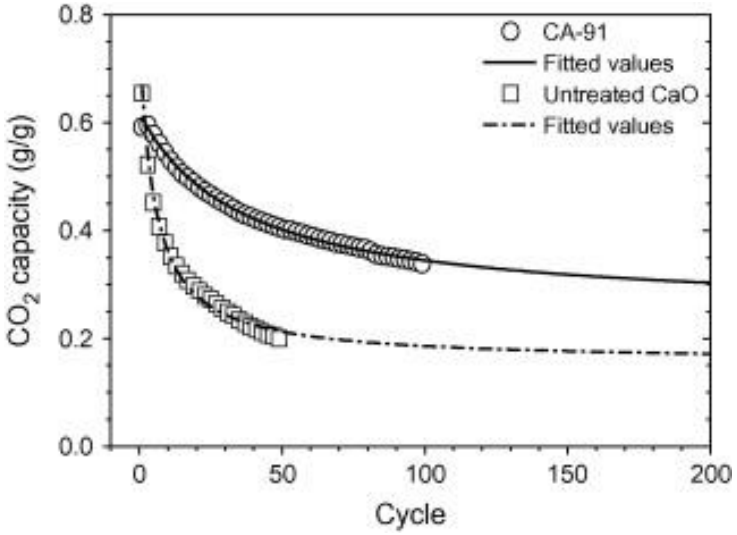

Figure 3-10: Evaluation of the long-term cycles of sample CA-91 (with 9% Al_2O_3) and untreated CaO in TGA (carbonation 650 °C for 30 min in 20% CO_2; calcination at 850 °C for 10 min in 20% CO_2) [102]

A modification of this method was proposed by Li et al. [103] using glycerol and water instead of citric acid in an attempt to reduce reagent costs. The resulting sorbent also exhibited better results than raw limestone. Li et al. [104] also developed a similar technique using carbide slag instead of limestone, which exhibited better CO_2 uptake than carbide slag without modification.

A less expensive route for obtaining an alumina support utilises kaolin [105]. In this study kaolin was calcined, the CaO was dispersed in water and ethanol and then metakaolin was added at different ratios. Finally, the mixture was acid-activated with hydrochloric acid, dried and calcined. The results exhibited higher carbonation in the first few cycles, but the sintering of the particles was also higher than for natural material.

SiO_2 can be used as a support in a similar way to the alumina-based sorbents. In such a study, 12 g of limestone was diluted in water and then added to a gelatinous solution containing 0.72 g of type A gelatine and 45 g of water. Then the mixture was added to an acidified sodium silicate solution, stirred, thermally treated and activated by calcination at 600 °C [106]. The resulting sorbent was then pelletised due to the initial unsuitability for use in FBs. These samples showed an increase in the carbonation conversion rate of 25% compared to

natural sorbents after 50 cycles; this was believed to be related to the creation of a mesoporous silica framework structure.

MgO has also been proposed as a support [107] showing slightly better performance than natural dolomite, indicating that molecular level mixing of CaO and MgO can be achieved with this methodology. Finally, in a recent study carried out by Zhao et al. [108], the effect of ZrO_2 as an additive to improve stability was studied. $Ca(OH)_2$ was mixed with hydrolysed zirconyl nitrate under vigorous stirring, then aged, dried and calcined. The most durable composition under severe calcination conditions (950 °C and 100% CO_2) was 30% $CaZrO_3$/70% CaO powder with a capture capacity of 0.36 g of CO_2/g sorbent in cycle 1, declining to 0.31 by cycle 30.

In some of these studies the sorbents were exposed to heat treatment, which caused an increase in the porosity of the resulting sorbent. Moreover, if additives or supports were included in the solution the stability of the synthetic particles was improved, which resulted in an increase of reactivity (see Table 3-5). However, further studies of these materials in FB environments need to be performed in order to investigate attrition resistance and to determine the performance of the particles in long series of cycles. Also, these techniques use heat for the particle production (at high or low temperature) of the material before calcination, which adds extra cost to the process due to the high energy consumption before sorbents enter the reactor. Moreover, the precursors needed are fairly expensive materials.

Table 3-5: Summary of synthetic sorbents derived from organic-acid precursors

Organic-acid precursor and support	Reactor	Conditions	Main findings	References
Citric acid with aluminium nitrate	TGA	Calcination 850°C in 100% N_2 (%vol) Carbonation 600°C in 20% CO_2	Activation of material with four-step heating (high energy consumption), better porous structure and higher sintering resistance than natural limestone (0.30 g/g after 200 cycles and 0.17 g/g after 200 for limestone)	[102]
Glycerol-water solution and aluminium nitrate	Dual fixed-bed reactor	Calcination 850-950°C in 100% N_2 or	The modified structure was $CaO/Ca_3Al_2O_6$; the CO_2 uptake capacity after 50 cycles was	[103]

hydrate (limestone)		CO_2 (%vol) Carbonation 650-725°C in 15% CO_2	six times higher (0.43 g/g) than natural limestone. The sintering resistance was higher than untreated sorbent	
Glycerol-water solution and aluminium nitrate hydrate (carbide slag)	TGA	Calcination 850°C in 100% N_2 (%vol) Carbonation 700°C in 15% CO_2	Synthetic sorbent had 2.5 times higher CO_2 capacity than carbide slag by the 20th cycle. The sintering of new sorbent was higher due to the mechanical support of $Ca_3Al_2O_6$	[104]
Ethanol-water solution and metakaolin	Twin fixed-bed	Calcination 850°C in 100% N_2 (%vol) Carbonation 700°C in 15% CO_2	Enhanced sintering of CaO and loss of sorption during cycles, higher conversion from 0.3 to 0.65 after 25 cycles	[105]
Gelatine-water with acidified sodium silicate then pelletised	TGA	Calcination 850°C in 100% N_2 (%vol) Carbonation 650°C in 100% CO_2	This method did not produce suitable particles for FB operation so they had to be pelletised. The carbonation conversion rate was 25% higher than limestone after 50 cycles	[106]
Aqueous solution of Ca and Mg acetates	TGA	Calcination 758°C in 100% He (%vol) Carbonation 758°C in 100% CO_2	Higher conversion than dolomite (53 wt% CO_2 after 50 cycles for the treated sample and 26 wt% CO_2 for dolomite) due to molecular mixing of CaO and MgO	[107]
Ethanol with ammonium hydroxide solution and ZrO nitrate	TGA	Calcination 800°C in air (mild conditions) 100% CO_2 (severe conditions) (%vol) Carbonation 650°C in 15% CO_2	The Zr-modified sorbents had more favourable performance. Under severe conditions the most durable composition was produced with a composition of 30% $CaZrO_3$/70% CaO	[108]

3.6.2 Sol-gel combustion synthesis

This method was first proposed by Luo et al. [109] for CaO-based sorbents and their work was extended in a subsequent study [110]. It included the following procedure: Predetermined quantities of $La(NO_3)_3.6H_2O$ or $Al(NO_3)_3.9H_2O$ and $Ca(NO_3).4H_2O$ were added to distilled water with a weight ratio of CaO to La_2O_3 of 80:20 and the mole ratio of water to metal ions of about 40:1. Citric acid was added, stirred and dried to form the sol, which was then left at ambient temperature for 18 h to form a gel. The gel was dried, and then calcined in a muffle furnace at 850 °C for 2 h. Sorbents generated in this study showed better performance than those containing mayenite ($Ca_{12}Al_{14}O_{33}$) in their structure due

to the effect of La_2O_3 in delaying sintering and absorbing extra CO_2 in the process. However, the problem of loss in reactivity was still present.

The process is illustrated in Figure 3-11.

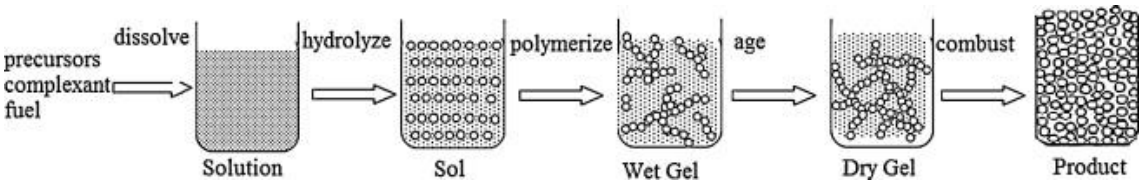

Figure 3-11: Manufacturing steps of the standard sol-gel combustion process [111]

Further studies were performed by Luo et al. [111] using a simplified method. The main differences between the methods were that the duration of the process steps was shortened, and the amount of water used was significantly less. They concluded that the standard sol-gel method produced sorbents with high CO_2 capture under mild calcination conditions (800 °C under 100% N_2) and could maintain a quite high reactivity of 0.20 gCO_2/gsorbent after 20 cycles, under more realistic calcination conditions, 950 °C in the presence of 100% CO_2. The porous microstructure was found to be favourable for the reaction and the sintering resistance was better than natural limestone.

Other materials have been prepared [112] following similar techniques containing primarily two phases: $Ca_9Al_6O_{18}$ and CaO, and Figure 3-12 provides SEM images comparing the pure CaO and the modified sorbent. It can be seen how the structure of the sol-gel material is less sintered when compared to the pure CaO.

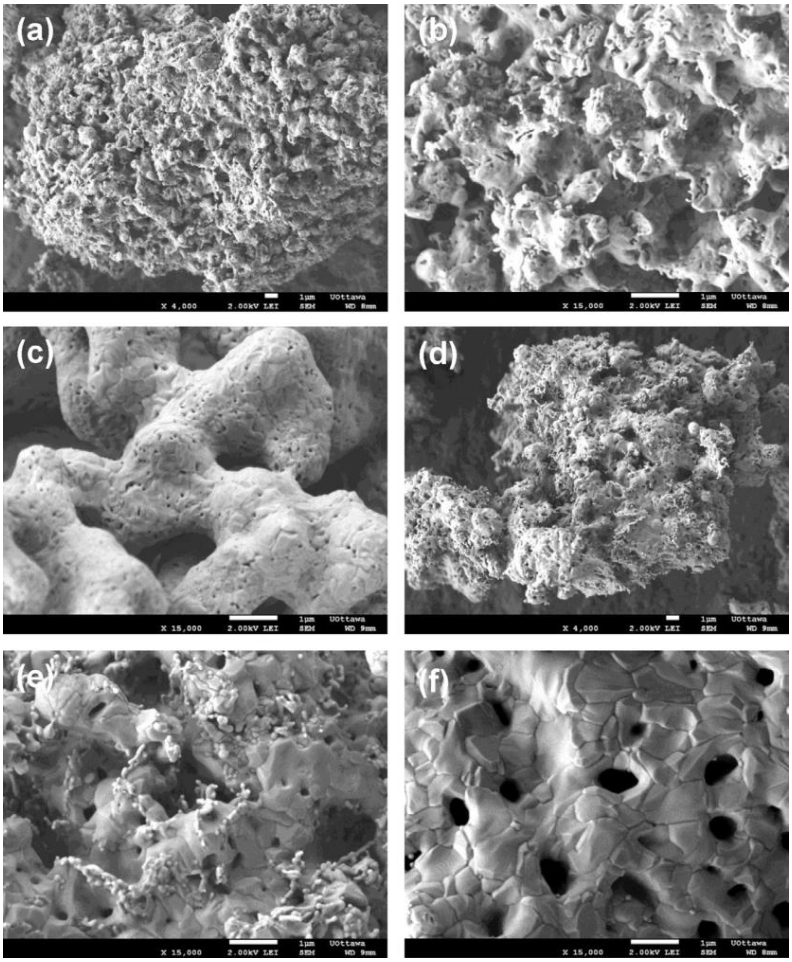

Figure 3-12: SEM images of CaO SG (sol gel) and pure CaO. (a) and (b) CaO SG mild conditions; (c) pure CaO mild conditions; (d) and (e) CaO SG under severe conditions; (f) pure CaO under severe condition [112]

The stability of this sorbent was attributed to the dispersion of $Ca_9Al_6O_{18}$ in the CaO matrix, which eventually controlled sintering.

Angeli et al. [113] used triethanolamine (TEA) as a complexing agent and $Ca(NO_3)\cdot 4H_2O$ and $Al(NO_3)_3.9H_2O$ as metal precursors. The formation of TEA-ion complexes ensured that the dispersion of Ca and Al formed a coral-like structure. The sorbent showed higher stability than previous sorbents [32]. Nonetheless, the high temperatures in calcination and the presence of CO_2 increased sintering.

Different supports, such as Zr, can be used in sol-gel techniques [114-116]. These showed a similar CO_2 uptake than the other particles synthesised with this procedure.

Although the porosity and stability were increased using this method in all the studies mentioned, a number of issues need to be addressed before such approaches can be applied on a large scale, including the attrition properties, the effect of gaseous impurities (SO_2), and the cost and lack of availability of large quantities of the modified sorbent.

Recently, there have been efforts to mitigate attrition of the particles by producing pellets using extrusion equipment in order to increase mechanical strength. In a recent study, the high reactivity of the sol-gel CaO powder was retained and its cyclic durability was higher than limestone and sol-gel powder [117]. However, this process needs further study with regard to attrition and durability of this sorbent in a FB environment. It is likely possible that these materials would need besides the costly preparation process including some type of granulation that would result in a cost rise and even a more complex processing procedure (see Table 3-6).

Table 3-6: Summary table for sol-gel combustion method

Support precursor	Reactor	Conditions	Main findings	References
$La(NO)_3$ or $Al(NO_3)_3$	Twin fixed-bed	Calcination 850°C in 100% N_2 (%vol) Carbonation 850°C in 100% CO_2	$La(NO)_3$ as an additive showed better performance (0.58 g $CO_2/g_{sorbent}$ after 11 cycles) than $Al(NO_3)_3$ (0.48 g $CO_2/g_{sorbent}$ after 11 cycles) using SGCS (Sol-gel-combustion-synthesis method). The baseline CaO captured 0.2 0.58 g $CO_2/g_{sorbent}$ after 11 cycles.	[109]
$La(NO)_3$	Fixed-bed reactor	Calcination 850°C in 100% N_2 (mild conditions) or 950°C in 100% CO_2 (severe conditions) (%vol) Carbonation 650°C in	Tested under realistic conditions and high CO_2 concentrations, with 20% carbonation conversion after 25 cycles for CaO and 42% carbonation conversion for the	[110]

		100% CO_2	the sol-gel derived sorbent	
$La(NO)_3$	TGA	Calcination 850°C in 100% N_2 (%vol) Carbonation 650°C in 15% CO_2	Compared simplified method with standard sol-gel method, the latest gave better results with a 49% conversion for the standard after 20 cycles and a 28% for the simplified sol-gel method	[111]
Aluminium isopropoxide(Al(O-iPr)$_3$)	TGA	Calcination 800, 850, 900, 930°C in 100% N_2 (%vol) Carbonation 650, 700°C in 100% CO_2	A phase of $Ca_9Al_6O_{18}$ was formed stabilising the structure and controlling sintering; attrition of sorbents produced by this method was an issue. The cyclic sorption was of 58.9 wt % adsorption for the sol gel material and a 34.8 wt% for pure CaO after 32 cycles	[112]
Aluminium nitrate hydrate (TEA as complexing agent)	TGA	Calcination 800°C in 100% N_2 (%vol) Carbonation 690°C in 15% CO_2	The complexing agent ensured the uniform distribution of Ca and Al ion which increased the stability of the sorbent with a 81% conversion after 50 cycles compared to 53% of pure CaO	[113]
High aluminium-based cement	TGA	Calcination 850°C in 100% N_2 (%vol) Carbonation 650°C in 15% CO_2	Pelletised material was prepared to solve attrition challenges with promising results with 0.43gCO_2/$g_{sorbent}$ after 50 cycles when compared to 0.09 g CO_2/$g_{sorbent}$ of lime	[117]

3.6.3 Precipitated calcium carbonate (PCC)

Gupta and Fan [31] performed synthesis of CO_2 sorbents using PCC. The procedure bubbled CO_2 through a $Ca(OH)_2$ slurry. PCC achieved high capture capacity which was accredited to the low predisposition of meso-porous sorbents to pore filling and plugging. In TGA testing, almost complete regenerability of PCC was found during the first 2–3 cycles; however, the long-term reactivity under a large number of cycles was not studied.

The design of a slurry bubble column was proposed to produce precipitated calcium carbonate using $Al(NO_3)_3 \cdot 9H_2O$ and $Ca(OH)_2$ slurry [118]. TGA tests with this sorbent were quite positive, showing a high conversion of 33% by the 33rd cycle. Nonetheless, FB reactor experiments showed that the inert support was not an effective component in comparison with unmodified PCC.

MgO was proposed as a support for the co-precipitation technique. Aqueous solutions containing Ca acetate and Mg acetate with 1 M Na_2CO_3 were precipitated, filtered, washed, dried and calcined. In this study several techniques for the addition of MgO were studied. The one that gave the worst performance was the co-precipitation technique which produced sorbents with less than 10% carrying capacity after 30 cycles [107].

The porosity of the material is increased by this procedure, but there is no in-depth study of the mechanical properties of the particles produced using this methodology, and it is expected that the particles will be mechanically weak due to the production method. Also, the scalability must be carefully investigated in order to see if this method is economically feasible at large scale (see Table 3-7).

Table 3-7: Summary table for PCC

Method	Reactor	Conditions	Main findings	References
Slurry bubble column for PCC	TGA	Carbonation 550, 600, and 650°C in 100% CO_2 Cyclic conversion: Calcination 700°C in 100% N_2 (%vol) Carbonation 700°C in 100% CO_2	Natural sorbents failed to carbonate completely. The PCC sorbent achieved 90% conversion in carbonation. The cyclic studies did not show relevant sintering in PCC at 700°C	[31]
Slurry bubble column for PCC	TGA	Calcination 900°C in 15% CO_2 (%vol) Carbonation 650°C in 15% CO_2	The highest capacity was the pure PCC with 20 $gCO_2/g_{sorbent}$ (%) after 15 cycles	[118]

3.6.4 Dry mixture and coating

Dry mixing of two precursors is probably the simplest way of producing a synthetic sorbent for the CaL process. This has been studied for materials with Si as an inert solid support [119, 120]. The calcium precursor and support are mixed in a ball-mill-like device, then pressed into a disc shape and calcined in N_2 atmosphere.

Ca_2SiO_4 reacts with CO_2 during the carbonation while SiO_2 acts as an inert support. The results showed a CaO conversion of 41% in the 13th cycle at 800 °C in 15% CO_2 [119]. MgO has also been physically mixed with $Ca(CH_3COO)_2$ using a ball mill and calcined afterwards, showing great stability and CO_2 capacity of 43% after 50 carbonation/calcination cycles [107]. Luo et al. [121] added La_2O_3 and $CaCO_3$ with dry physical mixing. This sorbent showed slightly better performance than natural limestone. However, such marginal improvements are likely to be overshadowed by cost issues, which may make this technique impractical for large-scale projects.

Coating is another technique that can be employed to produce suitable particles for CaL. Atomic Layer Deposition (ALD) deposits thin films of functional materials using sequential, self-limiting surface reactions allowing control of the thickness deposited on the particle [122, 123]. ALD was used to coat limestone particles with amorphous silica [124]. The coated particles exhibited a stable capture capacity during tests. This indicates that the nanosilica coating acts as a thermally stable support to mitigate sintering of lime during the calcination stage.

Peng et al. [125] developed another methodology for nano/micron-particle coating called self-assembly template synthesis (SATS) which followed a procedure to coat micron-Al_2O_3 with nano-TiO_2. The material was synthesised with SATS as well as prepared by wet impregnation with CaO (80 wt%) and Al_2O_3 (20 wt%) and limestone obtained from calcium acetate monohydrate. These three resulting sorbents were tested in a TGA at 700 °C with 10 vol% CO_2 for carbonation and pure N_2 for calcination to represent mild conditions and at 900 °C in pure CO_2 to represent more realistic calcination conditions. The

SATS sorbent exhibited much better CO_2 capture capacity in both mild and extreme conditions with approximately 0.47 gCO_2/gsorbent after 30 cycles in comparison with 0.27 gCO_2/gsorbent for the CaO. Peng et al. [126] performed tests in a batch FB with the same materials. The findings agree with the results mentioned before with a CO_2 capture capacity of 0.78 $molCO_2$/molCaO after 10 carbonation/calcination cycles.

Dry mixing is the simplest and most inexpensive technique to incorporate a support material into a CaO-based matrix. However, the enhancement in performance appears to be marginal; therefore, unless other materials show a greater improvement in conversion, this method provides limited benefits.

There is a clear advantage in using ALD, which is the extremely stable material than can maintain a high reactivity over long series of cycles. Such high reactivity is caused by the insertion of a thermally stable support that delays sintering. Nonetheless, there are several drawbacks to this technique. Namely, the process of the ALD reaction, needed to coat the material, is very slow. This would be a major limitation for the production of large quantities of this sorbent. Moreover, there are several limitations on the materials that can be used as a coating agent (i.e., the precursors have to be volatile, but not decompose) [127].

3.6.5 Granulation

Granulation of materials for utilisation in CaL is a method of incorporating a support material into CaO to obtain a highly attrition-resistant material. However, such treatments must not adversely affect the sorbent reactivity. Thus for example, Manovic and Anthony [128] suggested that Na_2CO_3 and bentonite, although possessing the required binding properties, are not suitable due to their sintering and loss of CO_2-capture capacity. XRD analysis revealed that local eutectic mixtures were formed. The authors recommended the use of calcium aluminate cement as it does not enhance sintering of the material. These cements also have other benefits such as fast setting, good refractory properties, low cost and ready availability.

Pelletisation with calcium aluminate cements was further explored by Wu et al. [129]. The particles were tested in a TGA with repeated carbonation/calcination cycles at 800 °C. Further, attrition tests were performed in an atmospheric bubbling FB. The results showed better performance for the pelletised material with and without the cement binder and higher attrition resistance during fluidisation in a bubbling bed than regular limestone. Moreover, the particles containing the aluminate cement showed more stable CO_2 carrying capacity over long-term cycle tests.

Later, the acidification of these pellets was investigated [130] as an option to improve the performance of pelletised sorbent. Samples acidified with 10% acetic acid solution exhibited better behaviour than samples treated with acid vapours. However, the acid and the modification procedure are neither simple nor inexpensive and this technique, therefore, appears to offer marginal benefits. The same group also proposed using kaolin as a potential precursor for $Al(OH)_3$ (using a leaching method) and raw kaolin for the pelletisation of acetified limestone [131]. This procedure displayed better results than the raw kaolin due to the dispersion of α-Al_2O_3 generated by the leached $Al(OH)_3$ which enhanced the resistance and stability of the sorbents and the accessibility of CO_2 to the interior of the pellets.

While granulation devices are usually used for this technique, extrusion equipment can also be employed [132]. The samples in this study exhibited good attrition resistance and mechanical strength; commercial cement from Kerneos Aluminate Technology containing 37 wt% CaO and 39.8% Al_2O_3 was used as a binder and also as a support material. The difference in CaO conversion between the samples used in this investigation is shown in Figure 3-13. Carbide slag has also been used as an initial material for extruded-spheronised pellets [133]. In this work the addition of biomass and the use of cement with 50 wt% Al_2O_3 were studied as well as the effect of calcination temperature and pellet size. The results demonstrated that cement addition should be limited to 10 wt% in order to maintain a high CO_2 capture capacity.

Pellets doped with pre-washed rice husk showed better CO_2 uptake than un-doped particles.

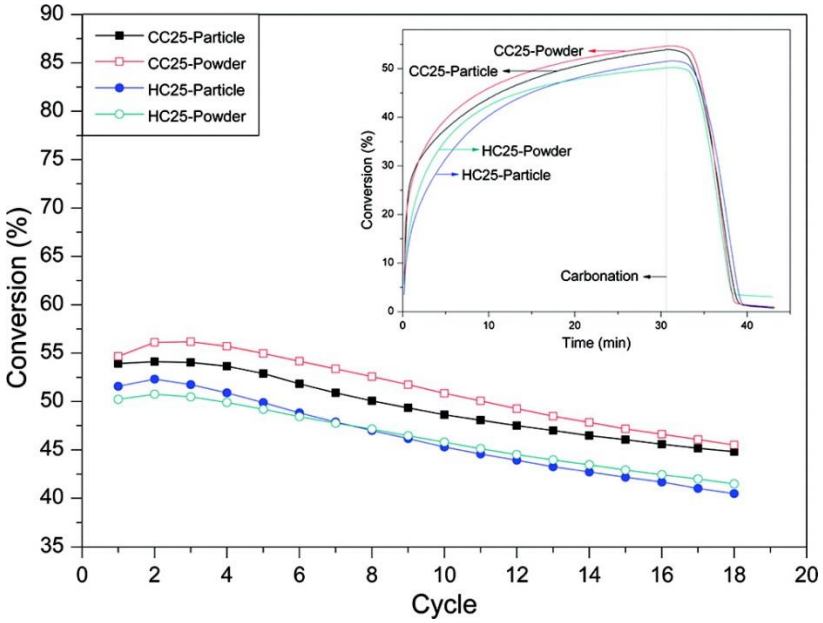

Figure 3-13: CaO conversion of original extruded particles and crushed limestone (CC- reagent calcium hydroxide used as a precursor, HC- commercial hydrated lime used as a precursor) [132]

Knight et al. [134] have performed attrition tests with pellets prepared at CanmetENERGY, Canada. Experimental results suggested that cement-bound pellets underwent attrition to a similar or greater degree than natural limestone. The pellets that showed the best results were silica-coated. However, more tests need to be performed varying the size and humidity as well as further analysis on the kinetics, economics and environmental properties of such sorbents.

Ridha et al. [135] performed attrition tests in a pilot dual FB on calcium aluminate cement pellets (90 wt% lime, 10 wt% calcium aluminate cement) using Cadomin limestone from Canada and Spanish limestones. The results showed that around 50% of the sorbent by mass was smaller than 250 μm. The authors concluded that the size distribution of the pellets indicated that the attrition tendencies were similar regardless of the type of limestone used.

Ridha et al. [136] noted that biomass was potentially a readily available and inexpensive material for increasing the porosity of the pelletised sorbent particles, and in their work the resulting sorbents demonstrated capture capacity of 0.41 gCO_2/g sorbent (prepared with 10% powdered leaves) after 20 cycles with 15% steam present. Before the addition of the templating material to the pelletiser, the biomass was ground and sieved to <30 μm in diameter. Pellets with leaves, cardboard, date seeds and white soft wood were studied. The most promising material was the one templated with leaves, which exhibited a 33.3% higher CO_2 capture than pellets without leaves. All the particles with biomass components displayed better results than those without biomass. Erans et al. [137] studied flour as a biomass-templating material in both TGA and bubbling FB. The synthetic materials displayed better performance than limestone; however, BFB testing proved that the attrition and fragmentation in biomass-templating materials is higher than for calcium aluminate pellets.

Materials used for templating pellets have been further studied by Sun et al. [138] where three different types of pellets were produced: non-shell pellets, core-in-shell with cement shells, and core-in-shell pellets with cement and lime shells. These samples were tested in a TGA (carbonation 650 °C in 15 vol% CO_2, calcination 900 °C in 100 vol% N_2). The most promising sample taking into account the capture capacity and sorbent strength was the material with 10% lime added to the cement shell, which demonstrated a capture of 0.165 gCO_2/g calcined sorbent after 17 cycles. The authors suggested that adding lime to the inert shell in small quantities had a beneficial effect in both the capture capacity and mechanical strength.

Granulation holds several benefits such as incorporation of a support material that stabilises the structure, the formation of pores during the pelletisation process, and the possibility of incorporating pore-forming materials to achieve a better pore structure (see Table 3-8). It is also a relatively easy technique to scale up that uses cheap materials for its production process. One of the most important benefits of pelletisation is that not only is the use of binders enabled, but it allows combining oxygen carriers and catalysts in order to make

composite materials for the integration of CaL and chemical looping combustion (CLC) [139].

Table 3-8: Summary table for granulation

Base material and/or binder and method	Reactor	Conditions	Main findings	References
Bentonites, calcium aluminate cements Extrusion through sieve	TGA	Calcination 850°C in 100% N_2 (%vol) Carbonation 850°C in 100% CO_2	Bentonites enhanced sintering because of the formation of certain compounds $Ca_2(SiO_4)$ and $Ca_5(SiO_4)_2CO_3$ Calcium aluminate cements had very promising properties due to fast setting, good refractory properties and their low cost with a 42% conversion after 30 cycles	[128]
Calcium aluminate cement (10%) Mechanical pelletiser	TGA-reactivity Bubbling FB-attrition	TGA: Calcination 800°C in 100% N_2 (%vol) Carbonation 800°C in 25% CO_2 Bubbling FB: 2 h 800°C in continuous fluidisation	Higher CO_2 uptake in carbonation/calcination cycles than plain limestone. Higher resistance to attrition than plain material. Cement stabilised the CO_2 carrying capacity and increased resistance to sintering with 27 mg CO_2/100mg$_{sorbent}$ after 90 cycles for the cement supported pellets and 18 mg CO_2/mg$_{sorbent}$ for $Ca(OH)_2$ pellets	[129]
Calcium aluminate cement (10%) Treated with acetic acid and commercial vinegar Extrusion through sieve	TGA	Calcination 850°C in 100% N_2 or 920°C in 100% CO_2 (%vol) Carbonation 650°C in 15% CO_2	Acetification was a possible method of enhancing pellet performance, but attrition effects may have increased 10% acetic acid solution enhanced morphology, while vinegar showed worse pore volume and surface area Tests performed under mild conditions and results showed marginal benefit with an increase of 0.1 g CO_2/g$_{sorbent}$	[130]
Kaolin binder or $Al(OH)_3$ binder (obtained from	TGA	Calcination 920°C in 100% CO_2(%vol)	Pellets prepared with $Al(OH)_3$ binders exhibited higher CO_2	[131]

acid leaching of metakaolin) Acetification with acetic acid		Carbonation 650°C in 15% CO_2	uptake than kaolin binder, but it was marginal of 0.05 g $CO_2/g_{sorbent}$ after 30 cycles. Kaolin appears inadequate as a binder	
Commercial cement Extrusion using a 16 twin-screw extruder	TGA-reactivity Friability tester-attrition	TGA: Calcination 900°C in 100% N_2 (%vol) Carbonation 650°C in 15% CO_2 Friability tester: 2000 and 4000 rotations	Screw-extrusion particles displayed good attrition resistance and mechanical strength Preparation method had no effect on the chemical performance under the tested conditions with a marginal difference of around 2% conversion after 20 cycles	[132]
Extruded-spheronised	TGA	Calcination 850°C in 100% N_2 (%vol) Carbonation 650°C in 15% CO_2	Pellets doped with pre-washed rice husk showed better performance with 41.58% conversion for the 5% wt addition of rice husk after 25 cycles Cement addition should be limited to 10 wt%	[133]
Crushed limestone Calcium aluminate cement pellets Pellets without binder	Air jet apparatus-attrition testing	Temperature 20±3 or 500±5°C Atmospheric pressure Times 0,1,5,12,24 and 36 (h) Superficial gas velocity(m/s) 10 (20°C, 500°C) or 0.457 (500°C)	Pellets experienced similar attrition to crushed limestone and were highly sensitive to humidity.	[134]
Calcium aluminate cement	Attrition testing Dual FB (0.1 MW_{th})	Velocity carbonator:2-2.6 m/s T_{carb}=650°C Velocity calciner 0.5-0.8 m/s T_{calc}=650°C	Pellets experienced similar attrition to limestone. 50% of particles were recuperated as fines	[135]
Biomass used for templating: cardboard, maple leaves, date seed and white soft wood Calcium aluminate cement as binder	TGA	Calcination 850°C in air Carbonation 650°C in 15% CO_2 (15% steam in some tests)	Leaf-derived biomass pellets showed higher porosity than all the other types of biomass, increasing also the CO_2 uptake. Optimal content 10% biomass with a 33.3% more CO2 captured than biomass-free pellets after 20 cycles.	[136]

			Tests with steam exhibited better performance of the biomass-templated sorbents	
Biomass used for templating: commercial wheat white flour Calcium aluminate cement as binder Doped with sea-water	TGA	Carbonation 650°C in 15% CO_2 Calcination 850°C in N_2 Carbonation 650°C in 15% CO_2 Calcination 950°C in 100% CO_2 Carbonation 850°C in 90% CO_2 Calcination 850°C in 20% CO_2	The synthetic materials showed better performance than limestone under BFB conditions from 0.25 g/g for calcium aluminate pellets to below 0.1 g/g for limestone after 10 cycles	[137]
Calcium aluminate, rice husk as pore-forming material and inert or semi-reactive shells	BFB TGA	Calcination 900°C in 100% N_2 (%vol) Carbonation 650°C in 15% CO_2	The addition of limestone to the inert shell proved to be beneficial for the reactivity and improved the structure with a maximum with 60% lime added to the shell (0.293 g/g after 17 cycles) when compared to the inert shells (0.132 g/g)	[138]

3.6.6 Nanomaterials

Nano-$CaCO_3$ was investigated with a TGA, which showed a residual activity double what regular limestone would present after 100 cycles. The conversion (X) is presented in Figure 3-14, which shows a residual conversion of 20% and a first-cycle conversion of 89% [140].

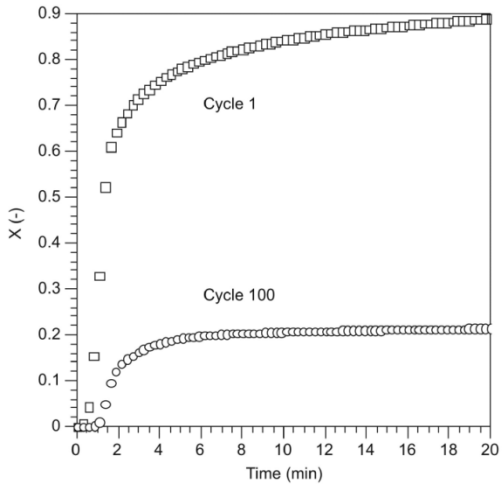

Figure 3-14: Conversion (*X*) for nano-$CaCO_3$ in the first carbonation and 100th carbonation [140]

Liu et al. [141] compared the capture performance from synthetic precursors including nano-particles. All the samples were subjected to 9 carbonation/calcination cycles in a TGA. The solids obtained from nano-sized precursors exhibited a slower decay in conversion, which suggests that those materials are less susceptible to sintering [141].

Another attempt to use nano-sized calcium carbonate as a precursor for the sorbent was made by Wu et al. [142], and the results confirmed that nano-calcium carbonate is a better precursor than $Ca(OH)_2$ and micro $CaCO_3$. Wu and Zhu [143] coated the surface of nano-$CaCO_3$ with a nano-TiO_2 using a solution containing $Ti(OH)_4$. The resulting material was heated and calcined, and TGA tests showed a constant reactive sorption capacity of 5.3 mol/kg after 10 cycles (under carbonation at 600 °C in 0.02 MPa CO_2 partial pressure and calcination at 750 °C using N_2). In comparison, the uncoated material showed a capacity of 1.6 mol/kg after the same number of carbonation/calcination cycles. These results suggest that the higher melting point of the $CaTiO_3$ developed as the coating layer after calcination reduced sintering.

An alternative method for producing nano-particles is flame spray pyrolysis (FSP), in which precursor droplets are converted into solid nano-particles in flames. This has been proposed as an inexpensive large-scale production method for various types of reactive powders [144]. Different sorbents were

produced using this technique, doping the particles with silica, titanium, chromium oxide, cobalt oxide, zirconia and ceria [145]. Nano-CaO exhibited increased capture capacity and the performance of the sorbents generated by FSP was better than that of the sorbents prepared from regular wet methods.

Liu et al. [146] investigated wet mixing of calcium and magnesium salts of d-gluconic acid. The particles exhibited well-distributed CaO nano-particles coated with MgO, which the authors suggested acted as a barrier to avoid sintering. The TGA experiments displayed a constant CO_2 capture capacity over 24 cycles of 0.56 (650 °C for 30 min for carbonation using 15% CO_2 in the flue gas, and calcination at 900 °C for 10 min in 100% N_2).

An alternative to the materials mentioned above was proposed by Li et al. [147]: mixing a 2-propanol slurry containing $Ca(CH_3COO)_2$ and $MgAl_2O_4$ particles. The particles were then dried and calcined, and experiments were performed in a TGA and fixed bed. Both experiments demonstrated the superior capture capacity of the $CaO/MgAl_2O_4$, compared to CaO/MgO particles prepared with the same technique and natural dolomite. The thermal and mechanical properties of $MgAl_2O_4$ added as a support were beneficial for the particles as they interfered with the agglomeration of the nano-CaO particles, which minimised the sintering.

The production of these materials has several benefits such as the advantageous properties of supports (high melting point, stabilisation of structure), as well as the benefit of using nanoparticles on their own (slower decay in conversion). However, these methods are difficult to scale up and much more expensive than using natural limestone or granulated material; therefore, a compromise between durability, cost and adsorption capacity has to be made. Attrition also has to be studied with such materials, and generally the lack of attrition studies on new materials represents a potential major limitation for determining their suitability for calcium looping applications.

3.7 Reactivation of spent sorbent

Once the sorbent has been used for a long series of cycles, the residual reactivity is very low. For the CaL process to be feasible at commercial scale, a method should be found to re-use the potentially very large quantities of spent sorbent, thereby avoiding the necessity of disposal. Besides, the cost of synthetic sorbents is a critical parameter for the feasibility of the technology making their reactivation even more important [148].

3.7.1 Hydration

Hydration can be used not only as a pre-treatment to make limestone more reactive but also as a reactivation technique for spent sorbent. Hydration is beneficial due to the formation of cracks in the CaO particles creating paths to the interior of the particles and, therefore, improving CO_2 capture [149]. Another positive effect of hydration is the formation of larger pores, which make the particles less susceptible to pore blockage [150].

Reactivation can be achieved utilising water [151, 152], water vapour or steam [153, 154]. Generally, calcination/carbonation reactors are not designed for hydration. Therefore, a new vessel would be required so that the used sorbent can be reactivated. The hydration reaction between CaO and water is exothermic, which raises two considerations: the dehydration is endothermic, and the heat produced in the hydrator needs to be integrated with the power plant or the process in order to maintain overall efficiency [153]. It is also essential that the material that needs to be hydrated comes from the calciner, due to the fact that the material from the carbonator is likely to show minimal reactivation compared to calcined material [88, 155].

The most effective way of hydrating spent sorbent is water hydration [151, 152]. Used sorbent reactivated with water for 1 min can reach 70% of the initial conversion of natural sorbent. There are many factors that affect the hydration of synthetic sorbents, but ultrasonic hydration could be a solution for reactivating this type of material [151], which was first proposed by Wang et al. [156] to enhance hydration in sulphated sorbent. However, direct water

hydration is far from ideal due to the energy penalty caused by drying humid hydrated lime. Therefore, steam hydration is proposed as the best method for reactivation [153, 154]. Another advantage of steam over water is that spent sorbent exhibits high reactivity towards steam, allowing small pores to be produced. More investigations [155, 157] have been conducted with promising results using steam as the hydration procedure as shown in Figure 3-15 and from an industrial point of view it seems more likely that steam would be used rather than liquid water.

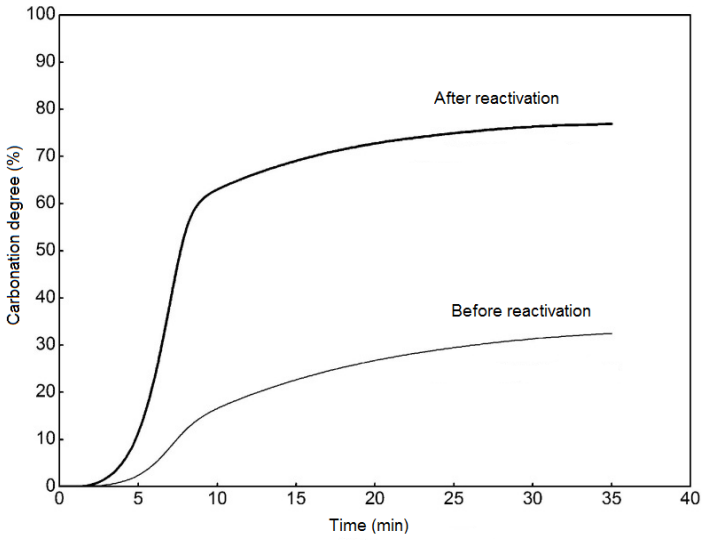

Figure 3-15: Effect of hydration on sorbent activity (after the first cycle in tube furnace)

However, the results seen in Figure 3-15 only demonstrated the effect of reactivated lime during the first cycle after the hydration, while the most important parameter for the CaL cycle is long-term reactivity. The results shown in Figure 3-16 indicate that the improvement in the reactivity in the first cycle actually continues over a relatively high number of cycles [150]. This is attributed to the enhanced rate of carbonation in the diffusion-controlled regime [158].

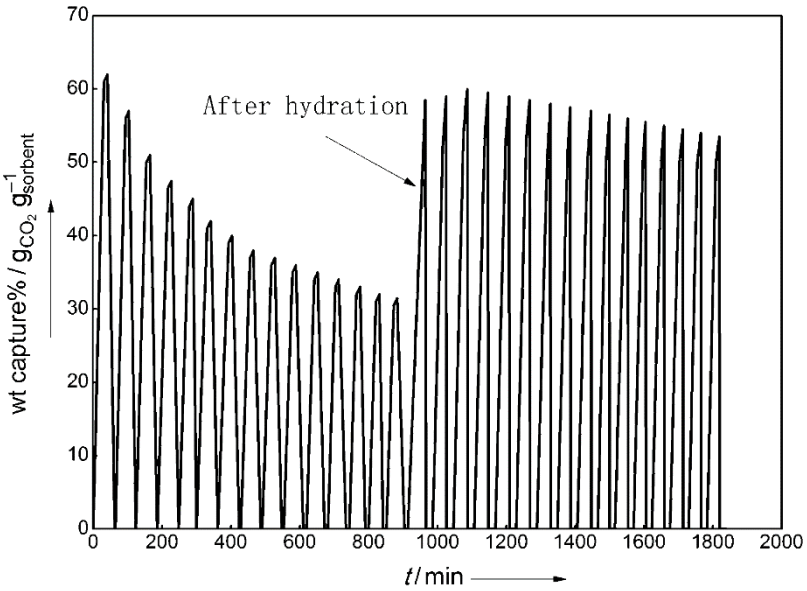

Figure 3-16: Effect of hydration on decay rate of CO_2 sorption of CaO sorbent (the hydration was performed after the 15th cycle) [150]

However, it is interesting to note that Sun et al. [88] reported poor capture performance after hydration; it was later found that if the hydrated sample was exposed to temperatures above 750 °C after reactivation, the beneficial effect was effectively eliminated [159]. The carbonation of $Ca(OH)_2$ is faster than CaO [160, 161], so it has been suggested that the hydration vessel for post-combustion operation should be positioned before the carbonator, taking special care in selecting the carbonation temperature.

While the benefits of using hydration as a means to reactivate the sorbent are numerous (e.g., low price of water as a reactivating chemical, easy procedure and scale up of the hydration technique and high reactivity of the treated sorbent), an extra reactor will increase the cost and complexity of the plant. Another drawback for the technique is the high attrition of hydrated particles, which is a challenge for FB operation [47, 149, 162]. An extra step (i.e., granulation or extrusion) would be required to overcome the mechanically weak particles, which will incur a rise in price.

3.7.2 Re-pelletisation technique

The re-pelletisation process uses water to re-bind the pellets. There is a double effect when using this method for reactivation purposes. The porosity of the particles is increased and some unreacted CaO in the core is exposed at the surface. Moreover, water used to re-pelletise the sorbent hydrates the material increasing its performance further.

This phenomenon was first studied in the field for sulphur capture for flue gas desulphurisation, where it was demonstrated that wet mixing was beneficial compared to dry mixing for re-pelletisation of spent material [163].

This technique could be used for CaL. Lu et al. [164] proposed pelletisation of hydrated lime as an acceptable solution for attrition of the hydrated material. Manovic and Anthony [165] mixed calcined limestone with calcium aluminate cement using extrusion through a sieve as a technique for obtaining pellets. These pellets were cycled 300 times, under isothermal conditions at 850 °C with 100% CO_2 for calcination and 100% N_2 for carbonation (using a tube furnace to make spent sorbent). They were then removed following calcination, before being ground and remade by addition of water and extrusion through a sieve. TGA tests showed that the fresh pellets and the ones made with spent sorbent showed very similar results exhibiting 33–34% conversion after 30 cycles at 700 °C in an atmosphere of 20% CO_2, N_2 balance for carbonation, and 950 °C in pure CO_2 for calcination.

The spent sorbent from a pilot plant was pelletised using a mechanical granulator [166]. Three types of granules were made: with no binder; with 10% calcium aluminate cement; and with a cement-free core, cement-containing mixture. This last type of pellet was prepared in a two-step process. Spent sorbent with no cement was hydrated, granulated and dried. Then, these pellets were added to the vessel with cement to be pelletised forming a cement shell around the cement–free pellet. The results for the pellets were then compared to the spent sorbent from the power plant, showing improvement in reactivity. Although the reactivity was increased, the pellets did not show the level of

conversion seen in fresh limestone due to sulphation during cycles, as can be seen in Figure 3-17.

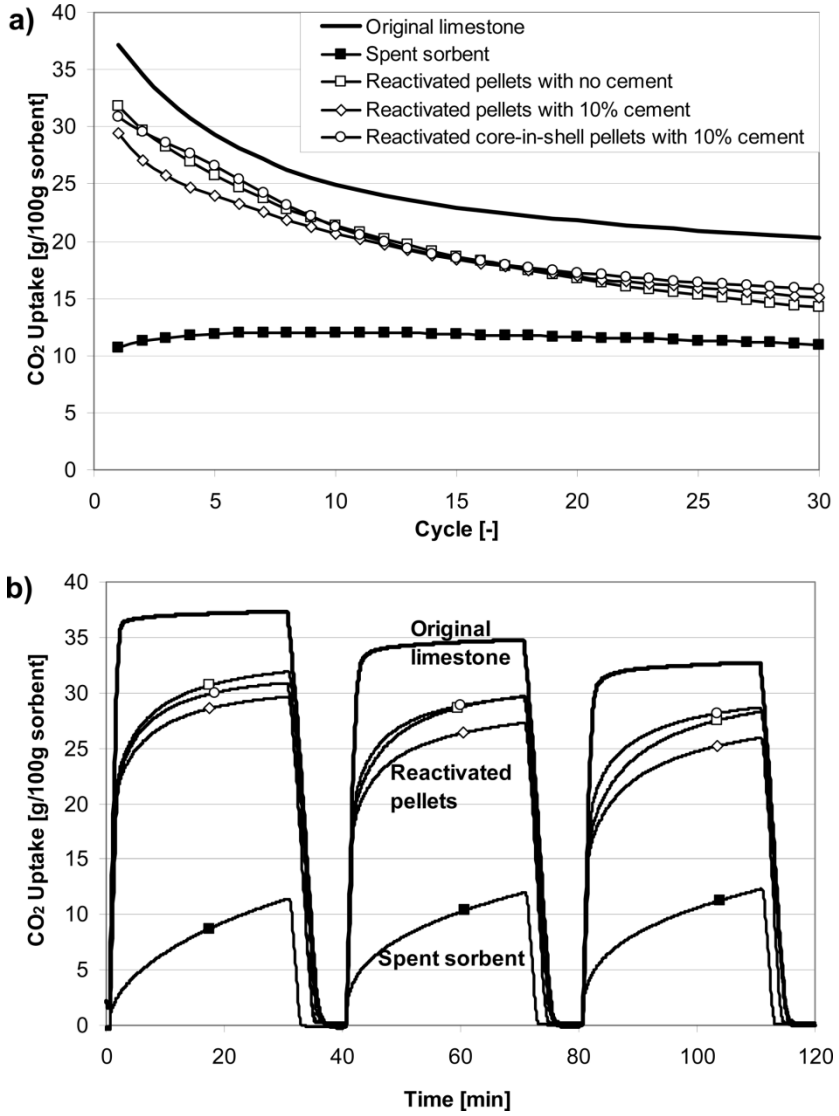

Figure 3-17: CO_2 capture performance of tested sorbents: (a) CO_2 capture capacity during 30 cycles and (b) conversion profiles during the first three cycles. Conditions: carbonation in 50% CO_2 (N_2 balance) for 30 min, calcination in 100% N_2 for 10 min, isothermally at 800 °C [166]

As a reactivation technique remaking of pellets would be beneficial from the economic perspective as the materials are cheap (deactivated material and water). Moreover, the procedure would be easy to implement as it is the same as the production method explained in the granulation subsection. It has a clear advantage over hydration, as the material is hydrated and pelletised at the

same time. Therefore, the reactivity is increased but the material is less subjected to attrition.

3.7.3 Extended carbonation time and re-carbonation

To understand the benefits of this technique a more detailed explanation of the reaction of CaO with CO_2 is needed. The carbonation reaction has two stages: a fast kinetically-controlled stage and a slow diffusion-controlled stage as shown in Figure 3-18 [32]. The more time the solid spends in the slow diffusion stage, the more reactive the particle is in the next calcination due to the increasing volume of the particle which will result in a more porous structure, which is advantageous for the process.

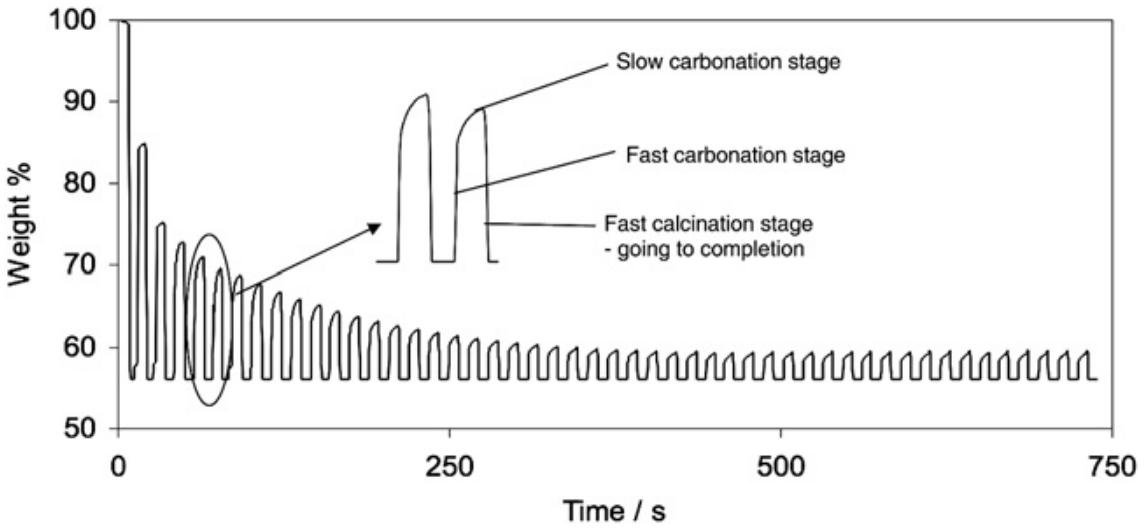

Figure 3-18: Repeated calcination/carbonation cycles of limestone in a TGA [32]

This phenomenon was first studied for energy storage where it was noted that if the slow diffusion stage was completed then the flow of CO_2 during calcination would increase porosity and increase the surface area for the next cycle [48].

This was first noted for CaL by Sun, Lim and Grace [49] who showed that marginal increase in carbonation times had a positive outcome on the capture capacity over several cycles. Chen et al. [92] stated that extending the carbonation time substantially helped to recover some capture ability of the sorbents. Although this recovery decreased with increasing number of cycles,

the samples that experienced extended carbonation time showed better reactivity than the ones that did not.

Further work demonstrated that carbonation time has a robust effect on carrying capacity. If the carbonation time increased, the residual conversion also increased [31].

Arias et al. [60] proposed incorporating this into the CaL scheme with a recarbonation reactor. This would maintain a quasi-optimal carrying capacity by carbonating the solids with pure CO_2 from the calciner. This hypothesis was verified using a TGA, increasing the residual carrying capacity from 7% to 16%. The design of a reactor for this purpose was suggested recently [167], although the idea was first proposed by Salvador et al. in 2003 [50] and [168]. The results for the modelled re-carbonator are displayed in Figure 3-19, which clearly indicates the increased conversion versus recarbonation time.

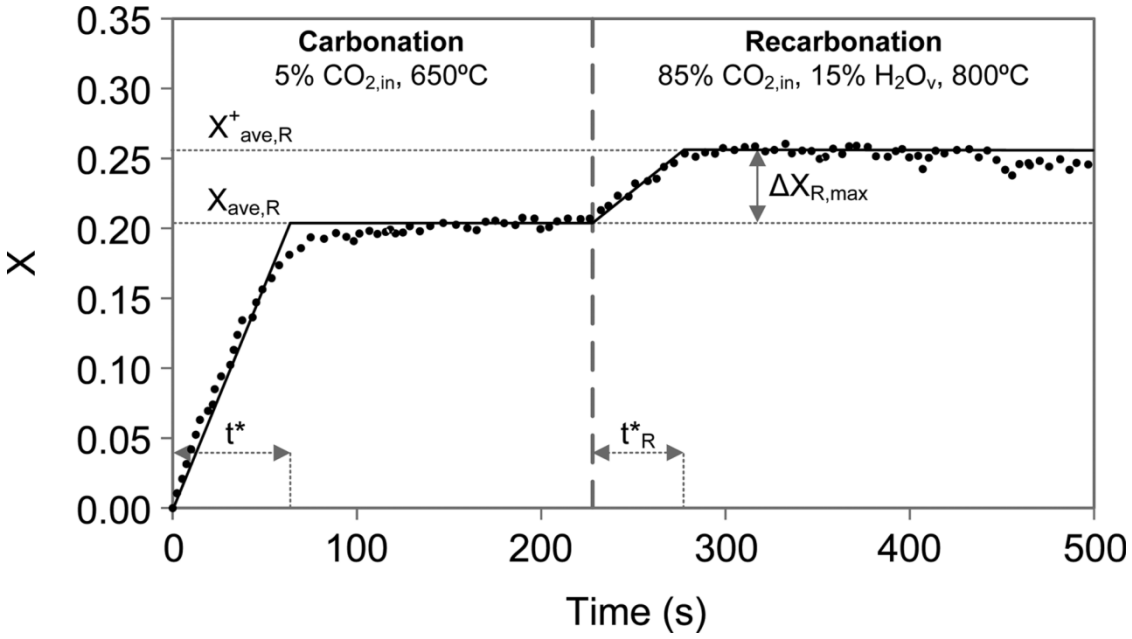

Figure 3-19: Example of a typical conversion versus time curve during carbonation and recarbonation stages [167]

Manovic and Anthony [68] have shown that recarbonation can have an adverse effect, further accelerating the decay of CaO conversion. This was confirmed in a recent publication where the authors suggested that this process leads to an intensification of diffusion-controlled carbonation, which causes defects due to

intense bulk stresses [169]. Further studies need to be carried out regarding the potential of this process to better understand the effects on the sorbent due to the contradictory results that can be found in the literature.

3.8 Conclusions

Although limestone would be initially preferred as a CaL sorbent due to its low cost, ready availability and possible re-use, once spent, as a feedstock for the cement industry, there are several drawbacks to its use: in particular, the reactivity decay caused by sintering, the potentially high attrition rate for many limestones, and vulnerability of limestone to sulphation in practical systems. A number of solutions have been reviewed in order to overcome these challenges. First, enhancement of natural sorbents can be achieved, reducing their reactivity decay by means of some simple procedures, such as using calcium hydroxide as a precursor, and thermal pre-treatment. In addition, novel synthesis methods have been developing during the past decade to obtain particles with upgraded properties. The techniques vary from fairly simple procedures such as granulation and dry mixing to very complex processes like sol-gel combustion synthesis and co-precipitation.

There is a need to study the scalability of these complex processes. The preferred processes would be, at least at an initial stage of deployment, techniques that are already proven in industry such as granulation or extrusion. Another important factor is the cost of the material since one of the main advantages of CaL is the low sorbent cost. The last important concern with respect to sorbents is the suitability of the particles for use in FBs. Some of the methods presented here require modifications to fine particles (nano-materials or PCC) in order for them to be usable in a reactor of this kind. Consequently, the cost of granulation of this material should be added to the overall process costs and evaluation, which risks making such approaches prohibitively costly. Moreover, reactivation techniques should also be carefully investigated to determine their appropriateness at commercial scale as an alternative approach to preparing synthetic sorbents.

3.9 References

[1] IEA, 2015. CO_2 emissions from fuel combustion. IEA Publications, Paris, France.

[2] Nakicenovic, N., Alcamo, J., Grubler, A., Riahi, K., Roehrl, R.A., Rogner, H.H. and Victor, N., 2000. Special report on emissions scenarios (SRES), a special report of Working Group III of the intergovernmental panel on climate change. Cambridge University Press.

[3] Watson R.T., Albritton D.T. IPCC, Climate change 2001: Synthesis report A. Contribution of working groups I, II and III to the third assessment report on intergovernmental panel on climate change.

[4] IEA, 2014. World energy outlook. IEA Publications, Paris, France.

[5] Fan, L.S., 2011. Chemical looping systems for fossil energy conversions. John Wiley & Sons.

[6] Herzog, H., Eliasson, B. and Kaarstad, O., 2000. Capturing greenhouse gases. Scientific American, 282(2), pp. 72-79.

[7] Rackley, S., 2009. Carbon capture and storage. Gulf Professional Publishing.

[8] Li, F. and Fan, L.S., 2008. Clean coal conversion processes–progress and challenges. Energy & Environmental Science, 1(2), pp. 248-267.

[9] MacDowell, N., Florin, N., Buchard, A., Hallett, J., Galindo, A., Jackson, G., Adjiman, C.S., Williams, C.K., Shah, N. and Fennell, P., 2010. An overview of CO_2 capture technologies. Energy & Environmental Science, 3(11), pp. 1645-1669.

[10] Supap, T., Idem, R., Tontiwachwuthikul, P. and Saiwan, C., 2006. Analysis of monoethanolamine and its oxidative degradation products during CO_2 absorption from flue gases: A comparative study of GC-MS, HPLC-RID, and CE-DAD analytical techniques and possible optimum combinations. Industrial & Engineering Chemistry Research, 45(8), pp. 2437-2451.

[11] Veawab, A., Tontiwachwuthikul, P. and Chakma, A., 2001. Investigation of low-toxic organic corrosion inhibitors for CO_2 separation process using aqueous MEA solvent. Industrial & Engineering Chemistry Research, 40(22), pp. 4771-4777.

[12] Aaron, D. and Tsouris, C., 2005. Separation of CO_2 from flue gas: a review. Separation Science and Technology, 40(1-3), pp. 321-348.

[13] Chi, S. and Rochelle, G.T., 2002. Oxidative degradation of monoethanolamine. Industrial & Engineering Chemistry Research, 41(17), pp. 4178-4186.

[14] Goff, G.S. and Rochelle, G.T., 2004. Monoethanolamine degradation: O_2 mass transfer effects under CO_2 capture conditions. Industrial & Engineering Chemistry Research, 43(20), pp. 6400-6408.

[15] Fytianos, G., Ucar, S., Grimstvedt, A., Hyldbakk, A., Svendsen, H.F. and Knuutila, H.K., 2016. Corrosion and degradation in MEA based post-combustion CO_2 capture. International Journal of Greenhouse Gas Control, 46, pp .48-56.

[16] Li, K., Leigh, W., Feron, P., Yu, H. and Tade, M., 2016. Systematic study of aqueous monoethanolamine (MEA)-based CO_2 capture process: techno-economic assessment of the MEA process and its improvements. Applied Energy, 165, pp. 648-659.

[17] Xiong, Y., Luo, P. and Hua, B., 2014. Energy consumption analysis of air separation process for oxy-fuel combustion system. Advanced Materials Research.

[18] Idem, R., Wilson, M., Tontiwachwuthikul, P., Chakma, A., Veawab, A., Aroonwilas, A. and Gelowitz, D., 2006. Pilot plant studies of the CO_2 capture performance of aqueous MEA and mixed MEA/MDEA solvents at the University of Regina CO_2 capture technology development plant and the boundary dam CO_2 capture demonstration plant. Industrial & Engineering Chemistry Research, 45(8), pp. 2414-2420.

[19] Bhown, A.S. and Freeman, B.C., 2011. Analysis and status of post-combustion carbon dioxide capture technologies. Environmental Science & Technology, 45(20), pp. 8624-8632.

[20] Dean, C.C., Blamey, J., Florin, N.H., Al-Jeboori, M.J. and Fennell, P.S., 2011. The calcium looping cycle for CO_2 capture from power generation, cement manufacture and hydrogen production. Chemical Engineering Research and Design, 89(6), pp. 836-855.

[21] Hamilton RH, Herzog H, Parsons JE. Cost and U.S. public policy for new coal power plants with carbon capture and sequestration. Energy Procedia, 2009, pp. 4487–4494.

[22] Blyth, W., Bradley, R., Bunn, D., Clarke, C., Wilson, T. and Yang, M., 2007. Investment risks under uncertain climate change policy. Energy Policy, 35(11), pp. 5766-5773.

[23] Markewitz, P., Kuckshinrichs, W., Leitner, W., Linssen, J., Zapp, P., Bongartz, R., Schreiber, A. and Müller, T.E., 2012. Worldwide innovations in the development of carbon capture technologies and the utilization of CO_2. Energy & Environmental Science, 5(6), pp. 7281-7305.

[24] Hanak, D.P., Anthony, E.J. and Manovic, V., 2015. A review of developments in pilot-plant testing and modelling of calcium looping process for CO_2 capture from power generation systems. Energy & Environmental Science, 8(8), pp. 2199-2249.

[25] Shimizu, T., Hirama, T., Hosoda, H., Kitano, K., Inagaki, M. and Tejima, K., 1999. A twin fluid-bed reactor for removal of CO_2 from combustion processes. Chemical Engineering Research and Design, 77(1), pp. 62-68.

[26] Alonso, M., Rodríguez, N., Grasa, G. and Abanades, J.C., 2009. Modelling of a fluidized bed carbonator reactor to capture CO_2 from a combustion flue gas. Chemical Engineering Science, 64(5), pp. 883-891.

[27] Lasheras, A., Ströhle, J., Galloy, A. and Epple, B., 2011. Carbonate looping process simulation using a 1D fluidized bed model for the carbonator. International Journal of Greenhouse Gas Control, 5(4), pp. 686-693.

[28] Valverde, J.M., 2013. A model on the CaO multicyclic conversion in the Ca-looping process. Chemical Engineering Journal, 228, pp. 1195-1206.

[29] Lu, D.Y., Hughes, R.W. and Anthony, E.J., 2008. Ca-based sorbent looping combustion for CO_2 capture in pilot-scale dual fluidized beds. Fuel Processing Technology, 89(12), pp. 1386-1395.

[30] Alvarez, D. and Abanades, J.C., 2005. Determination of the critical product layer thickness in the reaction of CaO with CO_2. Industrial & Engineering Chemistry Research, 44(15), pp. 5608-5615.

[31] Gupta, H. and Fan, L.S., 2002. Carbonation− calcination cycle using high reactivity calcium oxide for carbon dioxide separation from flue gas. Industrial & Engineering Chemistry Research, 41(16), pp. 4035-4042.

[32] Blamey, J., Anthony, E.J., Wang, J. and Fennell, P.S., 2010. The calcium looping cycle for large-scale CO_2 capture. Progress in Energy and Combustion Science, 36(2), pp. 260-279.

[33] Yin, J., Qin, C., Feng, B., Ge, L., Luo, C., Liu, W. and An, H., 2013. Calcium looping for CO_2 capture at a constant high temperature. Energy & Fuels, 28(1), pp. 307-318.

[34] Valverde, J.M., Sanchez-Jimenez, P.E., Perejon, A. and Perez-Maqueda, L.A., 2013. CO_2 multicyclic capture of pretreated/doped CaO in the Ca-looping process. Theory and experiments. Physical Chemistry Chemical Physics, 15(28), pp. 11775-11793.

[35] Hanak, D.P., Biliyok, C., Anthony, E.J. and Manovic, V., 2015. Modelling and comparison of calcium looping and chemical solvent scrubbing retrofits for CO_2 capture from coal-fired power plant. International Journal of Greenhouse Gas Control, 42, pp. 226-236.

[36] Romano, M.C., 2012. Modeling the carbonator of a Ca-looping process for CO_2 capture from power plant flue gas. Chemical Engineering Science, 69(1), pp. 257-269.

[37] Abanades, J.C., Anthony, E.J., Wang, J. and Oakey, J.E., 2005. Fluidized bed combustion systems integrating CO_2 capture with CaO. Environmental Science & Technology, 39(8), pp. 2861-2866.

[38] Mantripragada, H.C. and Rubin, E.S., 2014. Calcium looping cycle for CO_2 capture: Performance, cost and feasibility analysis. Energy Procedia, 63, pp. 2199-2206.

[39] Zhao, M., Minett, A.I. and Harris, A.T., 2013. A review of techno-economic models for the retrofitting of conventional pulverised-coal power plants for post-combustion capture (PCC) of CO_2. Energy & Environmental Science, 6(1), pp. 25-40.

[40] Abanades, J.C., Grasa, G., Alonso, M., Rodriguez, N., Anthony, E.J. and Romeo, L.M., 2007. Cost structure of a postcombustion CO_2 capture system using CaO. Environmental Science & Technology, 41(15), pp. 5523-5527.

[41] Cormos, C.C., 2014. Economic evaluations of coal-based combustion and gasification power plants with post-combustion CO_2 capture using calcium looping cycle. Energy, 78, pp. 665-673.

[42] Cormos, C.C., 2015. Assessment of chemical absorption/adsorption for post-combustion CO_2 capture from Natural Gas Combined Cycle (NGCC) power plants. Applied Thermal Engineering, 82, pp. 120-128.

[43] Romeo, L.M., Abanades, J.C., Escosa, J.M., Paño, J., Giménez, A., Sánchez-Biezma, A. and Ballesteros, J.C., 2008. Oxyfuel carbonation/calcination cycle for low cost CO_2 capture in existing power plants. Energy Conversion and Management, 49(10), pp. 2809-2814.

[44] Borgwardt, R.H., 1989. Sintering of nascent calcium oxide. Chemical Engineering Science, 44(1), pp. 53-60.

[45] Sun, P., Grace, J.R., Lim, C.J. and Anthony, E.J., 2007. The effect of CaO sintering on cyclic CO_2 capture in energy systems. AIChE Journal, 53(9), pp. 2432-2442.

[46] Fennell, P.S., Pacciani, R., Dennis, J.S., Davidson, J.F. and Hayhurst, A.N., 2007. The effects of repeated cycles of calcination and carbonation on a variety of different limestones, as measured in a hot fluidized bed of sand. Energy & Fuels, 21(4), pp. 2072-2081.

[47] Blamey, J., Paterson, N.P., Dugwell, D.R. and Fennell, P.S., 2010. Mechanism of particle breakage during reactivation of CaO-based sorbents for CO_2 capture. Energy & Fuels, 24(8), pp. 4605-4616.

[48] Barker, R., 1973. The reversibility of the reaction $CaCO_3 \rightleftarrows CaO + CO_2$. Journal of Applied Chemistry and Biotechnology, 23(10), pp. 733-742.

[49] Sun, P., Lim, C.J. and Grace, J.R., 2008. Cyclic CO_2 capture by limestone-derived sorbent during prolonged calcination/carbonation cycling. AIChE Journal, 54(6), pp. 1668-1677.

[50] Salvador, C., Lu, D., Anthony, E.J. and Abanades, J.C., 2003. Enhancement of CaO for CO_2 capture in an FBC environment. Chemical Engineering Journal, 96(1), pp. 187-195.

[51] Lysikov, A.I., Salanov, A.N. and Okunev, A.G., 2007. Change of CO_2 carrying capacity of CaO in isothermal recarbonation− decomposition cycles. Industrial & Engineering Chemistry Research, 46(13), pp. 4633-4638.

[52] Coppola, A., Scala, F., Salatino, P. and Montagnaro, F., 2013. Fluidized bed calcium looping cycles for CO_2 capture under oxy-firing calcination conditions: Part 1. Assessment of six limestones. Chemical Engineering Journal, 231, pp. 537-543.

[53] Coppola, A., Montagnaro, F., Salatino, P. and Scala, F., 2012. Attrition of limestone during fluidized bed calcium looping cycles for CO_2 capture. Combustion Science and Technology, 184(7-8), pp. 929-941.

[54] Coppola, A., Montagnaro, F., Salatino, P. and Scala, F., 2012. Fluidized bed calcium looping: the effect of SO_2 on sorbent attrition and CO_2 capture capacity. Chemical Engineering Journal, 207, pp. 445-449.

[55] Abanades, J.C., Rubin, E.S. and Anthony, E.J., 2004. Sorbent cost and performance in CO_2 capture systems. Industrial & Engineering Chemistry Research, 43(13), pp. 3462-3466.

[56] Chen, S., Xiang, W., Wang, D. and Xue, Z., 2012. Incorporating IGCC and CaO sorption-enhanced process for power generation with CO_2 capture. Applied Energy, 95, pp. 285-294.

[57] Lisbona, P., Martínez, A. and Romeo, L.M., 2013. Hydrodynamical model and experimental results of a calcium looping cycle for CO_2 capture. Applied Energy, 101, pp. 317-322.

[58] Jia, L., Hughes, R., Lu, D., Anthony, E.J. and Lau, I., 2007. Attrition of calcining limestones in circulating fluidized-bed systems. Industrial & Engineering Chemistry Research, 46(15), pp. 5199-5209.

[59] Grasa, G.S. and Abanades, J.C., 2006. CO_2 capture capacity of CaO in long series of carbonation/calcination cycles. Industrial & Engineering Chemistry Research, 45(26), pp. 8846-8851.

[60] Arias, B., Grasa, G.S., Alonso, M. and Abanades, J.C., 2012. Post-combustion calcium looping process with a highly stable sorbent activity by recarbonation. Energy & Environmental Science, 5(6), pp. 7353-7359.

[61] Wang, J., Manovic, V., Wu, Y. and Anthony, E.J., 2010. A study on the activity of CaO-based sorbents for capturing CO_2 in clean energy processes. Applied Energy, 87(4), pp. 1453-1458.

[62] González, B., Alonso, M. and Abanades, J.C., 2010. Sorbent attrition in a carbonation/calcination pilot plant for capturing CO_2 from flue gases. Fuel, 89(10), pp. 2918-2924.

[63] Chen, H., Zhao, C., Yang, Y. and Zhang, P., 2012. CO_2 capture and attrition performance of CaO pellets with aluminate cement under pressurized carbonation. Applied Energy, 91(1), pp. 334-340.

[64] Arias, B., Diego, M.E., Abanades, J.C., Lorenzo, M., Diaz, L., Martínez, D., Alvarez, J. and Sánchez-Biezma, A., 2013. Demonstration of steady state CO_2 capture in a 1.7 MW_{th} calcium looping pilot. International Journal of Greenhouse Gas Control, 18, pp. 237-245.

[65] Sánchez-Biezma, A., Paniagua, J., Diaz, L., Lorenzo, M., Alvarez, J., Martínez, D., Arias, B., Diego, M.E. and Abanades, J.C., 2013. Testing postcombustion CO_2 capture with CaO in a 1.7 MW_{th} pilot facility. Energy Procedia, 37, pp. 1-8.

[66] Ströhle, J., Junk, M., Kremer, J., Galloy, A. and Epple, B., 2014. Carbonate looping experiments in a 1MW_{th} pilot plant and model validation. Fuel, 127, pp. 13-22.

[67] Dieter, H., Hawthorne, C., Zieba, M. and Scheffknecht, G., 2013. Progress in calcium looping post combustion CO_2 capture: successful pilot scale demonstration. Energy Procedia, 37, pp. 48-56.

[68] Manovic, V. and Anthony, E.J., 2008. Parametric study on the CO_2 capture capacity of CaO-based sorbents in looping cycles. Energy & Fuels, 22(3), pp. 1851-1857.

[69] Manovic, V., Charland, J.P., Blamey, J., Fennell, P.S., Lu, D.Y. and Anthony, E.J., 2009. Influence of calcination conditions on carrying capacity of CaO-based sorbent in CO_2 looping cycles. Fuel, 88(10), pp. 1893-1900.

[70] Li, Y.J., Zhao, C.S., Duan, L.B., Liang, C., Li, Q.Z., Zhou, W. and Chen, H.C., 2008. Cyclic calcination/carbonation looping of dolomite modified with acetic acid for CO_2 capture. Fuel Processing Technology, 89(12), pp. 1461-1469.

[71] Chrissafis, K., Dagounaki, C. and Paraskevopoulos, K.M., 2005. The effects of procedural variables on the maximum capture efficiency of CO_2 using

a carbonation/calcination cycle of carbonate rocks. Thermochimica Acta, 428(1), pp. 193-198.

[72] Valverde, J.M., Sanchez-Jimenez, P.E. and Perez-Maqueda, L.A., 2015. Ca-looping for postcombustion CO_2 capture: A comparative analysis on the performances of dolomite and limestone. Applied Energy, 138, pp. 202-215.

[73] Itskos, G., Grammelis, P., Scala, F., Pawlak-Kruczek, H., Coppola, A., Salatino, P. and Kakaras, E., 2013. A comparative characterization study of Ca-looping natural sorbents. Applied Energy, 108, pp. 373-382.

[74] Deshpande, N. and Yuh, B., 2013. Screening of Multiple Waste Animal Shells as a Source of Calcium Sorbent for High Temperature CO_2 Capture. Sustainable Enviornment Research, 23, pp. 227-232.

[75] Sacia, E.R., Ramkumar, S., Phalak, N. and Fan, L.S., 2013. Synthesis and regeneration of sustainable CaO sorbents from chicken eggshells for enhanced carbon dioxide capture. ACS Sustainable Chemistry & Engineering, 1(8), pp. 903-909.

[76] Ives, M., Mundy, R.C., Fennell, P.S., Davidson, J.F., Dennis, J.S. and Hayhurst, A.N., 2008. Comparison of different natural sorbents for removing CO_2 from combustion gases, as studied in a bench-scale fluidized bed. Energy & Fuels, 22(6), pp. 3852-3857.

[77] Shan, S., Ma, A., Hu, Y., Jia, Q., Wang, Y. and Peng, J., 2016. Development of sintering-resistant CaO-based sorbent derived from eggshells and bauxite tailings for cyclic CO_2 capture. Environmental Pollution, 208, pp. 546-552.

[78] Wu, S.F., Beum, T.H., Yang, J.I. and Kim, J.N., 2007. Properties of Ca-base CO_2 sorbent using $Ca(OH)_2$ as precursor. Industrial & Engineering Chemistry Research, 46(24), pp. 7896-7899.

[79] Hughes, R.W., Lu, D., Anthony, E.J. and Wu, Y., 2004. Improved long-term conversion of limestone-derived sorbents for in situ capture of CO_2 in a

fluidized bed combustor. Industrial & Engineering Chemistry Research, 43(18), pp. 5529-5539.

[80] González, B., Blamey, J., McBride-Wright, M., Carter, N., Dugwell, D., Fennell, P. and Abanades, J.C., 2011. Calcium looping for CO_2 capture: sorbent enhancement through doping. Energy Procedia, 4, pp. 402-409.

[81] Al-Jeboori, M.J., Nguyen, M., Dean, C. and Fennell, P.S., 2013. Improvement of limestone-based CO_2 sorbents for Ca looping by HBr and other mineral acids. Industrial & Engineering Chemistry Research, 52(4), pp. 1426-1433.

[82] Al-Jeboori, M.J., Fennell, P.S., Nguyen, M. and Feng, K., 2012. Effects of different dopants and doping procedures on the reactivity of CaO-based sorbents for CO_2 capture. Energy & Fuels, 26(11), pp. 6584-6594.

[83] Sun, R., Li, Y., Liu, H., Wu, S. and Lu, C., 2012. CO_2 capture performance of calcium-based sorbent doped with manganese salts during calcium looping cycle. Applied Energy, 89(1), pp. 368-373.

[84] Chen, H., Zhao, C. and Yu, W., 2013. Calcium-based sorbent doped with attapulgite for CO_2 capture. Applied Energy, 112, pp. 67-74.

[85] Manovic, V., Fennell, P.S., Al-Jeboori, M.J. and Anthony, E.J., 2013. Steam-enhanced calcium looping cycles with calcium aluminate pellets doped with bromides. Industrial & Engineering Chemistry Research, 52(23), pp. 7677-7683.

[86] González, B., Blamey, J., Al-Jeboori, M.J., Florin, N.H., Clough, P.T. and Fennell, P.S., 2016. Additive effects of steam addition and HBr doping for CaO-based sorbents for CO_2 capture. Chemical Engineering and Processing: Process Intensification, 103, pp. 21-26.

[87] Reddy, E.P. and Smirniotis, P.G., 2004. High-temperature sorbents for CO_2 made of alkali metals doped on CaO supports. The Journal of Physical Chemistry B, 108(23), pp. 7794-7800.

[88] Sun, P., Grace, J.R., Lim, C.J. and Anthony, E.J., 2008. Investigation of attempts to improve cyclic CO_2 capture by sorbent hydration and modification. Industrial & Engineering Chemistry Research, 47(6), pp. 2024-2032.

[89] Manovic, V. and Anthony, E.J., 2008. Thermal activation of CaO-based sorbent and self-reactivation during CO_2 capture looping cycles. Environmental Science & Technology, 42(11), pp. 4170-4174.

[90] Albrecht, K.O., Wagenbach, K.S., Satrio, J.A., Shanks, B.H. and Wheelock, T.D., 2008. Development of a CaO-based CO_2 sorbent with improved cyclic stability. Industrial & Engineering Chemistry Research, 47(20), pp. 7841-7848.

[91] Manovic, V., Anthony, E.J., Grasa, G. and Abanades, J.C., 2008. CO_2 looping cycle performance of a high-purity limestone after thermal activation/doping. Energy & Fuels, 22(5), pp. 3258-3264.

[92] Chen, Z., Song, H.S., Portillo, M., Lim, C.J., Grace, J.R. and Anthony, E.J., 2009. Long-term calcination/carbonation cycling and thermal pretreatment for CO_2 capture by limestone and dolomite. Energy & Fuels, 23(3), pp. 1437-1444.

[93] Li, Y., Zhao, C., Chen, H., Liang, C., Duan, L. and Zhou, W., 2009. Modified CaO-based sorbent looping cycle for CO_2 mitigation. Fuel, 88(4), pp. 697-704.

[94] Li, Y., Zhao, C., Chen, H. and Liu, Y., 2009. Enhancement of Ca-Based Sorbent Multicyclic Behavior in Ca Looping Process for CO_2 Separation. Chemical Engineering & Technology, 32(4), pp. 548-555.

[95] Ridha, F.N., Manovic, V., Macchi, A. and Anthony, E.J., 2012. The effect of SO_2 on CO_2 capture by CaO-based pellets prepared with a kaolin derived $Al(OH)_3$ binder. Applied Energy, 92, pp. 415-420.

[96] Adanez, J., Fierro, V., García-Labiano, F. and Palacios, J., 1997. Study of modified calcium hydroxides for enhancing SO_2 removal during sorbent injection in pulverized coal boilers. Fuel, 76(3), pp. 257-265.

[97] Li, Y.J., Zhao, C.S., Qu, C.R., Duan, L.B., Li, Q.Z. and Liang, C., 2008. CO_2 capture using CaO modified with ethanol/water solution during cyclic calcination/carbonation. Chemical Engineering & Technology, 31(2), pp. 237-244.

[98] Sun, R., Li, Y., Wu, S., Liu, C., Liu, H. and Lu, C., 2013. Enhancement of CO_2 capture capacity by modifying limestone with propionic acid. Powder Technology, 233, pp. 8-14.

[99] Li, Y., Sun, R., Liu, H. and Lu, C., 2011. Cyclic CO_2 capture behavior of limestone modified with pyroligneous acid (PA) during calcium looping cycles. Industrial & Engineering Chemistry Research, 50(17), pp. 10222-10228.

[100] Ridha, F.N., Manovic, V., Wu, Y., Macchi, A. and Anthony, E.J., 2013. Post-combustion CO_2 capture by formic acid-modified CaO-based sorbents. International Journal of Greenhouse Gas Control, 16, pp. 21-28.

[101] Ridha, F.N., Manovic, V., Macchi, A., Anthony, M.A. and Anthony, E.J., 2013. Assessment of limestone treatment with organic acids for CO_2 capture in Ca-looping cycles. Fuel Processing Technology, 116, pp. 284-291.

[102] Zhang, M., Peng, Y., Sun, Y., Li, P. and Yu, J., 2013. Preparation of $CaO–Al_2O_3$ sorbent and CO_2 capture performance at high temperature. Fuel, 111, pp. 636-642.

[103] Li, Y., Shi, L., Liu, C., He, Z. and Wu, S., 2015. Studies on CO_2 uptake by $CaO/Ca_3Al_2O_6$ sorbent in calcium looping cycles. Journal of Thermal Analysis and Calorimetry, 120(3), pp. 1519-1528.

[104] Li, Y., Su, M., Xie, X., Wu, S. and Liu, C., 2015. CO_2 capture performance of synthetic sorbent prepared from carbide slag and aluminum nitrate hydrate by combustion synthesis. Applied Energy, 145, pp. 60-68.

[105] Wang, K., Guo, X., Zhao, P. and Zheng, C., 2010. Cyclic CO_2 capture of CaO-based sorbent in the presence of metakaolin and aluminum (hydr)oxides. Applied Clay Science, 50(1), pp. 41-46.

[106] Li, C.C., Wu, U.T. and Lin, H.P., 2014. Cyclic performance of $CaCO_3$@ $mSiO_2$ for CO_2 capture in a calcium looping cycle. Journal of Materials Chemistry A, 2(22), pp. 8252-8257.

[107] Li, L., King, D.L., Nie, Z. and Howard, C., 2009. Magnesia-stabilized calcium oxide absorbents with improved durability for high temperature CO_2 capture. Industrial & Engineering Chemistry Research, 48(23), pp. 10604-10613.

[108] Zhao, M., Bilton, M., Brown, A.P., Cunliffe, A.M., Dvininov, E., Dupont, V., Comyn, T.P. and Milne, S.J., 2014. Durability of CaO-CaZrO3 sorbents for high-temperature CO_2 capture prepared by a wet chemical method. Energy & Fuels, 28(2), pp. 1275-1283.

[109] Luo, C., Zheng, Y., Ding, N. and Zheng, C., 2011. Enhanced cyclic stability of CO_2 adsorption capacity of CaO-based sorbents using La_2O_3 or $Ca_{12}Al_{14}O_{33}$ as additives. Korean Journal of Chemical Engineering, 28(4), pp. 1042-1046.

[110] Luo, C., Zheng, Y., Ding, N., Wu, Q., Bian, G. and Zheng, C., 2010. Development and performance of CaO/La_2O_3 sorbents during calcium looping cycles for CO_2 capture. Industrial & Engineering Chemistry Research, 49(22), pp. 11778-11784.

[111] Luo, C., Zheng, Y., Zheng, C., Yin, J., Qin, C. and Feng, B., 2013. Manufacture of calcium-based sorbents for high temperature cyclic CO_2 capture via a sol–gel process. International Journal of Greenhouse Gas Control, 12, pp. 193-199.

[112] Radfarnia, H.R. and Sayari, A., 2015. A highly efficient CaO-based CO_2 sorbent prepared by a citrate-assisted sol–gel technique. Chemical Engineering Journal, 262, pp. 913-920.

[113] Angeli, S.D., Martavaltzi, C.S. and Lemonidou, A.A., 2014. Development of a novel-synthesized Ca-based CO_2 sorbent for multicycle operation: parametric study of sorption. Fuel, 127, pp. 62-69.

[114] Wang, B., Yan, R., Lee, D.H., Zheng, Y., Zhao, H. and Zheng, C., 2011. Characterization and evaluation of Fe_2O_3/Al_2O_3 oxygen carrier prepared by sol–gel combustion synthesis. Journal of Analytical and Applied Pyrolysis, 91(1), pp. 105-113.

[115] Wang, B., Song, X., Wang, Z. and Zheng, C., 2014. Preparation and application of the sol–gel combustion synthesis-made $CaO/CaZrO_3$ sorbent for cyclic CO_2 capture through the severe calcination condition. Chinese Journal of Chemical Engineering, 22(9), pp. 991-999.

[116] Broda, M. and Müller, C.R., 2014. Sol–gel-derived, CaO-based, ZrO_2-stabilized CO_2 sorbents. Fuel, 127, pp. 94-100.

[117] Luo, C., Zheng, Y., Xu, Y., Ding, H., Zheng, C., Qin, C. and Feng, B., 2015. Cyclic CO_2 capture characteristics of a pellet derived from sol–gel CaO powder with $Ca_{12}Al_{14}O_{33}$ support. Korean Journal of Chemical Engineering, 31, pp. 1-5.

[118] Florin, N. and Fennell, P., 2011. Synthetic CaO-based sorbent for CO_2 capture. Energy Procedia, 4, pp. 830-838.

[119] Wang, M., Lee, C.G. and Ryu, C.K., 2008. CO_2 sorption and desorption efficiency of Ca_2SiO_4. International Journal of Hydrogen Energy, 33(21), pp. 6368-6372.

[120] Valverde, J.M., Perejón, A. and Perez-Maqueda, L.A., 2012. Enhancement of fast CO_2 capture by a nano-SiO_2/CaO composite at Ca-looping conditions. Environmental Science & Technology, 46(11), pp. 6401-6408.

[121] Luo, C., Zheng, Y., Ding, N., Wu, Q., Bian, G. and Zheng, C., 2010. Development and performance of CaO/La_2O_3 sorbents during calcium looping cycles for CO_2 capture. Industrial & Engineering Chemistry Research, 49(22), pp. 11778-11784.

[122] George, S.M., 2009. Atomic layer deposition: an overview. Chemical Reviews, 110(1), pp. 111-131.

[123] Puurunen, R.L., 2005. Surface chemistry of atomic layer deposition: A case study for the trimethylaluminum/water process. Journal of Applied Physics, 97(12), 9.

[124] Soria-Hoyo, C., Valverde, J.M., Van Ommen, J.R., Sánchez-Jiménez, P.E., Pérez-Maqueda, L.A. and Sayagués, M.J., 2015. Synthesis of a nanosilica supported CO_2 sorbent in a fluidized bed reactor. Applied Surface Science, 328, pp .548-553.

[125] Peng, W., Xu, Z., Luo, C. and Zhao, H., 2015. Tailor-Made Core–Shell $CaO/TiO_2–Al_2O_3$ Architecture as a High-Capacity and Long-Life CO_2 Sorbent. Environmental Science & Technology, 49(13), pp. 8237-8245.

[126] Peng, W., Xu, Z. and Zhao, H., 2016. Batch fluidized bed test of SATS-derived $CaO/TiO_2–Al_2O_3$ sorbent for calcium looping. Fuel, 170, pp. 226-234.

[127] Langereis, E., Heil, S.B.S., Knoops, H.C.M., Keuning, W., Van De Sanden, M.C.M. and Kessels, W.M.M., 2009. In situ spectroscopic ellipsometry as a versatile tool for studying atomic layer deposition. Journal of Physics D: Applied Physics, 42(7), 073001.

[128] Manovic, V. and Anthony, E.J., 2009. Screening of binders for pelletization of CaO-based sorbents for CO_2 capture. Energy & Fuels, 23(10), pp. 4797-4804.

[129] Wu, Y., Manovic, V., He, I. and Anthony, E.J., 2012. Modified lime-based pellet sorbents for high-temperature CO_2 capture: reactivity and attrition behavior. Fuel, 96, pp. 454-461.

[130] Ridha, F.N., Manovic, V., Wu, Y., Macchi, A. and Anthony, E.J., 2013. Pelletized CaO-based sorbents treated with organic acids for enhanced CO_2 capture in Ca-looping cycles. International Journal of Greenhouse Gas Control, 17, pp. 357-365.

[131] Ridha, F.N., Manovic, V., Macchi, A. and Anthony, E.J., 2012. High-temperature CO_2 capture cycles for CaO-based pellets with kaolin-based binders. International Journal of Greenhouse Gas Control, 6, pp. 164-170.

[132] Qin, C., Yin, J., An, H., Liu, W. and Feng, B., 2011. Performance of extruded particles from calcium hydroxide and cement for CO_2 capture. Energy & Fuels, 26(1), pp. 154-161.

[133] Sun, J., Liu, W., Hu, Y., Wu, J., Li, M., Yang, X., Wang, W. and Xu, M., 2016. Enhanced performance of extruded–spheronized carbide slag pellets for high temperature CO_2 capture. Chemical Engineering Journal, 285, pp. 293-303.

[134] Knight, A., Ellis, N., Grace, J.R. and Lim, C.J., 2014. CO_2 sorbent attrition testing for fluidized bed systems. Powder Technology, 266, pp. 412-423.

[135] Ridha, F.N., Lu, D.Y., Symonds, R.T. and Champagne, S., 2016. Attrition of CaO-based pellets in a 0.1 MW_{th} dual fluidized bed pilot plant for post-combustion CO_2 capture. Powder Technology, 291, pp. 60-65.

[136] Ridha, F.N., Wu, Y., Manovic, V., Macchi, A. and Anthony, E.J., 2015. Enhanced CO_2 capture by biomass-templated $Ca(OH)_2$-based pellets. Chemical Engineering Journal, 274, pp. 69-75.

[137] Erans, M., Beisheim, T., Manovic, V., Jeremias, M., Patchigolla, K., Dieter, H., Duan, L. and Anthony, E.J., 2016. Effect of SO_2 and steam on CO_2 capture performance of biomass-templated calcium aluminate pellets. Faraday Discussions, 192, pp. 97-111.

[138] Sun, J., Liu, W., Hu, Y., Li, M., Yang, X., Zhang, Y. and Xu, M., 2015. Structurally improved, core-in-shell, CaO-based Sorbent pellets for CO_2 capture. Energy & Fuels, 29(10), pp. 6636-6644.

[139] Manovic, V. and Anthony, E.J., 2011. CaO-based pellets with oxygen carriers and catalysts. Energy & Fuels, 25(10), pp. 4846-4853.

[140] Florin, N.H. and Harris, A.T., 2009. Reactivity of CaO derived from nano-sized $CaCO_3$ particles through multiple CO_2 capture-and-release cycles. Chemical Engineering Science, 64(2), pp. 187-191.

[141] Liu, W., Low, N.W., Feng, B., Wang, G. and Diniz da Costa, J.C., 2009. Calcium precursors for the production of CaO sorbents for multicycle CO_2 capture. Environmental Science & Technology, 44(2), pp. 841-847.

[142] Wu, S.F., Li, Q.H., Kim, J.N. and Yi, K.B., 2008. Properties of a nano CaO/Al_2O_3 CO_2 sorbent. Industrial & Engineering Chemistry Research, 47(1), pp. 180-184.

[143] Wu, S.F. and Zhu, Y.Q., 2010. Behavior of $CaTiO_3$/nano-CaO as a CO_2 reactive adsorbent. Industrial & Engineering Chemistry Research, 49(6), pp. 2701-2706.

[144] Ashgriz, N. ed., 2011. Handbook of atomization and sprays: theory and applications. Springer Science & Business Media.

[145] Lu, H., Khan, A., Pratsinis, S.E. and Smirniotis, P.G., 2008. Flame-made durable doped-CaO nanosorbents for CO_2 capture. Energy & Fuels, 23(2), pp. 1093-1100.

[146] Liu, W., Feng, B., Wu, Y., Wang, G., Barry, J. and Diniz da Costa, J.C., 2010. Synthesis of sintering-resistant sorbents for CO_2 capture. Environmental Science & Technology, 44(8), pp. 3093-3097.

[147] Li, L., King, D.L., Nie, Z., Li, X.S. and Howard, C., 2010. $MgAl_2O_4$ spinel-stabilized calcium oxide absorbents with improved durability for high-temperature CO_2 capture. Energy & Fuels, 24(6), pp. 3698-3703.

[148] Fennell P.S., Anthony E.J, 2015. End use of lime-based sorbents from calcium looping systems. Calcium and Chemical Looping Technology Power Generation Carbon Dioxide Capture, pp. 153–67.

[149] Wu, Y., Blamey, J., Anthony, E.J. and Fennell, P.S., 2010. Morphological changes of limestone sorbent particles during carbonation/calcination looping cycles in a thermogravimetric analyzer (TGA) and reactivation with steam. Energy & Fuels, 24(4), pp. 2768-2776.

[150] Yu, F.C., Phalak, N., Sun, Z. and Fan, L.S., 2011. Activation strategies for calcium-based sorbents for CO_2 capture: a perspective. Industrial & Engineering Chemistry Research, 51(4), pp. 2133-2142.

[151] Yin, J., Zhang, C., Qin, C., Liu, W., An, H., Chen, G. and Feng, B., 2012. Reactivation of calcium-based sorbent by water hydration for CO_2 capture. Chemical Engineering Journal, 198, pp. 38-44.

[152] Coppola, A., Salatino, P., Montagnaro, F. and Scala, F., 2014. Reactivation by water hydration of the CO_2 capture capacity of a calcium looping sorbent. Fuel, 127, pp. 109-115.

[153] Arias, B., Grasa, G.S. and Abanades, J.C., 2010. Effect of sorbent hydration on the average activity of CaO in a Ca-looping system. Chemical Engineering Journal, 163(3), pp. 324-330.

[154] Han, L., Wang, Q., Ma, Q., Guan, J., Luo, Z. and Cen, K., 2010. Hydration reactivation of CaO-based sorbent for cyclic calcination-carbonation reactions. In Proceedings of the 20th international conference on fluidized bed combustion (pp. 726-731). Springer Berlin Heidelberg.

[155] Manovic, V. and Anthony, E.J., 2007. Steam reactivation of spent CaO-based sorbent for multiple CO_2 capture cycles. Environmental Science & Technology, 41(4), pp. 1420-1425.

[156] Wang, J., Wu, Y. and Anthony, E.J., 2005. The hydration behavior of partially sulfated fluidized bed combustor sorbent. Industrial & Engineering Chemistry Research, 44(22), pp. 8199-8204.

[157] Fennell, P.S., Davidson, J.F., Dennis, J.S. and Hayhurst, A.N., 2007. Regeneration of sintered limestone sorbents for the sequestration of CO_2 from combustion and other systems. Journal of the Energy Institute, 80(2), pp. 116-119.

[158] Materić, B.V., Sheppard, C. and Smedley, S.I., 2010. Effect of repeated steam hydration reactivation on CaO-based sorbents for CO_2 capture. Environmental Science & Technology, 44(24), pp. 9496-9501.

[159] Martínez, I., Grasa, G., Murillo, R., Arias, B. and Abanades, J.C., 2011. Evaluation of CO_2 carrying capacity of reactivated CaO by hydration. Energy & Fuels, 25(3), pp. 1294-1301.

[160] Anthony, E.J., Jia, L., Woods, J., Roque, W. and Burwell, S., 2000. Pacification of high calcic residues using carbon dioxide. Waste Management, 20(1), pp. 1-13.

[161] Jia, L. and Anthony, E.J., 2000. Pacification of FBC ash in a pressurized TGA. Fuel, 79(9), pp. 1109-1114.

[162] Manovic, V., Lu, D. and Anthony, E.J., 2008. Steam hydration of sorbents from a dual fluidized bed CO_2 looping cycle reactor. Fuel, 87(15), pp. 3344-3352.

[163] Jia, L., Wang, J. and Anthony, E.J., 2003. Reactivation of fluidised bed combustor ash for sulphur capture. Chemical Engineering Journal, 94(2), pp. 147-154.

[164] Lu, D.Y., Hughes, R.W., Reid, T. and Anthony, E.J., 2009. Hydration and pelletization of $CaCO_3$-derived sorbents for in-situ CO_2 capture. In Proceedings of the 20th International Conference on Fluidized Bed Combustion (pp. 569-575). Springer Berlin Heidelberg.

[165] Manovic, V. and Anthony, E.J., 2011. Reactivation and remaking of calcium aluminate pellets for CO_2 capture. Fuel, 90(1), pp. 233-239.

[166] Manovic, V., Wu, Y., He, I. and Anthony, E.J., 2012. Spray water reactivation/pelletization of spent CaO-based sorbent from calcium looping cycles. Environmental Science & Technology, 46(22), pp. 12720-12725.

[167] Diego, M.E., Arias, B., Grasa, G. and Abanades, J.C., 2014. Design of a novel fluidized bed reactor to enhance sorbent performance in CO_2 capture systems using CaO. Industrial & Engineering Chemistry Research, 53(24), pp. 10059-10071.

[168] Anthony E.J., Lu D., Salvador C., 2003. Pre-treatment of lime-based sorbents using hydration. U.S Patent Application No.10/577,540.

[169] Valverde, J.M., Sanchez-Jimenez, P.E. and Perez-Maqueda, L.A., 2014. Calcium-looping for post-combustion CO_2 capture. On the adverse effect of sorbent regeneration under CO_2. Applied Energy, 126, pp. 161-171.

4 EFFECTS OF SO_2 AND STEAM ON CO_2 CAPTURE PERFORMANCE OF BIOMASS-TEMPLATED CALCIUM ALUMINATE PELLETS

María Erans[1], Theodor Beisheim[2], Vasilije Manovic[1], Michal Jeremias[1], Kumar Patchigolla[1], Heiko Dieter[2], Lunbo Duan[1] and Edward J Anthony[1]

[1] Combustion and CCS Centre, Cranfield University, Bedford, Bedfordshire, United Kingdom

[2] IFK, University of Stuttgart, Pfaffenwaldring 23, Stuttgart, United Kingdom

Submitted 29th February 2016, Accepted 29th March 2016

Published in Faraday Discussions, 2016, 192, 97-111.

DOI: 10.1039/c6fd00027d

Statement of contributions of joint authorship

María Erans conducted the literature review on the subject, planned and performed the experiments, drafter and critically reviewed this manuscript. Also, María analysed the results and produced figures and tables in this paper. Heiko Dieter and Theodor Beisheim assisted María Erans in carrying out the BFB experiments and in modifying the set-up of the plant. Vasilije Manovic, Michal Jeremias, Lunbo Duan, Kumar Patchigolla and Edward J Anthony proof-read and critically commented on the manuscript before its submission to Faraday Discussions.

Abstract

Four types of synthetic sorbents were developed for high-temperature post-combustion calcium looping CO_2 capture using Longcal limestone. Pellets were prepared with: lime and cement (LC); lime and flour (LF); lime, cement and flour (LCF); and lime, cement and flour doped with seawater (LCFSW). Flour was used as a templating material. All samples underwent 20 cycles in a TGA under two different calcination conditions. Moreover, the prepared sorbents were tested for 10 carbonation/calcination cycles in a 68 mm-internal-diameter

bubbling fluidized bed (BFB) in three environments: with no sulphur and no steam; in the presence of sulphur; and with steam. When compared to limestone, all the synthetic sorbents exhibited enhanced CO_2 capture performance in the BFB experiments, with the exception of the sample doped with seawater. In the BFB tests, the addition of cement binder during the pelletisation process resulted in the increase of CO_2 capture capacity from 0.08 g CO_2 per g sorbent (LF) to 0.15 g CO_2 per g sorbent (LCF) by the 10^{th} cycle. The CO_2 uptake in the presence of SO_2 dramatically declined by the 10^{th} cycle; for example, from 0.22 g CO_2 per g sorbent to 0.05 g CO_2 per g sorbent in the case of the untemplated material (LC). However, as expected all samples showed improved performance in the presence of steam, and the decay of reactivity during the cycles was less pronounced. Nevertheless, in the BFB environment, the templated pellets showed poorer CO_2 capture performance. This is presumably because of material loss due to attrition under the FB conditions. By contrast, the templated materials performed better than untemplated materials under TGA conditions. This indicates that the reduction of attrition is critical when employing templated materials in realistic systems with FB reactors.

4.1 Introduction

It is widely accepted that CO_2 emissions are the most contributing factor affecting climate change. Decreasing anthropogenic CO_2 emissions, especially from power sector, which accounted for at least one third of the total greenhouse gas emissions in 2010 [1] is one of the main goals of climate change mitigation strategies. Carbon capture and storage (CCS) has been proposed to mitigate CO_2 emission from power plants [2–5].

Currently, the carbon capture technology that is the closest to the market is amine scrubbing [4] with its first commercial-scale plant opened in October 2014 in Canada [6]. However, there are many problems associated with this technology such as degradation of the expensive solvent and the corrosive nature of typical solvents such as monoethanolamine (MEA) [7–13]. Due to these challenges other options are increasingly being explored for CO_2 capture, such as calcium looping (CaL) [14].

CaL systems are comprised of two interconnected fluidised beds which function as a carbonator and calciner respectively. The CO_2 is captured by a lime-based sorbent in the carbonator at 600–700 °C, and a high-purity CO_2 stream is produced in the calciner at 850–950 °C. This process has many advantages, such as the use of a cheap natural sorbent [15, 16] and a low energy penalty [17]. However, there are two major challenges associated with this technology: the sorbent reactivity decay over reaction cycles, and the attrition of the particles due to the mechanical and thermal stresses experienced in a fluidized bed environment. These challenges demand increasing sorbent makeup (i.e. the use of fresh sorbent) [18].

Considerable research efforts have been made towards developing new sorbents that have a more stable reactivity over many cycles, using techniques such as sol–gel combustion [19–27], organic/acid modifications [28–34], calcium carbonate precipitation [33, 35, 36], and granulation [37–44], among others. Most of these methods have proven to produce materials that have higher capture capacity than natural sorbents. However, although these modifications can result in a better sorbent performance, they are potentially

expensive due to the cost of the materials required and the use of multiple process steps [45, 46].

Granulation is a promising technique for the preparation of sorbents; it allows chemical doping and also the improvement of mechanical strength using binders such as bentonites, kaolin, alumina and calcium aluminate cements, and it appears to be easily scalable. Recently, Ridha et al. [43] explored the templating of pellets using cheap biomass sources; the resulting sorbent displayed a higher pore volume and CO_2 capture than biomass-free pellets.

Doping has also been previously explored as a means to reduce the decay of activity of natural materials. Salvador et al. [47] demonstrated that NaCl improved the relative capture capacity by maintaining it at 40% after 10 cycles due to the resulting changes in the pore structure for TGA tests. However, NaCl markedly decreased the CO_2 capture of the treated lime when tested in a fluidised bed reactor (FBR) compared to the untreated material. Other materials such as KCl and K_2CO_3 [48], manganese salts [49], MgCl and $Mg(NO_3)_2$ [50] and $CaBr_2$ [51,52] have also produced improvement in pore structure, pore volume and pore size. However, in some cases, alkali-metal precursors used as dopants, such as lithium chloride, produced poorer performance in the treated sample than that of natural limestone [53].

The reduction in reactivity over many cycles is aggravated by the presence of SO_2, due to the irreversible reaction between CaO and SO_2 to form $CaSO_4$ [54–56]. Unfortunately, calcium sulphate is stable at typical CaL temperatures, whichleads to a dramatic decay in carbonation conversions during the cycling due to the formation of a $CaSO_4$ layer. Pacciani et al. [57] discovered that sulfation is enhanced in carbonation/calcination cycles for synthetic sorbents. Stanmore and Gilot [58] reported that the simultaneous capture of CO_2 and SO_2 causes more sintering than SO_2 capture alone.

The use of pelletised material in the presence of SO_2 has been studied by Manovic and Anthony [59]. They found that particles composed of lime and calcium aluminate cement exhibited a higher sulfation rate (89%) than that of natural limestone (30%). Ridha et al. [60] also studied the effect of sulfation in

pelletised particles prepared using kaolin as a binder; the results showed strong deactivation of all sorbents tested, but it was more pronounced in the case of the pelletised material, which is in agreement with previous results from the same group [59].

Steam is always present in flue gas due to the combustion process, and it has been experimentally simulated by, for example, 15 vol% steam addition during the carbonation stages of CO_2 capture experiments [61,62]. These studies show that the presence of steam increased the CO_2 uptake substantially in a bench-scale FBC, possibly due to enhanced solid-state diffusion in the product layer [63].

This work explores the effect of SO_2 and steam on calcium aluminate pellets as cheap synthetic CaL sorbents, templated by biomass and doped with seawater. CO_2 uptake was measured during the carbonation/calcination cycling of the sorbent performed using a TGA, and a bubbling FB was used to provide realistic test conditions and to allow us to study the effects of attrition.

4.2 Experimental

4.2.1 Materials

Longcal limestone from the United Kingdom was used as a lime precursor. Commercial calcium aluminate cement, CA-14, manufactured by Almatis Inc., was used as a binder in the pelletisation process and as a source of Al_2O_3. Commercial flour was used as the biomass templating material. Artificial seawater (Complete Aquatics) was used for doping purposes; this water is treated with NaOCl, to leave only a small additional amount of Na and Cl.

4.2.2 Pellet preparation procedure

Four types of materials were prepared: (i) 10% calcium aluminate cement and 90% calcined limestone (LC), (ii) 10% flour and 90% calcined limestone (LF), (iii) 10% flour, 10% calcium aluminate cement and 80% calcined limestone (LCF), and (iv) 10% flour, 10% calcium aluminate cement and 80% calcined lime doped with seawater (LCFSW). The pellets were prepared in a Glatt TMG

1/6 granulator. The desired powder proportional quantities (1 kg batches) were introduced into the pelletizer vessel (4 L) and mixed. The mixing was carried out inside the vessel by two sets of blades (the chopper and the agitator) while continuously spraying with water (ca. 1 L during the procedure) for pelletisation. A more detailed explanation of this procedure can be found in the work done by Manovic et al. [64]. The particles were then sieved and the size fraction 0.3–0.6 mm was collected. The material was air dried for 24 h before storage and the samples produced are described in Table 4-1.

Table 4-1: Materials used in the preparation of samples

Sample	Lime (wt %)	Calcium aluminate cement (wt %)	Flour (wt %)	Type of water used in the pelletisation process
LC	90	10	0	Deionized water
LF	90	0	10	Deionized water
LCF	80	10	10	Deionized water
LCFSW	80	10	10	Seawater

4.2.3 CO_2 capture cycles

A Perkin Elmer Diamond TG/DTA thermogravimetric analyser (TGA) was used for repeated carbonation/calcination cycles. The samples were tested under two conditions; in the first, carbonation was performed for 20 min at 650 °C under 15% CO_2, while the calcination was carried out for 10 min at 850 °C under 100% N_2. In the second round of tests, the carbonation was performed for 20 min at 650 °C under 15% CO_2, and the calcination was carried out for 10 min at 950 °C under 100% CO_2. Under the latter set of conditions, during the transition between calcination and carbonation, the atmosphere was switched to 100% N_2 below 900 °C to avoid carbonation under non-desired conditions. The heating ramp was set to 40 °C min^{-1} for the heating stage and 20 °C min^{-1} for the cooling stage. All the sorbents underwent 20 cycles with the first calcination performed in air to allow the combustion of the biomass.

In addition to the TGA, a lab-scale bubbling fluidised bed (BFB) was used for testing carbonation/calcination cycles to ensure testing under more realistic

conditions [65]. The BFB was 68 mm ID; it was operated at atmospheric pressure and heated to the desired temperature by means of an external electric furnace. The distributor plate consists of four bubble caps and a cyclone downstream of the fluidised bed is used to avoid excessive particle concentration in the flue gas. After the cyclone, the gas was filtered and cooled. A fraction of the exhaust gas was continuously sampled to measure CO_2 and SO_2 concentration with ABB EL3020 infrared (CO_2 and SO_2) photometers in order to monitor the progress of the reactions. The layout of the experimental equipment used is exhibited in Figure 4-1.

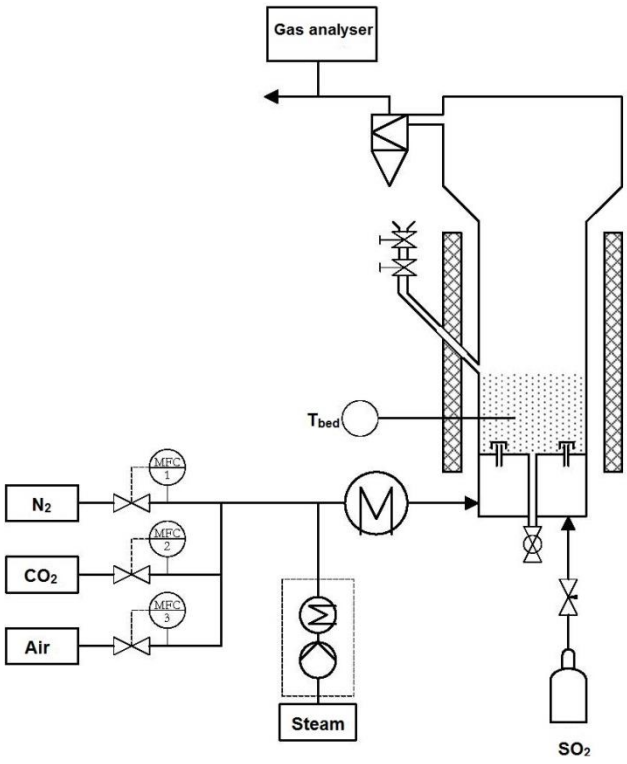

Figure 4-1: Overview of laboratory-scale fluidised-bed system

For the BFB tests, 100 g of sorbent was diluted with 1.5 kg of silica sand to avoid excessive increase of temperature in the bed during carbonation. Due to the temperature change limitations caused by the thermal inertia of the BFB, all the experiments were performed isothermally at 850 °C with 90 vol% CO_2 during the carbonation and 20 vol% CO_2 during the calcination. The duration of both calcination and carbonation was 15 min (with the first calcination performed in air to allow the combustion of the biomass).

The effects of sulphur and steam were also investigated in the BFB following the same procedure as above with a sand-diluted bed and isothermal conditions for carbonation/calcination at 850 °C. To measure the effect of SO_2 a new series of experiments was performed. For these tests, the concentration of CO_2 was maintained at the same level as in the experiments with no SO_2. The SO_2 concentration was set to 1500 ppm for both carbonation and calcination, simulating non-desulphurised flue gas from high-sulphur-coal combustion entering the carbonator and burning high-sulphur coal in the oxy-fuel calciner.66 A high impact on the carbonation degree and the CO_2 uptake was expected. The concentration of oxygen during carbonation and calcination was kept constant at 3 vol%.

The effect of steam was also studied in the BFB. The steam is normally present both in the calciner and carbonator due to the moisture content in fuels and due to steam formation during combustion. The selected steam content was 15 vol% during the carbonation and calcination, in accordance with previously published work [63]. The CO_2 concentration during calcination was maintained at 20 vol% on a wet basis, and during the carbonation the CO_2 concentration was set at 80 vol% on a wet basis.

For all the fluidised-bed experiments, 10 cycles were performed while maintaining the bed velocity at 0.5 m s^{-1} (bubbling regime) for the whole duration of each experiment.

4.2.4 Sample characterization

Elementary analysis of the samples was performed using ICP-OES (inductively coupled plasma optical emission spectrometry). Compression strength tests were performed using an FGE-5XY Digital Force Gauge. For each sample, 31 measurements were made to ensure the validity of the data for the raw material. Mercury porosimetry was performed using an AutoPore IV 9500 for analysis of the total pore area and porosity.

4.3 Results and discussion

4.3.1 Sorbent characterization

The ICP-OES and carbon analyses of the limestone and the samples are given in Table 4-2.

Table 4-2: Elementary analysis of the sorbents used

Component (wt %)	Limestone	LC	LF	LCF	LCFSW
Al_2O_3	0.082	5.63	0.218	4.73	5.22
BaO	0.007	0.007	0.007	0.005	0.015
CaO	53.9	58.4	58.2	52.4	57.3
Fe_2O_3	0.015	0.033	0.040	0.027	0.030
K_2O	0.007	0.006	0.037	0.023	0.051
MgO	0.185	0.208	0.210	0.197	0.335
MnO_2	0.008	0.008	0.009	0.008	0.010
Na_2O	0.053	0.071	0.052	0.056	0.806
P_2O_5	0.007	0.011	0.035	0.022	0.012
SO_3	0.034	0.039	0.122	0.055	0.234
SiO_2	0.701	1.20	0.770	0.267	0.292
SrO	0.017	0.018	0.018	0.017	0.018
TiO_2	0.006	0.015	0.013	0.006	0.007
Total oxides	55.1	65.7	59.7	57.8	64.4
TC (total carbon)	42.7	12.8	28.1	25.6	15.4
Water at 105°C	0.10	0.10	0.10	0.10	0.10
Water at 950°C	0.10	22.3	15.9	20.5	23.1
Total	98.0	100.8	103.8	103.9	102.9

Raw pellets made from calcined limestone and 10% aluminate cement (LC) show the highest crushing strength resistance (Figure 4-2). It was expected that cement-containing pellets (LC and LCF) would have higher crushing strength than non-cement containing particles (LF) due to the presence of cement. However, LCFSW was also prepared with a cement containing mixture and its crushing strength is very low. It is possible that the lower crushing strength is due to the negative effects of seawater doping, probably caused by the excess

of NaCl in the dopant media [67]. Limestone was not tested for crushing strength due to the small particle size (average size of 180 mm) when compared to the size range of the materials produced (300–600 mm).

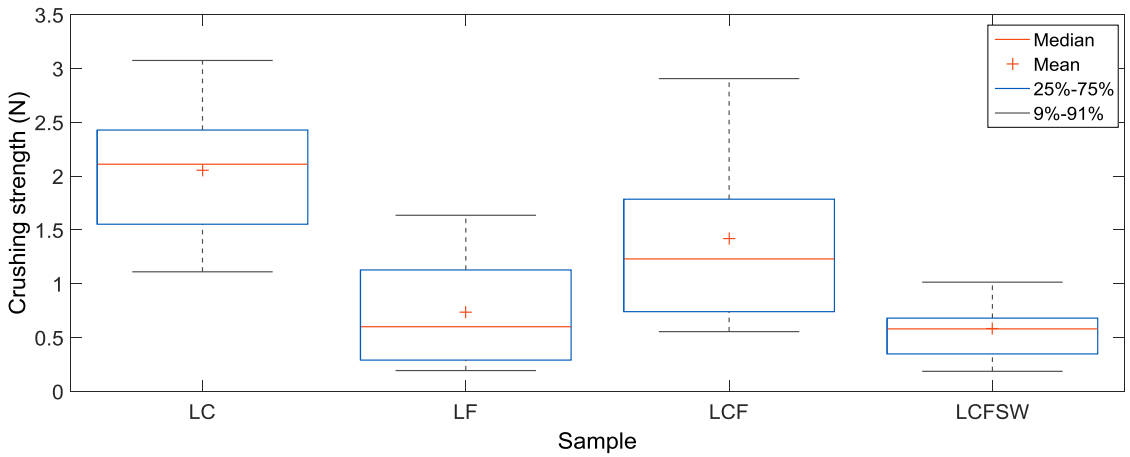

Figure 4-2: Crushing strength of non-calcined samples

In Table 4-3, the results of mercury porosimetry for LC and LCF are shown in order to compare the effect that the addition of flour has on the sorbent pore size. As expected, the addition of flour has a positive effect, increasing both the porosity and the total pore area of the resulting material.

Table 4-3: Mercury porosimetry for LC and LCF

Sample	Porosity (%)	Total pore area (m^2 g^{-1})
LC	53.3	14.95
LCF	68.4	17.173

4.3.2 Reactivity tests

4.3.2.1 TGA tests

The final TGA results over 20 cycles under the previously mentioned conditions are shown in Figure 4-3 (samples calcined at 850 °C in pure N_2) and Figure 4-4 (samples calcined at 950 °C in pure CO_2). The main aim of these tests was to compare the synthetic sorbents prepared using the pelletisation method in order

to assess if flour or any similar material used as a biomass-templating material would be suitable for calcium looping processes.

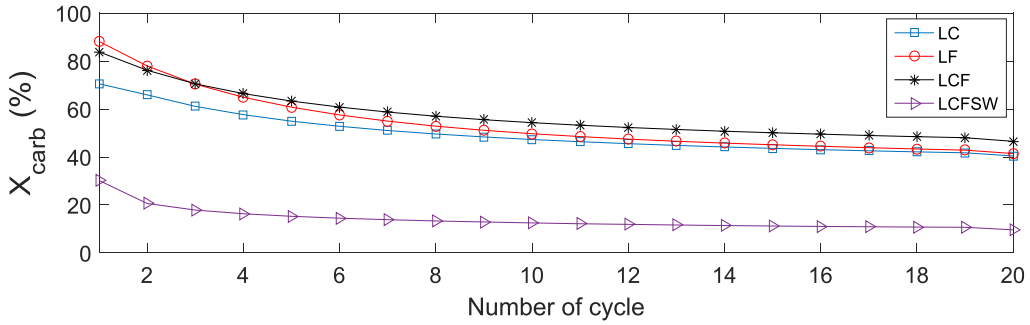

Figure 4-3: TGA carbonation conversion of sorbents calcined under N_2 atmosphere (10 min calcination at 850 °C in 100 vol% N_2 and 20 min carbonation at 650 °C in 15 vol% CO_2)

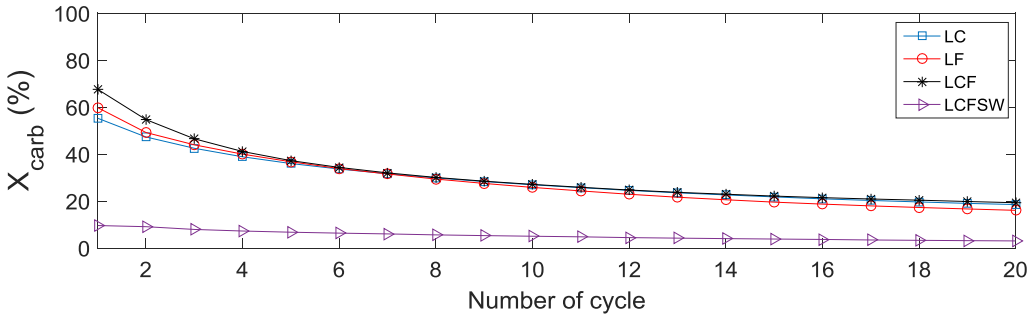

Figure 4-4: TGA carbonation conversion of sorbents calcined under CO_2 atmosphere (10 min calcination at 950 °C in 100 vol% CO_2 and 20 min carbonation at 650 °C in 15 vol% CO_2)

The carbonation conversion of all pellets was higher when they were calcined at 850 °C in pure N_2 (Figure 4-3) compared to the calcination at 950 °C in pure CO_2 (Figure 4-4). The use of seawater (LCFSW) instead of deionized water (LCF) during the pelletisation process had a very dramatic effect in terms of decreasing the carbonation conversion from 16% to 3% in the 20th cycle in CO_2 calcination conditions (and from 46.5% to 9.6% in the case of calcination with pure N_2;Figure 4-3). The other samples showed quite uniform behaviour for the calcination in pure CO_2 (Figure 4-4). In the tests performed under mild conditions (calcination at 850 °C in pure N_2; Figure 4-3), the biomass-templated pellets (both LF and LCF) showed better carbonation conversions than LC in

the first ten cycles, but afterwards their conversions remained only slightly higher (6%) than the conversion for LC.

4.3.2.2 BFB tests

The behaviour of the pellets compared to the original limestone in a real BFB over 10 cycles is shown in Figure 4-5. It can be seen that all of the pellets performed better than the initial limestone after the third cycle. The sorbent performance was increased from 0.03 g CO_2 per g sorbent for the limestone to 0.22 g CO_2 per g sorbent for LC, 0.07 g CO_2 per g sorbent for LF, 0.12 g CO_2 per g sorbent for LCF and 0.05 g CO_2 per g sorbent for LCFSW in the 10th cycle.

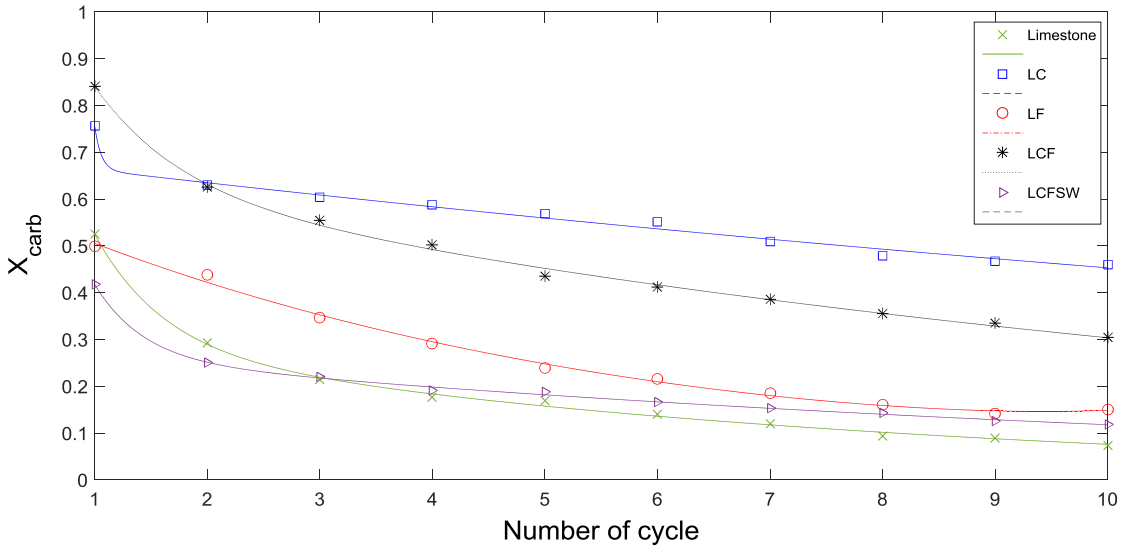

Figure 4-5: Carbonation conversion of the prepared pellets and original limestone in BFB; carbonation at 850 °C for 15 min; calcination at 850 °C for 15 min

It can be observed that the addition of calcium aluminate cement has a clear effect on the biomass-doped pellets, increasing their CO_2 uptake by 71% (LCF compared to LF). This phenomenon can be attributed to the presence of the mesoporous Al_2O_3 phase, which increases the porosity of the sample [68], as well as the increased attrition resistance and decreased elutriation rate.

LCFSW pellets exhibited only a marginal improvement of 0.02 g CO_2 per g sorbent by the 10th cycle (compared to the limestone), indicating that doping

with seawater did not increase the performance of the sorbent. It was also apparent that the addition of biomass to LC reduced the CO_2 uptake from 0.22 g CO_2 per g sorbent to 0.12 g CO_2 per g sorbent by the 10th cycle. This suggests that flour templating of the pellets did not improve the resistance towards degradation experienced during the carbonation–calcination cycles.

Figure 4-6 shows how the sorbents behaved under high SO_2 concentration conditions (1500 ppm). Here, all sorbents behaved poorly when compared to the results without SO_2 addition (Figure 4-5). Even in the case of the best sorbent, LC, there was a significant loss of activity. In this case, the CO_2 capture capacity declined from 0.22 g CO_2 per g sorbent to 0.05 g CO_2 per g sorbent by the 10th cycle. This highlights the need to desulphurise flue gas, especially when dealing with synthetic sorbents.

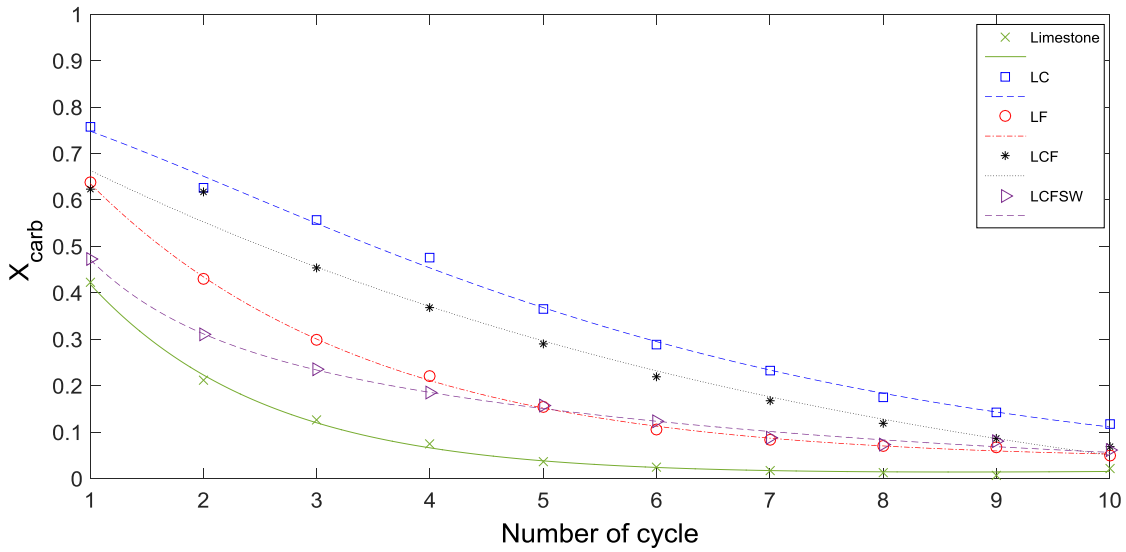

Figure 4-6: Carbonation conversion of pellets and original limestone with 1500 ppm SO_2; carbonation at 850 °C for 15 min; calcination at 850 °C for 15 min in BFB

For the biomass-containing materials (LF, LCF and LCFSW) the capacity after 10 cycles was found to be very similar at around 5% carbonation. This also represents (when compared to Figure 4-5) a very dramatic decline, especially for LCF, which had a 31% carbonation degree in the 10th cycle without SO_2 addition. These results can be explained by the progressive build-up of a sulfate

layer, which reduces CO_2 diffusion in the pores of the pellets and limestone particles [69].

The effect of steam addition on *Xcarb* is shown in Figure 4-7. The addition of steam increased the degree of carbonation for all the sorbents. In accordance with previous observations, such as those of Ridha et al. [40], the drastic decline observed in the first cycle when cycling without steam is no longer observed when the steam is introduced. In the 10th cycle, LC had a CO_2 uptake of 0.25 g CO_2 per g sorbent, which is 14% more than in the case without steam. LCF adsorbed 25% more CO_2 (0.12 g CO_2 per g sorbent to 0.15 g CO_2 per g sorbent) in the 10th cycle. The other sorbents (limestone, LF and LCFSW) also improved their capture capacity but their CO_2 uptake was still below 0.1 g CO_2 per g sorbent.

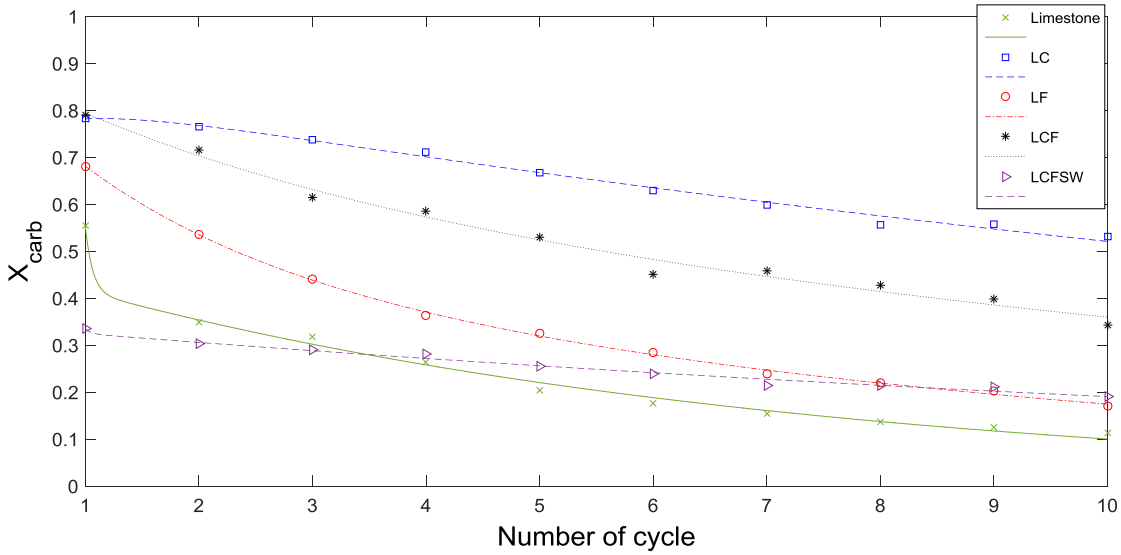

Figure 4-7: Carbonation conversion of pellets and original limestone with 15% steam in BFB; carbonation at 850 °C for 15 min; calcination at 850 °C for 15 min

4.4 Conclusions

This work examined the CO_2 capture performance of CaO-based sorbents (limestone, calcium aluminate pellets, biomass-doped pellets with and without binder, and biomass-templated pellets doped with seawater). All of the biomass-containing pellets were made from flour chosen as a cheap biomass source to enhance the CO_2 uptake. The biomass-free pellets showed superior

capture capacity compared with the biomass-containing pellets when cycles were performed in a BFB; the non-biomass-containing sample (LC) had the highest capacity in all cases. However, when pellets were tested in a TGA under both conditions (calcination at 850 °C in pure N_2 and calcination at 950°C, 100% CO_2), the biomass and cement-containing pellets (LCF) had the highest conversion. It appears that the biomass-containing pellets are more prone to attrition, so their mechanical strength needs to be improved during the preparation process. This increased attrition is in agreement with the crushing strength results, where the biomass-containing particles showed markedly lower results than biomass-free particles. The CO_2 uptake by the biomass-free pellets (LC) in the 10th cycle was 0.22 g CO_2 per g sorbent under normal conditions, 0.25 g CO_2 per g sorbent with 15 vol% of steam and 0.05 g CO_2 per g sorbent under 1500 ppm of SO_2 during carbonation and calcination, indicating a very dramatic effect of sulphur addition. The most important difference between the biomass-containing material (LF) and the biomass and cement containing material (LCF) is the presence of a binder (10% calcium aluminate cement in LCF), which has a great impact with a 71.4% higher CO_2 uptake for the cement-containing sample under normal conditions, an 87.5% increase of CO_2 uptake for the same pellets with 15 vol% steam, and around the same conversion under high sulphur conditions. Although biomass-templating for pelletising Ca-based sorbents could be a beneficial technique to improve reactivity, it is clear that a means of increasing mechanical strength is required, and that attrition for these systems needs to be better understood.

4.5 References

[1] UNEP, The Emissions Gap Report 2012, United Nations Environment Programme (UNEP), Nairobi, Kenya, 2012.

[2] Siefert N.S., and Litster, S., 2013. Exergy and economic analyses of advanced IGCCCCS and IGFC-CCS power plants, Applied Energy, 107, pp. 315–328.

[3] Boot-Handford, M.E., Abanades, J.C., Anthony, E.J., Blunt, M.J., Brandani, S., Mac Dowell, N., Fernández, J.R., Ferrari, M.C., Gross, R., Hallett, J.P. and

Haszeldine, R.S., 2014. Carbon capture and storage update. Energy & Environmental Science, 7(1), pp. 130-189.

[4] Fan, L.S., 2011. Chemical looping systems for fossil energy conversions. John Wiley & Sons.

[5] Herzog, H., Eliasson, B. and Kaarstad, O., 2000. Capturing greenhouse gases. Scientific American, 282(2), pp .72-79.

[6] Idem, R., Wilson, M., Tontiwachwuthikul, P., Chakma, A., Veawab, A., Aroonwilas, A. and Gelowitz, D., 2006. Pilot plant studies of the CO_2 capture performance of aqueous MEA and mixed MEA/MDEA solvents at the University of Regina CO_2 capture technology development plant and the boundary dam CO_2 capture demonstration plant. Industrial & Engineering Chemistry Research, 45(8), pp. 2414-2420.

[7] Supap, T., Idem, R., Tontiwachwuthikul, P. and Saiwan, C., 2006. Analysis of monoethanolamine and its oxidative degradation products during CO_2 absorption from flue gases: A comparative study of GC-MS, HPLC-RID, and CE-DAD analytical techniques and possible optimum combinations. Industrial & Engineering Chemistry Research, 45(8), pp. 2437-2451.

[8] Veawab, A., Tontiwachwuthikul, P. and Chakma, A., 2001. Investigation of low-toxic organic corrosion inhibitors for CO_2 separation process using aqueous MEA solvent. Industrial & Engineering Chemistry Research, 40(22), pp. 4771-4777.

[9] Aaron, D. and Tsouris, C., 2005. Separation of CO_2 from flue gas: a review. Separation Science and Technology, 40(1-3), pp. 321-348.

[10] Chi, S. and Rochelle, G.T., 2002. Oxidative degradation of monoethanolamine. Industrial & Engineering Chemistry Research, 41(17), pp. 4178-4186.

[11] Goff, G.S. and Rochelle, G.T., 2004. Monoethanolamine degradation: O_2 mass transfer effects under CO_2 capture conditions. Industrial & Engineering Chemistry Research, 43(20), pp. 6400-6408.

[12] Fytianos, G., Ucar, S., Grimstvedt, A., Hyldbakk, A., Svendsen, H.F. and Knuutila, H.K., 2016. Corrosion and degradation in MEA based post-combustion CO_2 capture. International Journal of Greenhouse Gas Control, 46, pp. 48-56.

[13] Li, K., Leigh, W., Feron, P., Yu, H. and Tade, M., 2016. Systematic study of aqueous monoethanolamine (MEA)-based CO_2 capture process: techno-economic assessment of the MEA process and its improvements. Applied Energy, 165, pp. 648-659.

[14] Blamey, J., Anthony, E.J., Wang, J. and Fennell, P.S., 2010. The calcium looping cycle for large-scale CO_2 capture. Progress in Energy and Combustion Science, 36(2), pp .260-279.

[15] Lasheras, A., Ströhle, J., Galloy, A. and Epple, B., 2011. Carbonate looping process simulation using a 1D fluidized bed model for the carbonator. International Journal of Greenhouse Gas Control, 5(4), pp. 686-693.

[16] Dean, C.C., Blamey, J., Florin, N.H., Al-Jeboori, M.J. and Fennell, P.S., 2011. The calcium looping cycle for CO_2 capture from power generation, cement manufacture and hydrogen production. Chemical Engineering Research and Design, 89(6), pp. 836-855.

[17] Romano, M.C., 2012. Modeling the carbonator of a Ca-looping process for CO_2 capture from power plant flue gas. Chemical Engineering Science, 69(1), pp. 257-269.

[18] Lu, D.Y., Hughes, R.W. and Anthony, E.J., 2008. Ca-based sorbent looping combustion for CO_2 capture in pilot-scale dual fluidized beds. Fuel Processing Technology, 89(12), pp. 1386-1395.

[19] Luo, C., Zheng, Y., Ding, N. and Zheng, C., 2011. Enhanced cyclic stability of CO_2 adsorption capacity of CaO-based sorbents using La_2O_3 or $Ca_{12}Al_{14}O_{33}$ as additives, Korean Journal of Chemical Engineering, 28 (4), pp. 1042–1046.

[20] Luo, C., Zheng, Y., Ding, N., Wu, Q., Bian, G. and Zheng, C., 2010. Development and performance of CaO/La_2O_3 sorbents during calcium looping

cycles for CO_2 capture. Industrial & Engineering Chemistry Research, 49(22), pp. 11778-11784.

[21] Luo, C., Zheng, Y., Zheng, C., Yin, J., Qin, C. and Feng, B., 2013. Manufacture of calcium-based sorbents for high temperature cyclic CO_2 capture via a sol–gel process. International Journal of Greenhouse Gas Control, 12, pp. 193-199.

[22] Radfarnia, H.R. and Sayari, A., 2015. A highly efficient CaO-based CO_2 sorbent prepared by a citrate-assisted sol–gel technique. Chemical Engineering Journal, 262, pp. 913-920.

[23] Angeli, S.D., Martavaltzi, C.S. and Lemonidou, A.A., 2014. Development of a novel-synthesized Ca-based CO_2 sorbent for multicycle operation: parametric study of sorption. Fuel, 127, pp. 62-69.

[24] Wang, B., Yan, R., Lee, D.H., Zheng, Y., Zhao, H. and Zheng, C., 2011. Characterization and evaluation of Fe_2O_3/Al_2O_3 oxygen carrier prepared by sol–gel combustion synthesis. Journal of Analytical and Applied Pyrolysis, 91(1), pp. 105-113.

[25] Wang, B., Song, X., Wang, Z. and Zheng, C., 2014. Preparation and application of the sol–gel combustion synthesis-made $CaO/CaZrO_3$ sorbent for cyclic CO_2 capture through the severe calcination condition. Chinese Journal of Chemical Engineering, 22(9), pp .991-999.

[26] Broda, M., Müller, C. R., 2014. Sol –gel-derived, CaO-based, ZrO_2-stabilized CO_2 sorbents. Fuel, 127, pp. 94–100.

[27] Luo, C., Zheng, Y., Xu, Y., Ding, H., Zheng, C., Qin, C. and Feng, B., 2015. Cyclic CO_2 capture characteristics of a pellet derived from sol–gel CaO powder with $Ca_{12}Al_{14}O_{33}$ support. Korean Journal of Chemical Engineering, 31, pp. 1-5.

[28] Zhang, M., Peng, Y., Sun, Y., Li, P. and Yu, J., 2013. Preparation of CaO–Al_2O_3 sorbent and CO_2 capture performance at high temperature. Fuel, 111, pp. 636-642.

[29] Li, Y., Shi, L., Liu, C., He, Z. and Wu, S., 2015. Studies on CO_2 uptake by $CaO/Ca_3Al_2O_6$ sorbent in calcium looping cycles. Journal of Thermal Analysis and Calorimetry, 120(3), pp. 1519-1528.

[30] Li, Y., Su, M., Xie, X., Wu, S. and Liu, C., 2015. CO_2 capture performance of synthetic sorbent prepared from carbide slag and aluminum nitrate hydrate by combustion synthesis. Applied Energy, 145, pp .60-68.

[31] Wang, K., Guo, X., Zhao, P. and Zheng, C., 2010. Cyclic CO_2 capture of CaO-based sorbent in the presence of metakaolin and aluminum hydroxides. Applied Clay Science, 50(1), pp. 41-46.

[32] Li, C.C., Wu, U.T. and Lin, H.P., 2014. Cyclic performance of $CaCO_3@mSiO_2$ for CO_2 capture in a calcium looping cycle. Journal of Materials Chemistry A, 2(22), pp. 8252-8257.

[33] Li, L., King, D.L., Nie, Z. and Howard, C., 2009. Magnesia-stabilized calcium oxide absorbents with improved durability for high temperature CO_2 capture. Industrial & Engineering Chemistry Research, 48(23), pp. 10604-10613.

[34] Zhao, M., Bilton, M., Brown, A.P., Cunliffe, A.M., Dvininov, E., Dupont, V., Comyn, T.P. and Milne, S.J., 2014. Durability of $CaO-CaZrO_3$ sorbents for high-temperature CO_2 capture prepared by a wet chemical method. Energy & Fuels, 28(2), pp. 1275-1283.

[35] Gupta, H. and Fan, L.S., 2002. Carbonation− calcination cycle using high reactivity calcium oxide for carbon dioxide separation from flue gas. Industrial & Engineering Chemistry Research, 41(16), pp. 4035-4042.

[36] Florin, N. and Fennell, P., 2011. Synthetic CaO-based sorbent for CO_2 capture. Energy Procedia, 4, pp .830-838.

[37] Manovic, V. and Anthony, E.J., 2009. Screening of binders for pelletization of CaO-based sorbents for CO_2 capture. Energy & Fuels, 23(10), pp. 4797-4804.

[38] Wu, Y., Manovic, V., He, I. and Anthony, E.J., 2012. Modified lime-based pellet sorbents for high-temperature CO_2 capture: reactivity and attrition behavior. Fuel, 96, pp. 454-461.

[39] Ridha, F.N., Manovic, V., Wu, Y., Macchi, A. and Anthony, E.J., 2013. Pelletized CaO-based sorbents treated with organic acids for enhanced CO_2 capture in Ca-looping cycles. International Journal of Greenhouse Gas Control, 17, pp.357-365.

[40] Ridha, F.N., Manovic, V., Macchi, A. and Anthony, E.J., 2012. High-temperature CO_2 capture cycles for CaO-based pellets with kaolin-based binders. International Journal of Greenhouse Gas Control, 6, pp. 164-170.

[41] Qin, C., Yin, J., An, H., Liu, W. and Feng, B., 2011. Performance of extruded particles from calcium hydroxide and cement for CO_2 capture. Energy & Fuels, 26(1), pp. 154-161.

[42] Knight, A., Ellis, N., Grace, J.R. and Lim, C.J., 2014. CO_2 sorbent attrition testing for fluidized bed systems. Powder Technology, 266, pp. 412-423.

[43] Ridha, F.N., Wu, Y., Manovic, V., Macchi, A. and Anthony, E.J., 2015. Enhanced CO_2 capture by biomass-templated $Ca(OH)_2$-based pellets. Chemical Engineering Journal, 274, pp .69-75.

[44] Manovic, V. and Anthony, E.J., 2011. CaO-based pellets with oxygen carriers and catalysts. Energy & Fuels, 25(10), pp. 4846-4853.

[45] Sun, P., Grace, J.R., Lim, C.J. and Anthony, E.J., 2008. Investigation of attempts to improve cyclic CO_2 capture by sorbent hydration and modification. Industrial & Engineering Chemistry Research, 47(6), pp. 2024-2032.

[46] Ridha, F.N., Manovic, V., Macchi, A., Anthony, M.A. and Anthony, E.J., 2013. Assessment of limestone treatment with organic acids for CO_2 capture in Ca-looping cycles. Fuel Processing Technology, 116, pp. 284-291.

[47] Salvador, C., Lu, D., Anthony, E.J. and Abanades, J.C., 2003. Enhancement of CaO for CO_2 capture in an FBC environment. Chemical Engineering Journal, 96(1), pp. 187-195.

[48] González, B., Blamey, J., McBride-Wright, M., Carter, N., Dugwell, D., Fennell, P. and Abanades, J.C., 2011. Calcium looping for CO_2 capture: sorbent enhancement through doping. Energy Procedia, 4, pp. 402-409.

[49] Sun, R., Li, Y., Liu, H., Wu, S. and Lu, C., 2012. CO_2 capture performance of calcium-based sorbent doped with manganese salts during calcium looping cycle. Applied Energy, 89(1), pp. 368-373.

[50] Al-Jeboori, M.J., Fennell, P.S., Nguyen, M. and Feng, K., 2012. Effects of different dopants and doping procedures on the reactivity of CaO-based sorbents for CO_2 capture. Energy & Fuels, 26(11), pp. 6584-6594.

[51] Manovic, V., Fennell, P.S., Al-Jeboori, M.J. and Anthony, E.J., 2013. Steam-enhanced calcium looping cycles with calcium aluminate pellets doped with bromides. Industrial & Engineering Chemistry Research, 52(23), pp. 7677-7683.

[52] Al-Jeboori, M.J., Nguyen, M., Dean, C. and Fennell, P.S., 2013. Improvement of limestone-based CO_2 sorbents for Ca looping by HBr and other mineral acids. Industrial & Engineering Chemistry Research, 52(4), pp. 1426-1433.

[53] Reddy, E.P. and Smirniotis, P.G., 2004. High-temperature sorbents for CO_2 made of alkali metals doped on CaO supports. The Journal of Physical Chemistry B, 108(23), pp. 7794-7800.

[54] Grasa, G.S., Alonso, M. and Abanades, J.C., 2008. Sulfation of CaO particles in a carbonation/calcination loop to capture CO_2. Industrial & Engineering Chemistry Research, 47(5), pp.1630-1635.

[55] Manovic, V. and Anthony, E.J., 2010. Competition of sulphation and carbonation reactions during looping cycles for CO_2 capture by CaO-based sorbents. The Journal of Physical Chemistry A, 114(11), pp. 3997-4002.

[56] Wu, Y., Wang, C., Tan, Y., Jia, L. and Anthony, E.J., 2011. Characterization of ashes from a 100 kW_{th} pilot-scale circulating fluidized bed with oxy-fuel combustion. Applied Energy, 88(9), pp. 2940-2948.

[57] Pacciani, R., Müller, C.R., Davidson, J.F., Dennis, J.S. and Hayhurst, A.N., 2009. Performance of a novel synthetic Ca-based solid sorbent suitable for desulfurizing flue gases in a fluidized bed. Industrial & Engineering Chemistry Research, 48(15), pp. 7016-7024.

[58] Stanmore, B.R. and Gilot, P., 2005. Review—calcination and carbonation of limestone during thermal cycling for CO_2 sequestration. Fuel Processing Technology, 86(16), pp. 1707-1743.

[59] Manovic, V., Anthony, E.J. and Loncarevic, D., 2009. SO_2 retention by CaO-based sorbent spent in CO_2 looping cycles. Industrial & Engineering Chemistry Research, 48(14), pp. 6627-6632.

[60] Ridha, F.N., Manovic, V., Macchi, A. and Anthony, E.J., 2012. The effect of SO_2 on CO_2 capture by CaO-based pellets prepared with a kaolin derived $Al(OH)_3$ binder. Applied Energy, 92, pp. 415-420.

[61] Donat, F., Florin, N.H., Anthony, E.J. and Fennell, P.S., 2012. Influence of high-temperature steam on the reactivity of CaO sorbent for CO_2 capture. Environmental Science & Technology, 46(2), pp. 1262-1269.

[62] Arias, B., Grasa, G., Abanades, J.C., Manovic, V. and Anthony, E.J., 2012. The effect of steam on the fast carbonation reaction rates of CaO. Industrial & Engineering Chemistry Research, 51(5), pp. 2478-2482.

[63] Manovic, V. and Anthony, E.J., 2010. Carbonation of CaO-based sorbents enhanced by steam addition. Industrial & Engineering Chemistry Research, 49(19), pp. 9105-9110.

[64] Manovic, V., Wu, Y., He, I. and Anthony, E.J., 2012. Spray water reactivation/pelletization of spent CaO-based sorbent from calcium looping cycles. Environmental Science & Technology, 46(22), pp. 12720-12725.

[65] Alonso, M., Criado, Y.A., Abanades, J.C. and Grasa, G., 2014. Undesired effects in the determination of CO_2 carrying capacities of CaO during TG testing. Fuel, 127, pp. 52-61.

[66] Coppola, A., Montagnaro, F., Salatino, P. and Scala, F., 2012. Fluidized bed calcium looping: the effect of SO_2 on sorbent attrition and CO_2 capture capacity. Chemical Engineering Journal, 207, pp. 445-449.

[67] Fennell, P.S., Pacciani, R., Dennis, J.S., Davidson, J.F. and Hayhurst, A.N., 2007. The effects of repeated cycles of calcination and carbonation on a variety of different limestones, as measured in a hot fluidized bed of sand. Energy & Fuels, 21(4), pp. 2072-2081.

[68] Manovic, V. and Anthony, E.J., 2009. CaO-based pellets supported by calcium aluminate cements for high-temperature CO_2 capture. Environmental Science & Technology, 43(18), pp. 7117-7122.

[69] Krishnan, S.V. and Sotirchos, S.V., 1994. Effective diffusivity changes during calcination, carbonation, recalcination, and sulfation of limestones. Chemical Engineering Science, 49(8), pp.1 195-208.

5 FRAGMENTATION OF BIOMASS-TEMPLATED CAO-BASED PELLETS

María Erans[1], Francesca Cerciello[2], Antonio Coppola[3], Osvalda Senneca[3], Fabrizio Scala[2], Vasilije Manovic[1] and Edward J Anthony[1]

[1] Combustion and CCS Centre, Cranfield University, Bedford, Bedfordshire, United Kingdom

[2] Dipartimento di Ingegneria Chimica dei Materiali e della Produzione Industriale, Università degli Studi di Napoli Federico II, P.le Tecchio 80, Naples, Italy

[3] Istituto di Ricerche sulla Combustione (C.N.R.), P.le Tecchio 80, Naples, Italy

Submitted 13th June 2016, Accepted 19th Semptember 2016

Published in Fuel, 2017, 187, 388-397

DOI: 10.1016/j.fuel.2016.09.061

Statement of contributions of joint authorship

María Erans conducted the literature review on the subject, planned and performed the experiments, drafter and critically reviewed this manuscript. Also, María analysed the results and produced figures and tables in this paper. Francesca Cerciello and Antonio Coppola assisted María Erans in carrying out the BFB and PHSR experiments. Vasilije Manovic, Osvalda Senneca, Fabrizio Scala and Edward J Anthony proof-read and critically commented on the manuscript before its submission to Fuel.

Abstract

The use of biomass templating materials with a cheap production method as an enhanced sorbent for CO_2 uptake has been proposed recently. However, the attrition and fragmentation behaviour of this type of material, which is a vital parameter for calcium looping sorbents, has not yet been investigated in detail. In this work the fragmentation behaviour of biomass-templated sorbents is

investigated. Three types of materials were prepared using a mechanical pelletiser: 1. lime and cement (LC); 2. lime and flour (LF); and 3. lime, cement and flour (LCF). These samples were heat treated in a pressurised heated strip reactor (PHSR) and in a bubbling fluidised bed (BFB) and changes in particle size distribution were measured to assess fragmentation. Results indicated that the addition of biomass enhances the propensity to undergo fragmentation. Upon heat treatment in the PHSR the particle size of LC was not modified significantly; on the contrary the mean particle diameter of LF decreased from 520 μm to 116 μm and that of LCF from 524 μm to 290 μm. Fragmentation tests in the BFB confirmed the trend: 67% of the particles of LF fragmented, against 53% of LCF and 18% of LC samples. The addition of cement to the LF samples partially counteracts this performance degradation with respect to attrition. However, calcium aluminate pellets (LC) showed the lowest rate of fragmentation amongst all of the samples tested.

Keywords: Calcium looping; Pellets; Biomass templating; Fragmentation

Highlights:

• Biomass-templated materials using flour as a cheap source of biomass were produced.

• Fragmentation was tested in PHSR and BFB simulating conditions at calciner entrance.

• Biomass addition was detrimental to the fragmentation resistance of the particles.

• This effect was partially neutralised by the inclusion of cement in the production.

• Results from both PHSR and BFB agreed in terms of behaviour of all particle types.

5.1 Introduction

Calcium looping (CaL) is a second-generation carbon capture technology, which uses a lime sorbent in dual fluidised-bed reactors; this technology depends on the following reversible exothermic calcium oxide carbonation reaction:

The typical reactor set-up consists of two interconnected fluidised-bed reactors. In the first reactor (the carbonator) the CaO-based sorbent captures CO_2 from power plant flue gas; this reaction occurs at a practical rate at 650–700 °C [1-3]. The carbonated sorbent is then transferred to the second reactor (the calciner) where CO_2 is released at high temperatures (850–950 °C). The regenerated material is then returned to the carbonator for the next cycle. However, there are several challenges with CaO-based sorbent whose CO_2 uptake decreases with increasing number of carbonation/calcination cycles. This decline in activity is mainly due to sintering during calcination because of the high temperatures necessary for calcination [4-8]. The CO_2 capture capacity of the fresh sorbent drops quickly during the initial cycles until an asymptotic value is achieved after about 20 or 30 cycles, which then remains almost constant over subsequent cycles and adopts typical values of about 0.08 g CO_2/gsorbent in the case of limestone [9]. This reduction in performance can be partially compensated by increasing the Ca/C ratio in the reactor (by increasing the purge of spent sorbent and the make-up ratio) or by modifying the properties of the particles [10]. However, this deactivation can also be caused by sulphation or ash fouling [11].

Natural sorbents (limestone and dolomite) are attractive due to their low cost, ready availability and, in the case of limestones, the potential suitability of the CaL purge material for the cement industry [12, 13]. However, significant research efforts are being made to modify limestone sorbents or create new synthetic sorbents using techniques such as sol-gel combustion [14-18], organic acid modifications [19-23], co-precipitation [24, 25] and granulation [26-32]. Such materials exhibited higher CO_2 uptake, in general, when compared to natural lime-based sorbents. However, the cost of these sorbents increases due

to such complex production procedures and the cost of the additives and may become prohibitively expensive.

One of the methods proposed to improve the performance of calcium looping sorbents was biomass templating [30]. Such biomass is potentially a cheap material for increasing the porosity of pelletised sorbents. Ridha et al. [30] observed that the capture capacity was 0.41 g CO_2/gsorbent after 20 cycles in the presence of 15% steam for sorbents with 10% of powdered leaves incorporated into the sorbent. This was an increase of 33.3% when compared to the untemplated materials after both samples underwent 20 cycles. The use of flour as a biomass templating material has been studied by Erans et al. [32]. These materials were tested in both a thermogravimetric analyser (TGA) and a bubbling fluidised bed (BFB), and the synthesised materials were shown to exhibit better performance than natural limestone. However, under BFB conditions the templated materials demonstrated higher rates of fragmentation and attrition compared to calcium aluminate pellets without the addition of biomass.

Attrition of lime based sorbents has been extensively investigated in previous studies [33-36]. There are several attrition/fragmentation mechanisms: primary fragmentation, which occurs when the sorbent is injected into the reactor due to thermal stresses and overpressures caused by CO_2 release from the calcination reaction; secondary fragmentation, which occurs due to mechanical stresses from collisions between particles and bed internals; and attrition by abrasion, which is also caused by mechanical stresses but generates finer particles when compared to secondary fragmentation [37]. It has also been reported that the attrition rate was higher during the initial cycles and then subsequently decreased [38, 39].

Previous results have shown the beneficial effect of biomass addition for the CO_2 uptake, as well as demonstrating the enhanced porous structure of the templated samples. However, there are discrepancies between TGA results and BFB results; and these differences are believed to be due to attrition and fragmentation. This work explores the effect of biomass templating in calcium

aluminate pellets with regard to fragmentation. Three different types of materials: one with the addition of calcium aluminate cement (LC), another with flour addition (LF) and one with both (LCF) have been tested in two different types of reactors; namely a pressurised heated strip reactor (PHSR) and bubbling fluidised bed under different conditions.

5.2 Experimental

5.2.1 Materials

Longcal limestone from the UK was used as a lime precursor. Commercial calcium aluminate cement, CA-14, manufactured by Almantis, was used as a binder in the pelletisation process and as a source of Al_2O_3. Commercial flour was used as the biomass templating material.

5.2.2 Pellet preparation procedure

Three types of materials were produced: (i) 10% calcium aluminate cement and 90% calcined limestone (LC); (ii) 10% flour and 90% calcined limestone (LF); and (iii) 10% flour, 10% calcium aluminate cement and 80% calcined limestone (LCF). The particles were prepared introducing the desired proportional quantities in 1 kg batches into a pelletiser vessel (4 L). The mixing took place inside the vessel by means of a chopper and agitator under a continuous water spray. A more detailed explanation of this procedure can be found elsewhere [27]. After pelletisation of the samples, the particles were sieved to different particle sizes. The material was air dried for 24 h before storage. The weight percentage of materials used in each sample can be found in Table 5-1.

Table 5-1: Materials used

Sample	Lime (wt %)	Calcium aluminate cement (wt %)	Flour (wt %)
LC	90	10	0
LF	90	0	10
LCF	80	10	10

5.2.3 Fragmentation experiments

For the fragmentation experiments two experimental systems have been used: a pressurised heated strip reactor and a bubbling fluidised bed.

The apparatus used for the first round of tests (the PHSR) achieves a heating rate of 4000 °C/s. Batches of particles of 500–710 μm are placed on the strip and heated up by physical contact with the strip and by thermal radiation from the semi-spherical cover of the reactor. Further details of this reactor are available elsewhere [40]. Tests have been carried out at 1 bar and 950 °C in pure N_2. The final temperature was held for 30 s in all experiments. After the test, particles were recovered and the experiments were repeated on fresh particles numerous times (~10–15 times) in order to collect a sufficiently large amount of material to perform further particle size analyses.

Further fragmentation tests were carried out in a lab-scale BFB in order to reproduce conditions typical of the first calcinations step. The BFB had a 40 mm ID, and was operated at atmospheric pressure and heated to the desired temperature by means of an external electric furnace. Calcination of the particles was performed under two conditions: 100 vol% air and 70 vol% CO_2/30 vol% air. The calcination time for all the experiments was 20 min to ensure complete calcination. These tests were repeated for two different particle size ranges: 500–710 μm and 250–500 μm.

For the BFB tests, 20 g of sorbent was diluted in 150 g of silica (particle size distribution of 850–1000 μm) sand to avoid excessive decrease of temperature in the bed during calcination, due to the endothermic reaction of the sorbent. All the experiments were performed isothermally at 900 °C.

It is important to note that in the present work the focus is on the first calcination step due to the fact that the highest attrition rate occurs in the first cycle rather than in the following cycles. Therefore, this first calcination is considered to provide a good indication of sorbent attrition behaviour [41, 42].

5.2.4 Sample characterisation

The biomass-containing materials (LF and LCF) were analysed by TGA in a Netzsch STA409 CD apparatus in order to investigate the effect of biomass pyrolysis and combustion throughout calcination of the templated sorbents. Two different types of tests have been carried out, namely, pyrolysis-calcination and combustion-calcination tests.

In pyrolysis-calcination tests the sample was dried in argon at 110 °C, and then the temperature was taken to 900 °C in argon with a ramp rate of 5 °C/min. At 900 °C the gas was switched from argon to air and the samples were held at isothermal conditions for 60 min, before being cooled at a rate of 20 °C/min.

In combustion-calcination tests the sample was exposed to air flow from the very beginning. It was dried at 110 °C and then taken to 370 °C with the heating rate of 10 °C/min. An isothermal step of 10 min in air was performed at 370 °C to allow combustion of biomass. Finally, the sample was heated to 900 °C at a similar heating rate and kept at this temperature for 10 min to allow calcination.

Approximately 30 mg of sample were used for each experiment, with a gas flow rate of 200 mL/min. In the case of LCF, additional tests were performed for the following particle size ranges: 710–500 μm and 250–500 μm in order to investigate the effect of particle size.

Sample morphology was observed with a FEI Inspect S Scanning Electron Microscope (SEM) with 20 kV of accelerating voltage under high vacuum. The calcined samples were put in the SEM chamber together with the ceramic pan. Before the analysis, the samples were coated with gold to avoid excessive charging. The porosimetry was studied using an AutoPore IV 9500 with mercury intrusion.

The particle size distribution was measured using the Mastersizer 2000 (Malvern, UK) and acetone was used as a carrier liquid. For X-ray diffraction analysis (XRD) a D2 Phaser (Bruker, Germany) apparatus with Cu Kα radiation (30 kV, 10 mA) was used. Scattered X-ray intensities were recorded between $2\theta = 5$ and 75° with a scan velocity of $0.052\theta\ s^{-1}$.

5.3 Results and discussion

5.3.1.1 Sorbent characterisation

Figure 5-1 and Figure 5-2 report the mass loss profiles obtained during TGA experiments of pyrolysis-calcination and combustion-calcination.

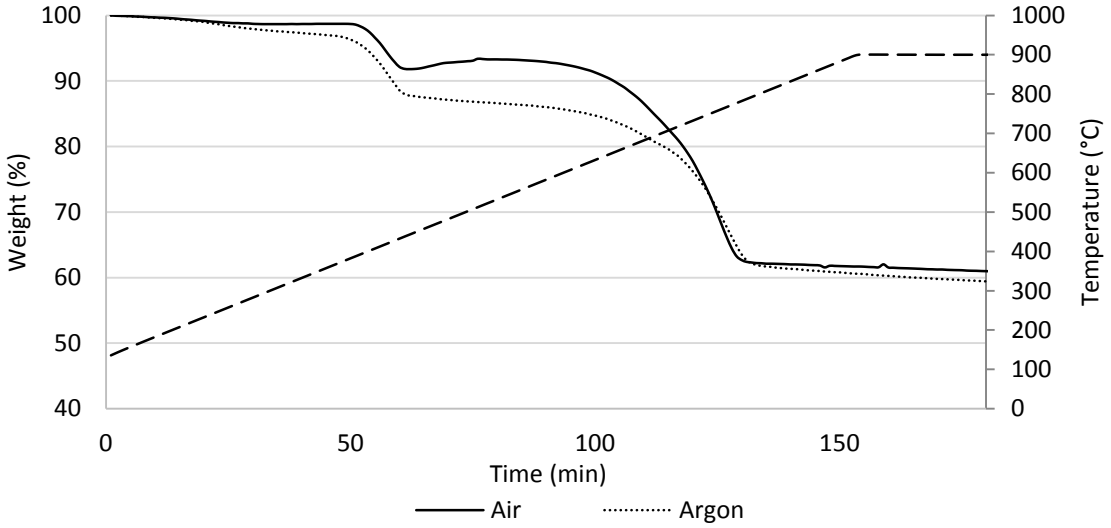

Figure 5-1: TG (%) and temperature of tests in air and argon of LF

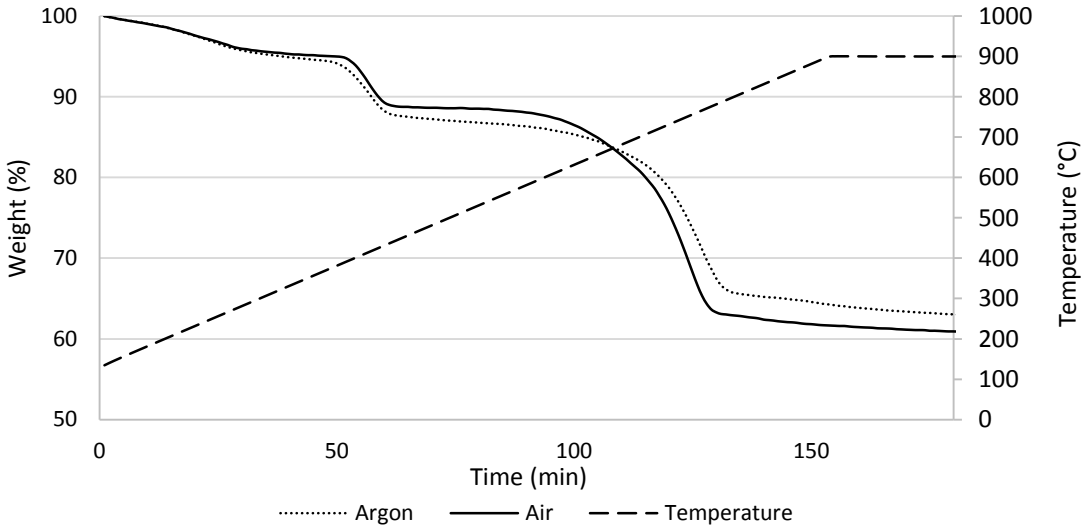

Figure 5-2: TG (%) and temperature of tests in air and argon of LCF

In the case of LF a first stage of mass loss is observed between 350 and 450 °C followed by a second stage of mass loss between 650 and 700 °C, which can be associated with flour pyrolysis and sorbent calcination, respectively.

Interestingly, the mass appears to be higher under pyrolysis conditions than under combustion, possibly due to the concurrent uptake of H_2O/CO_2 from air. In the combustion-calcination test a more noticeable uptake of CO_2 is evident above 450 °C. The release of CO_2 at still higher temperature supports the similar value of 60%, which is observed for the final residue after both pyrolysis-calcination and combustion-calcination of the flour templated samples.

In the case of LCF two stages of mass loss are observed associated with flour pyrolysis and sorbent calcination. The effect of CO_2 uptake in the combustion-calcination test is less striking for LCF than for LF, due to the smaller percentage of lime in LCF.

The fact that the final residue of the combustion-calcination tests exceeds that of the pyrolysis-calcination tests by 5% suggests that some structural changes in the cement phase might have occurred in air.

Figure 5-3, Figure 5-4 and Figure 5-5 show typical SEM images of LC, LF and LCF, respectively, after calcination. There are clear differences in structure: it is evident that the LC has a more compact structure, whilst LF has a more porous surface, as can be seen in Figure 5-4, due to the addition of flour, which creates mesopores in the structure. LCF displays a mixture of both structures, and it is definitely denser than LF; however, it has smaller pores and a more porous structure than LC.

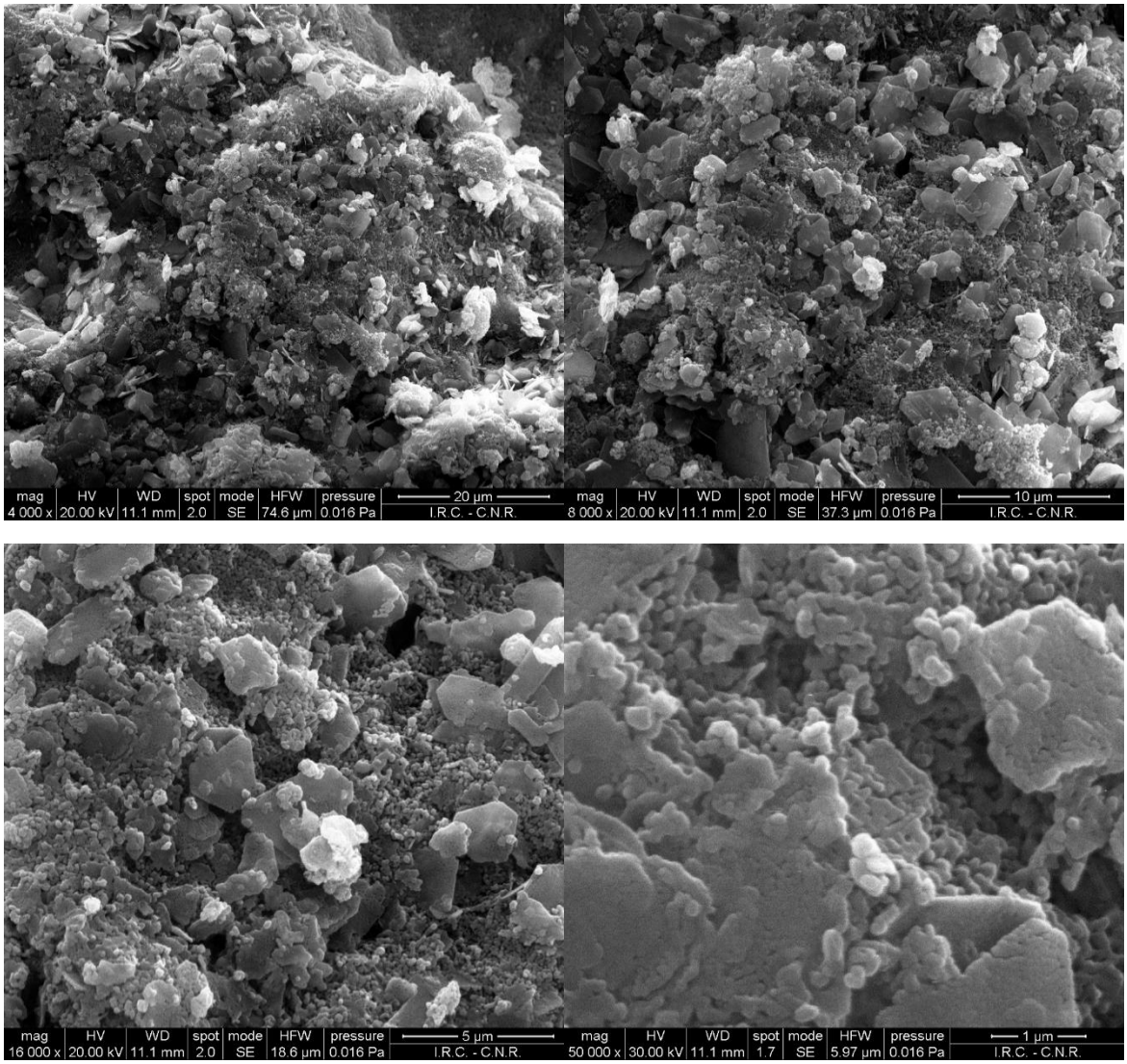

Figure 5-3: SEM images of calcined LC at 20 kV and different magnifications

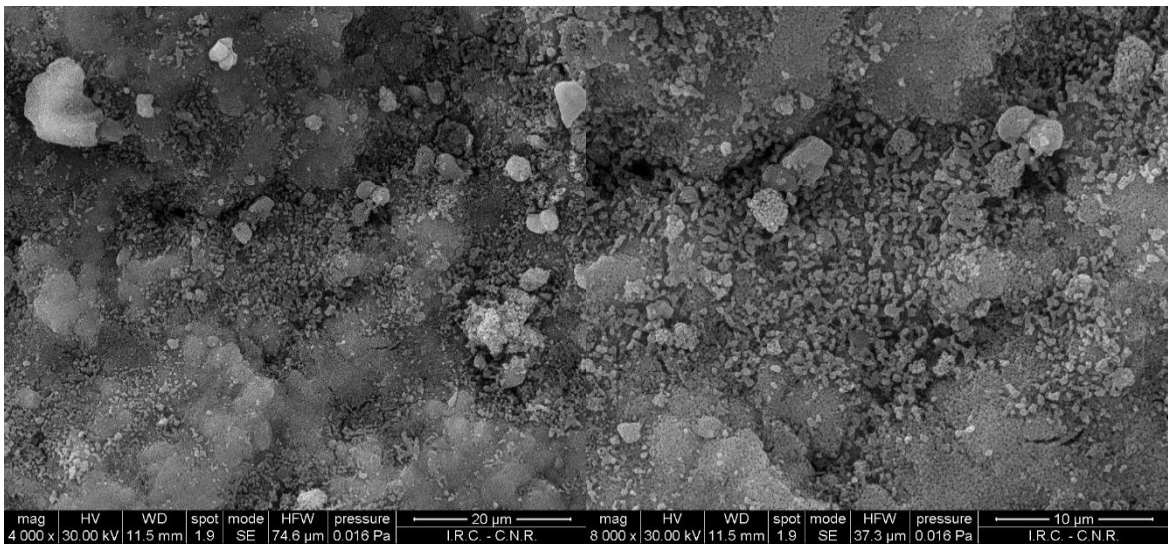

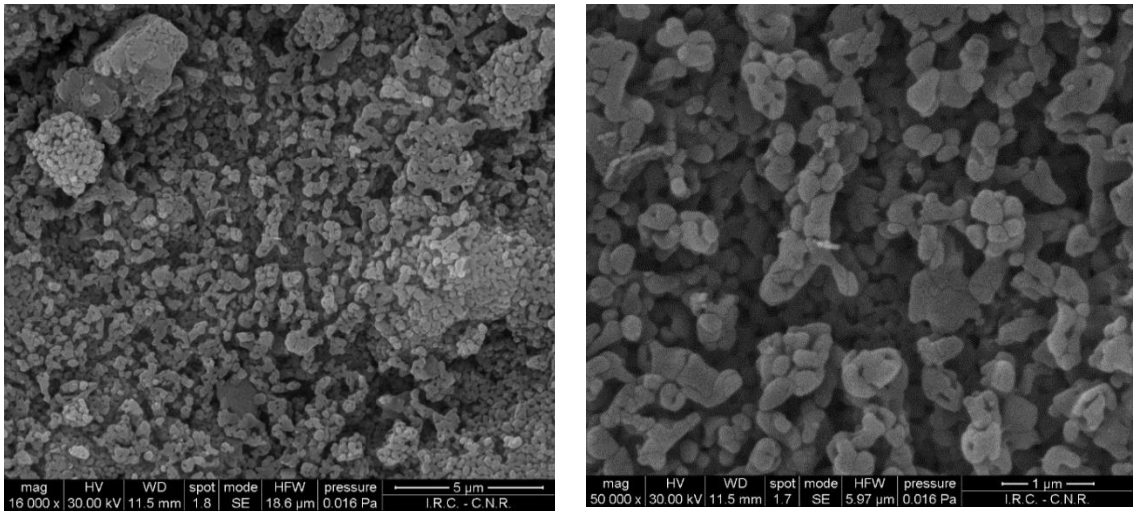

Figure 5-4: SEM images of calcined LF at 20 kV and different magnifications

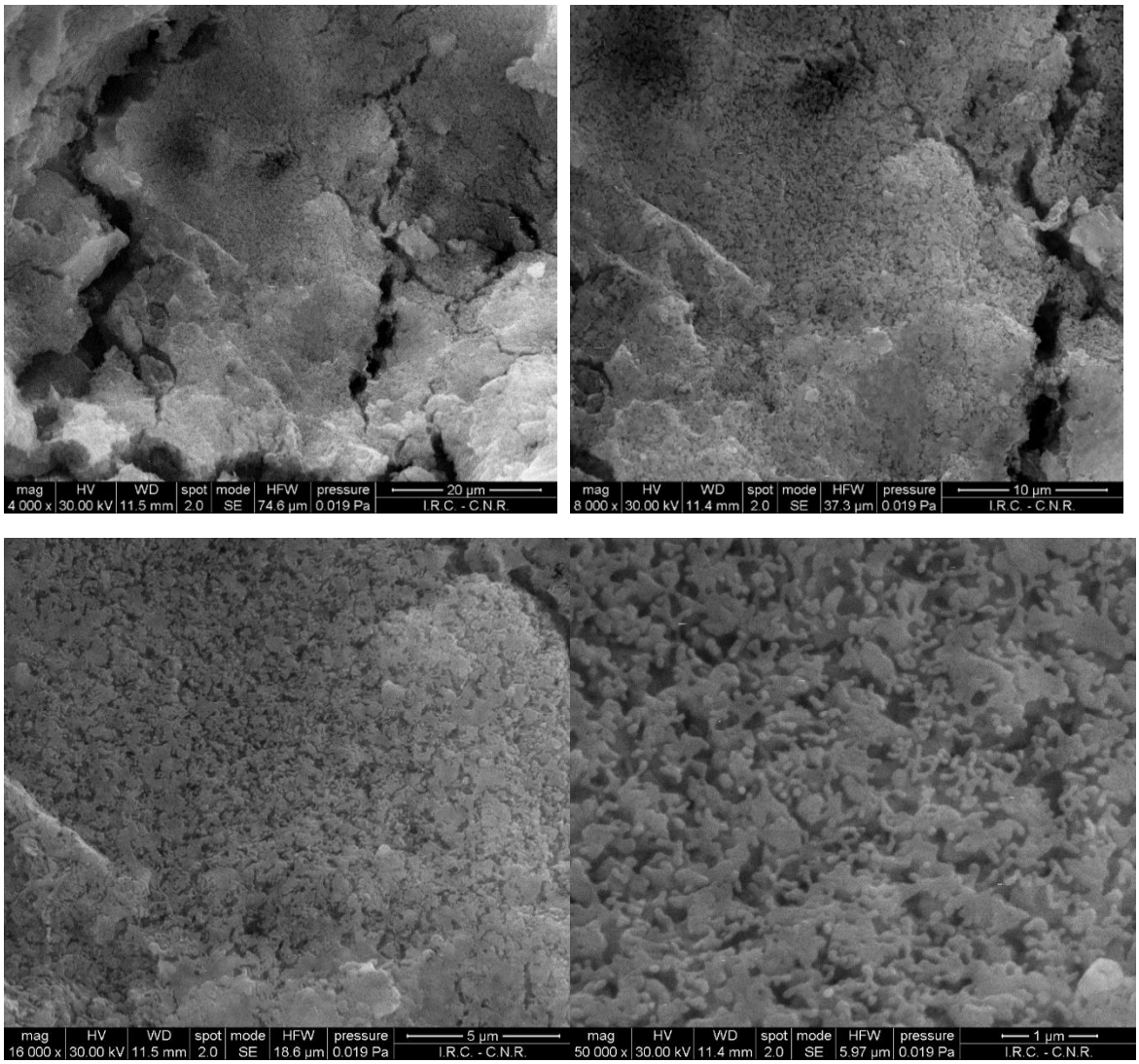

Figure 5-5: SEM images of calcined LCF at 20 kV and different magnifications

In Figure 5-6 the mercury intrusion pore volume (dV/dD) is shown. From these data, it can be inferred that there is a difference in the pore size distribution. In LC, there is a greater amount of larger pores (around 100 nm) than in LF and LCF and this was expected due to the addition of biomass; this addition creates smaller pores, as has been mentioned above. However, it can be seen that the total pore surface area is lower in the sample with biomass-only templating (LF) with a total pore area of 13.2 m^2/g compared to 15.0 m^2/g (LC). Further, this seems to be mitigated when adding cement, as the pore area is increased to 17.12 m^2/g (LCF). This increase in area is believed to be related to the mesoporous Al_2O_3 phase formed by the addition of the calcium aluminate cement in the pelletisation process [43].

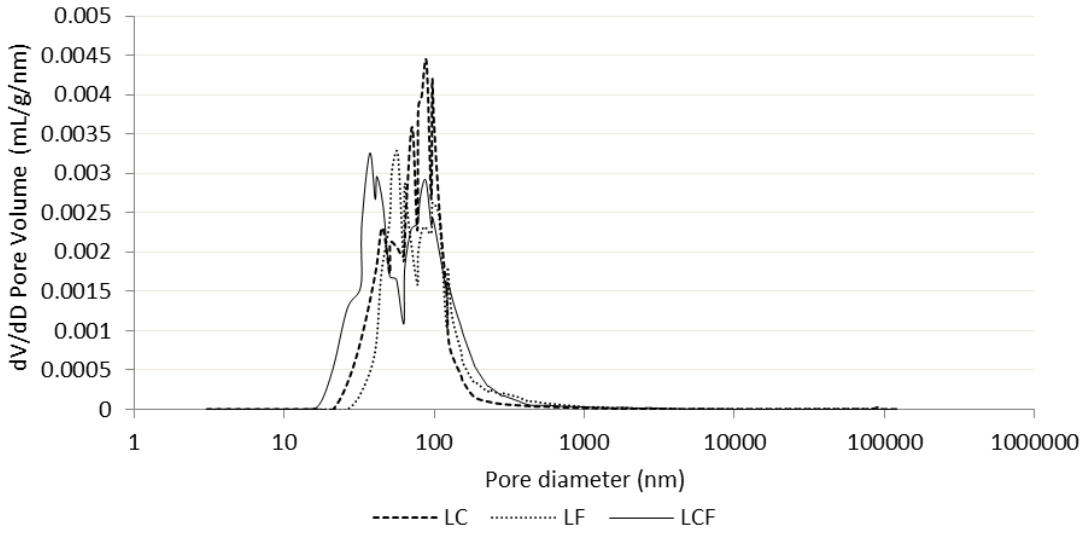

Figure 5-6: dV/dD pore volume vs pore diameter for calcined LC, LF and LCF

XRD analysis of the samples was also carried out for LC, LF and LCF. The results of this analysis can be seen in Figure 5-7. The differences in composition of the samples are mainly in the mayenite ($Ca_{12}Al_{14}O_{33}$) phase that forms from the reaction between calcium aluminate cement and lime in the production process. These outcomes have been well documented in earlier investigations [44, 45].

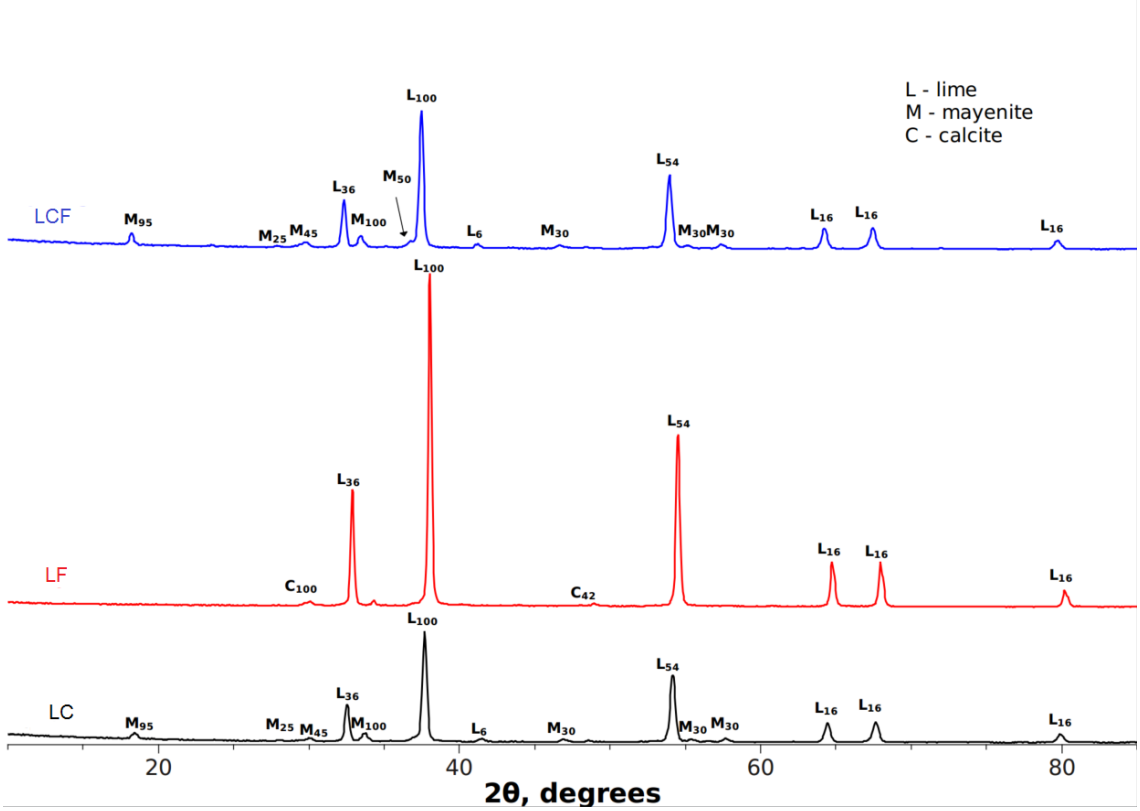

Figure 5-7: XRD of calcined LC, LF and LCF

5.3.2 Fragmentation tests

5.3.2.1 PSHR tests

The PHSR tests were performed repeatedly with raw samples until enough material was collected to analyse particle size distribution (PSD). In Figure 5-8, the PSD for LC is shown, comparing the raw material with the material after injection into the reactor, simulating the conditions at the entrance of the calciner. It can be seen that the PSDs are similar. However, it should be noted that the fine particles present in the raw sample probably became finer still, and could not be recovered after the PHSR experiment. Nonetheless, the mean diameter is almost equal in both the raw material and the treated sample.

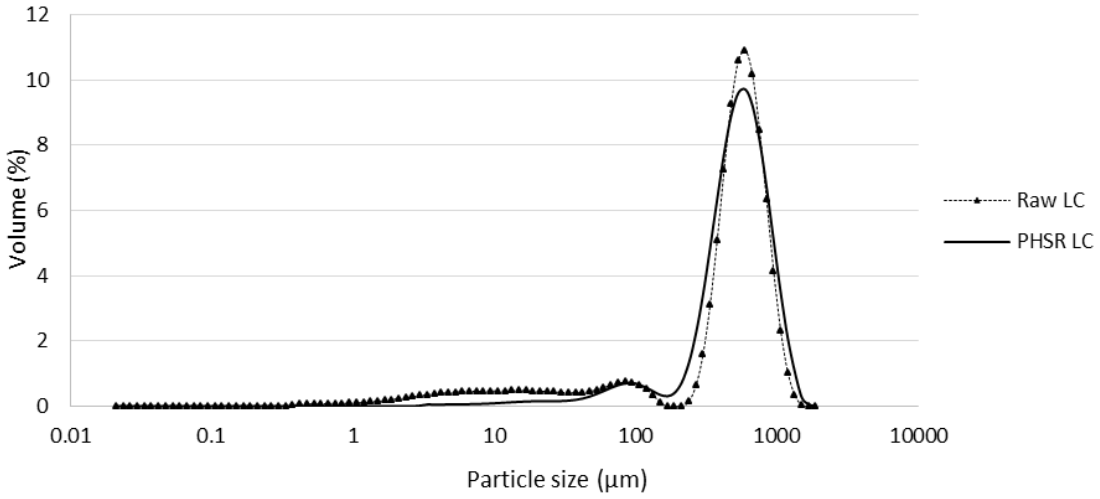

Figure 5-8: Particle size distribution of LC before and after the PHSR tests

The same distributions are shown for LF and LCF in Figure 5-9 and Figure 5-10, respectively. For LF the difference in the particle size distribution before and after the fragmentation experiment is quite significant, with major fragmentation occurring when the particles are treated at 950 °C, and the mean diameter decreases substantially from 520 µm to 116 µm. However, for LCF the change is less pronounced, although there is some fragmentation occurring when compared to LC; the change in mean diameter in LCF is smaller than for LF with a decrease from 524 µm to 290 µm. From these results, it can be inferred that the addition of biomass has a negative effect on the mechanical strength of the particles, making them more prone to fragmentation in the early stages of calcination presumably due to thermal stresses they experience. Nevertheless, the introduction of cement seems to have a positive effect in the biomass-templated particle with respect to fragmentation.

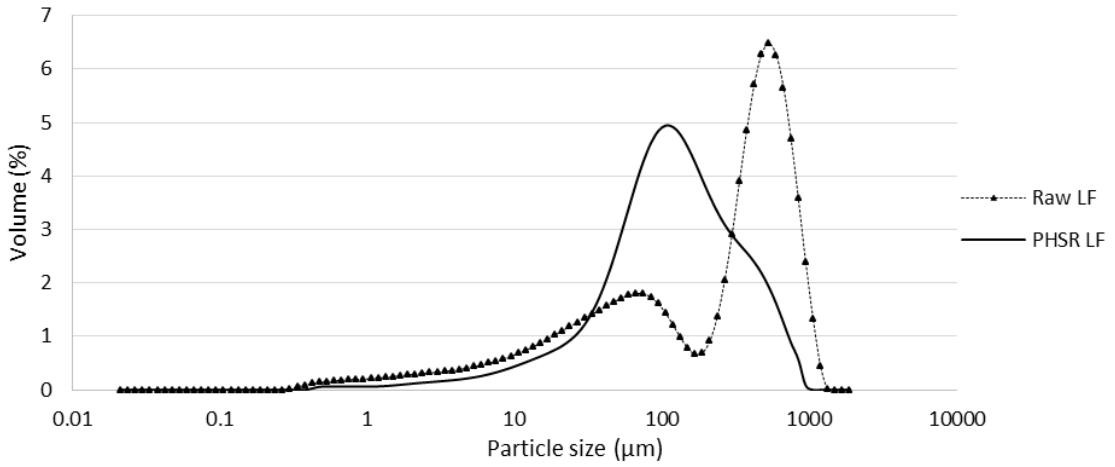

Figure 5-9: Particle size distribution of LF before and after the PHSR tests

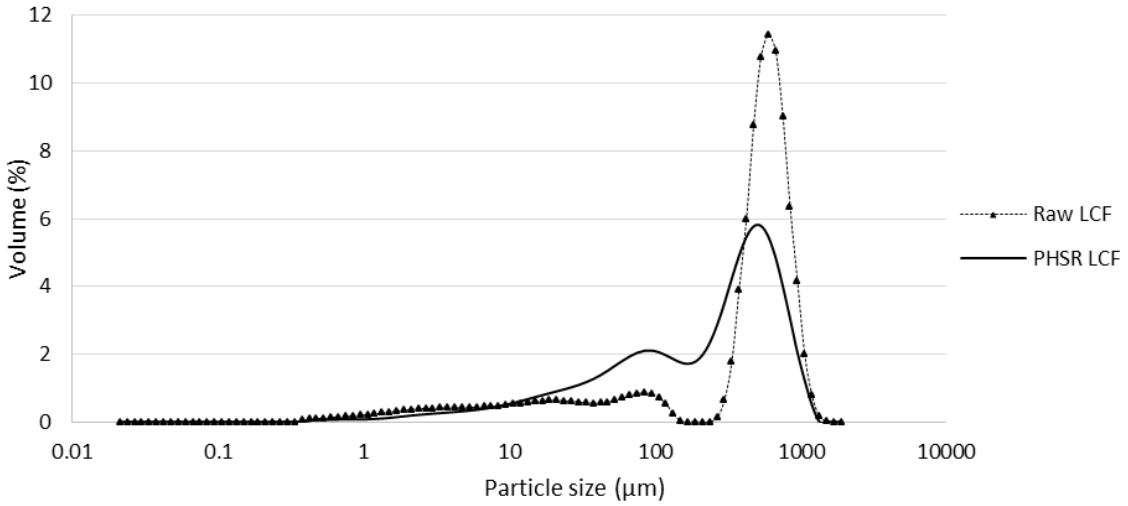

Figure 5-10: Particle size distribution of LCF before and after the PHSR tests

5.3.2.2 BFB experiments

Figure 5-11, Figure 5-12, Figure 5-13 and Figure 5-14 report the results of fragmentation tests in the fluidised bed reactor.

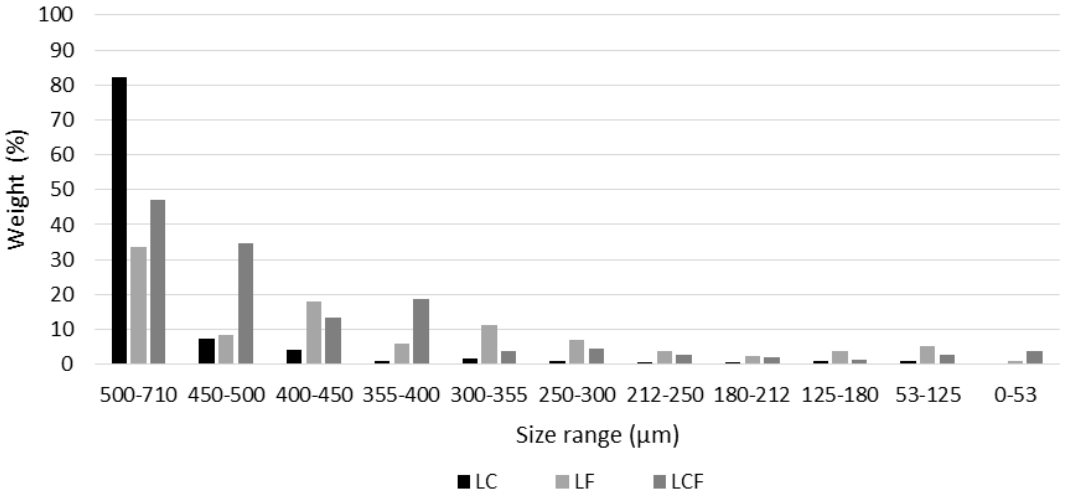

Figure 5-11: Weight distribution percentage of recovered material (500-710 µm, 900 °C in air)

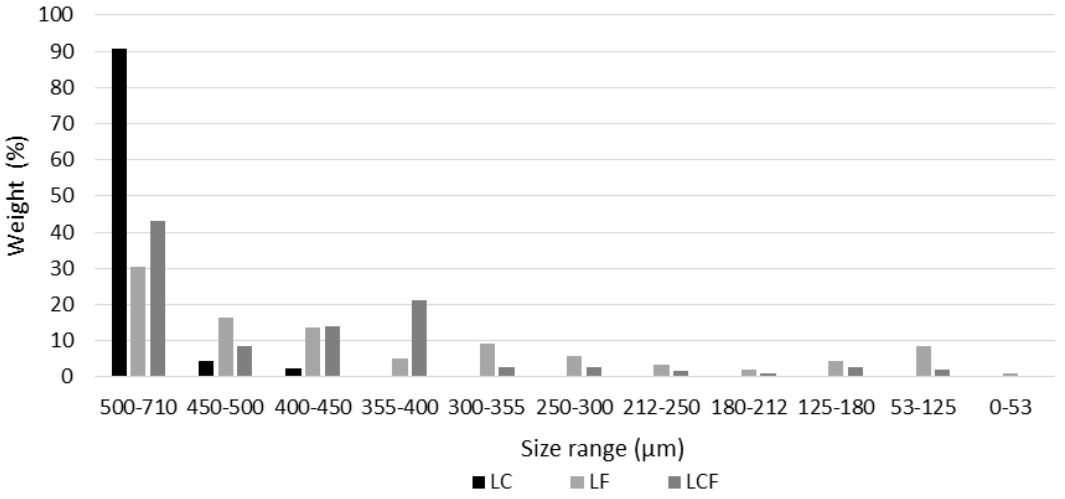

Figure 5-12: Weight distribution percentage of recovered material (500-710 µm, 900 °C in 70% vol CO_2, 30% vol air)

Figure 5-11 reports the PSDs after treating the samples of LC, LF and LCF of original size 500–710 µm in the fluidised bed reactor in air. There is a clear difference in the behaviour among samples; LC undergoes less fragmentation, with 82% of the samples retaining the initial size range, as compared to LF, with 33% of the sample in the initial size range and LCF, with 47% of the sample in the initial size range. However, as noted in the PHSR experiments, cement

addition has a positive effect making the particles less susceptible to fragmentation than the biomass-only templated material (LF).

Figure 5-12 reports the weight distribution of the material after calcination of the same samples in 70% CO_2 with balance of air. It can be seen that the material that fragments the most is LF with only 30% of the particles remaining in the initial size range, followed by LCF with 43% and LC with 90%.

The results of the same tests carried out on samples of smaller particle size (250–500 µm), are reported in Figure 5-13 and Figure 5-14. For calcination in air, LF has the highest fragmentation with only 67% of particles retaining the initial size, followed by LCF with 74% and LC with 94%. It can be seen that smaller particle sizes lead to less fragmentation of the material recovered in the reactor at the end of the tests.

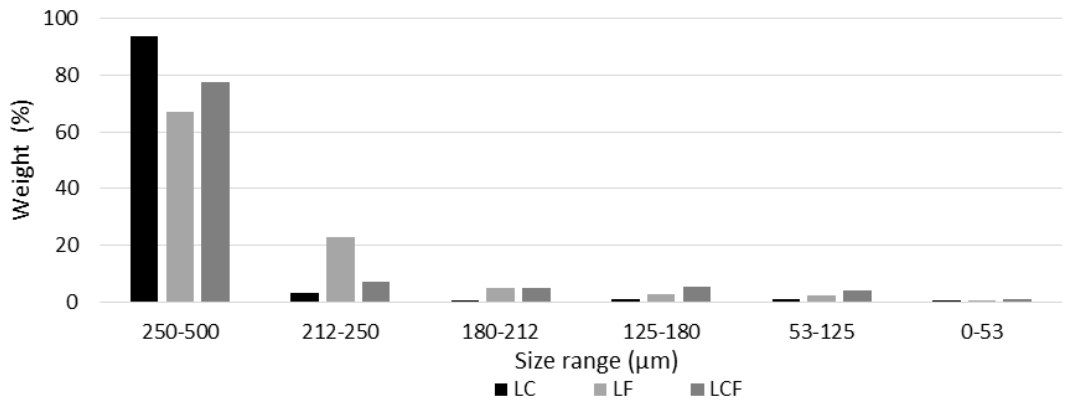

Figure 5-13: Weight distribution percentage of recovered material (250-500 µm, 900 °C in air)

For the smaller size particles (250–500 µm) calcined in 70% CO_2 with balance of air, the results were qualitatively similar to the other results. Nevertheless, the particles that remained in the reactor underwent less fragmentation than LF with 62% of particles in the initial size range, as was expected. The amount of fines (53–125 µm and 125–180 µm) is higher for LF (0.9 wt%) and LCF (0.08 wt%) than for LC (0.04 wt%), due to increased fragmentation created by biomass addition.

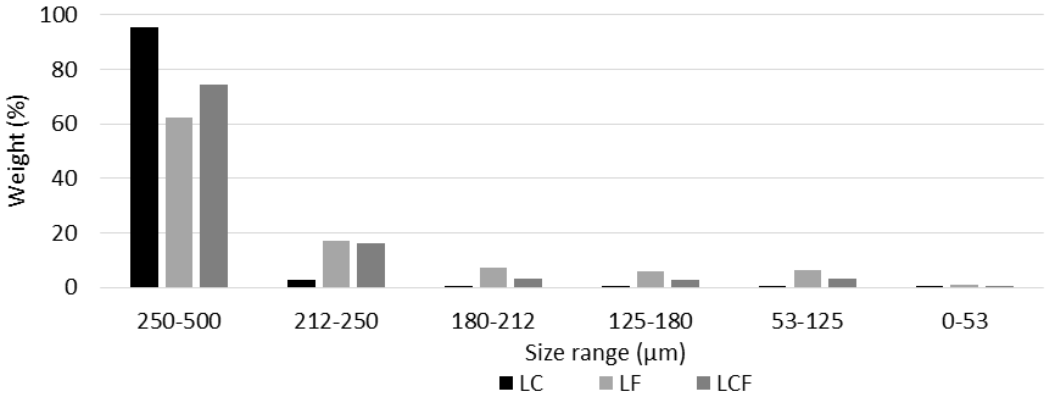

Figure 5-14: Weight distribution percentage of recovered material (250-500 µm, 900 °C in 70% vol CO_2, 30% vol air)

The percentage of material loss in the course of the BFB experiments is reported in Table 5-2. It can be seen that around 45% weight of LF was lost in the first calcination for smaller particles and around 30% for larger particles. This loss would be unacceptable for any real system. For LCF the losses were less significant for larger particles (between 4% and 8%), whilst for the smaller particles LCF behaved very similar to LF. The material that performed best was LC with a loss of around 3% for the smaller sample and 30% for the larger sample. Interestingly, the gas composition used in the calcination process did not affect the results significantly.

Table 5-2: Loss in sample weight during the BFB experiments

Sample	Loss of mass in weight (%) for 100% vol air		Loss of mass in weight (%) for 70% vol CO_2 and 30% vol air	
	250-500 µm	500-710 µm	250-500 µm	500-710 µm
LC	31.3	3.3	29.3	3.7
LF	45.4	27.4	46.8	30.5
LCF	41.5	3.4	48.4	8.7

It has been noted above that LCF and LF have similar behaviour for the smaller particle range; this could be due to the different composition in the larger LCF particles, which might incorporate more cement during the pelletisation process. This hypothesis was supported by comparing the results of pyrolysis-calcination TGA experiments carried out on LCF samples of different size cuts. The TG curves, reported in Figure 5-15 show a smaller water content for the larger particles which suggests that they contained more calcium aluminate cement

than the smaller size range particles. However, it should be noted that the particle size effect observed in Table 5-2 could be related to elutriation. The contribution of elutriation to the loss of bed material is in fact more noticeable the smaller the particle size is. Another point worth reiterating is that the main difference between both size ranges is the amount of cement present in each size cut. The effect of adding cement has been extensively studied in previous papers. There is a negative impact of adding cement because the particles have less active (CaO) material in them so that would negatively influence the CO_2 uptake, also cement reacts with lime to form mayenite ($Ca_{12}Al_{14}O_{33}$). However, a positive effect has also been found in which the addition of calcium aluminate cement stabilizes the structure of the particle due to a mesoporous Al_2O_3 phase that delays sintering and therefore decreases the reactivity decay over cycles [26, 44].

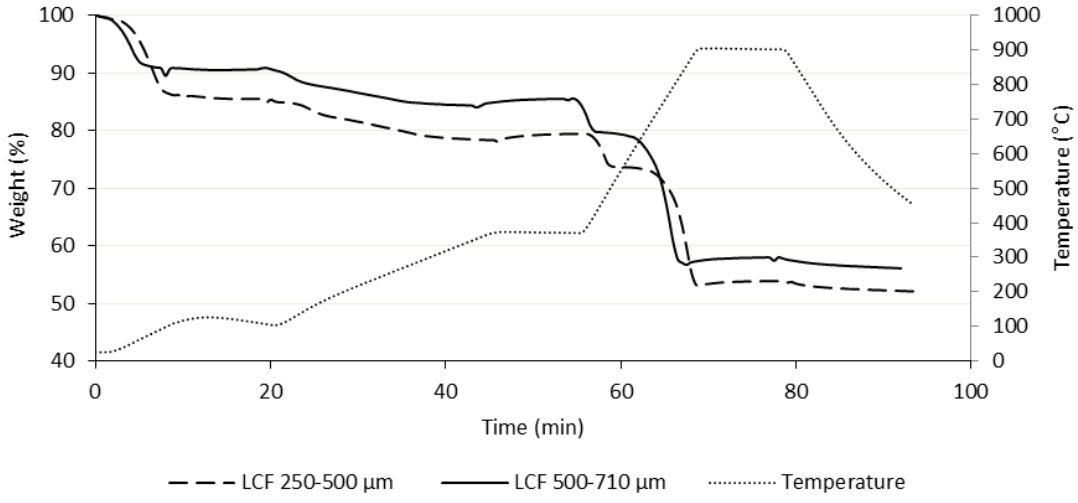

Figure 5-15: TG Results for LCF (250-500 µm) and LCF (500-710 µm) for the first calcination

5.4 Conclusions

Biomass-templated pellets for calcium looping appear to be a cheap and scalable alternative option to achieve high CO_2 uptake when compared with other synthetic materials for Ca looping. The reactivity of these templated materials has been previously investigated in both TGA and BFB. Here, LF

experienced the highest fragmentation in PHSR tests with a reduction in mean diameter of 404 μm compared to 234 μm for LCF and no change for LC. Moreover, in BFB, LF displayed the worst performance with a mass loss as high as 45.4 wt% for smaller particles in the air fluidisation case. The weight loss of this material was significantly higher than for LC with 31.3 wt% for the same case; this suggests that addition of biomass has a detrimental effect with regards to fragmentation. This effect is partially counteracted by the addition of calcium aluminate cement, which augments the resistance to fragmentation for LCF. However, the composition of LCF varied with particle size with the smaller range (250–500 μm) showing more elutriation of fines due to the pelletisation process, in which the larger particle size appeared to have incorporated more cement, leaving the smaller particles with a less stable structure. In consequence, smaller LCF particles were more prone to elutriate than the larger ones (500–710 μm). However, the particles that stayed in the reactor for the duration of the test underwent less fragmentation compared to the larger size range. It is clear that LC is the best material as regards fragmentation in all the cases explored, with a loss in mass as low as 3.3% for 500–710 μm particles in air calcination. The results for both techniques, BFB and PHSR, agree on the effects that biomass templating has on the fragmentation behaviour of these sorbents under calcium looping conditions, although the addition of cement partially mitigated this negative effect.

5.5 References

[1] Stanmore, B.R., Gilot, P., 2005. Review – calcination and carbonation of limestone during thermal cycling for CO_2 sequestration. Fuel Processing Technology, 86, pp. 1707–1743.

[2] Alonso, M., Rodríguez, N., González, B., Grasa G., Murillo, R., Abanades, J.C., 2010. Carbon dioxide capture from combustion flue gases with a calcium oxide chemical loop. International Journal of Greenhouse Gas Control, 4, pp. 167–173.

[3] Blamey, J., Anthony, E.J., Fang, J., Fennell, P.S., 2010. The calcium looping cycle for large- scale CO_2 capture. Progress in Energy and Combustion Science, 36, pp. 260–279.

[4] Sun, R., Li, Y., Liu, H., Wu, S., Lu, C., 2012. CO_2 capture performance of calcium-based sorbent doped with manganese salts during calcium looping cycle. Applied Energy, 89(1), pp. 368–373.

[5] Lysikov, A.I., Salanov, A.N., Okunev, A.G., 2007. Change of CO_2 carrying capacity of CaO in isothermal recarbonation–decomposition cycles. Industrial & Engineering Chemistry Research, 46, pp. 4633–4638.

[6] Abanades, J.C., 2202. The maximum capture efficiency of CO_2 using a carbonation/ calcination cycle of $CaO/CaCO_3$. Chemical Engineering Journal, 90, pp. 303–306.

[7] Blamey, J., Paterson, N.P.M., Dugwell, D.R., Fennell, P.S., 2010. Mechanism of particle breakage during reactivation of CaO-based sorbents for CO_2 capture. Energy & Fuels, 24, pp. 4605–4616.

[8] Rodríguez, N., Alonso, M., Abanades, J.C., 2010. Average activity of CaO particles in a calcium looping system. Chemical Engineering Journal,156, pp. 388–394.

[9] Grasa, G.S., Abanades, J.C., 2006. CO_2 capture capacity of CaO in long series of carbonation/calcination cycles. Industrial & Engineering Chemistry Research, 45, pp. 8846–8851.

[10] Lisbona, P., Martínez, A., Romeo, L.M., 2013. Hydrodynamical model and experimental results of a calcium looping cycle for CO_2 capture. Applied Energy, 101, pp. 317–322.

[11] Chen, S., Xiang, W., Wang, D., Xue, Z., 2012 Incorporating IGCC and CaO sorption- enhanced process for power generation with CO_2 capture. Applied Energy, 95, pp. 285–294.

[12] Lasheras, A., Ströhle, J., Galloy, A., Epple, B., 2011. Carbonate looping process simulation using a 1D fluidized bed model for the carbonator. International Journal Greenhouse Gas Control, 5, pp. 686–693.

[13] Dean, C.C., Blamey, J., Florin, N.H., Al-Jeboori, M.J., 2011. Fennell PS. The calcium looping cycle for CO_2 capture from power generation, cement manufacture and hydrogen production. Chemical Engineering Research and Design, 89, pp. 836–855.

[14] Luo, C., Zheng, Y., Ding, N., Wu, Q., Bian, G., Zheng, D., 2010. Development and performance of CaO/La_2O_3 sorbents during calcium looping cycles for CO_2 capture. Industrial & Engineering Chemistry Research, 49, pp. 11778–17784.

[15] Luo, C., Zheng, Y., Zheng, C., Yin, J., Qin, C., Feng, B.. 2013. Manufacture of calcium-based sorbents for high temperature cyclic CO_2 capture via a sol-gel process. International Journal Greenhouse Gas Control, 12, pp. 193–199.

[16] Radfarnia, H.R., Sayari, A., 2015. A highly efficient CaO-based CO_2 sorbent prepared by a citrate-assisted sol-gel technique. Chemical Engineering Journal, 262, pp. 913–920.

[17] Wang, B., Yan, R., Lee, D.H., Zheng, Y., Zhao, H., Zheng, C., 2011. Characterization and evaluation of Fe_2O_3/Al_2O_3 oxygen carrier prepared by sol-gel combustion synthesis. Journal Analytical Applied Pyrolysis, 91, pp. 105–113.

[18] Broda, M., Müller, C.R., 2014. Sol-gel-derived, CaO-based, ZrO_2-stabilized CO_2 sorbents. Fuel, 127, pp. 94–100.

[19] Zhang, M., Peng, Y., Sun, Y., Li, P., Yu, J., 2013. Preparation of $CaO-Al_2O_3$ sorbent and CO_2 capture performance at high temperature. Fuel, 111, pp. 636–642.

[20] Li, Y., Su, M., Xie, X., Wu, S., Liu, C., 2015. CO_2 capture performance of synthetic sorbent prepared from carbide slag and aluminum nitrate hydrate by combustion synthesis. Applied Energy, 145, pp. 60–68.

[21] Li, C.C., Wu, U.T., Lin, H.P., 2014. Cyclic performance of $CaCO_3.mSiO_2$ for CO_2 capture in a calcium looping cycle. Journal Material Chemistry A, 2(22), pp. 8252-8257.

[22] Li, L., King, D.L., Nie, Z., Howard, C., 2009. Magnesia-stabilized calcium oxide absorbents with improved durability for high temperature CO_2 capture. Industrial & Engineering Chemistry Research, 48, pp. 10604–10613.

[23] Zhao, M., Bilton, M., Brown, A.P., Cunliffe, A.M., Dvininov, E., Dupont, V., Comyn, T.P., Milne, S.J., 2014. Durability of $CaO–CaZrO_3$ sorbents for high-temperature CO_2 capture prepared by a wet chemical method. Energy & Fuels, 28, pp. 1275–1283.

[24] Gupta, H., Fan, L.S., 2002. Carbonation−calcination cycle using high reactivity calcium oxide for carbon dioxide separation from flue gas. Industrial & Engineering Chemistry Research, 41, pp. 4035–4042.

[25] Florin, N., Fennell, P.S., 2001. Synthetic CaO-based sorbent for CO_2 capture. Energy Procedia, 4, pp. 830–838.

[26] Manovic, V., Anthony, E.J., 2009. Screening of binders for pelletization of CaO-based sorbents for CO_2 capture. Energy & Fuels, 23, pp. 4797–4804.

[27] Wu, Y., Manovic, V., He, I., Anthony, E.J., 2012. Modified lime-based pellet sorbents for high-temperature CO_2 capture: Reactivity and attrition behaviour. Fuel, 96: 454–461.

[28] Ridha, F.N., Manovic, V., Macchi, A. and Anthony, E.J., 2012. High-temperature CO_2 capture cycles for CaO-based pellets with kaolin-based binders. International Journal of Greenhouse Gas Control, 6, pp. 164-170.

[29] Qin, C., Yin, J., An, H., Liu, W. and Feng, B., 2011. Performance of extruded particles from calcium hydroxide and cement for CO_2 capture. Energy & Fuels, 26(1), pp. 154-161.

[30] Ridha, F.N., Wu, Y., Manovic, V., Macchi, A. and Anthony, E.J., 2015. Enhanced CO_2 capture by biomass-templated $Ca(OH)_2$-based pellets. Chemical Engineering Journal, 274, pp. 69-75.

[31] Manovic, V. and Anthony, E.J., 2011. CaO-based pellets with oxygen carriers and catalysts. Energy & Fuels, 25(10), pp. 4846-4853.

[32] Erans, M., Beisheim, T., Manovic, V., Jeremias, M., Patchigolla, K., Dieter, H., Duan, L. and Anthony, E.J., 2016. Effect of SO_2 and steam on CO_2 capture performance of biomass-templated calcium aluminate pellets. Faraday Discussions, 192, pp. 97-111.

[33] Scala F, Cammarota A, Chirone R, Salatino P., 1997. Comminution of limestone during batch fluidized-bed calcination and sulfation. AIChE Journal, 43, pp. 363– 373.

[34] Scala, F., Salatino, P., Boerefijn, R. and Ghadiri, M., 2000. Attrition of sorbents during fluidized bed calcination and sulphation. Powder Technology, 107(1), pp.153-167.

[35] Scala, F. and Salatino, P., 2003. Dolomite attrition during fluidized-bed calcination and sulfation. Combustion Science and Technology, 175(12), pp. 2201-2216.

[36] Scala, F., Montagnaro, F. and Salatino, P., 2007. Attrition of limestone by impact loading in fluidized beds. Energy & Fuels, 21(5), pp. 2566-2572.

[37] Coppola, A., Scala, F., Salatino, P. and Montagnaro, F., 2013. Fluidized bed calcium looping cycles for CO_2 capture under oxy-firing calcination conditions: Part 1. Assessment of six limestones. Chemical Engineering Journal, 231, pp. 537-543.

[38] Coppola, A., Montagnaro, F., Salatino, P. and Scala, F., 2012. Limestone attrition during fluidized bed calcium looping cycles for CO_2 capture: the effect of SO_2. In Proceedings of the 35th Meeting of the Italian Section of The Combustion Institute.

[39] Coppola, A., Montagnaro, F., Salatino, P. and Scala, F., 2012. Fluidized bed calcium looping: the effect of SO_2 on sorbent attrition and CO_2 capture capacity. Chemical Engineering Journal, 207, pp. 445-449.

[40] Senneca, O. and Cortese, L., 2014. Thermal annealing of coal at high temperature and high pressure. Effects on fragmentation and on rate of combustion, gasification and oxy-combustion. Fuel, 116, pp. 221-228.

[41] Fennell, P.S., Pacciani, R., Dennis, J.S., Davidson, J.F. and Hayhurst, A.N., 2007. The effects of repeated cycles of calcination and carbonation on a variety of different limestones, as measured in a hot fluidized bed of sand. Energy & Fuels, 21(4), pp. 2072-2081.

[42] González, B., Alonso, M. and Abanades, J.C., 2010. Sorbent attrition in a carbonation/calcination pilot plant for capturing CO_2 from flue gases. Fuel, 89(10), pp. 2918-2924.

[43] Manovic, V. and Anthony, E.J., 2009. CaO-based pellets supported by calcium aluminate cements for high-temperature CO_2 capture. Environmental Science & Technology, 43(18), pp. 7117-7122.

[44] Manovic, V. and Anthony, E.J., 2009. Long-term behavior of CaO-based pellets supported by calcium aluminate cements in a long series of CO_2 capture cycles. Industrial & Engineering Chemistry Research, 48(19), pp. 8906-8912.

[45] Manovic, V. and Anthony, E.J., 2011. Reactivation and remaking of calcium aluminate pellets for CO_2 capture. Fuel, 90(1), pp. 233-239.

6 OPERATION OF A 25 KWTH CALCIUM LOOPING PILOT-PLANT WITH HIGH-OXYGEN CONCENTRATION IN THE CALCINER

María Erans, Michal Jeremias, Vasilije Manovic, Edward J Anthony

Combustion and CCS Centre, Cranfield University, Bedford, Bedfordshire, United Kingdom

Accepted in Journal of Visualized Experiments

Statement of contributions of joint authorship

María Erans conducted the literature review on the subject, planned and performed the experiments, drafter and critically reviewed this manuscript. Also, María analysed the results and produced figures and tables in this paper. Michal Jeremias and María Erans carried out all the experimental campaigns depicted in this paper in the 25 kW_{th} unit.Vasilije Manovic and Edward J Anthony proof-read and critically commented on the manuscript before its submission to Journal of Visualized Experiments.

Abstract

Calcium looping (CaL) is a post-combustion CO_2 capture technology that is suitable for retrofitting existing power plants. The CaL process uses limestone as a cheap and readily available CO_2 sorbent. While the technology has been widely studied, there are a few available options that could be applied to make it more economically viable. One of these is to increase the oxygen concentration in the calciner to reduce or eliminate the amount of recycled gas (CO_2, H_2O and impurities); therefore, decreasing or removing the energy necessary to heat the recycled gas stream. Moreover, there is a resulting increase in the energy input due to the change in the combustion intensity; this energy is used to enable the endothermic calcination reaction to occur in the absence of recycled flue gases. This paper presents the operation and first results of a CaL pilot plant with 100% oxygen combustion of natural gas in the calciner. The gas coming into the carbonator was a simulated flue gas from a

coal-fired power plant or cement industry. Several limestone particle size distributions are also tested to further explore the effect of this parameter on the overall performance of this operating mode. The configuration of the reactor system, the operating procedures, and the results are described in detail in this paper. The reactor showed good hydrodynamic stability and stable CO_2 capture, with capture efficiencies of up to 70% with a gas mixture simulating the flue gas of a coal-fired power plant.

6.1 Introduction

CO_2 emissions and the resulting global warming are critical environmental issues that have attracted a large amount of research in the past years. Carbon capture and storage (CCS) has been acknowledged as a potential technology for reducing CO_2 emissions to the atmosphere [1, 2]. The most challenging part of the CCS chain is the capture of CO_2, which is also the most costly stage [3]. In consequence, there has been a focus on developing new technologies for CO_2 capture from power plants and other industrial facilities.

CaL as a post-combustion CO_2 capture technology, was first proposed by Shimizu et al. [4] CO_2 is captured by a CaO-based sorbent at 600–700 °C in a reactor called a carbonator, and released by subsequent calcination at 850–950 °C (in a calciner) according to (6-1), to produce a high-purity CO_2 stream suitable for sequestration [5, 6]. The CaL cycle utilises fluidized beds, which represent an optimal configuration for this process, since they allow for large amounts of solids to be circulated easily from one reactor to the other [4, 7, 8].

$$CaO + CO_2 \leftrightarrow CaCO_3 \qquad \Delta H_{25°C} = -178.2\ kJ/mol \qquad \textbf{(6-1)}$$

This concept has been demonstrated at pilot scale by various groups and with different configurations and scales, such as the 0.2 MW_{th} pilot in Stuttgart, the 1 MW_{th} pilot in Darmstadt, the 1.7 MW_{th} pilot in La Pereda and the 1.9 MW_{th} unit in Taiwan [9-16]. Although this process has been proven, there are still possibilities for increasing its thermal efficiency, such as by modifying the standard operating conditions and changes in the design of the reactor configuration.

The use of heat pipes between the combustion and calciner has been studied instead of oxy-combusting fuel in the calciner: The results for the CO_2 capture performance are comparable with those of a conventional CaL pilot-plant, however, this process has higher plant efficiencies and lower CO_2 avoidance costs [17]. Martínez et al. [18] investigated the heat integration possibilities in

order to preheat the solid material entering the calciner and to reduce the heat needed in the calciner. The results showed 9% reduction in the coal consumption when compared with that of the standard case. Other studied possibilities for heat integration have also considered internal and external integration options [19].

One of the main problems of the CaL cycle from the economic point of view is to supply the energy needed in the calciner by means of fuel combustion [20]. Increasing the oxygen concentration in the calciner's inlet is proposed in order to reduce or even avoid the need of CO_2 recycle to the calciner. This alternative reduces the capital costs (reduced size of calciner and air separation units (ASU)), which can significantly improve the competitiveness of this process. The drastic change in the combustion conditions can be attained by exploiting the endothermic calcination reaction and the large $CaO/CaCO_3$ flow circulating from the carbonator operating at lower temperatures (neither advantage is available with the oxy-combustion technology).

This work aims to develop a standard operating procedure for running a CaL pilot plant with a Circulating Fluidized Bed (CFB) carbonator and a Bubbling Fluidized Bed (BFB) calciner with 100% O_2 concentration in the calciner's inlet. Several experimental campaigns have been run during the commissioning of the pilot plant to ensure proper operation as the oxygen concentration increased. Also, three limestone particle size distributions (100–200 μm; 200–300 μm; 300–400 μm) were studied to investigate how this parameter affects the elutriation of particles and capture efficiency in this operating mode.

6.2 Operating protocol

6.2.1 Material preparation

1. Sieve the limestone (around 50 kg of raw material) to the desired particle size distribution (300-400 μm or some other choice depending on the experiment) using a mechanical shacker. Put the sieved material in pots next to the calciner for feeding during the test.

2. Prepare the material in batches to be introduced in the reactor, the batches are generally 0.5 or 1 L (note 1 L of limestone is roughly 1.5 kg), but this can vary depending on the operating parameters.

6.2.2 Start-up procedure (Caution extremely high temperatures. Use suitable PPE such as gloves, eye glasses, laboratory coat and safety shoes)

6.2.2.1 Heat-up of reactors

1. Start low flow of N_2 in carbonator (60 L/min) and calciner (20 L/min) as well as loop-seals (10 L/min) (as seen in Fig.1) in the rotameters (as seen in Figure 1).

2. Turn on the carbonator transformers manually. Set the temperature of all electrical preheaters of the carbonator at 600 °C.

3. Start acquiring data data (for gases temperatures and pressure using the recording button in the software), these data includes temperatures, pressures and gas composition of both reactors. In Figure 6-1 and Figure 6-2, screenshots of the data acquisition system are shown.

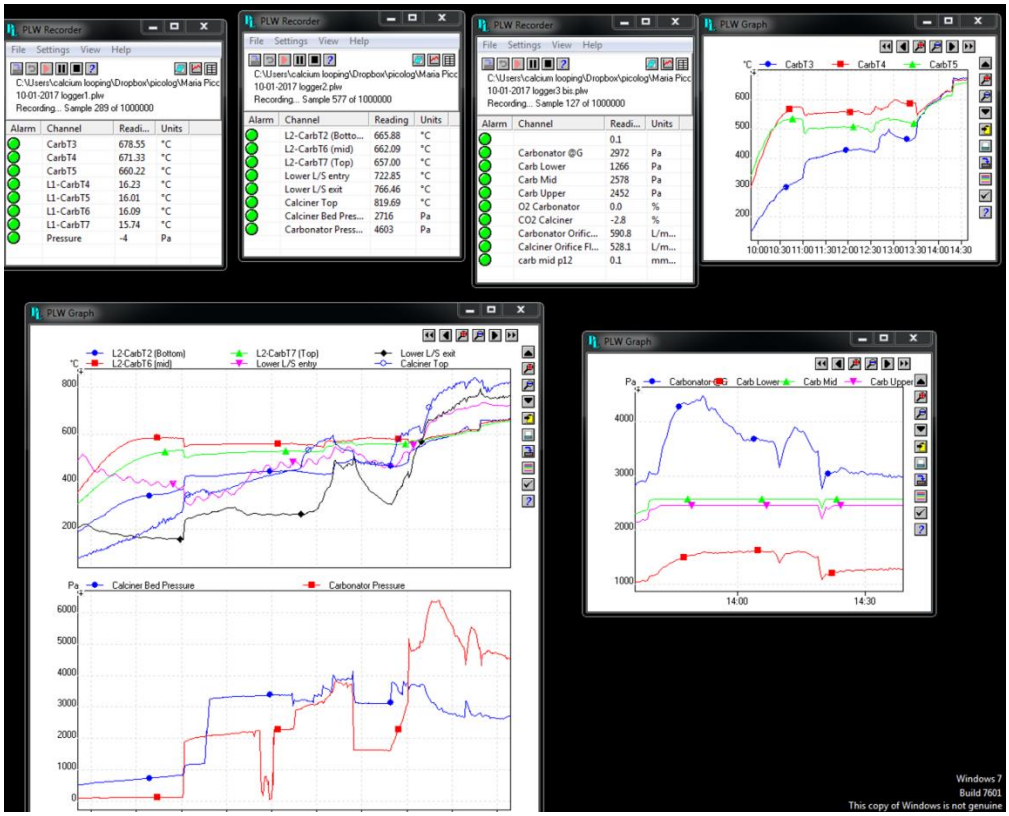

Figure 6-1: Screenshot of temperature and pressure data acquisition for both reactors

Figure 6-2: Screenshot of temperature data acquisition for the preheating system

4. Turn on the calciner gas preheaters and the heater around the calciner to a temperature of 600 °C measured inside the BFB via thermocouple. Note: Data such as temperature, pressures and gas composition are already being acquired as stated in step 2.1.3.

5. Put 3 L of the sieved limestone into the BFB in the calciner. First open the top valve, introduce the material in the down-pipe and close the top valve, then open the bottom valve so that the material flows into the reactor.

6. Heat the material in the BFB to above 650 °C (by the electrical heater around the calciner). Note: This usually takes ~ 1 h, during this time check the data acquisition and the pressures in the fluidized beds.

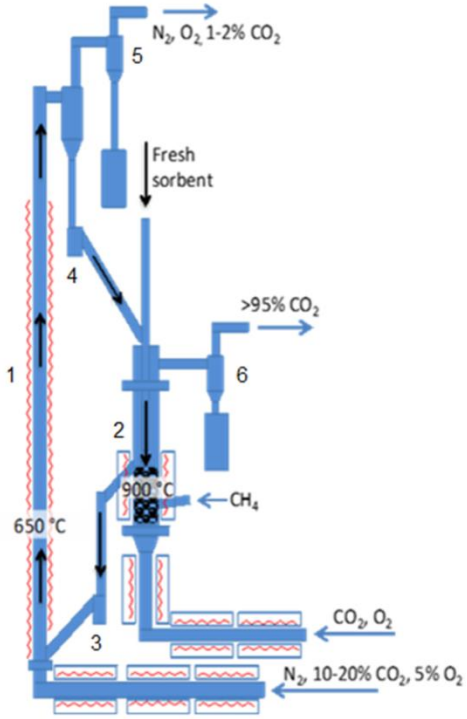

Figure 6-3: Schematic of the 25 kW_{th} CaL (CFB carbonator and BFB calciner): 1: carbonator; 2: calciner; 3: lower loop-seal; 4: upper loop-seal; 5: carbonator cyclone; 6: calciner cyclone

6.2.2.2 Start combustion in calciner

7. Increase the oxygen concentration in the calciner from 0 to 40% vol, making sure the concentration is stable before starting the combustion.

8. Start the stoichiometric flow of natural gas using a rotameter making sure the combustion is stable. Note: the natural gas flow should be increased carefully with checking that the data show that appropriate level of combustion reaction is occurring.

9. Increase the oxygen concentration in the calciner in 20% vol increments adjusting the natural gas flow rotameter to ensure stoichiometric combustion. Note: this process should be done with extreme care, if any suspicion arises that the combustion is not occurring as expected from preliminary calculations, stop the flow of natural gas and switch the oxygen flow for nitrogen for safe operation and identify the source of this discrepancy. The overall duration of this process is about 1 h.

10. Achieve 100% oxygen concentration natural gas combustion. Note: the temperature and gas composition data should be carefully followed throughout all the test, but especially when the combustion is taking place in 100% oxygen.

11. Add limestone in 0.5 L increments until there is 7 L in the fluidised bed. Calcine all the material in the fluidised bed of the calciner (the estimated calcination temperature is 800-850° for the batch present in the calciner and the calciner temperature for the following batches).

12. Increase the flow of N_2 in the carbonator to start the circulation. Check the circulation view port regularly to ensure proper circulation.

13. Calcine all the available limestone circulating in the rig, before starting the CO_2 capture.

6.2.3 Stable operation

1. Manually switch the carbonation gas from N_2 to 15% vol CO_2 using the rotameter, this would allow the calcined limestone to start capturing CO_2.

2. Adjust the flows in the calciner to achieve a stable 930-950 °C temperature in the calciner by regulating the flow of natural gas (NG) and oxygen (within optimal fluidisation regime), usually it is 100% O2 with enough bed material, but it is adjusted throughout the experiment.

3. When the material starts to decline in activity (above 5% CO_2 concentration at the exit of the carbonator, this is acquired every second in step 2.1.3), add more limestone.

6.2.4 Shut-down procedure

1. Manually turn off the natural gas flow and decrease oxygen flow, switch the gases in both reactors to N_2, Turn off all the heaters (calciner and carbonator).

2. Allow the temperature of the inventory of the rig to decrease (normally overnight), empty the reactors when they are at room temperature.

3. Weigh the extracted solids and perform a standard sieve analysis, characterise the material: porosimetry, composition (X-ray fluorescence spectrometry, XRF) [21,22] and microscopic structure (scanning electron microscopy, SEM).

6.3 Representative results

The experimental set-up is shown in Figure 6-3. The plant comprises two interconnected fluidized-beds. Namely, the carbonator is a CFB with 4.3 m height and 0.1 m ID; while the calciner is a BFB with 1.2 m height and 0.165 m ID. The solid transport from one reactor to the other is controlled by two loop-seals fluidized with nitrogen. Both reactors are fed a mixture of gas through a

preheating line, both reactors are electrically heated; moreover, the calciner is fed with natural gas in order to produce by combustion the heat needed for the endothermic calcination and to heat the circulating sorbent. The carbonator distributor plate has 8 nozzles, each of them with twenty 2 mm holes, whilst the calciner has 20 nozzles with six 1 mm holes each.

Three different experiments are discussed in this section. These tests provide an overview of the process of running the pilot plant from air (~20% vol O_2) to 100% vol O_2 at the calciner inlet. This work also explores the results of using different particle size distributions in this operational mode to see if this parameter has an impact on the overall performance of the system. The limestone used in this study has a minimum content of 98.25% $CaCO_3$.

6.3.1 Flue gas (15% vol. CO_2) with limestone (200–300 µm) 30% vol O_2

This first test with limestone fraction 200–300 µm was performed with the aim of testing the rig with limestone circulating between the two reactors within the rig as a starting point for the optimisation of its performance. During this test, a capture efficiency of 45% was achieved (Figure 6-4). This capture efficiency, E_{carb}, was calculated using the following formula [23]:

$$E_{carb} = \frac{F_{CO2} - F_{carb}}{F_{CO2}} \quad \textbf{(6-2)}$$

Where, F_{CO2} is the molar flow rate of CO_2 entering the carbonator and F_{carb} is the molar flow rate of CO_2 leaving the carbonator.

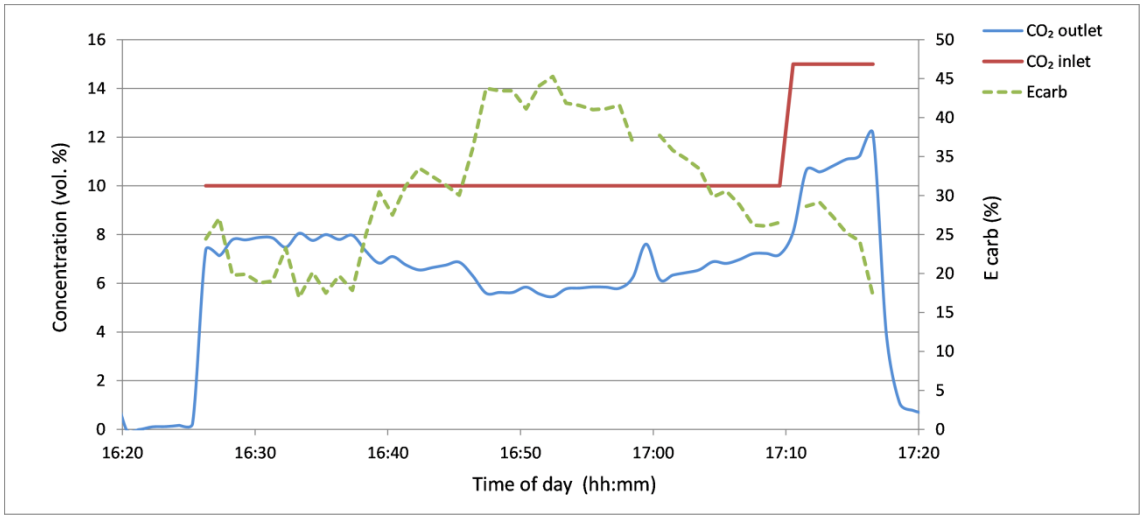

Figure 6-4: Concentration of CO_2 at inlet and at outlet of the carbonator and capture efficiency (E_{carb}) for 200–300 µm limestone with 30% O_2

The inferior capture efficiency during this experimental run was caused mainly by the supply of an insufficient quantity of heat to calcine all the limestone residing in the BFB. This caused a decrease of the $CaO/CaCO_3$ ratio in the carbonator feed. Another probable reason was the deactivation and carry-over of the lime particles from the calciner, which reduced the total bed inventory and the amount of sorbent present in the system.

After the experiment, a material balance of the inventory of the reactor was performed (Table 6-1). A shift towards smaller fractions can be observed, because of the attrition of the material in both fluidised beds.

Table 6-1: Weight balance of the material input and outputs for 200–300 µm limestone with 30% O_2

Fraction	Limestone in	Calciner+Carbonator	Cyclone Calciner	Cyclone Carbonator
Total mass (g)	9100	5000	500	20
250-300 µm	22%	24%	2%	0%
212-250 µm	47%	41%	6%	18%
150-212 µm	28%	34%	24%	18%

0-150 µm	3%	1%	69%	65%

6.3.2 Flue gas (15% CO_2) with limestone (100–200 µm) 100% O_2

In this test, the main aim was to explore the use of smaller limestone particles in order to investigate their possible beneficial effect on performance of the system. The secondary aim was to provide more heat to the calcination process in the BFB calciner by combusting the NG in highly concentrated oxygen, ideally up to 100% at the inlet.

During this test, we successfully tested the possibility of using pure O_2 at the inlet of the calciner, which offers the possibility of completely eliminating the recycle of off-gas needed for a standard oxy-fuel process. This is made possible by the heat consumption in the form of a circulating fluidised bed material and the continuous calcination reaction.

The use of smaller particles did not prove to have a beneficial effect on the carbonation process, which might have been expected based on the higher contact area between particles and the gas. However, there is some controversy in this matter as it appears that smaller particles have shown decreased reactivity due to higher content of impurities [24]. Practically all the added limestone with the size <150 µm was very quickly elutriated from the calciner to the downstream cyclone. Therefore, it was very difficult to maintain the necessary inventory of lime in the rig needed to achieve higher capture efficiency.

The results of the capture efficiency can be seen in Figure 6-5.

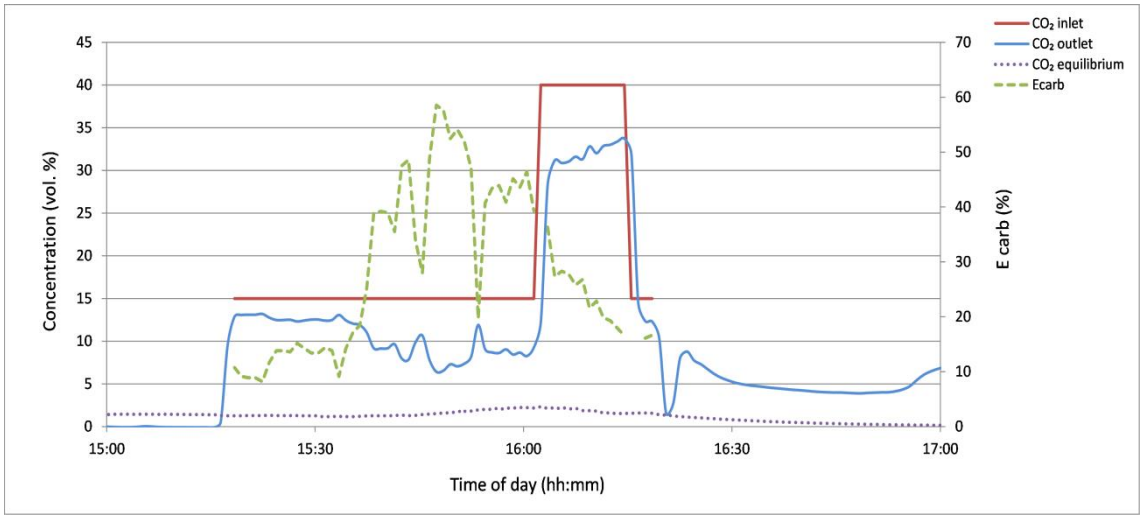

Figure 6-5: CO_2 concentration at inlet and at outlet of the carbonator and corresponding capture efficiency (E_{carb}) for 100–200 µm limestone with 100% O_2

When the balance of the inputs and outputs of the solids was performed after the test (Table 6-2), it was discovered that most of the material introduced into the rig during the experiment ended up in the cyclone of the calciner, which was probably the main cause of the low measured capture efficiency during this test.

Table 6-2: Balance of recovered material and its sieve analysis for 100–200 µm limestone with 100% O_2

Fraction	Limestone	Carbonator	Calciner	Cyclone calciner	Cyclone carbonator
Total mass (g)	19000	1200	2700	8700	360
>212-212 µm	0%	21%	2%	0%	39%
212-150 µm	18%	39%	73%	5%	42%
150-125 µm	40%	22%	13%	32%	10%
125-63 µm	41%	18%	12%	60%	9%
0-63 µm	2%	0%	0%	3%	1%

To conclude, the possibility of using pure O_2 at the inlet of the calciner was successfully tested, which offers the possibility to completely eliminate the

recycle of the off-gas needed for a standard oxy-fuel process. This is possible due to the heat sink provided in the form of circulating fluidised bed material and the continuous calcination reaction. However, the small particle size distribution (100-200 µm) was not beneficial for the capture process, due to the elutriation of the particles. It was extremely difficult to maintain the bed inventory needed to obtain a higher capture efficiency. Therefore, it was decided to investigate the use of bigger particles in the next experimental campaign.

6.3.3 Flue gas (15% CO_2) with limestone (300–400 µm) 100% O_2

During this trial, the performance of the fraction (300–400 µm) was tested so as to reduce the high material losses from the fluidised bed of the calciner as seen in previous runs. This was expected to enable retention of the necessary lime/limestone inventory needed for its efficient circulation and carbon capture. Due to use of an appropriate amount of sorbent circulating in the rig and sufficient heat provided by the combustion of natural gas in pure oxygen (releasing 18 kW), a stable capture efficiency of ca. 70% was achieved for more than 3 h, which is a very good result when considering the relatively short carbonator reactor tube and the consequent short contact time between the sorbent and CO_2. The concentration of CO_2 at the outlet of the carbonator was maintained below 5% vol. and fresh limestone (in 0.5 L batches) was added to the calciner when the concentration of CO_2 at the outlet of the carbonator exceeded this value. A stable experimental run was achieved with optimised conditions.

The process was begun using a standard procedure; i.e., first the reactor was heated up to 700°C, then 2.9 L of limestone was added into the calciner and heated up. The temperatures and gas concentrations in the calciner are shown in Figure 6-6. (Note that the numbers below correspond to those steps in Figure 6-6)

1) The air flow was replaced by the flow of a mixture of 40% O_2 and 60% N_2 and the combustion of NG in the fluidised bed was initiated (9.1 kW). The

limestone in the fluidised bed was heated above 800°C and 3 more batches of limestone (1 L) were added to the calciner.

2) While the limestone was calcining in the fluidised bed, the circulation of the lime/limestone was started by flowing preheated N_2 through the carbonator (at a velocity of 2.5 m/s at 650 °C). 0.9 L more limestone was added and a fresh O_2 cylinder was connected to the inlet of the calciner.

4) After reconnecting oxygen, the combustion was initiated again, this time in an inlet O_2 concentration of 70% (and 30% N_2), which led to a consumption of 14 kW of NG to reach an O_2 concentration at the outlet of around 5% (in wet gas).

5) Pure O_2 was introduced at the inlet of the calciner, which led to the heat release of 18 kW into the calciner and the carbonation was initiated in the carbonator by injecting 15% of CO_2. The efficiency of the carbonation (Figure 6-7) was the highest experienced yet on this reactor design (around 70%).

7) The gas velocity flowing through the bubbling fluidised bed of the calciner had to be lowered to 0.30 m/s (required by the desired temperature) to be able to maintain the temperature of about 930°C generated by the combustion of natural gas in pure O_2 (while maintaining the O_2 concentration in the off-gas to an industrially acceptable level below 5% vol.).

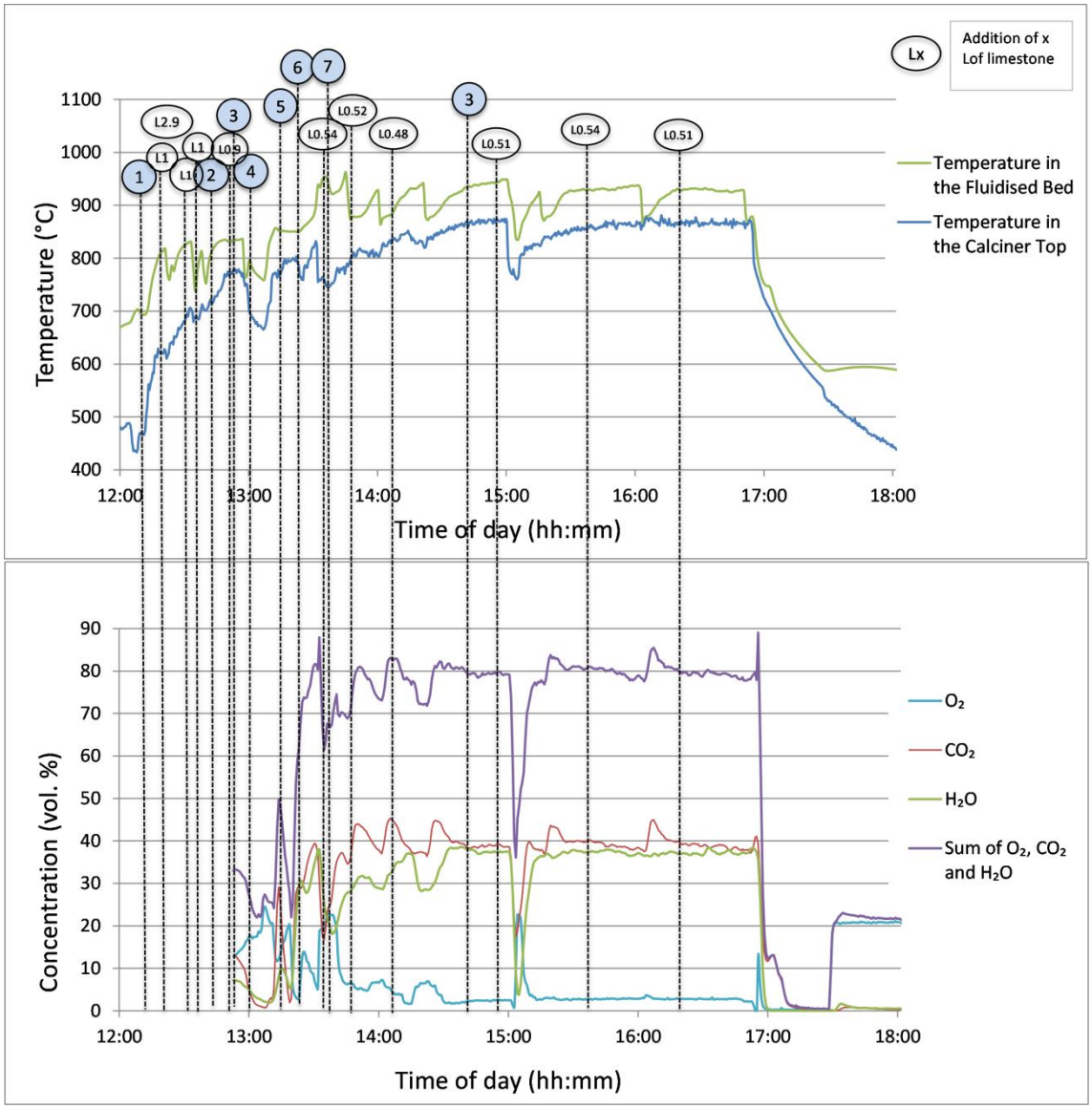

Figure 6-6: Temperature of the FB of the calciner and temperature and composition of the off-gas at its exit.

The temperature in the fluidised bed was maintained constant during the test by regulating the flow rate of NG and consecutively adjusting the flow rate of O_2 to achieve a calciner velocity of around 0.30 m/s. During the constant operation, the following energetic balance was observed: In the calciner, the oxygen was preheated to only 300 °C for safety reasons; hence, providing 0.5 kW in latent heat. Around 15.5 kW was released by the combustion of NG in the fluidised bed: only 5.3 kW was needed for a continuous calcination (when no fresh material was added), 3.6 kW to cover the latent heat of the off-gas

and ca. 7 kW for heating the circulating adsorbent and to cover the heat losses. In the carbonator, 3.2 kW was provided by the preheating of the gas (to 350 °C), and 5.4 kW was released by the carbonation process. Almost 5 kW was carried out of the carbonator as latent heat of the off-gas and 3.6 kW needed to be dissipated by heat losses to cover the heat released by the exothermic reaction while maintaining the temperature at 650 °C. When the carbonation process starts (and is effective) the temperature in the carbonator approaches 700 °C, which shifts the attainable thermodynamic equilibrium concentration of the outlet gas to higher values. This theoretical minimum concentration, dependent on the temperature in the carbonator, is depicted alongside the concentration measured during testing in Figure 6-7.

The carbonation process was initiated with ca. 6.7 L of limestone being present in the rig. An additional 0.54 L at the beginning of the carbonation (13:45 in Figure 6-7) resulted in the decrease of residual CO_2 in the gas below 5% vol. and this level was maintained throughout the test by additions of 0.5 L limestone batches (when the concentration of CO_2 at the exit of carbonator exceeded 5%. The time intervals between the additions of fresh limestone to the calciner were 15 min, 20 min, 50 min, 45 min and 50 minutes. Therefore, it can be concluded that for stable operation it would be necessary to add fresh sorbent corresponding to 0.5 L (750 g) of limestone approximately every 50 minutes, which is equivalent to a make-up ratio (F_0/F_{CO2}) of 6%, as described elsewhere [25], of 6%. The make-up ratio in these experiments was mainly influenced by the limestone (reactivity decay and elutriation). The value of this parameter was chosen based on the CO_2 concentration at the carbonator outlet, i.e. adding more limestone when it reached a 5% vol CO_2.

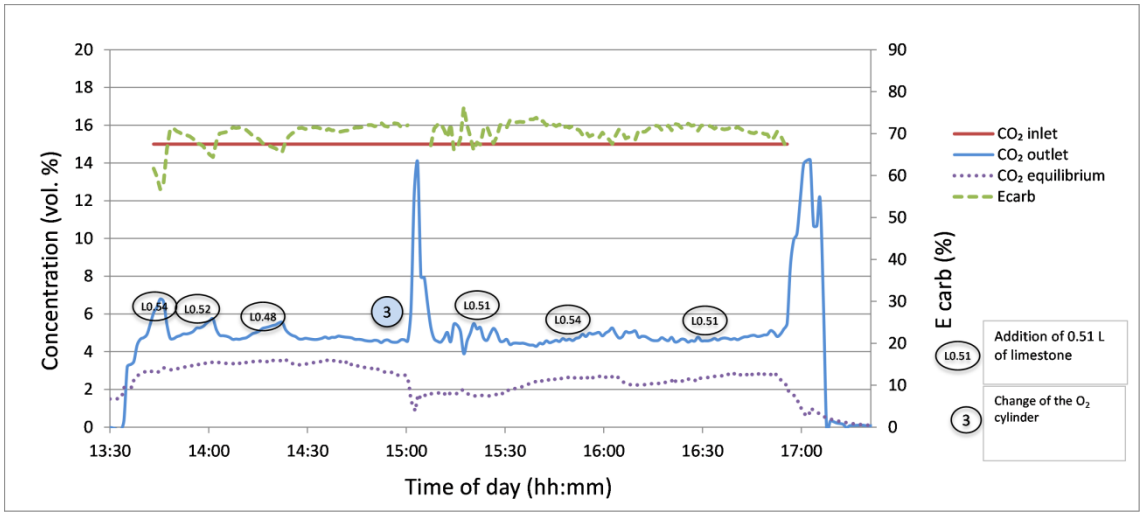

Figure 6-7: CO_2 concentration at inlet and at outlet of the carbonator and corresponding capture efficiency (E_{carb}) for 300–400 µm limestone with 100% O_2

The mass and molar balances of the inputs and outputs of solids from the rig are given in Table 6-3 and Table 6-4.

Table 6-3: Mass balance of solids and sieve analysis of the inputs (limestone) and outputs (other) for 300–400 µm limestone with 100% O_2

Fraction	Limestone in	Carbonator	Calciner	Cyclone calciner	Cyclone Carbonator
Total mass (g)	14000	1900	4200	2000	120
>355 µm	21%	16%	4%	0%	0%
300-350 µm	43%	45%	38%	1%	1%
250-300 µm	33%	26%	48%	3%	0%
212-250 µm	2%	4%	9%	7%	1%
150-212 µm	0%	3%	1%	35%	14%
63-150 µm	0%	5%	0%	41%	46%
0-63 µm	0%	0%	0%	12%	38%

Table 6-4: Molar balance estimate (10% humidity of the raw limestone, 75% wt. of the output in calcined state) for 300–400 µm limestone with 100% O_2

Fraction	Limestone in	Carbonator	Calciner	Cyclone calciner	Cyclone Carbonator	Difference (out – in)
Total mol	130	31	66	32	2	0
>355 µm	27	5	2	0	0	-20
300-350 µm	56	14	25	0	0	-17
250-300 µm	4	8	32	1	0	-2.6
212-250 µm	2	1	6	2	0	+6.9
150-212 µm	0	1	1	11	0	+13

63-150 µm	0	2	0	13	1	+16
0-63 µm	1	0	0	4	1	+4.1

Based on the sieving analysis, it can be concluded that the original fraction of limestone was retained mostly in circulation in the rig, while particles mostly <250 µm were carried over to the cyclone of the calciner. These particles result predominantly from the breakage/attrition of larger particles.

6.4 Discussion

The operation of the calciner with an inlet of 100% vol oxygen is achievable, based on exploiting the endothermic nature of the calcination reaction, as well as the fact that the solids circulate between the two reactors at different temperatures. This operating mode aims to make the CaL process more economically promising by reducing capital and operating costs. As the recycle of flue gas (mainly CO_2, water vapor and unreacted O_2) is reduced or even eliminated, the heat consumed to preheat this stream is lower. Therefore, less oxygen is needed and a smaller ASU would be required. As the gas flow would be lower in this configuration, the size of the calciner would be smaller for the same fluidization velocity.

A standard methodology was developed to ensure the safe operation of the high-oxygen concentration in the calciner. The results showed a capture efficiency of up to 70% in some of the performed experiments. Also, different particle size distributions were used in this reactor configuration (carbonator as a CFB; calciner as a BFB). The distributions were: 100–200 µm; 200–300 µm; 300–400 µm. For the smallest distribution (100–200 µm), however, there were elutriation issues and the majority of the bed inventory was found in the calciner's cyclone catch-pot. The best results were achieved with the largest particle size distribution (300–400 µm): an E_{carb} of ~ 70% was maintained throughout the experiment with a make-up ratio of about 6%.

This protocol was improved by minimizing the electrical heating provided to the gas and calciner when the natural gas is being combusted, in order to protect the tubes from electrical discharges caused by the heating elements.

Also, it has been noted that the O_2 concentration increase can be achieved more rapidly than in initial experimental campaigns, from 20% vol to 60% vol and 100% vol. It is important to highlight that the most critical steps in this process are the start of the combustion and the increase of the oxygen concentration, which can cause increased temperatures that will turn off the natural gas source if the temperature goes higher than 980 °C. Also, the material make-up is a concern as it can lower the temperature of the reactor and stop the combustion process, and therefore, it should be added in small batches.

With this methodology applied to this experimental rig, it is possible to test new synthetic materials, as well as materials improved via doping, thermal pre-treatment, chemical pre-treatment, etc. [26]. This protocol allows these new sorbents to be tested under realistic conditions providing a standard methodology for sorbent comparison. However, there are some challenges when applying this concept at larger scale, such as the use of coal in the calciner under these operating conditions. The use of solid fuels would increase the difficulty in calciner operation due to the high temperatures, which can lead to ash agglomeration and eventually defluidizing phenomena [27]. This needs further study in order to determine the feasibility of this protocol; however, the concept was proved successful at pilot-scale in this work using natural gas.

Another limitation arising from this study is the duration of the tests, with ~ 3 h of steady state operation per test; this is due to the heating process of the plant, which is a slow process. The average number of carbonation/calcination cycles experienced by a particle when circulating between reactors is not known. It is possible that the high oxygen concentration had a negative effect causing more sintering in the limestone particles. Further investigation of these challenges would help to assess the suitability of the protocol as a novel and feasible operating mode for CaL plants at a higher scale.

6.5 Acknowledgments

The research leading to these results has received funding from the European Community's Research Fund for Coal and Steel (RFCS) under grant agreement n° RFCR-CT-2014-00007. This work was funded by the UK Carbon Capture and Storage Research Centre (UKCCSRC) as part of Call 2 projects. UKCCSRC is supported by the Engineering and Physical Sciences Research Council (EPSRC) as part of the Research Council's UK Energy Programme, with additional funding from the Department of Business, Energy and Industrial Strategy (BEIS - formerly DECC). The authors would also like to thank Mr Martin Roskilly for his enormous help throughout the course of this work.

6.6 References

[1] Bernstein, L., Lee, A., Crookshank, S., 2011. Carbon dioxide capture and storage: a status report. Climate Policy, 6, pp. 241–246.

[2] Boot-Handford, M.E., Abanades, J.C., Anthony, E.J., Blunt, M.J., Brandani, S., Mac Dowell, N., Fernández, J.R., Ferrari, M.C., Gross, R., Hallett, J.P. and Haszeldine, R.S., 2014. Carbon capture and storage update. Energy & Environmental Science, 7(1), pp.130-189.

[3] Herzog, H.J., 2011. Scaling up carbon dioxide capture and storage: from megatons to gigatons. Energy Economics, 33(4), pp. 597-604.

[4] Shimizu, T., Hirama, T., Hosoda, H., Kitano, K., Inagaki, M., Tejima, K., 1999. A twin fluid-bed reactor for removal of CO_2 from combustion processes. Chemical Engineering Research and Design, 77(1), pp. 62–68.

[5] Blamey, J., Anthony, E. J., Wang, J., Fennell, P. S., 2010. The calcium looping cycle for large-scale CO_2 capture. Progress in Energy and Combustion Science, 36(2), pp. 260-279.

[6] Masnadi, M. S., Grace, J. R., Bi, X. T., Ellis, N., Lim, C. J., Butler, J. W., 2015. Biomass/coal steam co-gasification integrated with in-situ CO_2 capture. Energy, 83, pp. 326-336.

[7] Abanades, J. C., Anthony, E. J., Lu, D. Y., Salvador, C., Alvarez, D., 2004. Capture of CO_2 from combustion gases in a fluidized bed of CaO. AIChE Journal, 50(7), pp. 1614-1622.

[8] Hughes, R. W., Lu, D. Y., Anthony, E. J., Macchi, A., 2005. Design, process simulation and construction of an atmospheric dual fluidized bed combustion system for in situ CO_2 capture using high-temperature sorbents. Fuel Processing Technology, 86(14), pp. 1523-1531.

[9] Lu, D. Y., Hughes, R. W., Anthony, E. J., 2008. Ca-based sorbent looping combustion for CO_2 capture in pilot-scale dual fluidized beds. Fuel Processing Technology, 89(12), pp. 1386-1395.

[10] Hawthorne, C., Dieter, H., Bidwe, A., Schuster, A., Scheffknecht, G., Unterberger, S. and Käß, M., 2011. CO_2 capture with CaO in a 200 kW_{th} dual fluidized bed pilot plant. Energy Procedia, 4, pp. 441-448.

[11] Sánchez-Biezma, A., Ballesteros, J.C., Diaz, L., De Zárraga, E., Álvarez, F.J., López, J., Arias, B., Grasa, G. and Abanades, J.C., 2011. Postcombustion CO_2 capture with CaO. Status of the technology and next steps towards large scale demonstration. Energy Procedia, 4, pp. 852-859.

[12] Dieter, H., Hawthorne, C., Zieba, M. and Scheffknecht, G., 2013. Progress in calcium looping post combustion CO_2 capture: successful pilot scale demonstration. Energy Procedia, 37, pp.48-56.

[13] Arias, B., Diego, M.E., Abanades, J.C., Lorenzo, M., Diaz, L., Martínez, D., Alvarez, J. and Sánchez-Biezma, A., 2013. Demonstration of steady state CO_2 capture in a 1.7 MW_{th} calcium looping pilot. International Journal of Greenhouse Gas Control, 18, pp. 237-245.

[14] Ströhle, J., Junk, M., Kremer, J., Galloy, A., Epple, B., 2014. Carbonate looping experiments in a 1MW_{th} pilot plant and model validation. Fuel, 127, pp. 13-22.

[15] Bidwe, A. R., Hawthorne, C., Dieter, H., Dominguez, M. A., Zieba, M., Scheffknecht, G., 2014. Cold model hydrodynamic studies of a 200 kW_{th} dual

fluidized bed pilot plant of calcium looping process for CO_2 Capture. Powder Technology, 253, pp. 116-128.

[16] Chang, M.H., Chen, W.C., Huang, C.M., Liu, W.H., Chou, Y.C., Chang, W.C., Chen, W., Cheng, J.Y., Huang, K.E. and Hsu, H.W., 2014. Design and experimental testing of a 1.9 MW_{th} calcium looping pilot plant. Energy Procedia, 63, pp. 2100-2108.

[17] Reitz, M., Junk, M., Ströhle, J., Epple, B., 2016. Design and operation of a 300kW th indirectly heated carbonate looping pilot plant. International Journal of Greenhouse Gas Control, 54, pp. 272-281.

[18] Martínez, A., Lara, Y., Lisbona, P., Romeo, L. M., 2012. Energy penalty reduction in the calcium looping cycle. International Journal of Greenhouse Gas Control, 7, pp. 74-81.

[19] Perejón, A., Romeo, L. M., Lara, Y., Lisbona, P., Martínez, A., Valverde, J. M., 2016. The calcium-looping technology for CO_2 capture: on the important roles of energy integration and sorbent behavior. Applied Energy, 162, pp. 787-807.

[20] Mantripragada, H. C., Rubin, E. S., 2014. Calcium looping cycle for CO_2 capture: Performance, cost and feasibility analysis. Energy Procedia, 63, pp. 2199-2206.

[21] ASTM C1271-99(2012), Standard Test Method for X-ray Spectrometric Analysis of Lime and Limestone, ASTM International, West Conshohocken, PA, 2012, www.astm.org.

[22] ASTM C25-11e2, Standard Test Methods for Chemical Analysis of Limestone, Quicklime, and Hydrated Lime, ASTM International, West Conshohocken, PA, 2011, www.astm.org.

[23] Alonso, M., Rodríguez, N., Grasa, G., Abanades, J. C., 2009. Modelling of a fluidized bed carbonator reactor to capture CO_2 from a combustion flue gas. Chemical Engineering Science, 64(5), pp. 883-891.

[24] Manovic, V., Anthony, E. J., 2008. Parametric study on the CO_2 capture capacity of CaO-based sorbents in looping cycles. Energy & Fuels, 22(3), pp. 1851-1857.

[25] Duhoux, B., Mehrani, P., Lu, D. Y., Symonds, R. T., Anthony, E. J., & Macchi, A., 2016. Combined Calcium Looping and Chemical Looping Combustion for Post-Combustion Carbon Dioxide Capture: Process Simulation and Sensitivity Analysis. Energy Technology, 4(10), pp. 1158-1170.

[26] Erans, M., Manovic, V., Anthony, E. J., 2016. Calcium looping sorbents for CO_2 capture. Applied Energy, 180, pp. 722-742.

[27] Basu, P., 1982. A study of agglomeration of coal-ash in fluidized beds. The Canadian Journal of Chemical Engineering, 60, pp. 791–795.

7 PILOT TESTING OF ENHANCED SORBENTS FOR CALCIUM LOOPING

María Erans, Michal Jeremias, Vasilije Manovic, Edward J Anthony

Combustion and CCS Centre, Cranfield University, Bedford, Bedfordshire, United Kingdom

Draft prepared

Statement of contributions of joint authorship

María Erans conducted the literature review on the subject, planned and performed the experiments, drafter and critically reviewed this manuscript. Also, María Erans analysed the results and produced figures and tables in this paper. María Erans and Michal Jeremias carried out all the experimental campaigns depicted in this paper in the 25 kW_{th} unit. Vasilije Manovic and Edward J Anthony proof-read and critically commented on the manuscript.

Abstract

One of the main challenges for CO_2 capture using the calcium looping cycle is the reactivity decay of CaO-based sorbents with increasing number of cycles. In order to overcome this challenge, research has moved towards the investigation of enhanced sorbents in order to mitigate the decay in carrying capacity. However, this creates other potential problems related to the scalability of these production techniques and their effect on the production cost of such sorbents, and raises the question as to whether they can be used at larger scale. In this work limestone and two enhanced materials: (i) HBr-doped limestone with a novel surface impregnation technique and (ii) calcium aluminate pellets, are tested in a 25 kW_{th} pilotscale reactor in order to investigate their capture performance and mechanical stability under fluidised bed conditions. The unit set-up comprises a circulating fluidised bed (CFB) carbonator operating at ~650 °C and a bubbling fluidised bed (BFB) calciner operating at 900-950 °C. The HBr-doped limestone showed very promising

results in terms of both stability of the CO_2 uptake as well as low elutriation and attrition when compared to the pellets.

Keywords: carbon capture, calcium looping, CaO-based pellets, doping, pilot testing

7.1 Introduction

CO_2 emissions from power generation and industrial sectors have increased rapidly in recent decades. These emissions represent the greatest contributors to the greenhouse gas effect [1]. A portfolio of low-carbon technologies needs to be deployed in order to mitigate the effects that these emissions have in many natural systems, as well as the consequences this poses on human activities. Carbon capture and storage (CCS) is part of this portfolio and has been proposed for the power generation and carbon-intensive industrial sectors as a route for their decarbonation [2, 3].

Calcium looping (CaL) is a second-generation technology for CO_2 capture, which has attracted a fair amount of research activity [4]. In its fluidised bed form, it consists of two interconnected fluidised beds and is based on the reversible carbonation of lime. In the first reactor (carbonator) CaO-based material is carbonated at ~650°C with the CO_2 present in flue gas from power generation or carbon-intensive industrial processes; the saturated sorbent is then transferred to the second reactor (calciner) where the sorbent is regenerated (calcined) at high temperatures (~900-950°C). In order to provide the energy for the calcination reaction to occur, fuel is burnt in oxy-fuel conditions in the calciner. A schematic of a typical CaL configuration is presented in Figure 7-1.

This concept has been demonstrated at scales of up to 1.9 MW_{th} in different research institutions using different reactor configurations. Some examples of these plants are: the 200 kW_{th} pilot plant in IFK (Stuttgart), the 1.7 MW_{th} unit “La Pereda” developed by CSIC in Oviedo, the 1.9 MW_{th} unit in Taiwan, the 1 MW_{th} plant in Darmstadt, among others [5-11].

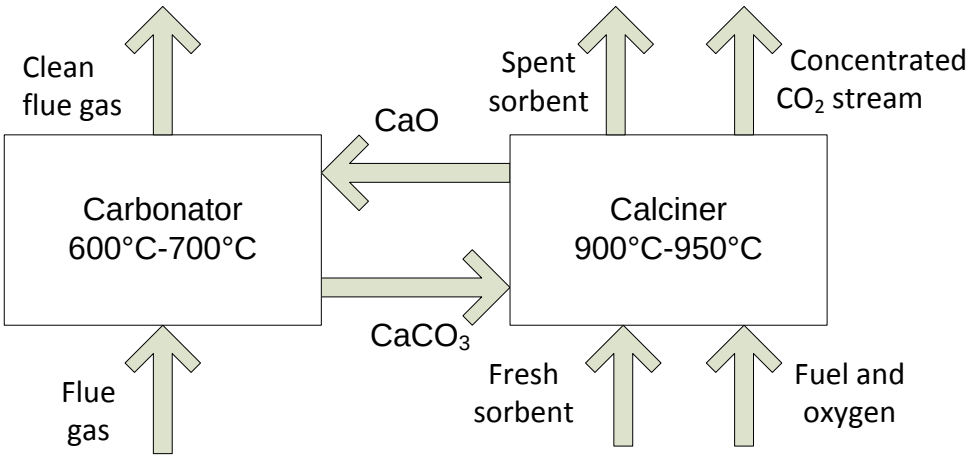

Figure 7-1: Schematic of the calcium looping cycle

One of the main challenges of this technology is the deactivation of sorbent over the capture/regeneration cycles [12-14]. In order to overcome this issue, several approaches have been explored such as the modification of natural materials and the development of synthetic sorbents with techniques such as: sol-gel combustion [14-19], organic acid modifications [20-24], co-precipitation [25, 26] and granulation [27-33]. Another important challenge, particularly at larger scale in fluidised bed reactors, is elutriation of the sorbent from the reactors, resulting in the loss of active material.

One of the enhancement methods proposed is doping limestone in order to increase its carrying capacity. Different mineral-acid dopants have been investigated such as: HBr, HCl, HNO_3 and HI. Their performance has been studied during carbonation/calcination cycles [34, 35], and it has been shown that such dopants can significantly improve the performance of the sorbents. However, the experimental results are not always consistent and it appears that the extent of the improvement depends on the combination of the specific limestone and doping agent, as well as the concentration of the dopant [34, 35]. The highest residual conversion was found using Havelock and Longcliffe limestones with an HBr solution containing 0.167 mol % HBr/$CaCO_3$ [35].

This work investigates the capture performance of enhanced CaO-sorbents at the pilot scale in a CFB carbonator and BFB calciner (25 kW_{th}). Specifically,

Longcal limestone doped with HBr using a novel surface impregnation technique and calcium aluminate pellets (90% lime and 10% calcium aluminate cement) were tested. Operating conditions were chosen to be as close as possible to the anticipated real conditions in CaL industrial systems.

7.2 Experimental

7.2.1 Materials

Longcal limestone from the UK was used as a $CaCO_3$ source. Commercial calcium aluminate cement, CA-14, manufactured by Almatis, was used as a binder in the pelletisation process and as a source of Al_2O_3. The limestone-doping solution was prepared by diluting 57 g of 47%-wt. HBr with deionised water to 1 L to reach a concentration of 0.33 mol/L HBr.

7.2.2 Sorbent preparation procedure

Two enhanced types of sorbent were produced: (i) pellets with 10% calcium aluminate cement and 90% calcined limestone; and (ii) HBr-doped limestone. The pellets were prepared by introducing 10% wt. calcium aluminate cement and 90% wt. calcined limestone in the pelletiser vessel. A comprehensive description of this technique can be found elsewhere [28]. After pelletisation of the samples, the particles were sieved to the desired particle size range and air dried for 24 h before storage. HBr was selected as a suitable dopant based on previous work [35]. However, this doping technique was deemed less suitable for larger samples, of the order of several kilograms. Therefore, the method was modified to be suitable for larger-scale production and to maintain the same HBr concentration of 0.17 % mol HBr/mol $CaCO_3$. 1 L of 0.33 mol/L HBr solution was evenly sprayed on 20 kg of Longcliffe limestone, while mixing the sample thoroughly to obtain a uniform distribution of the solution over the sample mass. After the impregnation, the sample was spread and dried for several days at ambient conditions.

7.2.3 Pilot plant description

The pilot plant (Figure 7-2) comprises a CFB carbonator (4.2 m long and 0.1 m ID) and a BFB calciner (1.2 m long and 0.165 m ID). The fluidising gases are pre-heated by electrically-heated pipes. The carbonator gas distributor has 8 nozzles with 20 2-mm holes each, whilst the calciner gas distributor has 20 nozzles, each with 6 1-mm holes. There are two cyclones in series at the exit of the carbonator: one to separate the bulk of the particles to be recycled to the calciner and the other one to prevent remaining particles from being emitted to the environment, while the calciner has only one cyclone. The carbonator and calciner are connected by two loop seals (upper and lower), which allow the controlled circulation of sorbent between the reactors. During the tests, the loop seals were fluidised by nitrogen. The reactors are electrically heated in order to reach the temperatures needed for stable operation. In addition, in order to reach the high temperatures necessary in the calciner and to provide enough heat for calcination, natural gas (NG) is burnt directly in the fluidised bed. Two gas analysers (ADC MGA-3000 series) are used to measure the gas compositions at the carbonator exhaust (CO_2 concentration) and calciner exit (CO_2, CO, O_2, CH_4 concentrations). Additionally, a Fourier Transform Infrared analyser (FTIR) (Protea, model FTPA-002) was used at the exhaust of the calciner to monitor the quality of combustion (H_2O, CO_2, CO, NO_x, SO_2, CH_4, C_2H_6, C_3H_8, C_2H_4, HCHO concentrations).

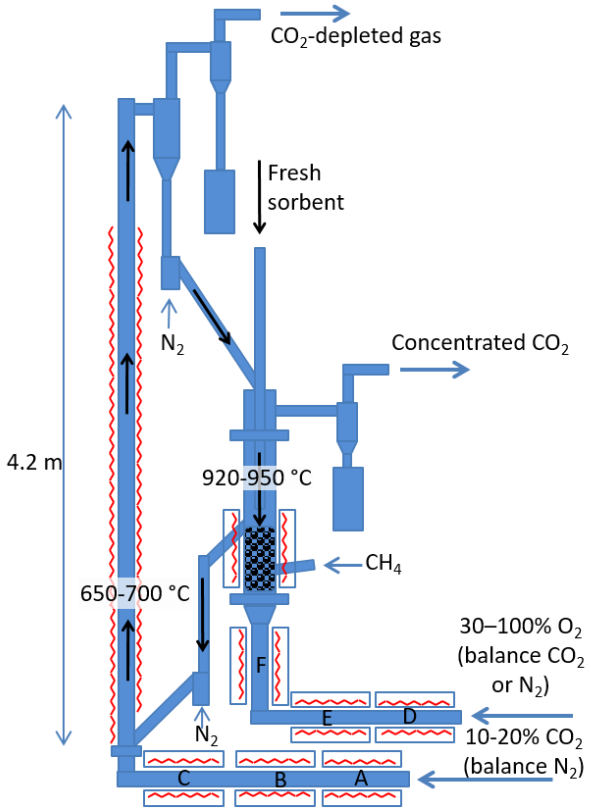

Figure 7-2: Schematic of the 25 kW_{th} pilot plant

7.3 Results and discussion

7.3.1 Standard procedure of an experimental run and a base case result with pure Longcliffe limestone

Operation of the reactor for the experiments described here was limited to working hours. Here, as a representative case, an experimental run described in detail elsewhere is presented [36]. In Figure 7-3, the temperature of the calciner, together with the gas analysis at its outlet measured by FTIR are presented through the experimental run.

The experimental run was started as follows: the pilot plant was first heated up to close to the desired temperatures by means of electrical furnaces surrounding the preheating lines, the carbonator and the BFB of the calciner, with only a low flow of N_2 passing through both reactors. When the temperature of the calciner's BFB reached 600°C, the first batch of limestone (3 L) was added to the reactor and was heated to 650°C by means of electrical

heating around the calciner with a flow of N_2 at velocity 0.35 m/s in the fluidised bed, i.e., under mild fluidising conditions. A portion of the N_2 was substituted by O_2 (to reach 40% vol. O_2) at the inlet of the calciner and the combustion of natural gas was started (by its self-ignition in the FB) at slightly over stoichiometric conditions (ER (stoichiometric ratio) 1.05). This corresponds to no. 1 in Figure 7-3. The temperature of the fluidised bed was quickly increased and when the calcination reaction started, more limestone (3x1 L) was added to be calcined. A chute is located at a height of 400 mm above the distributor of the calciner. When the bubbling fluidised bed reaches this level, the surplus material overflows by this chute to the lower loop seal and then to the carbonator. During the initial calcination of the first batch of limestone in the calciner, the flow of N_2 through the carbonator is maintained at a low level to prevent its transport back to the calciner. When nearly all material in the calciner was calcined, which can be tracked by a quick increase in temperature, the circulation of the material between carbonator and calciner was initiated by increasing the flow of N_2 to the carbonator to 2.5 m/s, thereby, transporting the sorbent from the carbonator to the cyclone where it is separated from the gas flow and then allowed to recirculate back to the calciner (no. 2 in Figure 7-3). No. 3 in Figure 7-3 depicts the change of the O_2 cylinder. To accelerate the calcination process and the heating of the additional limestone, the oxygen concentration in the in-flow to the calciner was increased in steps to 100% and a stoichiometric amount of methane was combusted in the fluidised bed (as depicted by no. 4 and 5 in Figure 7-3). After all the circulating material was calcined (as monitored by a steep increase in temperature in the calciner), a portion of the feed-in gas to carbonator was substituted with CO_2 (15%) and the carbonation reaction started (no. 6 in Figure 7-3 as monitored by the outlet concentration of CO_2 from the carbonator and by the endothermic calcination reaction occurring in the calciner). The temperature in the calciner during the steady state operation was regulated to be 920–950°C by adjusting the natural gas and O_2 flow rates to maintain the concentration of unconverted O_2 in the gas leaving the calciner at a very low level (around 5% vol.). The velocity was adjusted in the calciner

in no. 7 due to the excessive heat produced by the combustion, which caused an extreme increase in the temperature.

The performance of the carbonator is depicted in Figure 7-4**.** The CO_2 outlet concentration from the carbonator was maintained below 5% vol. by periodic addition of 0.5 L batches of fresh limestone to the calciner. This corresponds to stable capture efficiency, E_{carb}, of ca. 70%, calculated using the following formula [37]:

$$E_{carb} = \frac{F_{CO2} - F_{carb}}{F_{CO2}} \quad \textbf{(7-1)}$$

Where F_{CO2} is the molar flow rate of CO_2 entering the carbonator and F_{carb} is the molar flow rate of CO_2 leaving the carbonator. In this base case, a make-up ratio of 6% was needed to maintain this capture efficiency.

The size distribution of solids as determined after the experiment is summarised in Table 7-1, the samples recovered from the carbonator, calciner and their respective cyclones were analysed in order to measure their particle size distribution to have an understanding of the elutriation and attrition of the particles in such system.

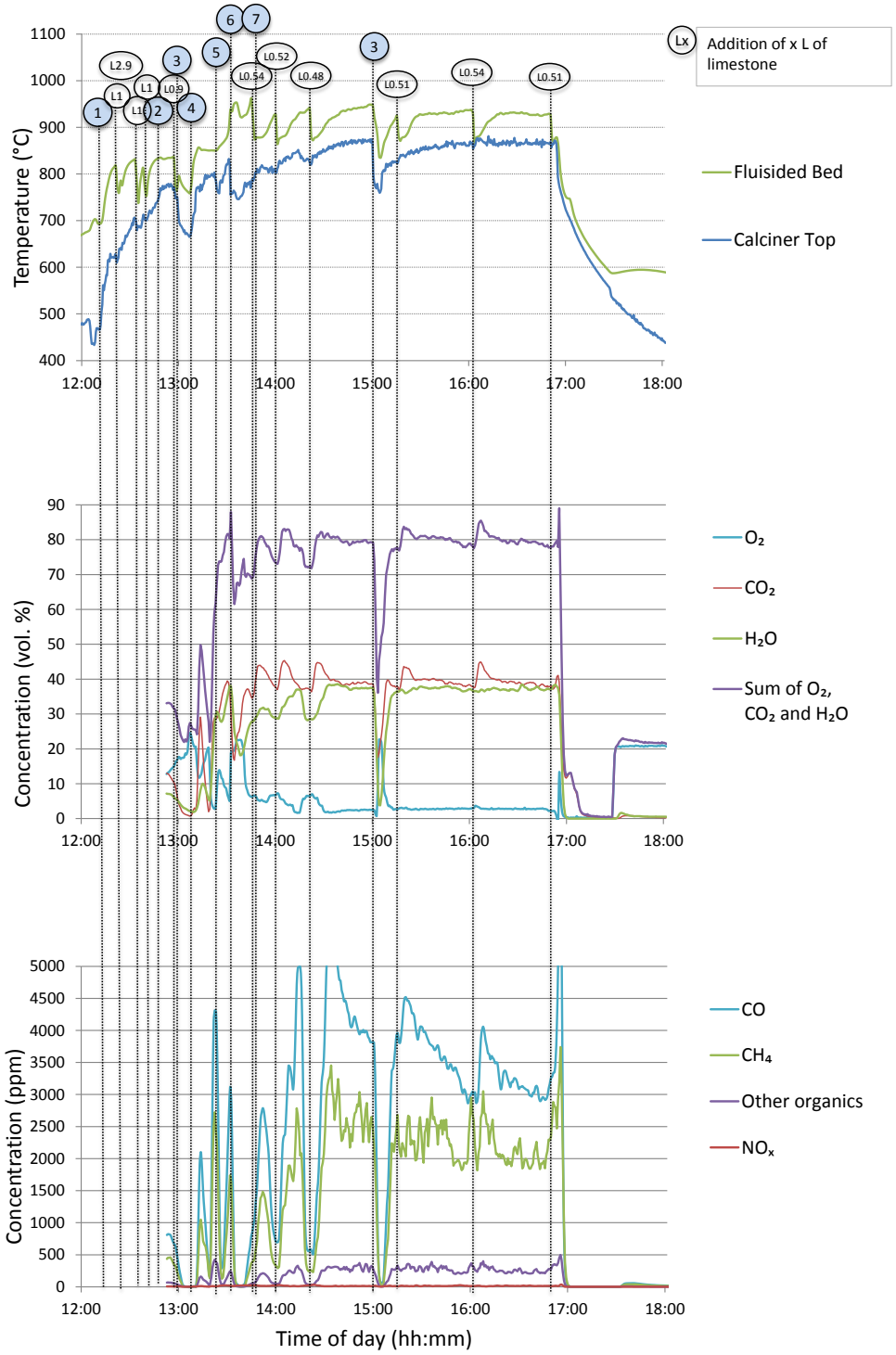

Figure 7-3: The temperatures in the FB of the calciner and the temperature and gas composition at the outlet of the reactor in the experiment with limestone. The "other organics" designates the sum of ethane, propane, ethene, and formaldehyde concentrations

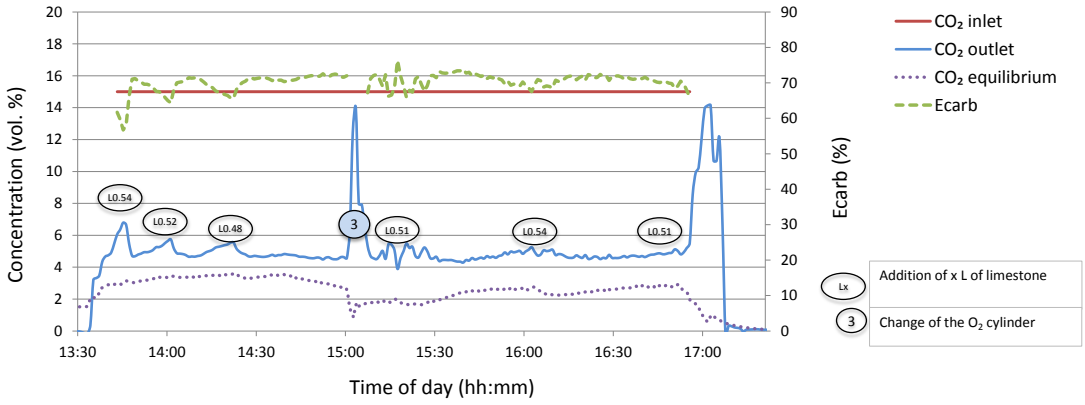

Figure 7-4: CO_2 concentration at the inlet and at the outlet of the carbonator and the corresponding carbonation efficiency, E_{carb}, in the experiment with limestone

Table 7-1: Weight balance of solids and sieve analysis of the inputs (limestone) and outputs

Fraction	Limestone in	Carbonator	Calciner	Cyclone calciner	Cyclone Carbonator
Total mass (g)	14000	1900	4200	2000	120
>355 µm	21%	16%	4%	0%	0%
300-350 µm	43%	45%	38%	1%	1%
250-300 µm	33%	26%	48%	3%	0%
212-250 µm	2%	4%	9%	7%	1%
150-212 µm	0%	3%	1%	35%	14%
63-150 µm	0%	5%	0%	41%	46%
0-63 µm	0%	0%	0%	12%	38%

7.3.2 HBr-doped sorbent tests

A test was performed with HBr-doped material, using the size fraction (300-400 µm). The setup of the test was the same as described in section 7.3.1. However, after heating 3 L of HBr-doped limestone, starting the combustion and inserting 2 more litres of limestone, there was a fault of the safety valve controlling NG flow (no. 2 in Figure 7-5). After its replacement, the NG (Natural Gas) combustion in 40 % O_2 was started and soon after this pure O_2 was used in the inlet of the calciner (no. 3, Figure 7-5).

The carbon capture from the carbonator inlet concentration (15% CO_2) was started (no. 4 in Figure 7-5) and the temperature in the fluidised bed of the

calciner was maintained at 930–950°C by adjusting the velocity of the calciner and the appropriate input of NG (15 kW) (no. 5 in Figure 7-5). Compared to the standard case with pure Longcliffe limestone (as described in 7.3.1), the CO_2 capture efficiency attained, seen in Figure 7-6, (E_{carb} = 70–80%) was higher with the same amount of limestone circulating in the rig.

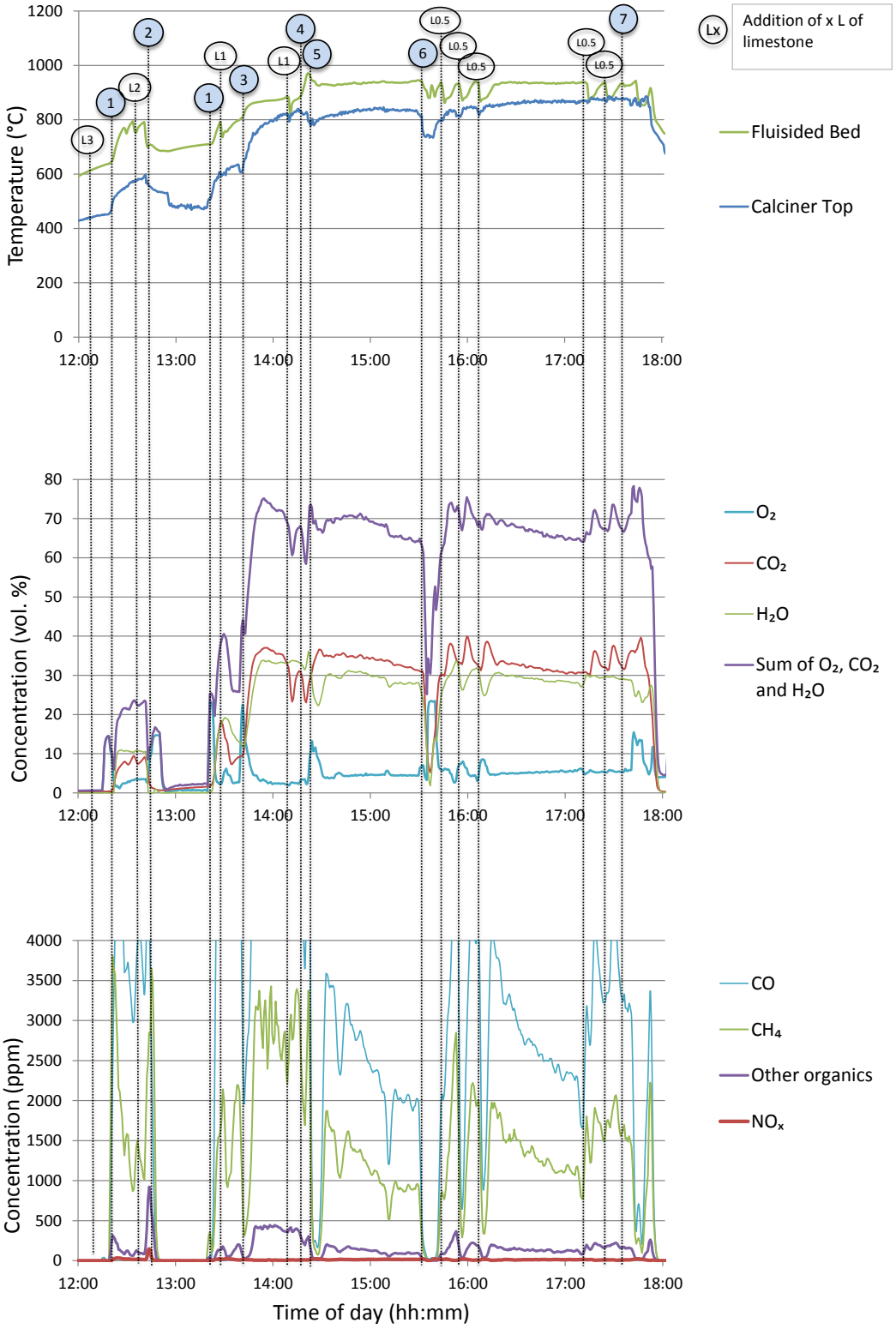

Figure 7-5: Temperatures of the FB and the freeboard of the calciner (top) and the composition of the off-gas from the calciner

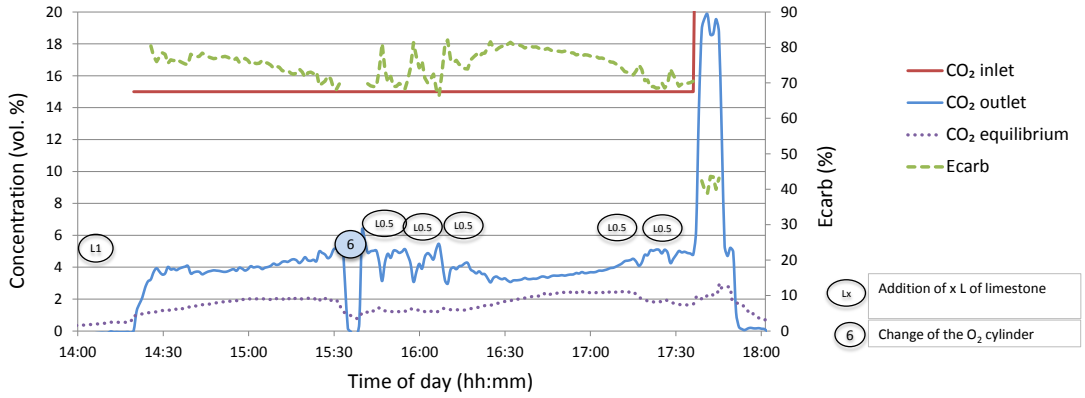

Figure 7-6: The residual concentration of CO_2 at the outlet of the carbonator compared to the inlet CO_2 concentration and the equilibrium CO_2 concentration for the experiment with HBr-doped limestone

The sieve analysis (Table 7-2) revealed that the doped material exhibited good mechanical properties with only about 400 g of material present in the cyclones out of more than 13 kg of material in the primary reaction loop. This was probably due to the lower shift to smaller particle sizes during the cycling. The X-ray fluorescence (XRF) and Brunauer-Emmett-Teller (BET) analyses of the samples recovered after the test are shown in Table 7-3.

Table 7-2: Weight balance of solids and sieve analysis of the inputs (HBr-doped limestone) and outputs

Fraction (weight %)	Limestone	Carbonator	Cyclone carbonator	Calciner	Cyclone calciner
Total mass (g)	13,300	3,100	50	3,990	370
>355 µm	13	5	3	4	17
300-355 µm	50	43	7	48	1
250-300 µm	34	43	11	37	2
212-250 µm	1	7	3	9	4
150-212 µm	0	2	3	1	10

63-150 µm	0	0	9	0	38
<63 µm	0	0	64	0	28

The fines in the cyclone at the outlet of the calciner exhibited a tendency to agglomerate, which was not observed in previous runs with un-doped Longcal limestone.

Table 7-3: BET, degree of calcination and XRF of the solids inputs and outputs

	HBr-doped limestone		**Carbonator out**		**Calciner out**		**Cyclone calciner**		**Cyclone carbonator**	
BET (m^2/g)	<1		1.88		2.33		1.14		<1	
Degree of calcination *			57 % wt calcined		81% wt calcined		19% wt calcined		5% wt calcined	
Weight %	Oxide	Oxide +CO_2	Oxide	Oxide +CO_2	Oxide	Oxide +CO_2	Oxide	Oxide +CO_2	Oxide	Oxide +CO_2
CaO	99	56	99	56	99	56	98	55	99	55
Br	0.29	0.13	0.032	0.014	0.025	0.011	0.088	0.04	0.57	0.26
MgO	0.26	0.19	0.34	0.24	0.33	0.23	0.3	0.21	0.26	0.18
SiO_2	0.14	0.1	0.17	0.12	0.1	0.070	0.37	0.26	0.19	0.13
Al_2O_3	0.11	0.1	0.086	0.063	0.061	0.045	0.29	0.21	0.042	0.083
SrO	0.036	0.016	0.030	0.014	0.030	0.013	0.038	0.02	0.033	0.015
MnO	0.019	ND	0.015	0.0071	0.015	0.0068	0.036	0.017	0.024	0.011
SO_3	0.014	ND	ND	ND	ND	ND	0.14	0.092	0.042	0.028
TiO_2	0.012	0.0053	0.011	ND	0.0066	ND	0.021	0.01	0.011	0.005
Fe_2O_3	0.011	0.0051	0.013	0.0058	ND	ND	0.34	0.16	0.095	0.044
Cl	0.005	ND	ND	ND	ND	ND	0.006	0.01	0.0081	0.0054

Cr_2O_3	ND	ND	ND	ND	ND	ND	0.093	0.04	0.042	0.019
K_2O	ND	ND	ND	ND	ND	ND	0.016	0.06	0.027	0.017
CO_2 (with CaO and MgO)	-	44	-	44	-	44	-	44	-	44
Before normalisation to 100%	75	97	90	117	94	123	83	108	78	102

*The degree of calcination is determined by calcining the material in the oven at 900°C for 2 h and is expressed as the theoretical concentration of CaO in the mixture of CaO and $CaCO_3$

It is interesting to note that the Br^- was concentrated mainly in the carbonator cyclone fraction. The smallest fraction of the limestone was found in this cyclone (see Table 7-2), and it can be reasonably hypothesised that Br^- is concentrated mainly at the surface of sorbent particles given the way it was originally introduced into the limestone. This surface is readily attrited during the circulation of the particles mainly due to mechanical abrasion generating very small particles [38], which are then collected in the carbonator cyclone, and these particles have the highest loading of Br^-. This suggests that the impregnation of the surface of the particle was only partly successful as the Br^- penetrated the particles only to a limited extent and mainly remains on its surface. However, the behaviour of the material during the test and the fact that low overall attrition and breakage of the particles was observed suggest that the doping technique was successful in terms of achieving an improvement in limestone behaviour for the CaL process. Also, it is important to highlight the effect that the HBr-doping of the surface had on the structure of the pores. It has been suggested previously that this type of enhancement method produces $CaBr_2$, which modifies the structure of the pores making them more favourable for the process [39]. This suggests that this phenomenon mitigates the sintering of the surface of the particles enhancing their CO_2 uptake and delaying sintering. Moreover, this method uses less HBr solution than the previously proposed technique of impregnating the whole

particle [35]. As the solution only impregnates the surface, while the amount of solution used is less, this is clearly a more cost-effective methodology for enhancement of sorbents at industrial scale.

7.3.3 Calcium aluminate pellets testing

The steps followed in this run can be seen in Figure 7-7. There were some challenges with the dosing of the material into the reactor. Namely, the pellet preparation procedure left the pellets substantially wet (18% wt. moisture). Therefore, introducing 100 g of pellets in the calciner released 42 L of steam (at 900 °C). Due to the excessive steam release during the dosing of the pellets, filling of the reactor was very slow. Therefore, after introducing 6.3 L of pellets, 4 L of doped limestone was added so that the circulation would begin. When there was enough material in the system, the oxygen concentration in the calciner was changed from 40% O_2 (no. 1 in Figure 7-7) to 50% O_2 (no. 2 in Figure 7-7), and then to 100% O_2 (no. 3 in Figure 7-7). There is a defluidisation of the system in no. 4 caused by changing the oxygen cylinder.

The start of carbonation is marked by no. 4, no. 5, no. 7, no. 8, no. 9 and no. 10 by the addition of 10%, 15%, 20%, 25%, 30% and 35% vol CO_2 into the carbonator, respectively.

The results are summarised in the following chart (Figure 7-8). The efficiency attained for carbonation was substantially lower than in the base case with pure Longcliffe limestone and in the abovementioned case with HBr-doped limestone. The main limitation is the amount of available adsorbent to react with CO_2 in the carbonator. Possible solutions would be the use of a taller carbonator which would allow longer retention and contact time of the calcined sorbent particles and the gas, or the use of more limestone circulating inside the rig between calciner and carbonator.

The capture efficiency of the experimental run with pellets mixed with doped limestone was lower compared to the previous experiments with HBr-doped limestone; however, the pellets showed that they can be used in combination with limestone for the CaL process. As shown in Table 7-4 and Table 7-5, it is

clear that some of the pellets were fragmented or attrited but the bulk of them was retained within the CaL rig.

This experimental run demonstrated that the spent material after reactivation and pelletisation [40] can be potentially reused in the operation of the calcium looping rig in combination with fresh limestone. In the current experiment in total 58% wt. of the solid inventory of the rig was pellets. However, there are some difficulties related to their use, such as the excessive release of steam during their quick heating above 900°C and their tendency to make agglomerates during their dosing and heating, which could be dealt with by a slower feeding rate, at the level of make-up.

Such challenges regarding this type of material could be mitigated by previously carbonating the pellets. This can be done by means of capturing residual CO_2 from low-emitting sources, such as for example the residual CO_2 concentration that leaves the carbonator (as can be seen in Figure 7-8). The capture with this type of material has also been studied previously at room temperature [41] with successful results. This would also enhance the conversion of the pellets, due to the fact that material that is previously carbonated exhibited better results than material which has been initially calcined [42]. This would not only improve the performance of synthetic materials in real systems due to the production of less mechanical stress within the particle due to steam release, but would also mitigate the emissions from CaL plants making the overall capture of these plants higher.

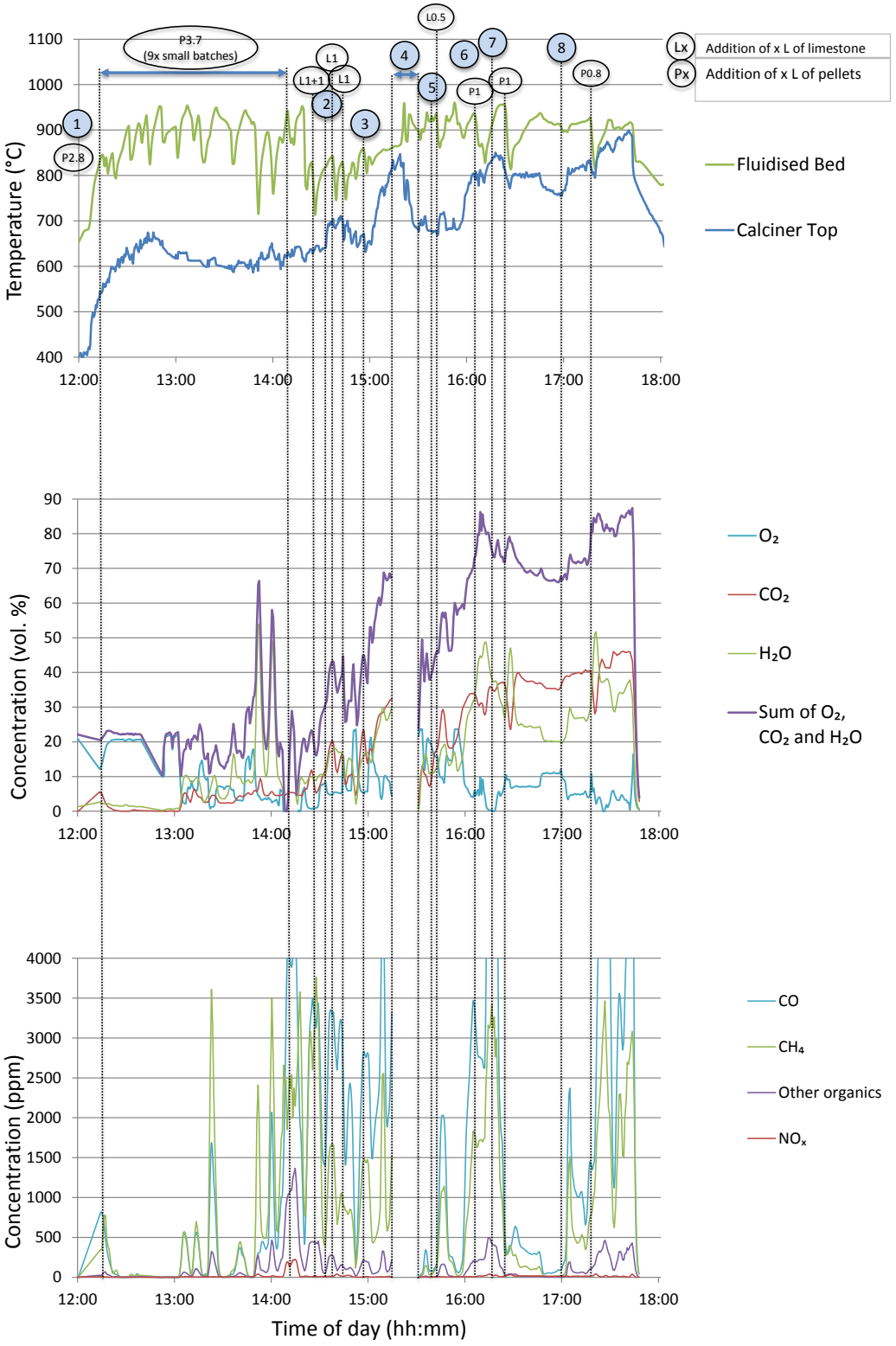

Figure 7-7: Temperatures of the FB and the freeboard of the calciner (top) and the composition of the off-gas from the calciner calciner for the experiment with pellets mixed with doped limestone

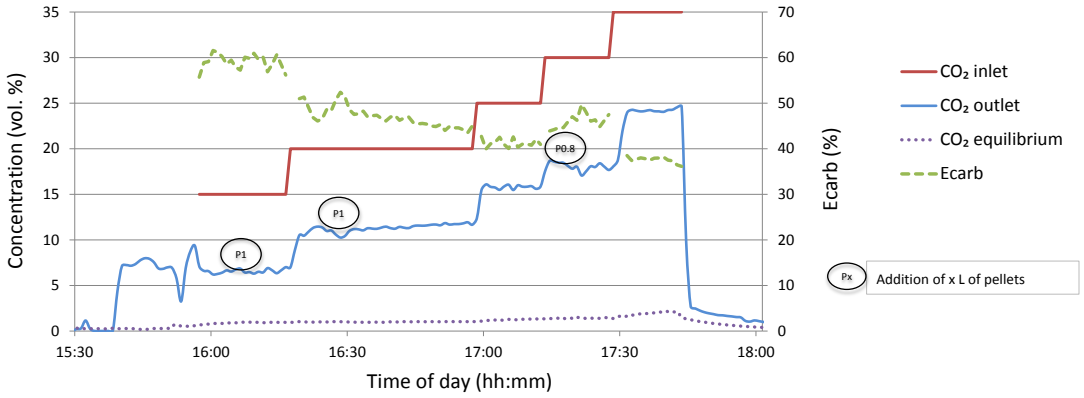

Figure 7-8: The residual concentration of CO_2 at the outlet of the carbonator compared to the inlet CO_2 concentration and the minimal thermodynamically achievable CO_2 residual concentration for the experiment with pellets mixed with doped limestone

Table 7-4: Weight balance of solids and sieve analysis of the inputs and outputs

Fraction (weight %)	Limestone	Pellets	Carbonator	Cyclone carbonator	Calciner	Cyclone calciner
Total mass (g)	6500	9100	3400	2600	3300	1100
>710 µm	0	27	29	1	2	6
600-710 µm	0	19	12	1	5	10
500-600 µm	0	19	12	2	10	14
425-500 µm	0	20	5	2	9	7
355-425 µm	13	11	9	2	15	17
300-355 µm	51	3	14	8	27	9

250-300 µm	34	1	15	18	25	19
212-250 µm	1	0	3	11	5	6
150-212 µm	0	0	1	17	1	4
63-150 µm	0	0	0	23	0	4
<63 µm	0	0	0	15	0	3

Table 7-5: BET, degree of calcination and XRF of the solids inputs and outputs

	Pellets in	**Carbonator out**	**Calciner out**	**Cyclone calciner**	**Cyclone carbonator**
BET (m2/g)	19	3	3.1	3.6	4.2
Degree of calcination *		58% wt calcined	65% wt calcined	59% wt calcined	76% wt calcined
Weight %	Oxide	Oxide	Oxide	Oxide	Oxide
CaO	93	94	95	97	96
Br	ND	0.057	0.043	0.10	0.056
MgO	0.27	0.30	0.32	0.28	0.30
SiO_2	0.13	0.22	0.1	0.17	0.15
Al_2O_3	6.9	5.4	4.5	2.1	2.9
SrO	0.03	0.029	0.032	0.032	0.032
MnO	0.020	0.016	0.016	0.017	0.017
SO_3	0.012	ND	0.012	0.016	0.019
TiO_2	0.031	ND	0.009	0.018	0.007
Fe_2O_3	0.026	0.015	0.016	0.035	0.033

Cl	ND	0.007	0.009	ND	0.006
Cr_2O_3	ND	ND	ND	ND	ND
K_2O	0.008	ND	ND	0.015	ND
CO_2 (with CaO and MgO)	-	-	-	-	-
Before normalisation to 100%	82	88	86	84	86

*The degree of calcination is determined by calcining the material in the oven at 900°C for 2 h and is expressed as the theoretical concentration of CaO in the mixture of CaO and $CaCO_3$

The results presented in Table 7-5 show that the pellets tend to remain in the system due to their high alumina content, as is demonstrated in the samples extracted from the carbonator and the calciner; this may also indicate low elutriation of pelletised particles due to their higher mechanical strength. As expected the Br- was mostly found in the cyclones due to the attrition from the surface of the particle as in the previous experiment.

7.4 Conclusions

The use of enhanced materials for CaL is studied at pilot-scale in this work. Here, a novel technique of impregnating the surface of limestone with HBr is described as well as the use of calcium aluminate pellets (90% lime and 10% calcium aluminate cement). The HBr-doped material showed good capture performance as well as good mechanical stability during stable operation. It should be noted that the surface of the particle was modified by the enhancement technique and hence as the particles attrited, most of the Br was found in the carbonator cyclone. Nonetheless the bromine treatment still delayed sintering, allowing for superior CO_2 capture and suitable for large-scale operation. However, the operation with calcium aluminate pellets proved to be more challenging, especially when dosing the material to the fluidised bed due to the release of steam from both the moisture in the pellets and its

hydroxide content. A way of avoiding this excessive release of steam would be to expose the pelletised material to low-concentration CO_2 sources, e.g., the exhaust gas coming from the carbonator (with residual CO_2 of around 2%) in order to pre-carbonate the hydroxides. As the pellet operation was more complex, some limestone was added to make the bed inventory sufficient to allow the circulation of solids. The pellets showed poorer performance when compared to the HBr limestone and their mechanical stability needs to be further explored.

7.5 References

[1] IPCC, Climate change 2007: synthesis report. Contribution of Working Groups I, II and III to the fourth assessment report of the intergovernmental panel on climate change. In: Pachauri KP, Reisinger A, editors. IPCC: Geneva, Switzerland; 2007.

[2] Bernstein, L., Lee, A. and Crookshank, S., 2006. Carbon dioxide capture and storage: a status report.

[3] Boot-Handford, M.E., Abanades, J.C., Anthony, E.J., Blunt, M.J., Brandani, S., Mac Dowell, N., Fernández, J.R., Ferrari, M.C., Gross, R., Hallett, J.P. and Haszeldine, R.S., 2014. Carbon capture and storage update. Energy & Environmental Science, 7(1), pp. 130-189.

[4] Erans, M., Manovic, V. and Anthony, E.J., 2016. Calcium looping sorbents for CO_2 capture. Applied Energy, 180, pp. 722-742.

[5] Hawthorne, C., Dieter, H., Bidwe, A., Schuster, A., Scheffknecht, G., Unterberger, S. and Käß, M., 2011. CO_2 capture with CaO in a 200 kW_{th} dual fluidized bed pilot plant. Energy Procedia, 4, pp. 441-448.

[6] Sánchez-Biezma, A., Ballesteros, J.C., Diaz, L., De Zárraga, E., Álvarez, F.J., López, J., Arias, B., Grasa, G. and Abanades, J.C., 2011. Postcombustion CO_2 capture with CaO. Status of the technology and next steps towards large scale demonstration. Energy Procedia, 4, pp. 852-859.

[7] Dieter, H., Hawthorne, C., Zieba, M. and Scheffknecht, G., 2013. Progress in calcium looping post combustion CO_2 capture: successful pilot scale demonstration. Energy Procedia, 37, pp. 48-56.

[8] Arias, B., Diego, M.E., Abanades, J.C., Lorenzo, M., Diaz, L., Martínez, D., Alvarez, J. and Sánchez-Biezma, A., 2013. Demonstration of steady state CO_2 capture in a 1.7 MW_{th} calcium looping pilot. International Journal of Greenhouse Gas Control, 18, pp. 237-245.

[9] Ströhle, J., Junk, M., Kremer, J., Galloy, A. and Epple, B., 2014. Carbonate looping experiments in a 1MW_{th} pilot plant and model validation. Fuel, 127, pp. 13-22.

[10] Bidwe, A.R., Hawthorne, C., Dieter, H., Dominguez, M.A., Zieba, M. and Scheffknecht, G., 2014. Cold model hydrodynamic studies of a 200 kW_{th} dual fluidized bed pilot plant of calcium looping process for CO_2 Capture. Powder Technology, 253, pp. 116-128.

[11] Chang, M.H., Chen, W.C., Huang, C.M., Liu, W.H., Chou, Y.C., Chang, W.C., Chen, W., Cheng, J.Y., Huang, K.E. and Hsu, H.W., 2014. Design and experimental testing of a 1.9 MW_{th} calcium looping pilot plant. Energy Procedia, 63, pp. 2100-2108.

[12] Chen, Z., Song, H.S., Portillo, M., Lim, C.J., Grace, J.R. and Anthony, E.J., 2009. Long-term calcination/carbonation cycling and thermal pretreatment for CO_2 capture by limestone and dolomite. Energy & Fuels, 23(3), pp. 1437-1444.

[13] Fennell, P.S., Pacciani, R., Dennis, J.S., Davidson, J.F. and Hayhurst, A.N., 2007. The effects of repeated cycles of calcination and carbonation on a variety of different limestones, as measured in a hot fluidized bed of sand. Energy & Fuels, 21(4), pp. 2072-2081.

[14] Grasa, G.S. and Abanades, J.C., 2006. CO_2 capture capacity of CaO in long series of carbonation/calcination cycles. Industrial & Engineering Chemistry Research, 45(26), pp. 8846-8851.

[15] Luo, C., Zheng, Y., Ding, N., Wu, Q., Bian, G. and Zheng, C., 2010. Development and performance of CaO/La_2O_3 sorbents during calcium looping cycles for CO_2 capture. Industrial & Engineering Chemistry Research, 49(22), pp. 11778-11784.

[16] Luo, C., Zheng, Y., Zheng, C., Yin, J., Qin, C. and Feng, B., 2013. Manufacture of calcium-based sorbents for high temperature cyclic CO_2 capture via a sol–gel process. International Journal of Greenhouse Gas Control, 12, pp. 193-199.

[17] Radfarnia, H.R. and Sayari, A., 2015. A highly efficient CaO-based CO_2 sorbent prepared by a citrate-assisted sol–gel technique. Chemical Engineering Journal, 262, pp. 913-920.

[18] Wang, B., Yan, R., Lee, D.H., Zheng, Y., Zhao, H. and Zheng, C., 2011. Characterization and evaluation of Fe_2O_3/Al_2O_3 oxygen carrier prepared by sol–gel combustion synthesis. Journal of Analytical and Applied Pyrolysis, 91(1), pp. 105-113.

[19] Broda, M. and Müller, C.R., 2014. Sol–gel-derived, CaO-based, ZrO_2-stabilized CO_2 sorbents. Fuel, 127, pp. 94-100.

[20] Zhang, M., Peng, Y., Sun, Y., Li, P. and Yu, J., 2013. Preparation of CaO–Al_2O_3 sorbent and CO_2 capture performance at high temperature. Fuel, 111, pp. 636-642.

[21] Li, Y., Su, M., Xie, X., Wu, S. and Liu, C., 2015. CO_2 capture performance of synthetic sorbent prepared from carbide slag and aluminum nitrate hydrate by combustion synthesis. Applied Energy, 145, pp. 60-68.

[22] Li, C.C., Wu, U.T. and Lin, H.P., 2014. Cyclic performance of $CaCO_3$@ $mSiO_2$ for CO_2 capture in a calcium looping cycle. Journal of Materials Chemistry A, 2(22), pp. 8252-8257.

[23] Li, L., King, D.L., Nie, Z. and Howard, C., 2009. Magnesia-stabilized calcium oxide absorbents with improved durability for high temperature CO_2

capture. Industrial & Engineering Chemistry Research, 48(23), pp. 10604-10613.

[24] Zhao, M., Bilton, M., Brown, A.P., Cunliffe, A.M., Dvininov, E., Dupont, V., Comyn, T.P. and Milne, S.J., 2014. Durability of CaO–$CaZrO_3$ sorbents for high-temperature CO_2 capture prepared by a wet chemical method. Energy & Fuels, 28(2), pp. 1275-1283.

[25] Gupta, H. and Fan, L.S., 2002. Carbonation− calcination cycle using high reactivity calcium oxide for carbon dioxide separation from flue gas. Industrial & Engineering Chemistry Research, 41(16), pp. 4035-4042.

[26] Florin, N. and Fennell, P., 2011. Synthetic CaO-based sorbent for CO_2 capture. Energy Procedia, 4, pp. 830-838.

[27] Manovic, V. and Anthony, E.J., 2009. Screening of binders for pelletization of CaO-based sorbents for CO_2 capture. Energy & Fuels, 23(10), pp. 4797-4804.

[28] Wu, Y., Manovic, V., He, I. and Anthony, E.J., 2012. Modified lime-based pellet sorbents for high-temperature CO_2 capture: reactivity and attrition behavior. Fuel, 96, pp. 454-461.

[29] Ridha, F.N., Manovic, V., Macchi, A. and Anthony, E.J., 2012. High-temperature CO_2 capture cycles for CaO-based pellets with kaolin-based binders. International Journal of Greenhouse Gas Control, 6, pp. 164-170.

[30] Qin, C., Yin, J., An, H., Liu, W. and Feng, B., 2011. Performance of extruded particles from calcium hydroxide and cement for CO_2 capture. Energy & Fuels, 26(1), pp. 154-161.

[31] Ridha, F.N., Wu, Y., Manovic, V., Macchi, A. and Anthony, E.J., 2015. Enhanced CO_2 capture by biomass-templated Ca $(OH)_2$-based pellets. Chemical Engineering Journal, 274, pp. 69-75.

[32] Manovic, V. and Anthony, E.J., 2011. CaO-based pellets with oxygen carriers and catalysts. Energy & Fuels, 25(10), pp. 4846-4853.

[33] Erans, M., Beisheim, T., Manovic, V., Jeremias, M., Patchigolla, K., Dieter, H., Duan, L. and Anthony, E.J., 2016. Effect of SO_2 and steam on CO_2 capture performance of biomass-templated calcium aluminate pellets. Faraday Discussions, 192, pp. 97-111.

[34] Al-Jeboori, M.J., Fennell, P.S., Nguyen, M. and Feng, K., 2012. Effects of different dopants and doping procedures on the reactivity of CaO-based sorbents for CO_2 capture. Energy & Fuels, 26(11), pp. 6584-6594.

[35] Al-Jeboori, M.J., Nguyen, M., Dean, C. and Fennell, P.S., 2013. Improvement of limestone-based CO_2 sorbents for Ca looping by HBr and other mineral acids. Industrial & Engineering Chemistry Research, 52(4), pp. 1426-1433.

[36] Erans, M., Jeremiáš, M., Manovic, V., and Anthony, E.J., 2017. Operation of a 25 kW_{th} calcium looping pilot-plant with high oxygen concentration in the calciner, Journal of Visualized Experiments, In press.

[37] Alonso, M., Rodríguez, N., Grasa, G., and Abanades, J. C., 2009. Modelling of a fluidized bed carbonator reactor to capture CO_2 from a combustion flue gas. Chemical Engineering Science, 64(5), pp. 883-891.

[38] Scala, F. Chirone, R., and Salatino, P., 2013. Attrition phenomena relevant to fluidized bed combustion and gasification systems, in Fluidized Bed Technologies for Near-Zero Emission Combustion and Gasification, F. Scala, Ed. Woodhead publishing Limited pp. 254–315.

[39] Manovic, V. and Anthony, E.J., 2010. Sintering and formation of a nonporous carbonate shell at the surface of CaO-based sorbent particles during CO_2-capture cycles. Energy & Fuels, 24(10), pp. 5790-5796.

[40] Manovic, V., Wu, Y., He, I. and Anthony, E.J., 2012. Spray water reactivation/pelletization of spent CaO-based sorbent from calcium looping cycles. Environmental Science & Technology, 46(22), pp. 12720-12725.

[41] Ridha, F.N., Manovic, V., Macchi, A. and Anthony, E.J., 2015. CO_2 capture at ambient temperature in a fixed bed with CaO-based sorbents. Applied Energy, 140, pp. 297-303.

[42] Materić, V., Edwards, S., Smedley, S.I. and Holt, R., 2010. $Ca(OH)_2$ superheating as a low-attrition steam reactivation method for CaO in calcium looping applications. Industrial & Engineering Chemistry Research, 49(24), pp. 12429-12434.

8 GENERAL DISCUSSION

It is widely accepted that carbon capture and storage is a vital technology for significantly reducing CO_2 emissions from the energy and industrial sectors; therefore, it would considerably help to mitigate the effects that these emissions have on global climate [1, 2].

Calcium looping is a second generation capture technology [3] that has attracted a great amount of research due to its benefits such as low efficiency penalties [4], and the fact that the sorbent used (limestone or Ca-based materials) is cheap, widely available and environmentally friendly [5, 6]. These reasons give this technology clear advantages when compared to the first generation of CO_2 capture technologies such as MEA scrubbing. However, there are some challenges that need to be addressed in order to deploy this technology at a large scale. A key challenge is the rapid capture capacity decay of limestone over increasing number of reaction cycles mainly due to sintering of the particles at high temperatures. Another important requirement for this technology is the reduction of heat needed in the calciner. Namely, the main energy penalty of the system is associated with the ASU, which is required in order to produce pure oxygen for the oxy-combustion of fuel in calciner needed to drive the endothermic calcination reaction. The research presented in this Thesis covers these two challanges as a way of improving the competitiveness of calcium looping. In particular, the development and testing of different materials (pelletised Ca-based materials and HBr-doped limestone), and the effects of high oxygen concentrations in the calciner have been studied in this work.

In terms of sorbent development, research has focused on the production of enhanced materials for calcium looping cycle, and the comprehensive literature review on natural, enhanced and synthetic sorbents are explored in Chapter 3. The research presented in the open literature to date was compiled in the form of a review paper, critically assessing the different production methods and the performance of the sorbents in terms of chemical reactivity and mechanical stability. It is important to highlight that areas for further research and

development are recommended, and the development of cheaper sorbents, employing simpler and sceleable methods, using widely available materials or even waste as binders and/or support for the production of enhanced Ca-based materials should be the main focus.

Several materials have been studied during the course of this investigation:

i) calcium aluminate pellets (90% calcined limestone, 10% calcium aluminate cement)

ii) biomass-templated pellets (90% calcined limestone, 10% commercial wheat flour)

iii) biomass-templated calcium aluminate pellets (80% calcined limestone, 10% commercial wheat flour and 10% calcium aluminate cement)

iv) sea-water-doped biomass-templated calcium aluminate pellets (80% calcined limestone, 10% commercial wheat flour and 10% calcium aluminate cement produced with sea water)

These materials were produced using the pelletisation technique, which served as an example of a cheap method for producing synthetic sorbents using a tabletop granulator. These materials were studied in a TGA and BFB under different conditions. In the TGA they were tested under mild and harsh (more realistic) calcination conditions. As expected, the results showed that the particles had lower carbonation conversion under realistic conditions. These sorbents were also tested in a bubbling fluidised bed (BFB) under: i) normal conditions (90% CO_2 vol carbonation at 850 °C, 20% vol CO_2 calcination at 850 °C both in balanced N_2), ii) with high concentrations of SO_2 (1500 ppm) in both carbonation and calcination, and iii) with a 15% steam in both carbonation and calcination.

The conclusion from these investigations is that the tested synthetic materials performed better than limestone under all explored conditions, which is a positive conclusion. As expected, the particles had a lower CO_2 uptake in presence of sulphur, which highlights the importance of desulphurising the flue

gas or using fuels with low sulphur content when synthetic sorbents are used. Moreover, the prepared materials had an improved CO_2 uptake in the presence of steam due to the enhanced solid state diffusion, which is in accordance with previous research [7]. It should be highlighted that the main novelty of this investigation is the production of novel biomass-templated materials and the experimental study of these materials in a realistic system (BFB) and under realistic conditions at pilot scale; something that cannot be found in the open literature in the case of synthetic CaO-based sorbents.

The material that showed the best performance among all of the materials produced for this study was the calcium aluminate pellets (produced with 90% calcined limestone and 10% calcium aluminate cement), followed by the biomass templated pellets with cement (80% calcined limestone, 10% flour and 10% calcium aluminate cement).

The fragmentation of these materials was also studied using two different techniques: i) PHSR (pressurised heated strip reactor) that measures the primary fragmentation due to thermal stresses in the first calcination; ii) BFB (bubbling fluidised bed), which measures the primary and secondary fragmentation due to the thermal stresses and the impacts of particles amongst each other and with the reactor walls. The results from this investigation showed that particles with biomass are more prone to fragment due to internal stresses caused by the release of combustion gases when the particles enter the reactor. This effect was partially counteracted by the addition of calcium aluminate cement with much less fragmentation when compared with the sorbent with just lime and biomass. It can be concluded from this investigation that biomass-templated materials have improved porous structure; however, their fragmentation behaviour is less desirable in terms of their use in fluidised beds. These results have been corroborated by the two experimental methods (PHSR and BFB), both of these methodologies provided the same results and are in good agreement.

Overall, it can be concluded that the pelletisation of biomass-templated sorbents is a useful technique for the production of sorbents with enhanced

morphology. However, the mechanical stability of these sorbents should be further improved in order to make them more attractive for large scale applications.

Calcium aluminate pellets and HBr-doped limestone were also tested in a 25 kW_{th} pilot-scale unit comprising a CFB carbonator and a BFB calciner, in order to prove the scalability of these two types of materials presented in Chapter 7. The calcium aluminate pellets were produced in the same methodology described in Chapters 4 and 5, with a granulator, and using 90% lime and 10% calcium aluminate cement. For the HBr doping, a new wet surface impregnation technique was developed in order to use the lowest quantity of HBr to make this process more economically favourable. It appears that the particle surface was modified with this enhancement method and even if the particles suffer from attrition this modification is still effective. The conclusion is supported by the fact that XRF analysis showed that most of the Br was found in the cyclones due to attrition of the particles in fluidised-bed operation. This doping technique resulted in superior CO_2 uptake when compared with that of natural limestone.

For the calcium aluminate pellets, there were some challenges, which should be noted; namely, feeding these materials resulted in the release of high amounts of steam. This caused problems with the backpressure in the calciner reactor, which resulted in the close-down of the combustion in preliminary tests. It was decided that the feeding should be performed in a more controlled manner, i.e. by feeding material in smaller batches. This mitigated the problems with the release of steam allowing more manageable operation. The XRF results showed that most of the pellets remained in the system, as most of the alumina content present in the samples was found in the carbonator and calciner, which indicates low elutriation of the pelletised particles.

This work also demonstrated the potential scalability of the pelletisation and doping techniques, as well as developing a new doping technique for large-scale CaL. These materials were tested at pilot scale, where several challenges were encountered for the first time, such as the difficulties with the feeding of calcium aluminate pellets. In order to solve this issue it is proposed that the

materials are carbonated first, in order to minimise the release of steam when the particles enter the reactor. This opens a wide range of possibilities such as the use of raw pellets to decarbonise low concentration CO_2 streams, such as the exhaust from the carbonator of a CaL plant. Another option would be to expose the raw pellets to the atmosphere in order to take CO_2 directly from the air (direct air capture) before feeding the material into the fluidised bed, which will decrease even further the emissions with the CaL cycle making it even more attractive to be used at industrial scale.

Another possibility investigated in this research work is the option of operating the calciner under high oxygen concentrations. The advantage of this strategy is that this operation mode can reduce or even eliminate the need for the recirculation of flue gas into the calciner as part of oxy-fired operation. It should be noted that this recirculated stream consumes heat in order to be heated up to the bed temperature in the calciner. Therefore, the proposed operation mode enables a reduction in both fuel and oxygen needed in the calciner, i.e. less the oxygen being produced by the ASU, and, consequently, a higher thermal efficiency of the process. Furthermore, this would mean a potential reduction in size of the calciner, and a reduction of capital cost (smaller calciner and ASU), which together with the reduction in operational cost (less oxygen and fuel being combusted) would result in lower economic penalties associated with the calcium looping process.

This alternative approach of improving performance has been investigated by performing various pilot-plant experimental campaigns in a 25 kW_{th} unit comprising a CFB carbonator and a BFB calciner. In these experiments natural gas was used as a fuel and the oxygen concentration was carefully increased until burning the NG in 100% vol O_2. This concept was proved to be effective when using natural gas as a fuel; however, there might be different challenges when feeding coal into the calciner. This should be carefully studied in order to assess the viability of this operational mode.

In conclusion, improvement mechanisms for different aspects of the CaL cycle have been investigated during the course of this work. As part of this research

project new enhanced synthetic materials have been produced (pelletised sorbents and HBr-doped limestone), these materials have been tested at different scales, under different conditions and for different parameters (reactivity and mechanical stability). Moreover, a route for decreasing the heat needed in the calciner has been explored with the operation with 100% vol O_2 in the calciner; this path was proven to be effective in Cranfield's 25 kW_{th} pilot plant.

8.1 References

[1] Fan, L.S., 2011. Chemical looping systems for fossil energy conversions. John Wiley & Sons.

[2] Herzog, H., Eliasson, B. and Kaarstad, O., 2000. Capturing greenhouse gases. Scientific American, 282(2), pp. 72-79.

[3] Markewitz, P., Kuckshinrichs, W., Leitner, W., Linssen, J., Zapp, P., Bongartz, R., Schreiber, A. and Müller, T.E., 2012. Worldwide innovations in the development of carbon capture technologies and the utilization of CO_2. Energy & Environmental Science, 5(6), pp. 7281-7305.

[4] Romano, M.C., 2012. Modeling the carbonator of a Ca-looping process for CO_2 capture from power plant flue gas. Chemical Engineering Science, 69(1), pp. 257-269.

[5] Lasheras, A., Ströhle, J., Galloy, A. and Epple, B., 2011. Carbonate looping process simulation using a 1D fluidized bed model for the carbonator. International Journal of Greenhouse Gas Control, 5(4), pp. 686-693.

[6] Dean, C.C., Blamey, J., Florin, N.H., Al-Jeboori, M.J. and Fennell, P.S., 2011. The calcium looping cycle for CO_2 capture from power generation, cement manufacture and hydrogen production. Chemical Engineering Research and Design, 89(6), pp. 836-855.

[7] Ridha, F. N., Manovic, V., Macchi, A., & Anthony, E. J., 2012. High-temperature CO_2 capture cycles for CaO-based pellets with kaolin-based binders. International Journal of Greenhouse Gas Control, 6, pp. 164-170.

9 GENERAL CONCLUSIONS AND RECOMMENDATIONS

9.1 General conclusions

In this chapter, the main conclusions resulting from the research conducted as part of this degree are explained below.

9.1.1 Sorbent development

A range of low cost CaO-based sorbents were produced to be used in CaL systems (namely, pelletised sorbents and doped material). Their performance has been assessed using different methods: thermogravimetric analyser (TGA), bubbling fluidised bed (BFB) and pilot-plant testing to determine their CO_2 capture performance. In addition, mechanical stability of most of these particles has been investigated using: crushing strength tests, a pressurised heated strip reactor (PHSR) and a BFB.

The production of calcium aluminate pellets (LC as named in Chapters 4 and 5) led to the conclusions detailed below:

- With regard to the material characterisation: the crushing strength tests indicated good mechanical stability with a mean value of 2.1 N, the SEM also showed these materials had good porosity. As expected XRD showed the formation of mayenite ($Ca_{12}Al_{14}O_{33}$) due to the reaction of the calcium aluminate cement and the lime during.
- TGA results showed good stability over numerous cycles, both with harsh calcination conditions (950 °C in 100% CO_2) and mild calcination conditions (850°C in 100% N_2) with 40.5% and 18.5% conversion respectively after 20 cycles.
- BFB results showed a much higher CO_2 uptake than limestone (0.22 g CO_2 per g sorbent compared to 0.03 g CO_2 per g sorbent after 10 cycles, respectively) possibly due to the higher mechanical strength as well as the stabilised mesoporous structure caused by the presence of mayenite in the pellets.
- The test with SO_2 showed a diminished reactivity in LC going from 0.22 g CO_2 per g sorbent without SO_2 to 0.05 g CO_2 per g sorbent with SO_2,

which was expected due to the formation of $CaSO_4$. Furthermore, the test with steam showed enhanced capture (0.25 g CO_2 per g sorbent) after 10 cycles. It was also noted that the decline of activity is less dramatic when steam is present, which has been reported in previous work.

- Fragmentation results showed that these particles possessed good mechanical stability, namely due to the fact that there was no diameter reduction in the pressurised heated strip reactor (PHSR). Their fragmentation in a BFB was characterised by the reduction in particle size and the loss of bed material during the first calcination LC was the best material in all the cases tested.
- Pilot plant testing of LC showed some challenges when using this type of material. Specifically, the release of steam was high during the feeding process into the calciner. Some solutions have been proposed to avoid this, such as carbonating the pellets with residual CO_2 stream (like the carbonator outlet), which will promote their performance.

The production of biomass-templated sorbents (LF, LCF and LCFSW as named in Chapters 4 and 5) led to the following conclusions.

- The crushing strength testing performed on these particles showed the different behaviour depending on composition. The difference between particles is substantial with LF having an average crushing strength of 0.74 N LCF, 1.4 N and LCFSW 0.58 N. This indicates the importance of adding cement into biomass-templated materials in order to achieve more mechanical stability.
- The capture results varied depending on the calcination conditions with conversion of 41.5 %, 46.5% and 9.6% conversion under mild conditions and 16.1 %, 19.3% and 3.0% at harsh calcination conditions for LF, LCF and LCFSW, respectively. It has been suggested that LCFSW had lower conversion than LCF due to the high sodium content present in the sample, which indicates that this pelletisation/doping method needs to be adjusted in order to achieve enhanced properties.

- With regard to the BFB results the templated materials showed diminished performance when compared with calcium aluminate pellets with 0.12 g CO_2 per g sorbent for LCF, 0.07 g CO_2 per g sorbent for LF and 0.05 g CO_2 per g sorbent for LFSW after 10 cycles. However, all of these materials performed better than the original limestone which had 0.03 g CO_2 per g sorbent after 10 cycles. It is important to note that the addition of cement helped sorbent particles perform better under standard conditions. For the experiments with SO_2 all the sorbents showed a similar decrease in their capture capacity after 10 cycles (LF, LCF and LC at around 5% carbonation conversion). These outcomes can be explained by the progressive build-up of a sulphate layer, which reduces CO_2 diffusion in the pores. Steam also helped their performance with an increase of uptake with 25% in LCF, and some improvement in LF and LCFSW.
- Fragmentation behaviour was found to be a key factor when dealing with this type of particles. This is mainly due to the fact that the biomass templating does not have a positive effect with regard to fragmentation, which resulted in a reduction in mean diameter of 404 μm in LF (comparing particle size distribution of the samples before and after PHSR tests). However, the addition of cement partially counteracted this phenomenon with a reduction in diameter of 234 μm in LCF. The results of the BFB experiments agreed with those in the PHSR.

The HBr-doped limestone demonstrated enhanced performance under pilot plant conditions; the conclusions obtained from this test are:

- Enhanced CO_2 capture is achieved, with less make-up for the same CO_2 capture; this is due to the enhanced porosity formed by this production method, especially at the surface of sorbent particles.
- Lower elutriation was experienced compared to the tests with limestone and substantially less material was found in the cyclone of the calciner (370 g vs. 2000 g in the previous run), as well as in the secondary cyclone of the carbonator. This appears to be due to reduced attrition of

the sorbent during the cycling between the two reactors, which means that the majority of the material resided circulating between carbonator and the calciner.

9.1.2 Pilot-plant experimental campaigns

Pilot plant campaigns have been performed during the course of this research. These included the commissioning of the modified unit and experimental campaigns with high oxygen concentrations and the use of enhanced materials for CaL.

- The modifications and the commissioning of the pilot plant were successful. Problems with the gas burners present before the construction were eliminated, allowing the material to be calcined to a higher extent at temperatures of up to 950 °C to simulate a realistic calcium looping system. This reconstruction also increased the flexibility of the plant allowing the feeding of different gas compositions in both the carbonator and the calciner.
- A standard operational procedure was developed in order to run experiments with high oxygen concentrations (up to 100% vol O_2 in natural gas). This operational mode allows reducing or even eliminating the recirculation of flue gas (mainly CO_2 and steam) in the calciner, which would reduce/eliminate the heat needed to bring this stream up to temperature. The operational mode was proved to be successful in campaigns with limestone, as well as doped-materials and calcium aluminate pellets verifying the validity of this operational procedure.
- The scalability of enhanced sorbents was demonstrated during this research project, namely, calcium aluminate pellets (90% lime, 10% calcium aluminate cement) and HBr-doped material. Pilot campaigns for both of these materials were performed, identifying the challenges that non-natural sorbents pose to the operational conditions of this unit. HBr-doped particles showed very stable capture performance throughout the tests and low elutriation when compared to the limestone used in the commissioning process. However, the properties of the calcium

aluminate pellets proved to be more challenging, especially from the point of view of feeding and the release of steam from the raw pellets, which caused problems with the bed inventory.

9.2 Recommendations for future research

The research carried out during the course of this PhD research has contributed towards the knowledge in the field of carbon capture through the investigation of novel sorbents and through the use of high oxygen concentrations in the calciner in calcium looping systems. This section deals with the limitations encountered as part of this work and possible future paths for research in these areas.

9.2.1 Sorbent development

The used of enhanced sorbents is of vital importance in the calcium looping cycle due to the rapid decay in activity experienced by natural sorbents. It is imperative to find or develop sorbents with improved properties that are cheap in order to make this process more economically viable and further increase its competitiveness with other options such as amine scrubbing.

In the author's opinion, pelletised sorbents would be an option to reduce the cost of Ca-based synthetic materials as well as to improve the strength of any type of synthetic material produced in powder form (i.e. sol gel combustion, PCC, sorbent from organic precursors). This production method can be easily scaled-up and it is widely used in the pharmaceutical and chemical industries. Biomass-templated sorbents were proposed as a way to increase porosity; however, some challenges were encountered due to the mechanical stress experienced by the sorbent particles. It has been demonstrated that this phenomenon can be partially counteracted by the addition of calcium aluminate cement.

There are other options that need to be explored in terms of pelletised sorbents, for example doping of sorbents when they are being pelletised (as in Chapter 4, but with optimal concentrations of sea water or HBr); there are also novel supports that could be used with this technique such as spinel (magnesium

aluminate) and there is also room to explore the behaviour of pelletised natural materials such as dolomite or other natural materials (i.e egg shells and fish bones) providing they are available in large enough quantities. These materials could be also tested at larger scale from TGA to pilot- demonstration-scale.

With regards to the novel doping of limestone with HBr, this technique could be applied to different materials, as it has been explained above (calcium aluminate pellets). Besides, this wet surface-impregnation technique can be used with other doping agents, which allows flexibility and also a decrease in the cost of previously proposed doping methods.

9.2.2 High oxygen concentrations in the calciner

There are several limiting factors in the pilot plant testing with high oxygen concentrations in the calciner which have to be resolved. Several new testing procedures are proposed, based on the experienced gained developing the operating procedure.

The concept of high oxygen concentrations in the calciner has been proved during the course of this work using natural gas as a fuel in the calciner. However, new challenges may arise when using coal as a fuel in this reactor, as this mode of operation needs to be done in an industrial scale CaL plant. In particular, attention has to be taken to avoid potential ash melting due to high temperatures inside the fluidised bed, which might lead to agglomeration of the bed material and eventually to defluidisation of the unit.

This phenomenon needs to be carefully investigated through the testing of different solid materials; not only coal, but co-firing biomass and coal would be interesting options. Also, this operational mode should be tested using two circulating fluidised beds as a carbonator and calciner to explore how reactor configuration, as well as parameters such as solid and gas velocities and residence time, can affect the heat consumption in the calciner.

APPENDICES

Appendix A CO_2 CAPTURE PERFORMANCE USING BIOMASS-TEMPLATED CEMENT-SUPPORTED LIMESTONE PELLETS

Lunbo Duan[1,2], Chengli Su[1], María Erans[2], Yingjie Li[3], Edward J Anthony[2] and Huichao Chen[1]

[1] Key Laboratory of Energy Thermal Conversion and Control, Ministry of Education, School of Energy and Environment, Southeast University, Nanjing 210096, China

[2] Combustion and CCS Centre, Cranfield University, Bedfordshire MK43 0AL, U.K.

[3] School of Energy and Power Engineering, Shandong University, Jinan 250061, China

Published in Industrial & Engineering Chemistry Research, 2016, 55(39), 10294-10300.

Abstract

Synthetic biomass-templated cement-supported CaO-based sorbents were produced by the granulation process for high-temperature postcombustion CO_2 capture. Commercial flour was used as the biomass and served as a templating agent. The investigation of porosity showed that the pellets with biomass or cement resulted in an enhancement of porosity. Four types of sorbents containing varying proportions of biomass and cement were subjected to 20 cycles in a thermogravimetric analyzer under different calcination conditions. After the first series of tests calcined below 850 °C in 100% N2, all composite sorbents clearly exhibited higher CO_2 capture activity than untreated limestone with the exception of sorbents doped by seawater. The biomass-templated cement-supported pellets exhibited the highest CO_2 capture level of 46.5% relative to 20.8% for raw limestone after 20 cycles. However, the enhancement in performance was substantially reduced under 950 °C calcination condition.

Considering the fact that both sorbents supported by cement exhibited relatively high conversion with a maximum value of 19.5%, cement-promoted sorbents appear to be better at resisting harsh calcination conditions. Although flour as biomass-templated material generated a significant enhancement in CO_2 capture capacity, further exploration must be carried out to find ways of maintaining outstanding performance for CaO-based sorbents under severe reaction conditions.

I&EC research
Industrial & Engineering Chemistry Research

Article

pubs.acs.org/IECR

CO_2 Capture Performance Using Biomass-Templated Cement-Supported Limestone Pellets

Lunbo Duan,[*,†,‡] Chenglin Su,[†] María Erans,[‡] Yingjie Li,[§] Edward J. Anthony,[‡] and Huichao Chen[†]

[†]Key Laboratory of Energy Thermal Conversion and Control, Ministry of Education, School of Energy and Environment, Southeast University, Nanjing 210096, China

[‡]Combustion and CCS Centre, Cranfield University, Bedfordshire MK43 0AL, U.K.

[§]School of Energy and Power Engineering, Shandong University, Jinan 250061, China

ABSTRACT: Synthetic biomass-templated cement-supported CaO-based sorbents were produced by the granulation process for high-temperature postcombustion CO_2 capture. Commercial flour was used as the biomass and served as a templating agent. The investigation of porosity showed that the pellets with biomass or cement resulted in an enhancement of porosity. Four types of sorbents containing varying proportions of biomass and cement were subjected to 20 cycles in a thermogravimetric analyzer under different calcination conditions. After the first series of tests calcined below 850 °C in 100% N_2, all composite sorbents clearly exhibited higher CO_2 capture activity than untreated limestone with the exception of sorbents doped by seawater. The biomass-templated cement-supported pellets exhibited the highest CO_2 capture level of 46.5% relative to 20.8% for raw limestone after 20 cycles. However, the enhancement in performance was substantially reduced under 950 °C calcination condition. Considering the fact that both sorbents supported by cement exhibited relatively high conversion with a maximum value of 19.5%, cement-promoted sorbents appear to be better at resisting harsh calcination conditions. Although flour as biomass-templated material generated a significant enhancement in CO_2 capture capacity, further exploration must be carried out to find ways of maintaining outstanding performance for CaO-based sorbents under severe reaction conditions.

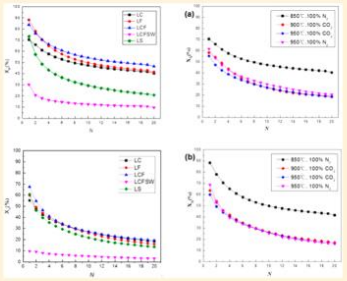

1. INTRODUCTION

Anthropogenic CO_2 emissions are widely considered as one main contributor to climate change, in particular power plants consuming fossil fuels produce ~40% of global CO_2 emissions.[1] Carbon capture and storage (CCS) technology is one promising and emerging way to mitigate CO_2 emissions effectively.[2,3] However, the cost of the CO_2 capture step contributes to ~80% of the whole cost associated with CCS.[4] Hence, it is of great importance to develop efficient and cost-effective CO_2 capture technologies. Several relatively mature CO_2 capture technologies, however, exhibit specific drawbacks. In the case of amine scrubbing, the degradation and regeneration of expensive solvents cause large economic and efficiency penalties.[4] In the case of oxy-fuel combustion, the air-separation unit (ASU) required is energy intensive and incurs large costs.[2] Therefore, the majority of research in this area aims to develop novel and potentially better carbon capture technology such as calcium looping (CaL) using solid CO_2 sorbents.

The CaL process is based on two reverse reactions for the formation and decomposition of $CaCO_3$, where CaO-based sorbents capture CO_2 (i.e., from flue gas) in a carbonation reactor, followed by regeneration of sorbents in a calcination reactor to fulfill a cycle. Natural limestone is regarded as one of the most suitable candidates for large scale CO_2 capture, due to its abundance and low cost as well as its potentially high initial CO_2 capture capacity of 0.786 g of CO_2/g of CaO. However, two major challenges associated with this technology should be addressed: (1) the sorbent reactivity decays rapidly with increasing number of reaction cycles because of sintering; (2) the attrition of the particles in an actual working environment can be excessive. As a result, a high makeup flow is required to compensate for the deactivation and elutriation of raw limestone to maintain desired CO_2 capture efficiency, but this damages the economics of the process. Thus, considerable research efforts have been focused on improving CO_2 capture performance of natural CaO-based sorbents and developing more stable ones over multiple cycles.

Several techniques have been proposed in previous works such as precipitation methods,[5,6] organic acid treatments,[7−11] chemical doping,[12,13] hydration,[12,14−17] and synthesis techniques of highly efficient sorbents, i.e., the sol−gel method,[18−21] carbon template,[19,22] and biomass template.[23] In terms of chemical doping method, different techniques and dopants have been used in recent work. Work carried out by González

Received: August 2, 2016
Revised: August 30, 2016
Accepted: September 9, 2016
Published: September 9, 2016

DOI: 10.1021/acs.iecr.6b02965
Ind. Eng. Chem. Res. 2016, 55, 10294−10300

et al. demonstrated that a 0.5 M solution of KCl enhanced long-term activity of limestone in both fluidized bed and TGA tests, in spite of decreasing reactivity for the initial cycle.[24] Other dopants were also investigated, such as NaCl,[25] $CaBr_2$,[12,26] MgCl, and $Mg(NO_3)_2$.[27] Various synthetic CO_2 sorbents have proved highly efficient. Ridha et al.[23] examined four types of biomass-templated CaO-based sorbents and noted that biomass materials improved the porosity of sorbents and biomass ash contributed to the enhancement of stabilization of pellets. Inert Al_2O_3 is now widely used as an additive to form inert support materials, i.e., $Ca_{12}Al_{14}O_{33}$ or $Ca_9Al_6O_{18}$ ($Ca_3Al_2O_6$),[17,18,28] which improves the stability of sorbents over multicycles. However, it should be noted that these modifications appear to be cost-ineffective because of the correspondingly high cost of materials and complex procedures, as well as potential problems for further scale up for commercialization. Granulation[10,12,15,16,29−32] has been proposed recently as a promising method, which allows the addition of various dopants and using kaolin[30,33] and/or cement[34] as binders to support sorbents.

Given that multiple CO_2 capture performance tests about synthetic sorbents, especially doped with biomass were carried out under correspondingly mild calcination condition (i.e., 850 °C). In this work, synthetic sorbents were produced through pelletization process, which were supported by calcium aluminate cement, templated by biomass, and also doped by seawater. Then CO_2 capture tests were performed in a TGA under mild and harsh conditions to compare the difference between observed characteristics.

2. EXPERIMENTAL SECTION

2.1. Materials and Pelletization. In this work, a batch of powdered Longcal limestone was used as the source of the CaO precursor. Commercial calcium aluminate cement, CA-14 (73% Al_2O_3, 27% CaO), from Almatis Inc. was chosen as the binder for pelletization; >80% of the powders were <45 μm in diameter. The biomass-templated material used was commercial flour. Artificial seawater (Complete Aquatics treated with moderate NaClO) was served for doping purposes.

The biomass-templated cement-supported limestone pellets were prepared by using TMG Tabletop granulator (Glatt HmGb). Raw limestone was calcined at 850 °C in air for 2 h before preparation. A batch of powdered materials (~800 g in total) was loaded into the pelletizer vessel (4 L). The pelletization process was achieved by the agitator and the chopper attached to the vessel with velocities of 500 and 2500 rpm, respectively. Water (~400 mL) was sprayed intermittently through a pressurized atomizing nozzle during the procedure, namely spraying for 1s at intervals of 4s. Usually, the amount of spraying water and the speed of two rotor blades play critical roles in controlling the final pellet size, it must be noted here that visual inspection of the mixture should be continuously performed, to ensure moderate water and desired particle size. More details about this pelletization procedure can be found elsewhere.[15,31] After pelletization, the pellets were air-dried and then the desired size particles of 0.1−0.6 mm were sieved out to storage. Four kinds of pellets were prepared with varying proportions of different dopants and calcined limestone. Combinations of the first letter of different materials were used to denote pellets, as seen in Table 1. Raw limestone was designated as LS for comparison.

2.2. Sorbents Characterization. Elementary analysis of the samples was performed using inductively coupled plasma optical emission spectrometry (ICP-OES) and the composition is given in Table 2. Prior to N_2 adsorption−desorption measurement using an accelerated surface area and porosimetry system (Micromeritics ASAP 2020), sorbents were decomposed into CaO in a muffle furnace at 850 °C in air for 15 min which also allowed the complete combustion of biomass. The BET surface area and BJH pore size distribution were derived from N_2 adsorption isotherms obtained at ~−196 °C. BET surface area distribution was derived from adsorption data, whereas the BJH pore volume distribution was derived from the corresponding desorption data. The surface morphology of pellets was observed by a Hitachi S-4800 scanning electron microscopy (SEM).

Table 1. Compositions of Materials Used in Different Preparation of Samples

sample[a]	lime (wt %)	cement (wt %)	flour (wt %)	type of water used
LC	90	10	0	deionized water
LF	90	0	10	deionized water
LCF	80	10	10	deionized water
LCFSW	80	10	10	sea water

[a]LC: lime and cement. LF: lime and flour. LCF: lime, cement and flour. LCFSW: lime, cement and flour doped by seawater.

Table 2. Elementary Analysis of All Sorbents

component (wt %)	LS	LC	LF	LCF	LCFSW
Al_2O_3	0.082	5.63	0.218	4.73	5.22
BaO	0.007	0.007	0.007	0.005	0.015
CaO	53.9	58.4	58.2	52.4	57.3
Fe_2O_3	0.015	0.033	0.040	0.027	0.030
K_2O	0.007	0.006	0.037	0.023	0.051
MgO	0.185	0.208	0.210	0.197	0.335
MnO_2	0.008	0.008	0.009	0.008	0.010
Na_2O	0.053	0.071	0.052	0.056	0.806
P_2O_5	0.007	0.011	0.035	0.022	0.012
SO_3	0.034	0.039	0.122	0.055	0.234
SiO_2	0.701	1.20	0.770	0.267	0.292
SrO	0.017	0.018	0.018	0.017	0.018
TiO_2	0.006	0.015	0.013	0.006	0.007
total oxides	55.1	65.7	59.7	57.8	64.4
TC (total carbon)	42.7	12.8	28.1	25.6	15.4
water at 105 °C	0.10	0.10	0.10	0.10	0.10
water at 950 °C	0.10	22.3	15.9	20.5	23.1
total	98.0	100.8	103.8	103.9	102.9

2.3. TGA Test. The CO_2 capture tests were performed using a thermogravimetric analyzer (TGA) with ~15 mg samples (particles size of <180 μm) loaded in a quartz tube (i.d. 20 mm). The gas flow rate was set at 100 mL min^{-1}, which was controlled by mass flowmeters. The heating rate and cooling rate were 40 and 20 °C min^{-1}, respectively. Two major conditions were studied in these tests: first, the samples were calcined at 850 °C in 100% N_2 (except for the initial cycle in air) for 5 min and then were carbonated at 650 °C under 15% CO_2 (N_2 balance) for 35 min. Second, the calcination process was carried out at 950 °C under 100% CO_2 (except for the initial cycle in air) for 5 min, and then the carbonation step was performed at 650 °C under 15% CO_2 (N_2 balance) for 35 min. All the sorbents were subjected to 20 cycles. Here, the atmosphere was switched from 100% CO_2 to 100% N_2 below

DOI: 10.1021/acs.iecr.6b02965
Ind. Eng. Chem. Res. 2016, 55, 10294−10300

900 °C during the transition between calcination and carbonation to avoid carbonation ahead of time. In addition, the initial cycle under both calcination conditions was in air to ensure the complete combustion of biomass.

3. RESULTS AND DISCUSSION

3.1. Porosity Characterization. The results of N_2 adsorption measurements are presented in Table 3. As can be seen, all the synthetic pellets presented larger BET surface area and BJH pore volume relative to untreated limestone except for LCFSW. Pellets containing flour and cement showed the highest pore surface area of 14.11 $m^2\ g^{-1}$ and pore volume of 0.110 $cm^3\ g^{-1}$ in comparison to 9.00 $m^2\ g^{-1}$ and 0.061 $cm^3\ g^{-1}$ for raw materials, respectively. This result can be attributed to the enhancement effect on porosity by biomass and cement, consistent with previous work.[12,23] Surprisingly, although LCFSW also contained these two types of additives, it exhibited inferior pore structure, actually far less than that of raw limestone. It is possible that the doping with too high levels of seawater produced an excess of Na^+ ion in the sorbent, which led to more pronounced sintering owing to the presence of the lower melting point of Na_2O. Additionally, as noted by Manovic et al.,[13] Na_2O might react with CaO and CO_2 to form lower melting point compounds ($Na_2Ca(CO_3)_2$/$Na_2Ca_2(CO_3)_3$), as a result, active CaO declined and sintering enhanced. This finding agrees with the previous work of Xu et al.[35] who found that calcined limestone doped by sea salt (main component is NaCl) experienced severe sintering during the cycles.

Table 3. Porosity Characterization of Five Type Pellets

sample	BET surface area (m^2/g)	BJH pore volume (cm^3/g)	av pore width, (nm)
LC	11.54	0.086	29.34
LF	12.60	0.093	30.93
LCF	14.11	0.110	28.30
LCFSW	4.03	0.017	16.32
LS	9.00	0.061	31.50

Figure 1 displays pore surface area and pore volume distribution of sorbent pellets. It can be seen in Figure 1a that all samples showed a bimodal pattern with peaks at 3−4 nm and 30−70 nm. The phenomenon revealed pores (<100 nm in diameter), especially mesopores, were mainly contributors to surface area, which is consistent with previous work.[23] The pore surface area profiles demonstrate that the additives used improved pore properties markedly. Similarly, there are two peaks in pore volume distribution, as can be seen in Figure 1b. However, given that the first peak at ~4 nm is very small, it is obvious that the significant increase in pore volume is attributed to the development of pores with size range of 30 nm ~100 nm. As expected, LCF exhibited the highest pore volume of 0.110 $cm^3\ g^{-1}$, corresponding to 83.3% higher than that of LS followed by LF and LC except for LCFSW. Accordingly, the addition of biomass and cement enables us to enhance the porous structure of limestone.

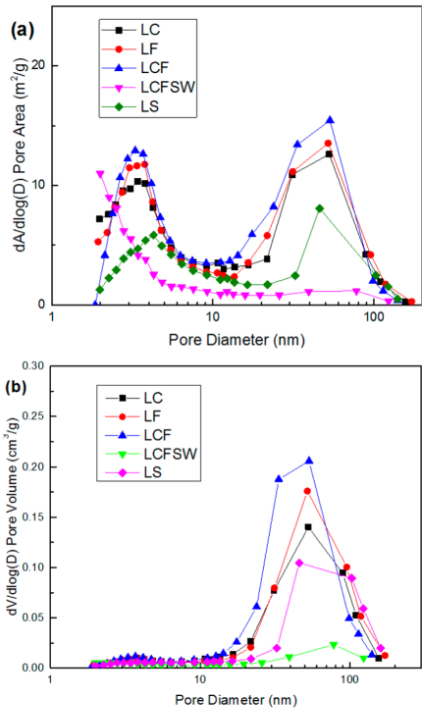

Figure 1. Porous structure distribution of all sorbents used: (a) pore area; (b) pore volume.

3.2. CO_2 Capture Performance. To compare these results with early studies, a typical reaction condition (calcination at 850 °C in 100% vol N_2) was carried out in TGA, and the carbonation conversion curves of four sorbents during the first two cycles are presented in Figure 2. There is a similar tendency for all treated pellets, which displays typically carbonation patterns with fast and slow reaction stages. On the fast stage, the reaction achieved a considerable conversion quickly controlled by chemical kinetics, followed by a slower stage controlled by diffusion. It is clear that biomass and cement doped prolonged the slow reaction stage. Moreover, when two profiles of LC and LCF are compared, it is also notable that biomass doped in sorbents had an effect on the fast reaction stage, which agrees with the finding by Ridha et al.[23]

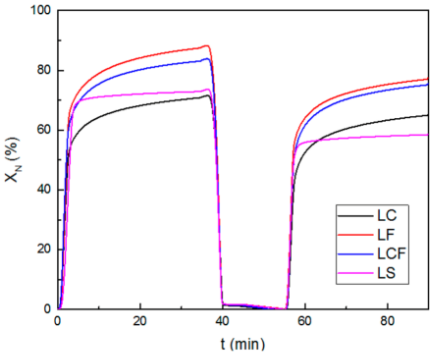

Figure 2. Conversion profiles during the first two cycles in TGA. Conditions: 10 min calcination at 850 °C in 100% vol N_2 and 20 min carbonation at 650 °C in 15% vol CO_2, N_2 balance.

DOI: 10.1021/acs.iecr.6b02965
Ind. Eng. Chem. Res. 2016, 55, 10294−10300

These results are ascribed to the enhancement in porosity, as shown in Table 3, whereas the shift between two reaction stages was so abrupt that the slow stage was hardly evident in the profile of LS. This appears to be connected with the closure of most of small pores in the rapid reaction stage, given the relatively narrow range of porosity seen in Figure 1b. In addition, the SEM image shown in the next chapter also displayed a smooth and solid surface pore structure for LS, which is easy to be covered by a layer of $CaCO_3$.[20,36] As a result, the resistance of CO_2 diffusion increased rapidly to retard the slower reaction.

The CO_2 capture performance of four synthetic pellets together with raw limestone is shown in Figure 3. All sorbents

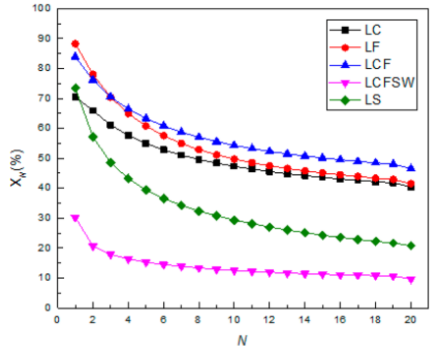

Figure 3. Conversion of the sorbent synthesized, tested 20 cycles of carbonation and calcination in TGA (10 min calcination at 850 °C in 100% vol N_2 and 20 min carbonation at 650 °C in 15% vol CO_2, N_2 balance).

showed monotonically declined profiles with multiple reaction cycles. In the first cycle, LF exhibited the highest conversion of 88.2%, compared to about 73.4% for LS. This can be explained by the fact that LF produced a surface area of 12.60 $m^2\ g^{-1}$, higher than that of 9.00 $m^2\ g^{-1}$ for LS, which was attributed to the addition of biomass. Usually, the high surface area in sorbent means better CO_2 carrying capacity. LC realized a conversion of 70.5% after the initial carbonation reaction, slightly lower than that of LS. It was proposed that Al_2O_3 in the binder reacts with CaO to form mayenite ($Ca_{12}Al_{14}O_{33}$); however, this part of the "CaO" cannot be used to capture CO_2.[28] After 20 capture cycles, LC showed a capture rate of 40.4%, compared to 20.8% of LS, corresponding to 57.3% and 28.3% of their initial conversion, respectively. It is apparent that cement can stabilize CaO-based sorbent over multiple reaction cycles, which is also likely due to the formation of inert mayenite. This result agrees with the finding in other studies that the inert material enables us to maintain sorbents with a stable capture capacity.[12,16] Interestingly, it should be noted that the final conversion of LF was 41.4%, slightly over that of LC, which appears to result from the presence of some small amount of residue (ash) in the sorbent after biomass combustion. As was reported earlier, treating CaO-based sorbents with an aqueous solution of a lower concentration of different mineral salts, such as KCl and K_2CO_3,[24] can improve the cyclic performances of the sorbents. It has been shown in Table 2 that the content of potassium salt in LF is 5 times as great as that in LC. Accordingly, this probably accounts for the somewhat higher CO_2 uptake for LF. As was expected, LCF, containing flour and cement, possessed the best CO_2 capture capacity, with the final conversion reaching 46.5%. By contrast, LCFSW showed rather poor capacity compared to other sorbents. This must be attributed to excessively inferior pore structure seen in Table 3. The later SEM images showed that quantities of cracks on the surface of LCFSW pellet, which means much severer sintering.

Usually, it is relatively reasonable to explore the process of CO_2 looping cycles under mild calcination conditions the in laboratory, if the goal is to collect sufficient experimental data for carrying out fundamental studies. However, to simulate industrial conditions, further experiments using realistic conditions need to be carried out. Figure 4 shows conversion

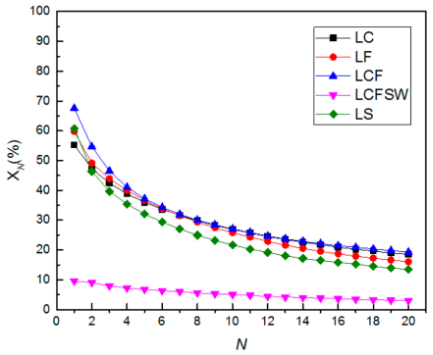

Figure 4. Conversion of the sorbent synthesized, tested 20 cycles of carbonation and calcination in TGA (10 min calcination at 950 °C in 100% vol CO_2 and 20 min carbonation at 650 °C in 15% vol CO_2, N_2 balance).

of sorbent synthesized in carbonation/calcination cycles, operated under harsh calcination conditions. In Figure 4, it is evident that the impact on capture capacity of synthesized sorbents clearly diminishes, although all synthesized sorbents exhibited higher CO_2 uptakes than their counterparts, if we exclude the initial cycle. This agrees with the result under prior calcination conditions. However, harsh conditions impaired the performance of sorbents. Conversion of LC was 55.3% in the first cycle, which decreased by 21.6% compared to that under 850 °C calcination condition. In a similar fashion, LF, LCF, and LS declined by 32.2%, 19.4%, and 17.2%, respectively. It is noticeable that these harsh conditions cause reduced CO_2 uptake. This is because severe calcination conditions cause more serious sintering, which was noted in previous studies.[33−35] It is also clear that the presence of cement is beneficial as compared to only biomass-treated materials under severe conditions. Thus, the optimized porosity structure produced by adding biomass is strongly affected by severe temperature conditions. After 20 cycles, the conversion of LS sharply dropped to 13.5%, equivalent to 22.2% of its initial value. This was close to the residual conversion noted in previous work.[37] Additionally, LC and LCF achieved almost the same conversion, 19.5% for LCF, as compared to 18.5% for LC, due presumably to the presence of an inert aluminate phase ($Ca_{12}Al_{14}O_{33}$). However, it should be pointed out that these levels were less than a residual activity of 28% for cement-supported pellets obtained under 800 °C isothermally by

DOI: 10.1021/acs.iecr.6b02965
Ind. Eng. Chem. Res. 2016, 55, 10294−10300

Manovic and Anthony.[38] Clearly, severe calcination conditions account for the dramatically reduced activity. By contrast, although LF still obtained a conversion of 16.0%, this was just 2.5% over that of LS, which is not a significant advantage when compared to the much better performance than LC after 20 cycles under milder condition. Except for the serious sintering under this harsh condition, as mentioned above, the ash remaining (especially the content of potassium salt) in sorbents may partially account for the satisfactory capacity of LF. Moderate potassium salt concentrations present in sorbent particles have proved to have positive impact on performance. Nevertheless, it must be noted here that the melting point of potassium carbonate is about 900 °C. Moreover, González et al.[24] found that potassium carbonate would vaporize above 900 °C by comparing the concentrations of potassium ions before and after cycling. Therefore, vaporization of potassium carbonate under 950 °C might partly account for the decline of capacity by a large margin for LF. Unfortunately, for TGA test, the low amounts of material produced containing potassium salts are insufficient for further chemical analysis, and a series of tests on lab-scale bubbling fluidized bed (BFB) will be performed in the future study. In addition, LCFSW showed rather poor capacity in both calcination conditions, which is set beyond the comparison of pellet capture capability.

Considering the various results observed under different calcination conditions, further explorations are necessary to examine the effect of high calcination temperature and high-concentration CO_2 atmosphere on the performance of additives. Subsequent tests at 900 °C in 100% CO_2 and at 950 °C in 100% N_2 were carried out, respectively. The experimental results obtained have been plotted in Figure 5. Figure 5a demonstrates different conversion profiles for LC. As can be seen, tests under 900 °C showed almost the same conversion with that at 950 °C in 100% CO_2 atmosphere, except for somewhat superiority in the first seven cycles. It can be concluded that the CO_2 uptake of cement-supported sorbent was clearly reduced at 900 °C, which is identical to that at 950 °C under pure CO_2 flows. LF exhibited a trend similar to that shown in Figure 5b. It has been reported that the high concentration of CO_2 during calcination may cause a dramatic decline on the reactivity of CaO-based sorbents.[39,40] To investigate the influence of different calcination atmosphere, LC and LF sorbents were subjected to reaction cycles at 950 °C in 100% N_2 to allow for comparisons. It is evident that the inert atmosphere plays a secondary role at a high calcination temperature of 950 °C, owing to the fact that the conversion of LC increased over ~3% on average through 20 cycles under pure N_2 gas flow compared with the case of a pure CO_2 atmosphere, as shown in Figure 5a. By contrast, three almost overlapping curves (seen in Figure 5b) indicate that high temperature takes up the predominant position for LF rather than the calcination atmosphere. Switching to pure inert calcination gas cannot increase CO_2 conversion at all. Accordingly, 900 °C can be regarded as extremely severe condition of damaging the reactivity of sorbents containing biomass. These results reveal that biomass-templated sorbents are more sensitive to high temperature than those supported by cement.

3.3. Surface Morphology. Figure 6 shows partial surface morphology images of LS, LC, LF, LCF, and LCFSW following 20 cycles after calcination at 850 or 950 °C. It is clear that the sintering of LS is much worse under 950 °C conditions, given the obvious decline of mesopores seen in Figure 6b. On the contrary, Figure 6c,e,g represented the morphology of LC, LF, and LCF after calcination at 850 °C. These images demonstrated the positive effect of doping sorbents with biomass and cement on porous structure transformation. LF (only containing biomass) shows an obviously sintered structure under severe temperature, as can be seen by comparing panels e and f of Figure 6, where very long and narrow pores were found because of the coalescence of small pores. The enhanced sintering seen here confirms the reduced impact on improving performance of sorbents by adding biomass like flour, when examined in TGA under 950 °C. In contrast, cement (Al_2O_3 actually) exhibited great durability and resisted damage from these harsh temperature conditions, as can be seen from Figure 6g,h. Furthermore, the structure from LCFSW suggests that the formations of compounds from the sea salts are detrimental for the structure of the pores. It is suggested that pores are replaced by the multiple cracks seen here as a result of formation of lower melting point compounds ($Na_2Ca(CO_3)_2$/$Na_2Ca_2(CO_3)_3$).

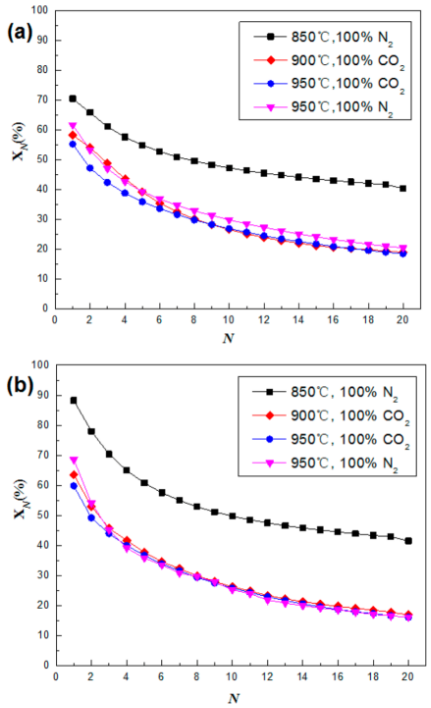

Figure 5. Effects of high temperature and high CO_2 concentration on reactivity of two synthetic sorbents: (a) LC; (b) LF.

4. CONCLUSION

In this work, four types of sorbents containing varying proportions of biomass and cement were synthesized by the pelletization process. Relative to the untreated limestone, both additives caused improvement on porous structure. In particular, biomass-templated cement-supported pellets exhibited the greatest porosity with high pore surface area and pore volume up to 14.11 $m^2\ g^{-1}$ and 0.110 $cm^3\ g^{-1}$,

DOI: 10.1021/acs.iecr.6b02965
Ind. Eng. Chem. Res. 2016, 55, 10294−10300

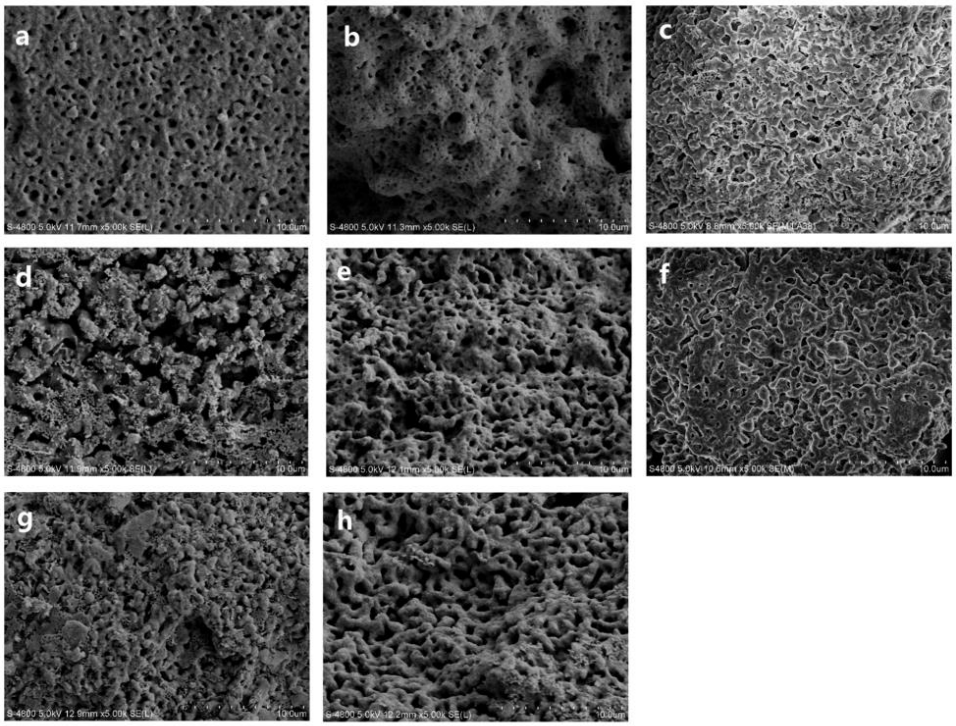

Figure 6. SEM images of samples after 20 carbonation/calcination cycles in TGA under different calcination conditions. Under 850 °C: (a), (c), (d), (e), and (g) for LS, LC, LCFSW, LF, and LCF, respectively. Under 950 °C: (b) LS, (f) LF, and (h) LCF.

respectively. Whereas the sorbents doped by seawater decreased significantly in porosity, here it is possible that the lower melting point of Na_2O caused pronounced sintering owing to the excess of Na^+ ion in this sorbent. A finding from the TGA test under a calcination temperature of 850 °C in N_2 demonstrated that all synthetic sorbents exhibited a significant increase in CO_2 uptake in comparison to raw limestone, wherein the biomass-templated cement-supported pellets produced the highest CO_2 capture rate of 46.5% relative to 20.8% for raw limestone after 20 cycles. This promising result was attributed to the enhancement of developed porosity and cyclic stability from the addition of biomass and calcium aluminate cement, respectively. However, this positive effect of biomass is substantially reduced for 950 °C calcinations after multicycles. This appears to be the result of pronounced sintering in this situation. Additionally, the vaporization of potassium carbonate under 950 °C may influence on the reduction of activity, given that it is noted that moderate potassium salt existing in pellets proved to have positive impact on performance. Further exploration to find more effective biomass dopants and/or enhancing the biomass-templated pellets will be carried out in subsequent studies.

■ AUTHOR INFORMATION

Corresponding Author

*L. Duan. Tel.: +86-25-83790147. E-mail address: duanlunbo@seu.edu.cn.

Notes

The authors declare no competing financial interest.

■ ACKNOWLEDGMENTS

Financial support from National Natural Science Foundation of China through Grant No. 51206023 and funding from the European Community's Research Fund for Coal and Steel (RFCS) under grant agreement No. RFCR-CT-2012-00008 are gratefully acknowledged.

■ REFERENCES

(1) IEA. *Energy technology perspectives 2010 -scenatios and strategies to 2050*, Paris, France, 2010; p 650.

(2) Boot-Handford, M. E.; Abanades, J. C.; Anthony, E. J.; Blunt, M. J.; Brandani, S.; Mac Dowell, N.; Fernández, J. R.; Ferrari, M.-C.; Gross, R.; Hallett, J. P.; Haszeldine, R. S.; Heptonstall, P.; Lyngfelt, A.; Makuch, Z.; Mangano, E.; Porter, R. T. J.; Pourkashanian, M.; Rochelle, G. T.; Shah, N.; Yao, J. G.; Fennell, P. S. Carbon capture and storage update. *Energy Environ. Sci.* **2014**, 7, 130−189.

(3) Herzog, H. J. Scaling up carbon dioxide capture and storage: From megatons to gigatons. *Energy Economics* **2011**, 33, 597−604.

(4) Rao, A. B.; Rubin, E. S. A technical, economic, and environmental assessment of amine-based CO_2 capture technology for power plant greenhouse gas control. *Environ. Sci. Technol.* **2002**, 36, 4467−4475.

(5) Karami, D.; Mahinpey, N. Highly Active CaO-Based Sorbents for CO_2 Capture Using the Precipitation Method: Preparation and Characterization of the Sorbent Powder. *Ind. Eng. Chem. Res.* **2012**, 51, 4567−4572.

DOI: 10.1021/acs.iecr.6b02965
Ind. Eng. Chem. Res. 2016, 55, 10294−10300

(6) Florin, N.; Fennell, P. Synthetic CaO-based sorbent for CO_2 capture. *Energy Procedia* **2011**, *4*, 830−838.
(7) Li, Y.; Shi, L.; Liu, C.; He, Z.; Wu, S. Studies on CO_2 uptake by $CaO/Ca_3Al_2O_6$ sorbent in calcium looping cycles. *J. Therm. Anal. Calorim.* **2015**, *120*, 1519−1528.
(8) Li, Y.; Su, M.; Xie, X.; Wu, S.; Liu, C. CO_2 capture performance of synthetic sorbent prepared from carbide slag and aluminum nitrate hydrate by combustion synthesis. *Appl. Energy* **2015**, *145*, 60−68.
(9) Zhao, M.; Bilton, M.; Brown, A. P.; Cunliffe, A. M.; Dvininov, E.; Dupont, V.; Comyn, T. P.; Milne, S. J. Durability of $CaO-CaZrO_3$ Sorbents for High-Temperature CO_2 Capture Prepared by a Wet Chemical Method. *Energy Fuels* **2014**, *28*, 1275−1283.
(10) Ridha, F. N.; Manovic, V.; Wu, Y.; Macchi, A.; Anthony, E. J. Pelletized CaO-based sorbents treated with organic acids for enhanced CO_2 capture in Ca-looping cycles. *Int. J. Greenhouse Gas Control* **2013**, *17*, 357−365.
(11) Ridha, F. N.; Manovic, V.; Wu, Y.; Macchi, A.; Anthony, E. J. Post-combustion CO_2 capture by formic acid-modified CaO-based sorbents. *Int. J. Greenhouse Gas Control* **2013**, *16*, 21−28.
(12) Manovic, V.; Fennell, P. S.; Al-Jeboori, M. J.; Anthony, E. J. Steam-Enhanced Calcium Looping Cycles with Calcium Aluminate Pellets Doped with Bromides. *Ind. Eng. Chem. Res.* **2013**, *52*, 7677−7683.
(13) Manovic, V.; Anthony, E. J.; Grasa, G.; Abanades, J. C. CO_2 looping cycle performance of a high-purity limestone after thermal activation/doping. *Energy Fuels* **2008**, *22*, 3258−3264.
(14) Blamey, J.; Manovic, V.; Anthony, E. J.; Dugwell, D. R.; Fennell, P. S. On steam hydration of CaO-based sorbent cycled for CO_2 capture. *Fuel* **2015**, *150*, 269−277.
(15) Manovic, V.; Wu, Y.; He, I.; Anthony, E. J. Spray water reactivation/pelletization of spent CaO-based sorbent from calcium looping cycles. *Environ. Sci. Technol.* **2012**, *46*, 12720−12725.
(16) Manovic, V.; Anthony, E. J. Reactivation and remaking of calcium aluminate pellets for CO_2 capture. *Fuel* **2011**, *90*, 233−239.
(17) González, B.; Liu, W.; Sultan, D. S.; Dennis, J. S. The effect of steam on a synthetic Ca-based sorbent for carbon capture. *Chem. Eng. J.* **2016**, *285*, 378−383.
(18) Angeli, S. D.; Martavaltzi, C. S.; Lemonidou, A. A. Development of a novel-synthesized Ca-based CO_2 sorbent for multicycle operation: Parametric study of sorption. *Fuel* **2014**, *127*, 62−69.
(19) Broda, M.; Müller, C. R. Sol−gel-derived, CaO-based, ZrO_2-stabilized CO_2 sorbents. *Fuel* **2014**, *127*, 94−100.
(20) Radfarnia, H. R.; Sayari, A. A highly efficient CaO-based CO_2 sorbent prepared by a citrate-assisted sol−gel technique. *Chem. Eng. J.* **2015**, *262*, 913−920.
(21) Luo, C.; Zheng, Y.; Ding, N.; Wu, Q.; Bian, G.; Zheng, C. Development and Performance of CaO/La_2O_3 Sorbents during Calcium Looping Cycles for CO_2 Capture. *Ind. Eng. Chem. Res.* **2010**, *49*, 11778−11784.
(22) Broda, M.; Muller, C. R. Synthesis of highly efficient, Ca-based, Al_2O_3-stabilized, carbon gel-templated CO_2 sorbents. *Adv. Mater.* **2012**, *24*, 3059−3064.
(23) Ridha, F. N.; Wu, Y.; Manovic, V.; Macchi, A.; Anthony, E. J. Enhanced CO_2 capture by biomass-templated $Ca(OH)_2$-based pellets. *Chem. Eng. J.* **2015**, *274*, 69−75.
(24) González, B.; Blamey, J.; McBride-Wright, M.; Carter, N.; Dugwell, D.; Fennell, P.; Abanades, J. C. Calcium looping for CO_2 capture: sorbent enhancement through doping. *Energy Procedia* **2011**, *4*, 402−409.
(25) Salvador, C.; Lu, D.; Anthony, E. J.; Abanades, J. C. Enhancement of CaO for CO_2 capture in an FBC environment. *Chem. Eng. J.* **2003**, *96*, 187−195.
(26) Al-Jeboori, M. J.; Nguyen, M.; Dean, C.; Fennell, P. S. Improvement of Limestone-Based CO_2 Sorbents for Ca Looping by HBr and Other Mineral Acids. *Ind. Eng. Chem. Res.* **2013**, *52*, 1426−1433.
(27) Al-Jeboori, M. J.; Fennell, P. S.; Nguyen, M.; Feng, K. Effects of Different Dopants and Doping Procedures on the Reactivity of CaO-based Sorbents for CO_2 Capture. *Energy Fuels* **2012**, *26*, 6584−6594.
(28) Zhou, Z.; Qi, Y.; Xie, M.; Cheng, Z.; Yuan, W. Synthesis of CaO-based sorbents through incorporation of alumina/aluminate and their CO_2 capture performance. *Chem. Eng. Sci.* **2012**, *74*, 172−180.
(29) Broda, M.; Manovic, V.; Anthony, E. J.; Muller, C. R. Effect of pelletization and addition of steam on the cyclic performance of carbon-templated, CaO-based CO_2 sorbents. *Environ. Sci. Technol.* **2014**, *48*, 5322−5328.
(30) Ridha, F. N.; Manovic, V.; Anthony, E. J.; Macchi, A. The morphology of limestone-based pellets prepared with kaolin-based binders. *Mater. Chem. Phys.* **2013**, *138*, 78−85.
(31) Wu, Y.; Manovic, V.; He, I.; Anthony, E. J. Modified lime-based pellet sorbents for high-temperature CO_2 capture: Reactivity and attrition behavior. *Fuel* **2012**, *96*, 454−461.
(32) Erans, M.; Beisheim, T.; Manovic, V.; Jeremias, M.; Patchigolla, K.; Dieter, H.; Duan, L.; Anthony, E. J. Effect of SO_2 and steam on CO_2 capture performance of biomass-templated calcium aluminate pellets. *Faraday Discuss.* **2016**, DOI: 10.1039/C6FD00027D.
(33) Ridha, F. N.; Manovic, V.; Macchi, A.; Anthony, E. J. High-temperature CO_2 capture cycles for CaO-based pellets with kaolin-based binders. *Int. J. Greenhouse Gas Control* **2012**, *6*, 164−170.
(34) Manovic, V.; Anthony, E. J. Screening of Binders for Pelletization of CaO-Based Sorbents for CO_2 Capture†. *Energy Fuels* **2009**, *23*, 4797−4804.
(35) Xu, Y.; Luo, C.; Zheng, Y.; Ding, H.; Zhang, L. Macropore-Stabilized Limestone Sorbents Prepared by the Simultaneous Hydration−Impregnation Method for High-Temperature CO_2 Capture. *Energy Fuels* **2016**, *30*, 3219−3226.
(36) Lu, H.; Reddy, E. P.; Smirniotis, P. G. Calcium Oxide Based Sorbents for Capture of Carbon Dioxide at High Temperatures. *Ind. Eng. Chem. Res.* **2006**, *45*, 3944−3949.
(37) Chen, Z.; Song, H. S.; Portillo, M.; Lim, C. J.; Grace, J. R.; Anthony, E. J. Long-Term Calcination/Carbonation Cycling and Thermal Pretreatment for CO_2 Capture by Limestone and Dolomite. *Energy Fuels* **2009**, *23*, 1437−1444.
(38) Manovic, V.; Anthony, E. J. Long-Term Behavior of CaO-Based Pellets Supported by Calcium Aluminate Cements in a Long Series of CO_2 Capture Cycles. *Ind. Eng. Chem. Res.* **2009**, *48*, 8906−8912.
(39) Manovic, V.; Anthony, E. J. CO_2 Carrying Behavior of Calcium Aluminate Pellets under High-Temperature/High-CO_2 Concentration Calcination Conditions. *Ind. Eng. Chem. Res.* **2010**, *49*, 6916−6922.
(40) Valverde, J. M.; Sanchez-Jimenez, P. E.; Perez-Maqueda, L. A. Effect of Heat Pretreatment/Recarbonation in the Ca-Looping Process at Realistic Calcination Conditions. *Energy Fuels* **2014**, *28*, 4062−4067.

DOI: 10.1021/acs.iecr.6b02965
Ind. Eng. Chem. Res. 2016, 55, 10294−10300

Appendix B ATTRITION STUDY OF CEMENT-SUPPORTED BIOMASS-ACTIVATED CALCIUM SORBENTS FOR CO_2 CAPTURE

Lunbo Duan[1, 2], Zhijian Yo[1], María Erans[2], Yingjie Li[3], Vasilije Manovic[2] and Edward J Anthony[2]

1 Key Laboratory of Energy Thermal Conversion and Control, Ministry of Education, School of Energy and Environment, Southeast University, Nanjing 210096, China

2 Combustion and CCS Centre, Cranfield University, Bedfordshire MK43 0AL, U.K.

3 School of Energy and Power Engineering, Shandong University, Jinan 250061, China

Published in Industrial & Engineering Chemistry Research, 2016, 55(35), 9476-9484.

Abstract

An enhanced CO_2 capacity was reported recently for biomass-modified Ca-based sorbent, but undesired attrition resistance was also observed. In this study, cement was used as a support for biomass-activated calcium sorbent during the granulation process to improve the poor mechanical resistance. Attrition tests were carried out in an apparatus focused on impact breakage to evaluate how the biomass addition and cement support influence the particle strength during Ca looping. The results showed that biomass addition impairs the mechanical strength and that a cement support can improve it, as reflected in the breakage probability and size change after impact of pellets that had experienced calcination and multiple calcination/carbonation cycles. Larger-sized particles suffered more intense attrition. The mechanical strength of the sorbents declined significantly after higher-temperature calcination but increased after carbonation. After multiple cycles, the mechanical strength of particles was greatly enhanced, but more cracks emerged. A semiempirical

formula for calculating the average diameter after attrition based on Rittinger's surface theory was developed. Observations of the morphology of the particles indicated that particles with more porosity and more cracks were more prone to breakage.

I&EC research
Industrial & Engineering Chemistry Research

Article

pubs.acs.org/IECR

Attrition Study of Cement-Supported Biomass-Activated Calcium Sorbents for CO_2 Capture

Lunbo Duan,*[,†,‡] Zhijian Yu,[†] María Erans,[‡] Yingjie Li,[§] Vasilije Manovic,[‡] and Edward J. Anthony[‡]

[†]Key Laboratory of Energy Thermal Conversion and Control, Ministry of Education, School of Energy and Environment, Southeast University, Nanjing 210096, China

[‡]Combustion and CCS Centre, Cranfield University, Cranfield, Bedfordshire MK43 0AL, U.K.

[§]School of Energy and Power Engineering, Shandong University, Jinan 250061, China

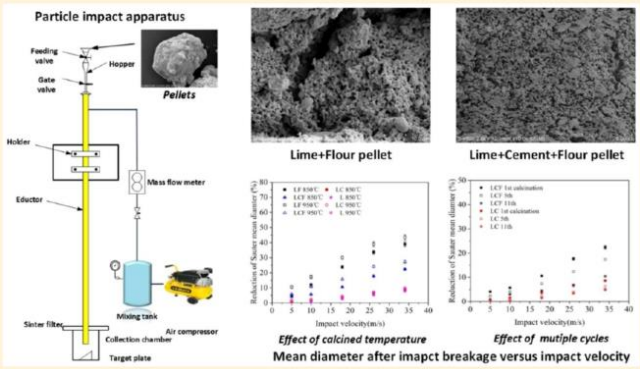

ABSTRACT: An enhanced CO_2 capacity was reported recently for biomass-modified Ca-based sorbent, but undesired attrition resistance was also observed. In this study, cement was used as a support for biomass-activated calcium sorbent during the granulation process to improve the poor mechanical resistance. Attrition tests were carried out in an apparatus focused on impact breakage to evaluate how the biomass addition and cement support influence the particle strength during Ca looping. The results showed that biomass addition impairs the mechanical strength and that a cement support can improve it, as reflected in the breakage probability and size change after impact of pellets that had experienced calcination and multiple calcination/carbonation cycles. Larger-sized particles suffered more intense attrition. The mechanical strength of the sorbents declined significantly after higher-temperature calcination but increased after carbonation. After multiple cycles, the mechanical strength of particles was greatly enhanced, but more cracks emerged. A semiempirical formula for calculating the average diameter after attrition based on Rittinger's surface theory was developed. Observations of the morphology of the particles indicated that particles with more porosity and more cracks were more prone to breakage.

1. INTRODUCTION

The calcination/carbonation cycles of calcium-based sorbents (also called calcium looping, or CaL) in dual-fluidized-bed systems represents a viable method for capturing CO_2 from fossil-fuel-fired power plants.[1−3] However, during operation, two main problems occur: continuous reactivity decay[4−6] due to the loss of micro- and mesopores and serious elutriation[7−10] resulting from the size reduction of the sorbent particles because of attrition. The latter occurs when the particles suffer wear during collisions with other particles and the reactor walls. Elutriation reduces the residence time of the particles in the furnace, increasing the sorbent makeup rates and, thus, the overall costs. Solving these problems requires improvements in reactivity and mechanical stability. However, very reactive particles are often not strong enough to survive in the high-temperature turbulent flow encountered in such reactors, whereas strong particles might not be reactive enough to capture CO_2 in a short time.

Many methods have been proposed to improve sorbent reactivity, as summarized by Valverde:[11] use of rigid porous materials as carriers of the Ca-based sorbents, use of additives to improve the sorbent thermal stability, reduction of the sorbent particle size to the nanometer scale, and use of synthetic precursors to produce novel sorbents with rich micropore structures. Recently, Chen et al.[12] reported that a

Received: June 21, 2016
Revised: August 10, 2016
Accepted: August 19, 2016
Published: August 19, 2016

DOI: 10.1021/acs.iecr.6b02393
Ind. Eng. Chem. Res. 2016, 55, 9476−9484

calcium-based sorbent doped with metal oxides through the sol−gel process exhibited enhanced reactivity by distributing the metal oxide particles at the molecular scale. Chen et al. also found that pressurized carbonation was beneficial for CO_2 capture.[13] Among possible additives, biomass additives[14] provide a cheap and efficient means of elevating the reactivity of the calcium sorbent, by improving the pore structure through biomass combustion. Also, the ash after combustion can serve as a composite framework. Our recent work[15] confirmed that biomass-activated calcium pellets (limestone + biomass) have better CO_2 capture performance than other tested pellets (limestone + cement and limestone + biomass + cement) in a thermogravimetric analyzer. Interestingly, the results obtained from a bubbling fluidized bed were not the same, and the biomass-activated pellet showed the poorest performance in that type of reactor. This is presumably because of material loss due to attrition under fluidized-bed (FB) conditions. It is well-known that cement is a good support for calcium-based sorbents[15−19] and that the reaction between CaO and alumina (Al_2O_3) to form mixed calcium−aluminum oxides (e.g., mayenite) results in the formation of an inert solid binder. The binder serves to reduce sintering of the CaO grains by providing an inert framework and helps improve the mechanical stability of the sorbent.[16]

There are several methods for evaluating the thermal stability of sorbent materials. The most common and direct method[20−22] is to carry out the reaction in a fluidized bed and measure the particle size of the materials after a number of reaction cycles. This method yields a value for attrition, but detailed information and the mechanism cannot be easily obtained because there are too many contributing factors. A Standard Test Method for the Determination of Attrition and Abrasion of Powdered Catalysts by Air Jets (D5757-00) proposed by the American Society for Testing and Materials (ASTM) has also been used[23−25] to evaluate the attrition properties of calcium-based sorbents through an air jet index (AJI, a unitless index that is numerically equal to the percentage attrition loss in 5 h). However, this method provides general information, obtained in a spouted bed rather than in the bubbling or fast beds that are usually used in calcium looping process. Scala and co-workers[26−29] proposed a single-particle impact apparatus in which particles accelerated by the gas stream strike a target, to test different limestones after calcination, desulfurization, and hydration. This setup was focused on attrition by impact damage, which occurs frequently in fluidized beds. Although the device could not simulate the entire attrition history of particles, the attrition resistance could be evaluated more accurately by this approach.

In this work, a system similar to that of Scala and co-workers was developed to investigate the attrition behavior of different calcium-based sorbents and evaluate how the addition of biomass and use of a cement support influence the mechanical strength of the sorbents. The effects of particle size, calcination temperature, carbonation, and multiple calcination/carbonation cycles on attrition resistance of sorbents were investigated. The relationship between the morphology characteristics and strengths of the sorbents was also fully explored.

2. EXPERIMENTAL SECTION

2.1. Sample Preparation. Longcal SP52 limestone from the United Kingdom, with a particle size of less than 125 μm, was calcined at 850 °C in a muffle furnace for 2 h. The product was then mixed with commercial flour (as the biomass binder used in this work), and a portion of the resulting mixture was mixed with calcium aluminate cement (CA-14 from Almatis Inc.).

The desired mixture was poured into a TMG tabletop mechanical granulator provided by Glatt GmbH to produce the sorbent pellets. The volume of the pelletizer vessel was 4 L, and the velocities of the agitator and chopper were 500 and 2500 rpm, respectively. About 1 L of deionized water was sprayed progressively during the operation. Then, the particles were air-dried for 12 h before being stored in a desiccator to avoid any reactions of the material with air.

Three types of pellets were prepared and are named according to their compositions: calcined limestone modified by addition of 10 wt % flour (LF), calcined limestone with addition of 10 wt % aluminate cement (LC), and the calcined limestone mixed with 10 wt % flour and 10 wt % cement (LCF). The constituents of the pellets are listed in Table 1, and

Table 1. Constituents of Sorbents (wt %)

component	LF	LC	LCF
calcined limestone	90	90	80
cement	–	10	10
flour	10	–	10

the compositions measured by X-ray fluorescence (XRF) are reported in Table 2. The increase of the K_2O mass in the LF and LCF samples seen in Table 2 indicates that the flour contained abundant potassium, which has been reported to be beneficial for reactivity improvement.[30] The CO_2 capture performances of these sorbents were reported in ref 15.

2.2. Apparatus and Procedures. Calcination, carbonation, and CaL cycles of the samples were carried out in a bubbling fluidized-bed reactor, as shown in Figure 1. The reactor consisted of a quartz reaction vessel heated by a two-stage external-resistance furnace. The first stage was used to preheat the gas to 300 °C, and the second stage was used to control the temperature of reaction. The quartz reaction vessel had an inner diameter of 25 mm and a length of 1800 mm. The gas distributor was a sintered plate. The height from the top of the reactor to the air distributor was 1000 mm. Fluidization gas, premixed using a mass flow-meter controller, was supplied from the bottom of the reactor. The concentration of CO_2 during carbonation was analyzed with a nondispersive infrared analyzer (Rosemount, NGA 2000) whose CO_2 range and precision were 50% and 0.5%, respectively.

The impact testing of the pellets was performed in the impact apparatus shown in Figure 2. The setup, in which particles accelerated by the gas stream hit a target, takes advantage of the approach proposed by Scala and co-workers.[26−29] The feeding unit was installed at the top and consisted of two valves. The first valve was closed after feeding to prevent the gas from escaping. The particles were stored in a hopper with a 1-mm-i.d. at the bottom section, so they stacked vertically. The second valve (gate valve) controlled the particles such that they fell into the eductor one by one. The eductor was 1.1 m in length and 10 mm in i.d. The gas flows into the tube from the side and the velocity were controlled by a mass flow meter. The particles, accelerated by the gas flow and gravity, impacted a stainless target at the bottom of the system. The target was set into the collection chamber 30 mm below the end of the tube and was inclined by 60° with respect to the vertical. This inclination was chosen by considering the effects

DOI: 10.1021/acs.iecr.6b02393
Ind. Eng. Chem. Res. 2016, 55, 9476−9484

Table 2. Compositions of Sorbents (wt %) by XRF

sample	CaO	Al_2O_3	K_2O	MgO	SiO_2	other	LOI[a]
limestone	55.0	0.084	0.007	0.189	0.715	0.230	43.78
LF	56.1	0.210	0.036	0.202	0.742	0.255	42.46
LC	57.9	5.585	0.006	0.206	1.190	0.254	34.86
LCF	50.4	4.552	0.022	0.190	0.257	0.176	44.40

[a]LOI = Loss on ignition.

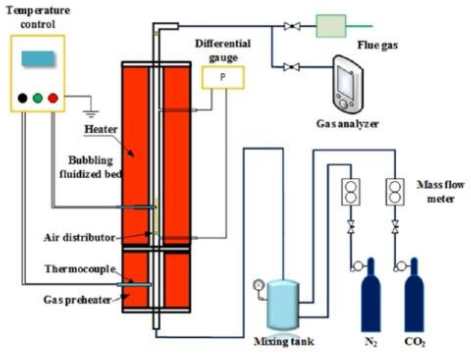

Figure 1. Scheme of the bubbling fluidized bed.

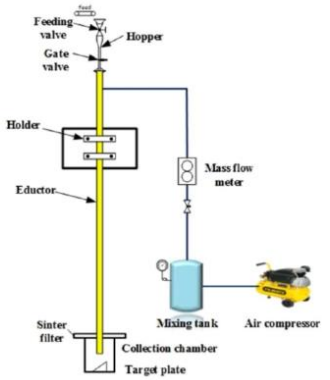

Figure 2. Impact apparatus diagram.

of rebounding particles. The chamber, 200 mm in height and 200 mm in i.d., was made of transparent Plexiglas suitable for use with a high-speed camera to track the particle location and, thereby, measure the particle velocity. The results showed that each particle was accelerated to nearly the gas velocity before it reached the target plate. The top section of the chamber was a sintered porous metal plate that could filter the entrained fine particles from the escaping gas. The chamber could be taken apart to allow for the collection of the particles after impact for further analysis.

The particles to be subjected to the impact test (described above) were obtained from the sorbent after calcination/carbonation tests in a FB reactor. About 25 g of pellets with sizes in the range of 0.4−0.6 mm were weighed for each FB test. Bed material was not used in these experiments. The first calcination was carried out at 850 °C in N_2 or at 950 °C in CO_2 for LF and LCF to decompose the biomass. Multiple CaL cycles were carried out by calcining the sample at 850 °C for 15 min in pure N_2 and carbonating it at 650 °C for 20 min in 15% (v/v) CO_2 with a balance of N_2. The fluidization number (U/U_{mf}) was about 4, and the fluidization velocity was 0.6 m/s. The gas volumetric flow rate through the flow meter was calibrated at different temperatures based on the equation of state of an ideal gas. The product was then sieved in the particle size range of 0.35−0.5 mm for impact tests.

About 2 g of pellets was used for each impact test at room temperature. The impact velocities were 5, 10, 18, 26, and 34 m/s, conforming to particle impact conditions near the gas distributor, in the bed, and in the cyclone. According to the calculations, the particles approached terminal velocity after accelerating through the eductor (1.1-m length). The terminal velocity was equal to the gas velocity plus the free-fall velocity of the particle. For particle sizes of 0.4 mm or less, the free-fall velocity is so small that it can be ignored in comparison to the gas velocity. If the mass of fragments collected after the impact test deviated by less than 1% from the initial mass, the test was considered to be satisfactory. Debris was sieved to determine the size distribution after each impact. Three parallel tests were performed to guarantee the reproducibility of the results for parts of the experiments.

The breakage probability,[31] f, is defined as

$$f = \frac{m_{\text{Debris}}}{m} \tag{1}$$

where m_{Debris} is the mass of debris whose size falls below the lower limit of the feed size interval and m is the total mass of particles. The Sauter mean diameter (d_{sv}) and the size reduction of d_{sv} were calculated according to the equations

$$d_{sv} = \frac{1}{\sum x_i/d_{pi}} \tag{2}$$

$$I = \frac{d_0 - d_{sv}}{d_0} \times 100\% \tag{3}$$

where x_i is the mass fraction of particles in the size interval of i, d_{pi} is the length of size interval of i, and d_0 is the initial mean size. Finally, the probability density function (PDF) of particle sizes was calculated as

$$\text{PDF}_i = \frac{x_i}{d_{pi}} \tag{4}$$

to describe the particle size distribution size distribution (PSD).

Morphology observations and microstructure tests were also performed to study the potential relationship between structure and mechanical strength. The pore microstructure was measured by nitrogen adsorption/desorption isotherm tests at −196.8 °C on a Micromeritics ASAP 2020-M analyzer. The

DOI: 10.1021/acs.iecr.6b02393
Ind. Eng. Chem. Res. 2016, 55, 9476−9484

morphology was observed by scanning electron microscopy (SEM).

3. RESULTS AND DISCUSSION

3.1. Impact Fragmentation of the Raw Sorbents. The breakage probabilities of raw samples of LF, LC, LCF, and limestone in the size range of 0.35−0.5 mm at different impact velocities are shown in Figure 3. The pellets subjected to higher

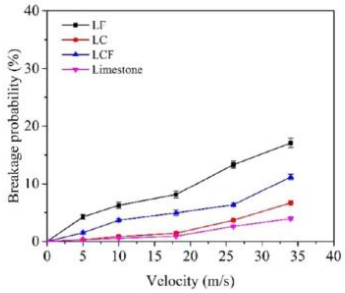

Figure 3. Breakage probabilities of different samples versus impact velocity (particle size range of 0.35−0.5 mm).

speeds suffered more intense breakage because they had higher momenta. The breakage probability of LF was found to be 4.2−17.1% at impact velocities in the range of 5−34 m/s, whereas the breakage probability of LC was 0.3−6.7% over the same velocity range. Thus, although the addition of biomass is beneficial for enhancing reactivity, it decreases the pellet strength. The breakage probability of LCF was found to be 1.5−11.2% in the same range of impact velocities (5−34 m/s), indicating that the addition of cement at room temperature can significantly improve the rigidity of sorbents compared to that LF pellets because the cement serves as only a physical binder and skeleton at this temperature. The LCF pellets, which were prepared by mixing biomass according to a commercial pelletization method, represent a possible candidate for CO_2 capture because they exhibit both reliable reactivity[15] and mechanical strength. The raw limestone and LC retained similar breakage probabilities at room temperature, except for a small deviation at 26−34 m/s. It appears that cement-supported sorbent can reach the strength of the original limestone.

The breakage probabilities of LC in the size ranges of 0.35−0.5, 0.5−0.6, and 0.6−0.85 mm at different impact velocities are shown in Figure 4. The fragmentation of pellets of the same material is sensitive to particle size, and particles with larger sizes suffer more intense breakage.

The critical stress of breakage can be obtained using the Griffith equation[32]

$$\sigma_f = \sqrt{2E\gamma_s/\pi c} \quad (5)$$

where σ_f is the critical breaking stress, E is the Young's modulus, γ_s is the surface energy of the material, and $2c$ is the length of the crack (equal to the particle size when the particle splits entirely). σ_f increases as the particle size decreases because the values of E and γ_s are constant for a given material. For fragmentation to occur, larger particles usually require large cracks as well as smaller critical stresses. Meanwhile, there is a

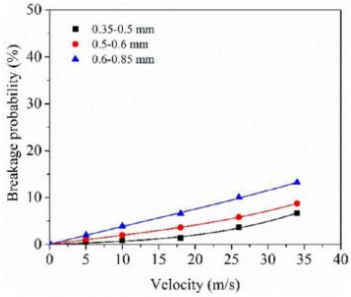

Figure 4. Effects of particle size on the breakage probability of LC at different impact velocities.

minimum size below which the critical stress cannot be reached and the particles are difficult to break further.

3.2. Effects of Calcination. Figure 5a displays the breakage probabilities of LF, LC, LCF, and limestone calcined at 850 and

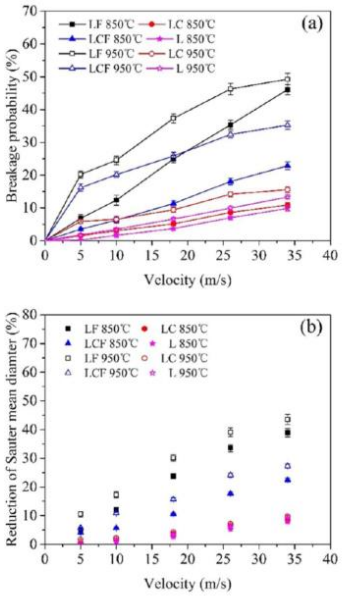

Figure 5. Effects of calcination temperature on different samples: (a) breakage probability, (b) reduction of Sauter mean diameter (original particle size range of 0.35−0.5 mm).

950 °C for 15 min (simulating the first calcination during calcium looping) at different impact velocities. The reductions of the Sauter mean diameters of the same samples versus impact velocity are shown in Figure 5b. All calcined samples exhibited higher breakage probabilities than the raw pellets for all tested impact velocities. This means that the mechanical strengths of the sorbents decline after calcination.[26,27] Furthermore, the curves of all samples calcined at 950 °C were higher than those of the samples calcined at 850 °C, which indicates that Ca-based sorbents suffer more from

DOI: 10.1021/acs.iecr.6b02393
Ind. Eng. Chem. Res. 2016, 55, 9476−9484

fragmentation at higher temperatures. The internal pressure stress, caused by the hindering of gas flow through the particle, and thermal stress usually increase at higher calcination temperatures, which generates cracks at the surfaces of samples and plays a vital role in diminution of particle strength.

At impact velocities in the range of 5−34 m/s, the breakage probability decreased from 6.8−46.1% for LF to 3.5−22.9% for LCF, and the reduction of Sauter mean size decreased from 5.0−38.9% for LF to 4.1−22.4% for LCF. Calcined LF was found to be more prone to fragmentation, whereas LCF containing cement showed much better attrition resistance.

Manovic and Anthony,[16] along with other workers,[33,35] have noted that, at the calcination temperature, some of the CaO from limestone could react with cement to form calcium aluminates, such as $Ca_{12}Al_{14}O_{33}$ (mayenite) or $Ca_3Al_2O_6$, for different Ca/Al ratios. The surface morphology of LCF after the first calcination at 850 °C is shown in Figure 6. The

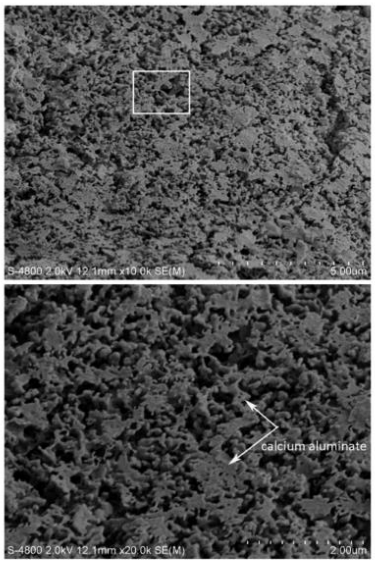

Figure 6. SEM images of LCF after the first calcination at 850 °C for 15 min.

appearance of calcium aluminate in Figure 6 is similar to that in images found elsewhere in the literature.[33,34] Calcium aluminate forms a stable cross-linked nanoscale framework, and CaO grains are embedded in the framework. A a result, unconsolidated grains are connected by those chemical bonds, and a tougher structure is obtained. The porous channels generated by the decomposition of biomass and $Ca(OH)_2$ can also be observed. This property leads to the poorer attrition resistance of LCF compared to LC.

Compared to limestone, LC suffers a marginally higher breakage probability and reduction of the Sauter mean size after calcination at different temperatures. These results agree well with the worse attrition resistance of calcined cement-supported pellets than of lime tested in an air jet apparatus reported by Knight et al.[23]

Figure 7 reports the probability density functions of the sizes (PSDs) of LF and LCF collected after impact. For both

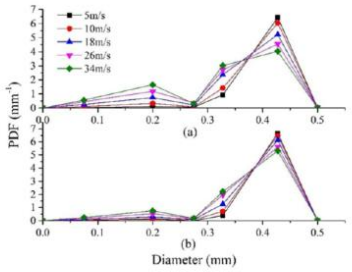

Figure 7. Probability density functions of particle size after impact: (a) LF calcined at 850 °C, (b) LCF calcined at 850 °C.

samples, the mass of particles in the feeding size range decreased noticeably, whereas the mass of particles in size intervals of 0−0.2 and 0.3−0.35 mm increased. Scala et al.[26] identified three types of typical breakage patterns that can be identified in the size distributions of fragments. Based on this concept, the calcined pellets of LF and LCF mostly undergo splitting (breakage into a relatively small number of fragments with sizes comparable to that of the parent particle), combined with moderate disintegration (extensive loss of particle connectivity, which results in the generation of a large number of small fragments), whereas the LCF pellets suffer less disintegration because their strength has been improved.

3.3. Effects of Multiple Calcination/Carbonation Cycles. *3.3.1. Effects of Multiple Calcinations.* LCF and LC were used to carry out 5 and 11 calcination/carbonation cycles. LF was not included in these tests because of its poorer strength. To facilitate the subsequent attrition test, the final step of the last cycle was calcination. The size range of the samples on which the impact tests were performed was 0.35−0.5 mm. Figure 8a reports the breakage probabilities of samples subjected to different numbers of cycles. The breakage probabilities of LC and LCF at impact velocities in the range of 5−34 m/s were 1.5−10.9% and 3.5−22.9%, respectively, after the first calcination; 0.9−9.2% and 3.0−18.7%, respectively, after the fifth calcination; and 0.7−6.1% and 2.1−14.0%, respectively, after the 11th calcination. Figure 8b reports the corresponding reductions of the Sauter mean diameters of LCF and LC. They decreased from 4.1−22.4% and 0.6−8.6%, respectively, after the first calcination to 0.8−10.4% and 0.2−4.9%, respectively, after the 11th calcination. It can be concluded that the attrition resistance was gradually enhanced after multiple calcinations.

Carbonation causes swelling of CaO as a result of the change in the molar volume from 16.9 $cm^3 \cdot mol^{-1}$ for CaO to 37.0 $cm^3 \cdot mol^{-1}$ for $CaCO_3$. Chemical stress was obvious at the surface of the particles that experienced swelling. The calcination of $CaCO_3$ resulted in excess internal pressure stress that was greater than the critical stress of the sorbents. Therefore, cracks inside and at the surfaces of the particles emerged as effects of iterative stress. Significantly increased cracking was observed in SEM images, as presented in the next section. According to Griffith's theory,[35] stress concentration will occur near cracks in solid materials. Therefore, particles with more cracks will suffer more attrition. Also, the porosity caused by the decomposition

DOI: 10.1021/acs.iecr.6b02393
Ind. Eng. Chem. Res. 2016, 55, 9476−9484

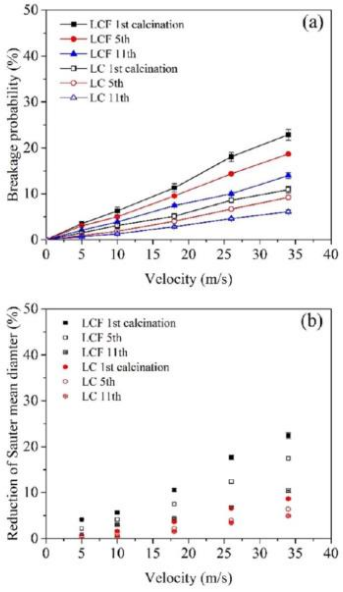

Figure 8. Effects of multiple calcinations on different samples: (a) breakage probability, (b) reduction of Sauter mean diameter (carbonation at 650 °C for 20 min in 15% CO_2, calcination at 850 °C for 15 min in pure N_2).

of biomass and $Ca(OH)_2$ contributes to the breakage of the pellets.

Figure 9 shows the surface morphology of LCF after the 11th calcination. Compared with Figure 6, the grains have merged

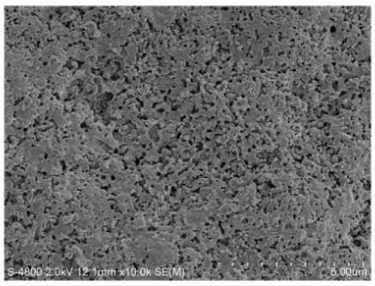

Figure 9. SEM image of LCF after the 11th calcination.

together, and the number of porous channels has decreased. It should be noted that this property could be caused by the combined effects of sintering and further CaO/Al_2O_3 reaction. A more compact structure forms, and it is more difficult to split this structure into smaller particles. The strength improvement resulting from the merging of grains and the decreasing of cracks means that the effects of grains merging are more important after multiple cycles because the total attrition resistance is enhanced.

3.3.2. Effects of Multiple Carbonations. Figure 10a shows the breakage probabilities of samples after the first and 11th

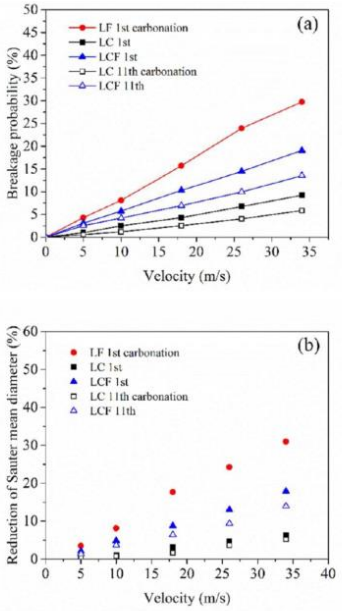

Figure 10. Effects of multiple carbonations on different samples: (a) breakage probability, (b) reduction of Sauter mean diameter (carbonation at 650 °C for 20 min in 15% CO_2, calcination at 850 °C for 15 min in pure N_2).

carbonations; the corresponding reductions of the Sauter mean diameter can be seen in Figure 10b. Compared to the results in Figure 5a, the breakage probabilities in the range of 5−34 m/s are 1.0−9.2%, 4.3−29.7%, and 3.1−19.1% for LC, LF, and LCF, respectively, after the first carbonation, which are lower than the results obtained after calcination of 1.5−10.9%, 6.8−46.1%, and 3.5−22.9%, respectively. Recarbonation is effective in reducing the propensity toward impact damage of the sorbent because the $CaCO_3$ shell can resist impact and the hardness of $CaCO_3$ is greater than that of CaO.[24]

The mechanical resistance of the samples was found to be enhanced after multiple carbonations. The reason is also the competitive effects between grains merging and cracks increasing.

Figure 11 shows the probability density functions of the size of LCF after the 11th carbonation and 11th calcination. The mass fraction of particles in the feeding size range decreased, whereas the particle fractions in the size ranges of 0.3−0.35 and 0.15−0.25 mm increased slightly. The breakage pattern of LCF after the 11th carbonation and calcination was mostly chipping (producing a few fragments with sizes much smaller than those of the mother particles) as a result of the enhanced strength caused by grain merging.

3.4. Modeling of Attrition. Rittinger's surface theory[36] indicates that the generation of new surface area of impacted particles is proportional to the total kinetic energy consumed. Chen et al.[37] reported that the impact attrition of limestone particles follows this theory and proposed a three-parameter attrition model of the form

DOI: 10.1021/acs.iecr.6b02393
Ind. Eng. Chem. Res. 2016, 55, 9476−9484

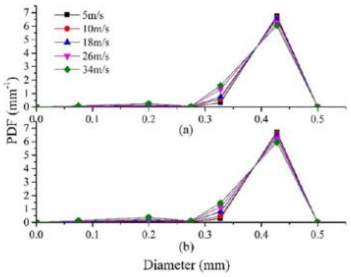

Figure 11. Probability density function of particle size after impact: (a) LCF after the 11th carbonation, (b) LCF after the 11th calcination.

$$\frac{d_0}{d_{sv}} = k_{Imp} v^2 N + \gamma \tag{6}$$

where d_0 is average diameter of feed particles, d_{sv} is the Sauter mean size after impact, k_{Imp} is a prefactor that can reflect the strength of particles, v is the impact velocity of the particles, N is the number of impact cycles, and γ is a constant.

In this work, $N = 1$ because impact cycles were not used. Figure 12 shows the relationship between d_0/d_{sv} and the square

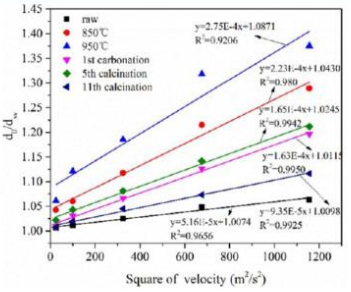

Figure 12. d_0/d_{sv} as a function of v^2 for LCF before and after different reactions.

of the impact velocity for LCF before and after different reactions. It can be seen that d_0/d_{sv} varies almost linearly with v^2. Least-squares fitting was performed based on eq 6, and the model coefficients of impact attrition are listed in Table 3. A confidence of 95% was employed in calculating the confidence intervals of the parameters.

The correlation coefficients (R^2) from Table 3 for all conditions have an average value of 0.9747. This means that the impact attrition of both raw LCF and LCF after calcination and multiple cycles of calcination also conforms to Rittinger's surface theory. The average diameter of the particles after impact is unknown, but velocities can be calculated by eq 6, and the accuracy can be guaranteed. According to Chen et al.'s research,[37] smaller values of k_{Imp} reflect higher particle strengths. Therefore, the raw pellets had the highest strength because their value of k_{Imp} was 0.516×10^{-4} s^2/m^2, which decreased after calcination to 2.75×10^{-4} s^2/m^2. The k_{Imp} value of the pellets after the 11th calcination was 0.935×10^{-4} s^2/m^2, which means that the strength had increased.

Table 3. Model Coefficients of Impact Attrition for LCF

	confidence intervals[a]				
sample	$k_{Imp} \times 10^4$ (s^2/m^2)	deviation	γ	deviation	R^2
raw LCF	0.516	±0.095	1.0074	±0.0059	0.9656
after calcination at 850 °C	2.23	±0.311	1.0430	±0.0192	0.9800
after calcination at 950 °C	2.75	±0.782	1.0871	±0.0483	0.9206
after first carbonation	1.63	±0.113	1.0115	±0.0070	0.9950
after fifth calcination	1.65	±0.124	1.0245	±0.0077	0.9942
after 11th calcination	0.935	±0.079	1.0098	±0.0049	0.9925

[a]95% confidence.

3.5. Microstructure Analysis. Figure13 presents the surface area and pore volume distributions of sorbents during

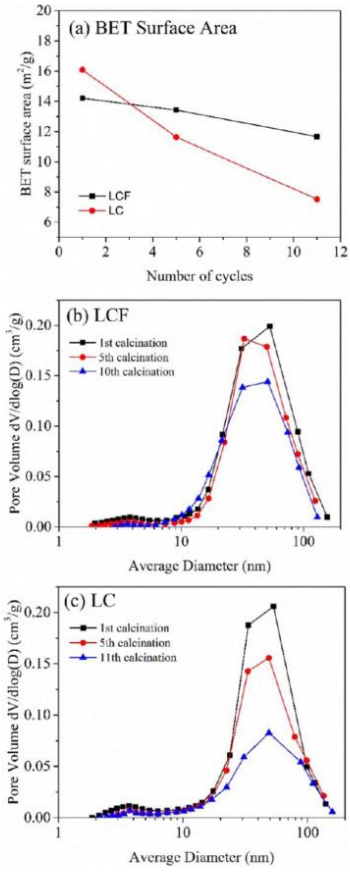

Figure 13. BET surface area and pore volume distributions of LCF and LC during multiple cycles.

DOI: 10.1021/acs.iecr.6b02393
Ind. Eng. Chem. Res. 2016, 55, 9476−9484

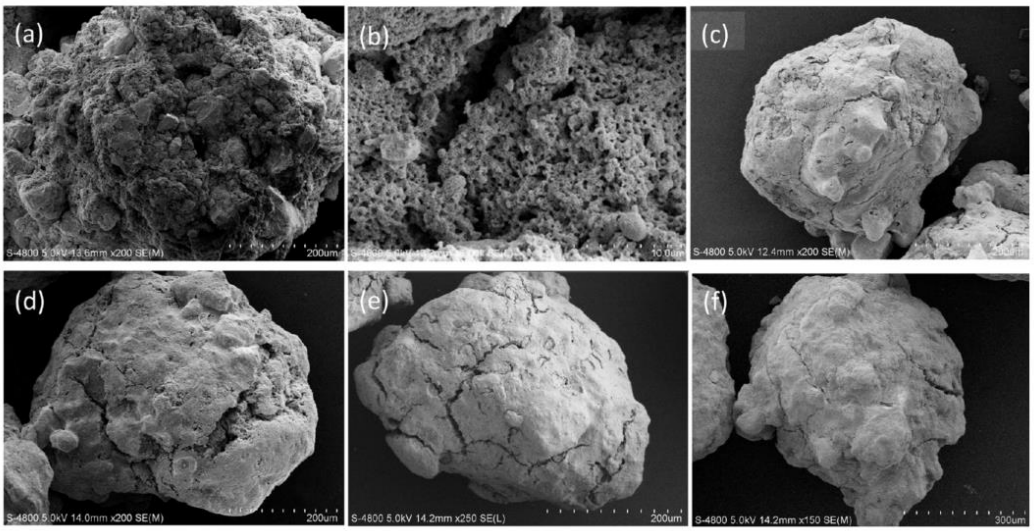

Figure 14. SEM images of sorbents after calcination: (a,b) LF after the first calcination at 850 °C, (c) LCF after the first calcination at 850 °C, (d) LCF after the first calcination at 950 °C, (e) LCF after the 11th calcination at 850 °C, (f) LC after the 11th calcination at 850 °C (carbonation at 650 °C for 20 min in 15% CO_2 in the cycle test).

multiple cycles. According to Figure13a, even though LC had a higher Brunauer−Emmett−Teller (BET) surface area in the initial cycle, it suffered a more severe surface area decrease after multiple cycles. Figure 13b,c suggests that the general pore volumes of both samples decreased after multiple reactions. The pore volume of LC reached a much lower level after the 11th cycle than that of LCF, which exhibited less of a decrease. Mesopores (2−50 nm) are beneficial for CO_2 capture, so the lower change in pore volume for LCF suggests a slower decay of the CO_2 capture capacity after multiple cycles than for LC, which is consistent with the results reported in section 3.1.

Although pore diameters greater than 300 nm cannot be assessed by N_2 absorption/desorption, it is apparent that grain merging occurred inside the pellets after long durations of high-temperature reaction because the CO_2 capacity declined. Also, the decrease of the porosity produced more compact structures, which can enhance the mechanical resistance.

SEM images of the sorbent pellets are presented in Figure 14. Figure 14a indicates that LF has a rugged and unconsolidated surface after the first calcination at 850 °C. Figure 14b shows that LF has ample pores of large size caused by burning out of the biomass, so the connections between grains are weak. This characteristic results in a low level of strength. The effect caused by adding cement to LF is prominent, as shown in Figure 14c. Unlike LF, the calcined LCF has a smooth and compact surface, which can improve attrition resistance. Comparison of panels c and d of Figure 14 shows that larger and more numerous cracks were generated on the sorbent surface after first calcination at 950 °C. By comparing panels c and e of Figure 14, one can see that more cracks emerged and the average size increased after the 11th calcination; cracks are unfavorable for reducing attrition because stress concentration and breakage occur along such cracks. Biomass addition was not found to influence the morphology significantly, because the calcined LC and LCF samples showed the same surface properties; see Figure 14e,f.

4. CONCLUSIONS

All of the modified lime-based sorbents for high-temperature CO_2 capture prepared in this work were granulated with a mechanical pelletizer. Impact tests were performed on both fresh materials and the materials after multiple CaL cycles. The results showed that the introduction of biomass was detrimental to the fragmentation resistance of the pellets, but the addition of cement could enhance the otherwise unsatisfactory mechanical strength. Smaller-sized particles were found to be more resistant to fragmentation. The attrition resistances of the sorbents declined significantly after higher-temperature calcination but were elevated after recarbonation and multiple cycles. A change in the major particle failure pattern from "splitting" after calcination to "chipping" after multiple cycles was observed. The impact attrition of LCF was also found to conform to the theory that the area of new surface generated is approximately proportional to the impact kinetic energy. Morphology analysis of the particles indicated that cracks caused by chemical stress during calcination and multiple cycles will impair the mechanical resistance, whereas compact structures with less porosity can endure higher impact loads.

■ AUTHOR INFORMATION

Corresponding Author

*Tel.: +86-25-83790147. E-mail: duanlunbo@seu.edu.cn.

Notes

The authors declare no competing financial interest.

■ ACKNOWLEDGMENTS

Financial support from the National Natural Science Foundation of China through Grant 51206023 and funding

DOI: 10.1021/acs.iecr.6b02393
Ind. Eng. Chem. Res. 2016, 55, 9476−9484

from the European Community's Research Fund for Coal and Steel (RFCS) under Grant Agreement RFCR-CT-2012-00008 are gratefully acknowledged.

REFERENCES

(1) Li, F.; Fan, L. S. Clean coal conversion processes−progress and challenges. *Energy Environ. Sci.* **2008**, *1*, 248−267.
(2) Blamey, J.; Anthony, E. J.; Wang, J.; Fennell, P. S. The calcium looping cycle for large-scale CO_2 capture. *Prog. Energy Combust. Sci.* **2010**, *36*, 260−279.
(3) Zhao, C.; Chen, X.; Anthony, E. J.; Jiang, X.; Duan, L.; Wu, Y.; Dong, W.; Zhao, C. Capturing CO_2 in flue gas from fossil fuel-fired power plants using dry regenerable alkali metal-based sorbent. *Prog. Energy Combust. Sci.* **2013**, *39*, 515−534.
(4) Lysikov, A. I.; Salanov, A. N.; Okunev, A. G. Change of CO_2 carrying capacity of CaO in isothermal recarbonation-decomposition cycles. *Ind. Eng. Chem. Res.* **2007**, *46*, 4633−4638.
(5) Alonso, M.; Rodríguez, N.; González, B.; Grasa, G.; Murillo, R.; Abanades, J. C. Carbon dioxide capture from combustion flue gases with a calcium oxide chemical loop. Experimental results and process development. *Int. J. Greenhouse Gas Control* **2010**, *4*, 167−73.
(6) Wang, C.; Zhou, X.; Jia, L.; Tan, Y. Sintering of Limestone in Calcination Carbonation Cycles. *Ind. Eng. Chem. Res.* **2014**, *53*, 16235−16244.
(7) Fennell, P. S.; Pacciani, R.; Dennis, J. S.; Davidson, J. F.; Hayhurst, A. N. The effects of repeated cycles of calcination and carbonation on a variety of different limestones, as measured in a hot fluidized bed of sand. *Energy Fuels* **2007**, *21*, 2072−2081.
(8) Charitos, A.; Hawthorne, C.; Bidwe, A. R.; Sivalingam, S.; Schuster, A.; Spliethoff, H.; Scheffknecht, G. Parametric investigation of the calcium looping process for CO_2 capture in a 10kW th dual fluidized bed. *Int. J. Greenhouse Gas Control* **2010**, *4*, 776−784.
(9) Coppola, A.; Scala, F.; Salatino, P.; Montagnaro, F. Fluidized bed calcium looping cycles for CO2 capture under oxy-firing calcination conditions Part 1. Assessment of six limestones. *Chem. Eng. J.* **2013**, *231*, 537−543.
(10) Wu, Y.; Manovic, V.; He, I.; Anthony, E. J. Modified lime-based pellet sorbents for high-temperature CO_2 capture: reactivity and attrition behavior. *Fuel* **2012**, *96*, 454−461.
(11) Valverde, J. M. Ca-based synthetic materials with enhanced CO_2 capture efficiency. *J. Mater. Chem. A* **2013**, *1*, 447−468.
(12) Chen, H.; Zhang, P.; Duan, Y.; Zhao, C. Reactivity enhancement of calcium based sorbents by doped with metal oxides through the sol−gel process. *Appl. Energy* **2016**, *162*, 390−400.
(13) Chen, H.; Zhao, C.; Yang, Y.; Zhang, P. CO_2 capture and attrition performance of CaO pellets with aluminate cement under pressurized carbonation. *Appl. Energy* **2012**, *91*, 334−340.
(14) Ridha, F. N.; Wu, Y.; Manovic, V.; Macchi, A.; Anthony, E. J. Enhanced CO_2 capture by biomass-templated $Ca(OH)_2$-based pellets. *Chem. Eng. J.* **2015**, *274*, 69−75.
(15) Erans, M.; Beisheim, T.; Manovic, V.; Jeremias, M.; Patchigolla, K.; Dieter, H.; Duan, L.; Anthony, E. J. Effect of SO_2 and steam on CO_2 capture performance of biomass-templated calcium aluminate pellets. *Faraday Discuss.* [Advance Article]. 10.1039/C6FD00027D. Published Online: Mar 29, 2016. http://pubs.rsc.org/en/content/articlelanding/2016/fd/c6fd00027d.
(16) Manovic, V.; Anthony, E. J. CaO-based pellets supported by calcium aluminate cements for high-temperature CO_2 capture. *Environ. Sci. Technol.* **2009**, *43*, 7117−7122.
(17) Manovic, V.; Anthony, E. J. Long-term behavior of CaO-based pellets supported by calcium aluminate cements in a long series of CO_2 capture cycles. *Ind. Eng. Chem. Res.* **2009**, *48*, 8906−8912.
(18) Ridha, F. N.; Manovic, V.; Macchi, A.; Anthony, E. J. CO_2 capture at ambient temperature in a fixed bed with CaO-based sorbents. *Appl. Energy* **2015**, *140*, 297−303.
(19) Manovic, V.; Wu, Y.; He, I.; Anthony, E. J. Spray water reactivation/pelletization of spent CaO-based sorbent from calcium looping cycles. *Environ. Sci. Technol.* **2012**, *46*, 12720−12725.
(20) Jia, L.; Hughes, R.; Lu, D.; Anthony, E. J.; Lau, I. Attrition of calcining limestones in circulating fluidized-bed systems. *Ind. Eng. Chem. Res.* **2007**, *46*, 5199−5209.
(21) Zhang, W.; Li, Y.; Duan, L.; Ma, X.; Wang, Z.; Lu, C. Attrition behavior of calcium-based waste during CO_2 capture cycles using calcium looping in a fluidized bed reactor. *Chem. Eng. Res. Des.* **2016**, *109*, 806−815.
(22) Materic, V.; Hyland, M.; Jones, M. I.; Holt, R. Investigation of the friability of Ca looping sorbents during and after hydration based reactivation. *Fuel* **2014**, *127*, 70−77.
(23) Knight, A.; Ellis, N.; Grace, J. R.; Lim, C. J. CO_2 sorbent attrition testing for fluidized bed systems. *Powder Technol.* **2014**, *266*, 412−423.
(24) Xiao, G.; Grace, J. R.; Lim, C. J. Evolution of Limestone Particle Size Distribution in an Air-Jet Attrition Apparatus. *Ind. Eng. Chem. Res.* **2014**, *53*, 15845−15851.
(25) Valverde, J. M.; Quintanilla, M. A. S. Attrition of Ca-based CO_2-adsorbents by a high velocity gas jet. *AIChE J.* **2013**, *59*, 1096−1107.
(26) Scala, F.; Montagnaro, F.; Salatino, P. Attrition of limestone by impact loading in fluidized beds. *Energy Fuels* **2007**, *21*, 2566−2572.
(27) Scala, F.; Salatino, P. Flue gas desulfurization under simulated oxyfiring fluidized bed combustion conditions: The influence of limestone attrition and fragmentation. *Chem. Eng. Sci.* **2010**, *65*, 556−561.
(28) Montagnaro, F.; Salatino, P.; Santoro, L.; Scala, F. The influence of reactivation by hydration of spent SO_2 sorbents on their impact fragmentation in fluidized bed combustors. *Chem. Eng. J.* **2010**, *162*, 1067−1074.
(29) Coppola, A.; Palladino, L.; Montagnaro, F.; Scala, F.; Salatino, P. Reactivation by Steam Hydration of Sorbents for Fluidized-Bed Calcium Looping. *Energy Fuels* **2015**, *29*, 4436−4446.
(30) González, B.; Blamey, J.; McBride-Wright, M.; Carter, N.; Dugwell, D.; Fennell, P.; Abanades, J. C. Calcium looping for CO_2 capture: Sorbent enhancement through doping. *Energy Procedia* **2011**, *4*, 402−409.
(31) Samimi, A.; Moreno, R.; Ghadiri, M. Analysis of impact damage of agglomerates: effect of impact angle. *Powder Technol.* **2004**, *143-144*, 97−109.
(32) Shipway, P. H.; Hutchings, I. M. Attrition of brittle spheres by fracture under compression and impact loading. *Powder Technol.* **1993**, *76*, 23−30.
(33) Wu, S. F.; Jiang, M. Z. Formation of a $Ca_{12}Al_{14}O_{33}$ nanolayer and its effect on the attrition behavior of CO_2-adsorbent microspheres composed of CaO nanoparticles. *Ind. Eng. Chem. Res.* **2010**, *49*, 12269−12275.
(34) Luo, C.; Zheng, Y.; Ding, N.; Zheng, C. Enhanced cyclic stability of CO_2 adsorption capacity of CaO-based sorbents using La_2O_3 or $Ca_{12}Al_{14}O_{33}$ as additives. *Korean J. Chem. Eng.* **2011**, *28*, 1042−1046.
(35) Anderson, T. L. *Fracture Mechanics: Fundamentals and Applications*, 3rd ed.; CRC Press: Boca Raton, FL, 2005.
(36) Ray, Y. C.; Jiang, T. S.; Wen, C. Y. Particle attrition phenomena in a fluidized bed. *Powder Technol.* **1987**, *49*, 193−206.
(37) Chen, Z.; Lim, C. J.; Grace, J. R. Study of limestone particle impact attrition. *Chem. Eng. Sci.* **2007**, *62*, 867−877.

DOI: 10.1021/acs.iecr.6b02393
Ind. Eng. Chem. Res. 2016, 55, 9476−9484

Appendix C RECONSTRUCTION OF THE 25KWTH CALCIUM LOOPING PILOT PLANT

Cranfield's 25 kW_{th} pilot plant underwent several modifications during the course of this research project. These upgrades are shown in Figure_Apx C-1.

a) Replacement of the carbonator and calciner gas burners by electrical preheating lines (Figure_Apx C-2, Figure_Apx C-3, Figure_Apx C-4 and Figure_Apx C-5) in order to provide a heated mixture of any desired gas composition to both reactors. These modifications broaden the use of this unit, which enable the simulation of many industrial and power generation sectors. Also, higher O_2 (for the calciner)/CO_2 (for carbonator/calciner) ratios can be used in the in the feed gas.

b) Deepening the bubbling fluidized bed of the calciner to ensure proper bubbling regime and a longer sorbent residence time. The calciner distributor was modified to improve the fluidization behaviour. Moreover, a high-temperature cyclone was added to the calciner's exhaust line (Figure_Apx C-6) so as to collect material that is carried over from the bubbling fluidised bed.

c) Additional electrical heating (8 kW_{th}) was installed around the calciner in order to achieve the temperature needed for the fuel ignition (above 650°C).

d) The fuel feeding system was put in place in order to directly inject the fuel into the calciner.

e) Trace heating (to 500°C) of the loop seals was installed combined with the preheating of nitrogen (to 200°C), which fluidises the circulating material.

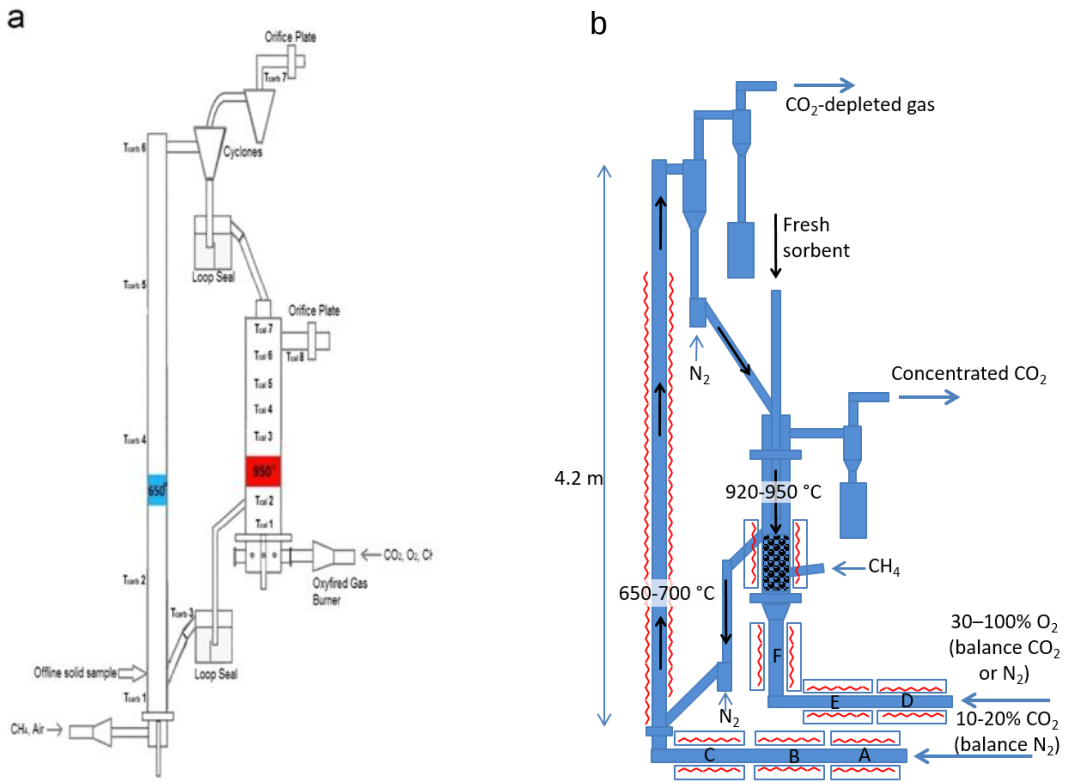

Figure_Apx C-1: 25 kW_{th} pilot plant before (a) and after (b) reconstruction

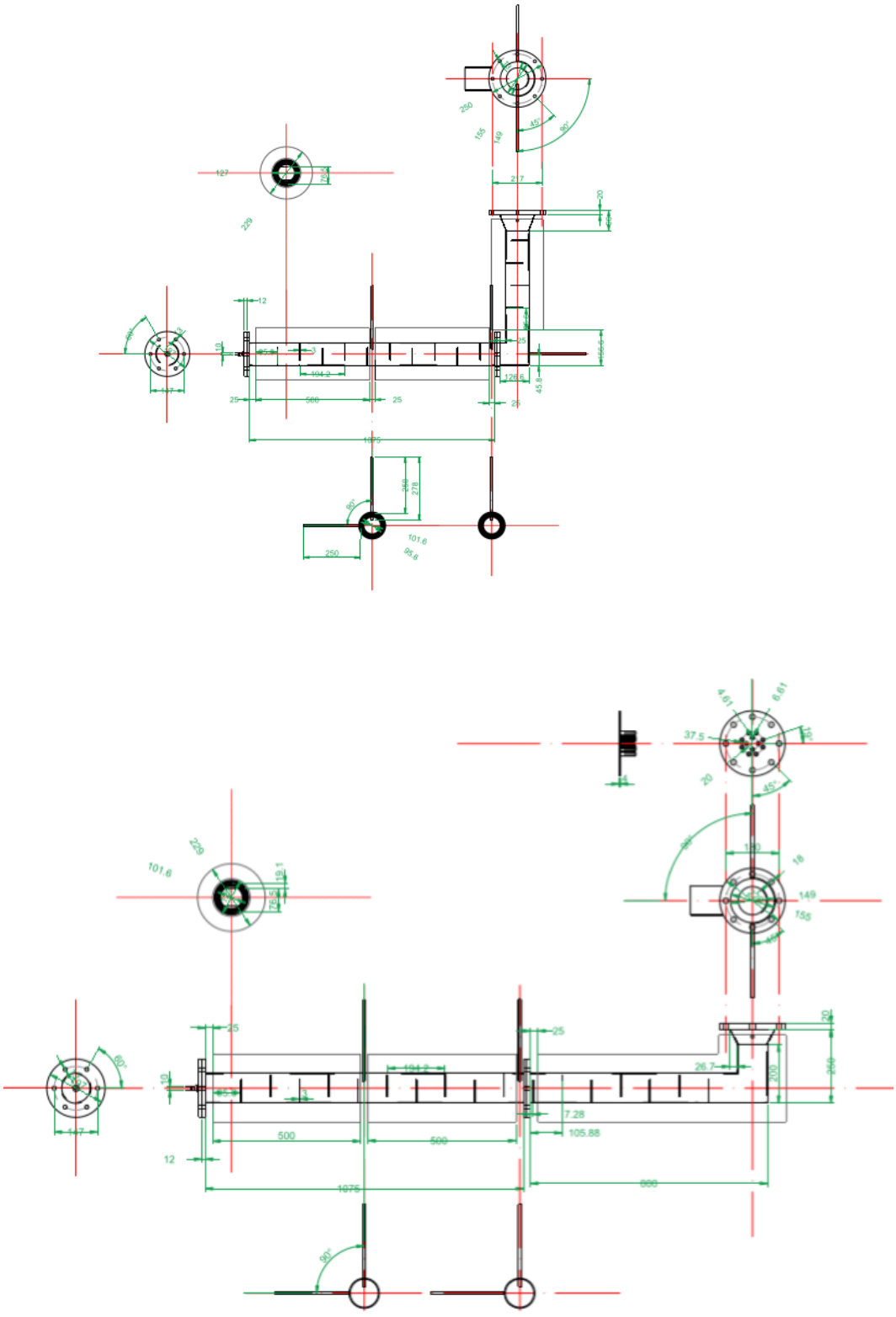

Figure_Apx C-2: Preheating tubes for calciner (up) and carbonator (down). Several inputs were included to enable us to inject steam and pollutants (SO_2, NO_x) into a hot gas of both calciner and carbonator

Figure_Apx C-3: Reconstructed calciner and fabricated new parts with new control unit and furnaces ready to be transported to Cranfield University

Figure_Apx C-4: Installation of the calciner with preheating line (top). Preheating line of the carbonator with installed electrical furnaces (bottom)

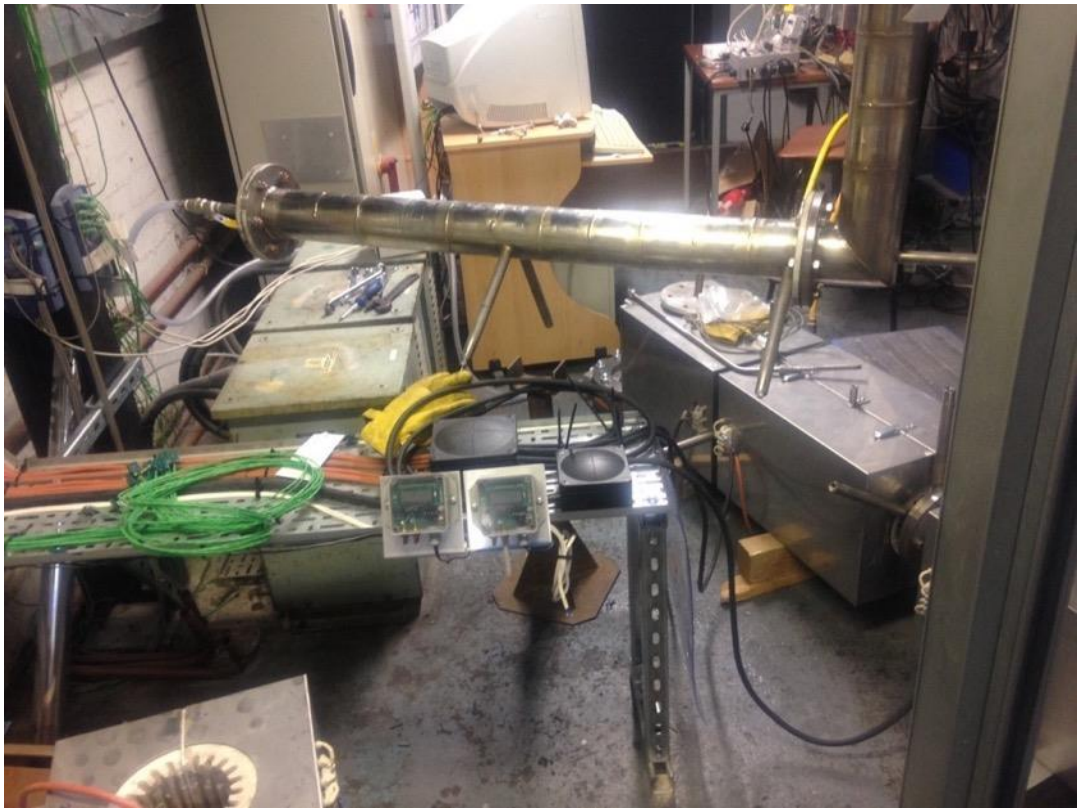

Figure_Apx C-5: Preheating line of the calciner, preheating line of the carbonator, wires from the control unit

Figure_Apx C-6: New hot cyclone being installed at the exit of the calciner to collect fines carried-over from the bubbling–fluidised-bed reactor

Appendix D COMISSIONING OF THE CALCIUM LOOPING PILOT PLANT

The first hot test in the upgraded unit was performed in order to reach the desired temperatures in the reactor needed for the calcium looping process (more than 900°C in the calciner and 650°C in the carbonator). This first heating is depicted in the following charts (Figure_Apx D-1).

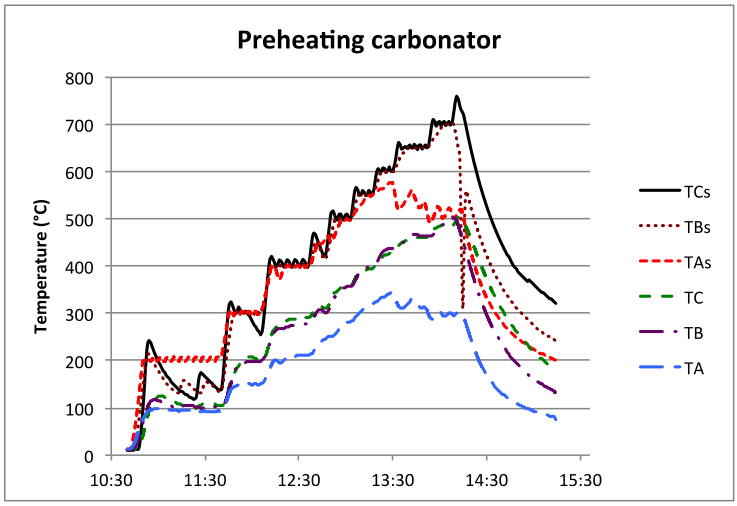

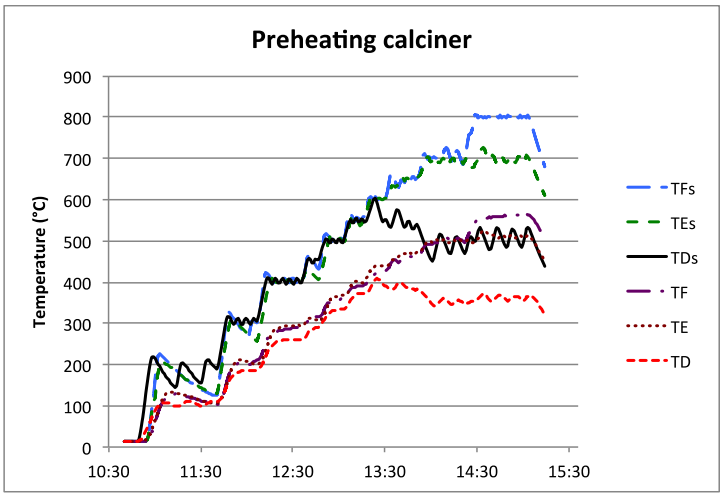

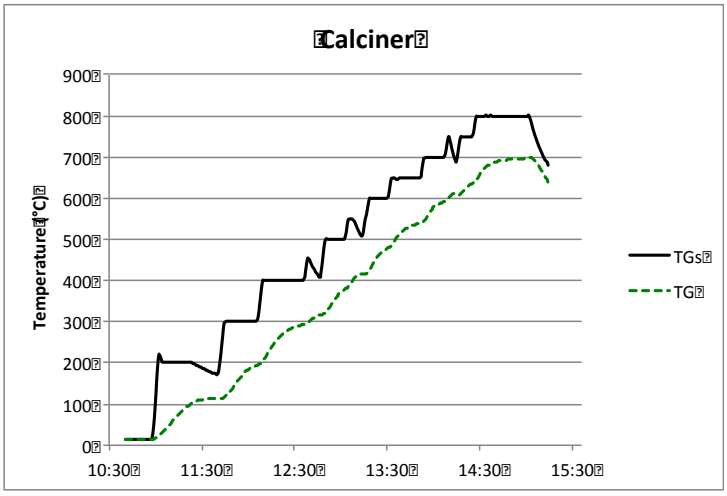

Figure_Apx D-1: First heating of the furnaces (TA–TG are temperatures of the gas measured inside the furnace and TAs–TGs are safety temperatures measured at the exterior of the tube near the heating elements of the furnaces)

Unfortunately, when the temperature of 700°C was reached in the rig, a cracking noise could be heard and gas leaking from the preheating tubes was detected. When the rig cooled down to ambient temperature, it was discovered that a discharge of electricity from the heating elements to the steel tube of the preheating occurred. This phenomenon melted a hole into the stainless steel tube (AISI 310). On closer inspection, hot spots were found under all the preheating furnaces (Figure_Apx D-2, Figure_Apx D-3 and Figure_Apx D-4).

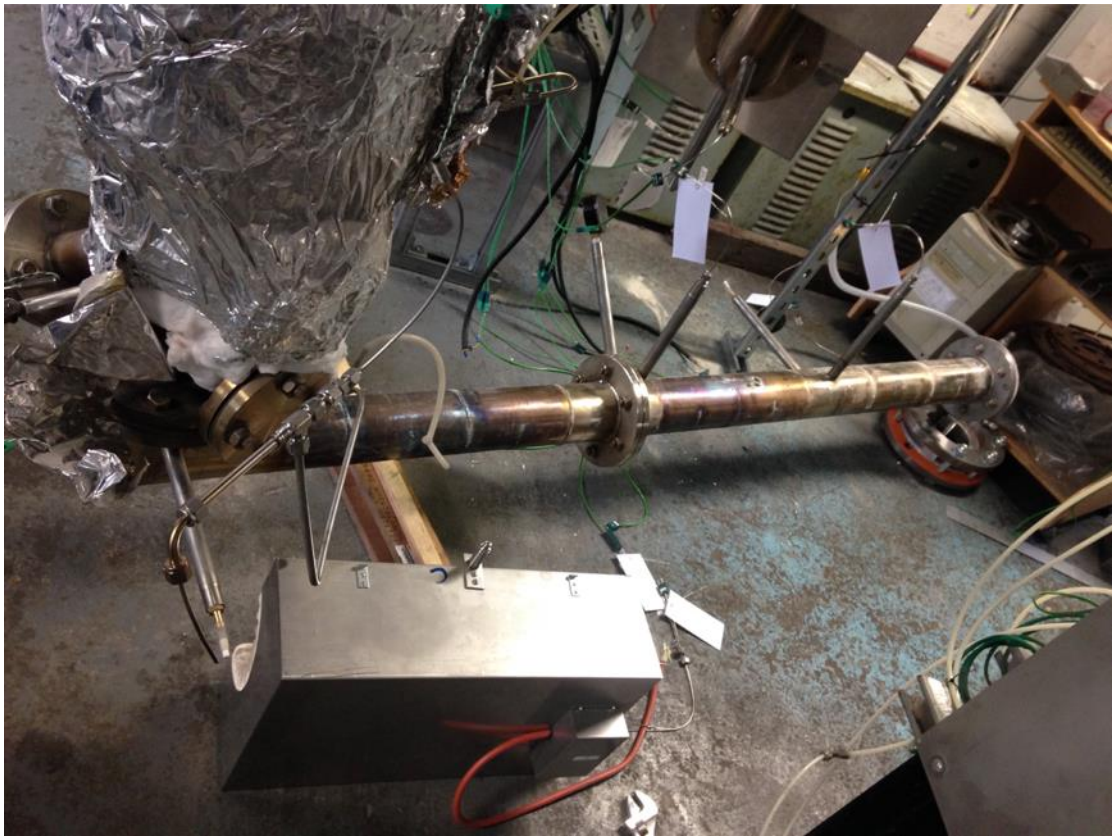

Figure_Apx D-2: The preheating unit of the carbonator after the first hot test. The hole can be seen in second segment on closer inspection.

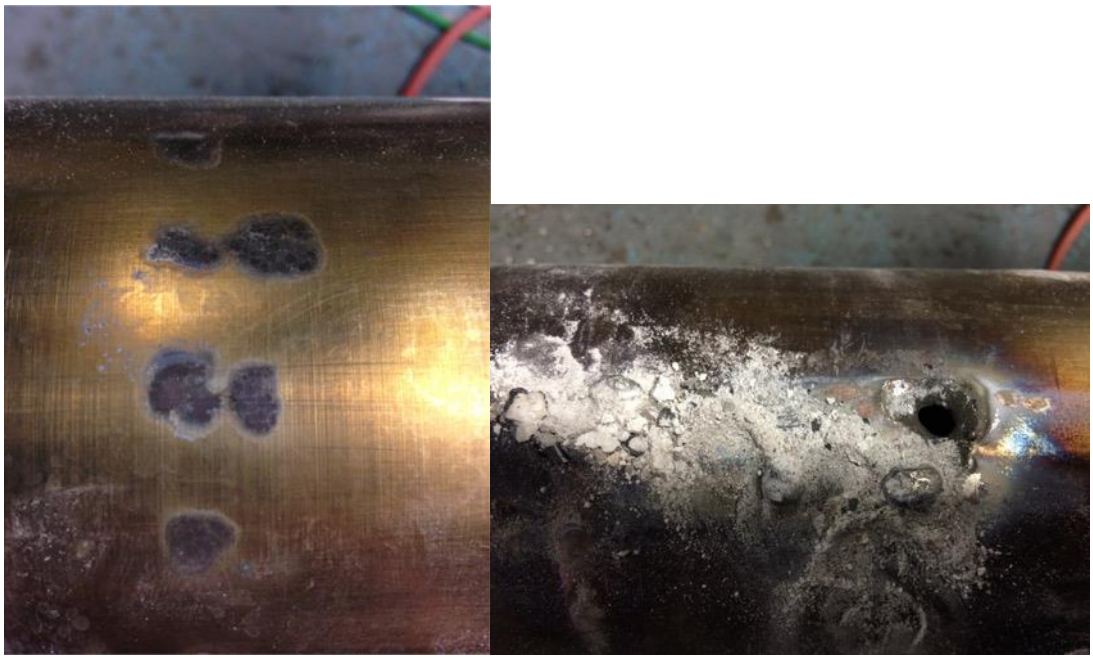

Figure_Apx D-3: Hot spots (left) and the melted hole into the stainless steel 310 (right)

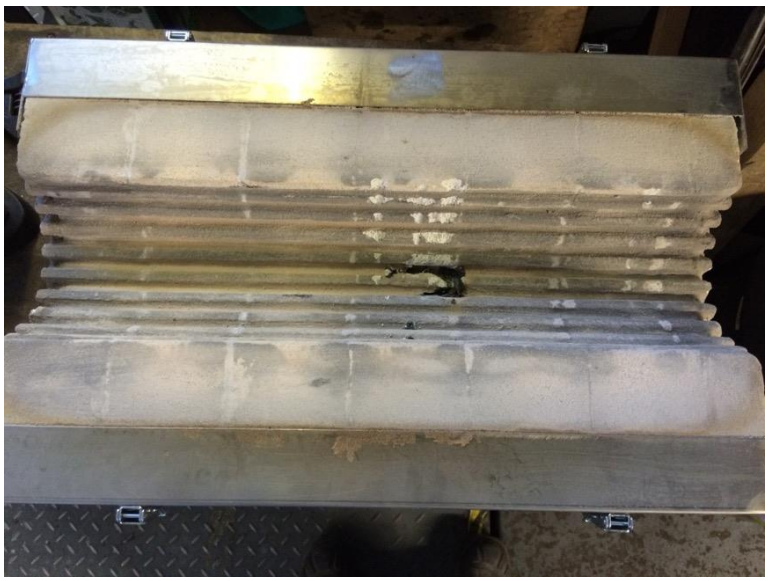

Figure_Apx D-4: Damaged furnace B

The damaged half of the furnace B was sent back to the supplier (Institute of Chemical Process Fundamentals in Prague) and the steel tube was repaired in a workshop in Cranfield University. Together with the supplier, the cause of the discharged was identified in the use of inappropriate refractory mastic (ALU-145 with composition 43% Al_2O_3, 52 % SiO_2 and 0.6% Fe_2O_3), which connects the segments of the furnaces and which becomes electrically conductive at temperatures above 700°C. This was confirmed by the measurement of its conductivity in a laboratory furnace (Figure_Apx D-5).

Figure_Apx D-5: Conductivity measurements of the refractory mastic used for the construction of the furnaces

To prevent further problems, several measures were applied.

a) The control software was modified to be able to set different (lower) safety temperatures for different furnaces.

b) The refractory mastic was partly removed (routed) from the furnaces not to be in touch with the steel tube (Figure_Apx D-6).

c) A support for the furnaces was installed to prevent their contact with the steel tubes.

d) Under three furnaces (C, F, G) with safety temperature higher than 600°C needed, a special mica sheet insulation (COGEBI Flexible Cogemicanite 132) was installed to prevent any possible further electrical discharge (Figure_Apx D-7).

Figure_Apx D-6: Removal of refractory mastic on critical parts of the furnaces

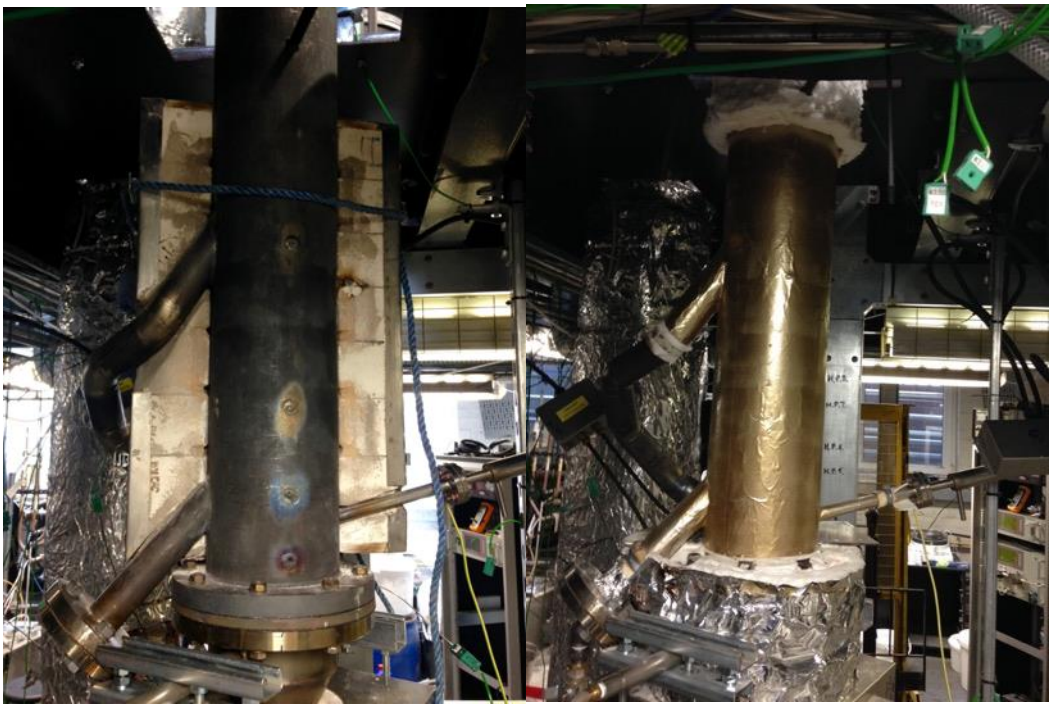

Figure_Apx D-7: Wrapping the calciner by mica sheet (COGEBI Flexible Cogemicanite 132) to protect it from potential electrical discharge from the electrical furnace

After applying the above-stated precautions, the heating was again tested. It was concluded that the necessary temperatures in both reactors can be achieved (the temperature profile of the carbonator is depicted in Figure_Apx D-8). Unfortunately, there was another electrical discharge, this time the electricity melted safety thermocouple of the heater G due to earthing issues (placed around the calciner). This issue caused not only the destruction of the thermocouple, but also the destruction of one half of the furnace (Figure_Apx D-9), which was returned to the supplier to be repaired.

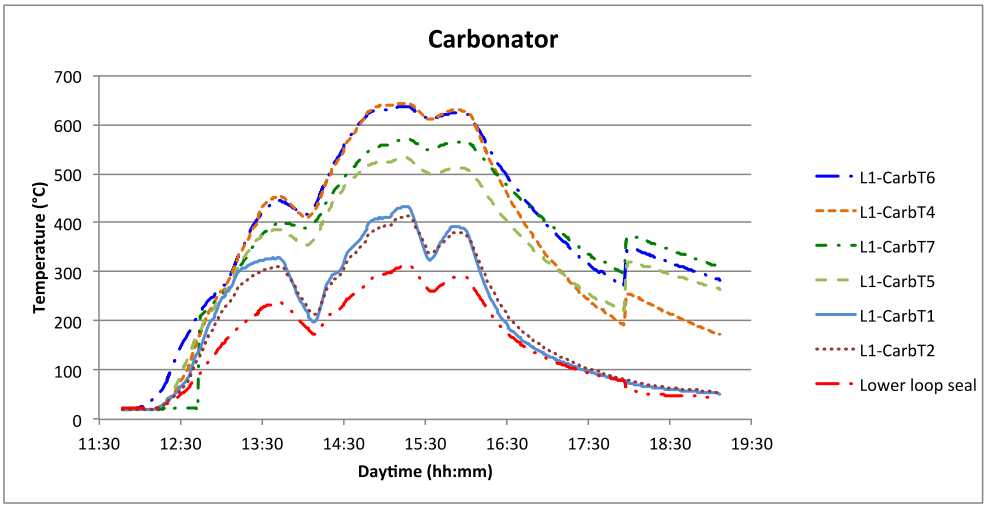

Figure_Apx D-8: Temperatures in the carbonator during the test 08/06/2016

Figure_Apx D-9: The damage of heater G by electrical discharge from heating elements to the safety thermocouple

After the installation of the fixed heater G, the heating was tested with silica sand as model non-reactive fluidised bed material. The aim was to observe its circulation between the two reactors and the performance of the loop seals.

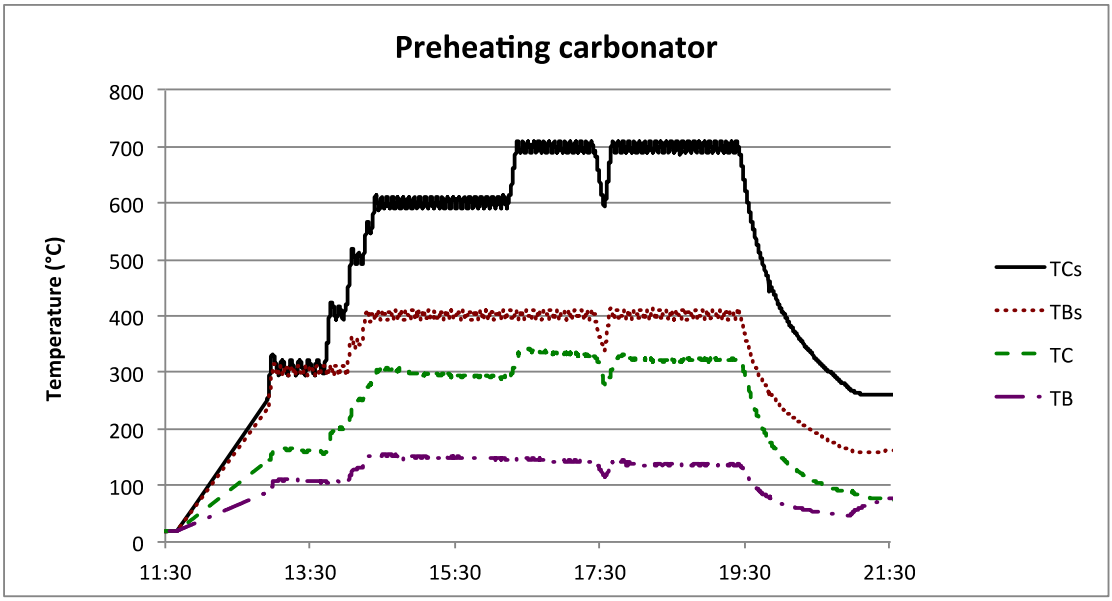
Preheating carbonator
Temperature (°C)
800
700
600
500
400
300
200
100
0
11:30
13:30
15:30
17:30
19:30
21:30
TCs
TBs
TC
TB

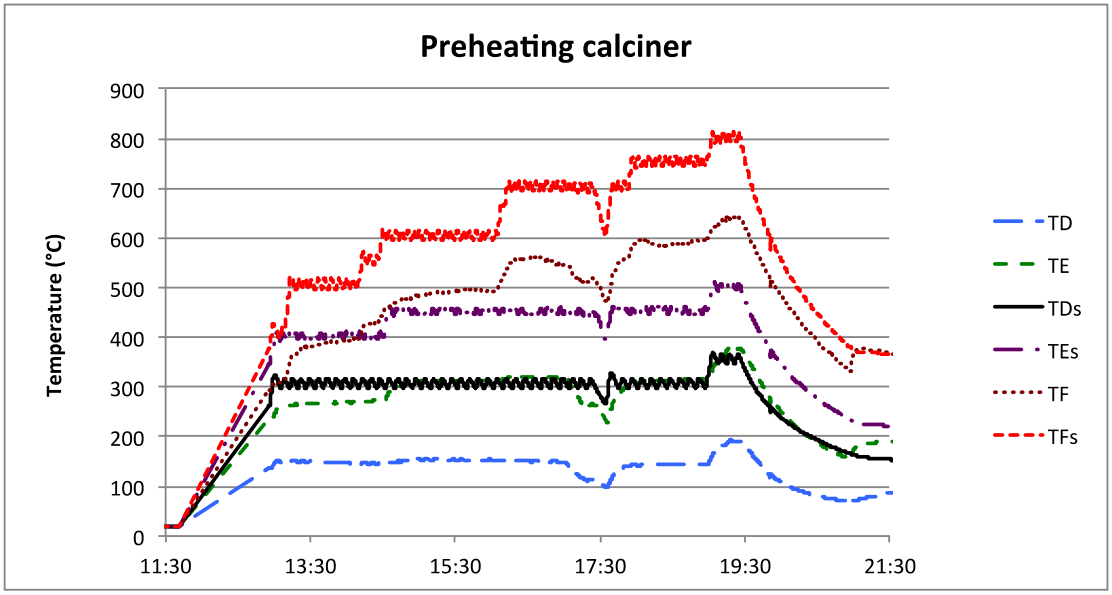
Preheating calciner
Temperature (°C)
900
800
700
600
500
400
300
200
100
0
11:30
13:30
15:30
17:30
19:30
21:30
TD
TE
TDs
TEs
TF
TFs

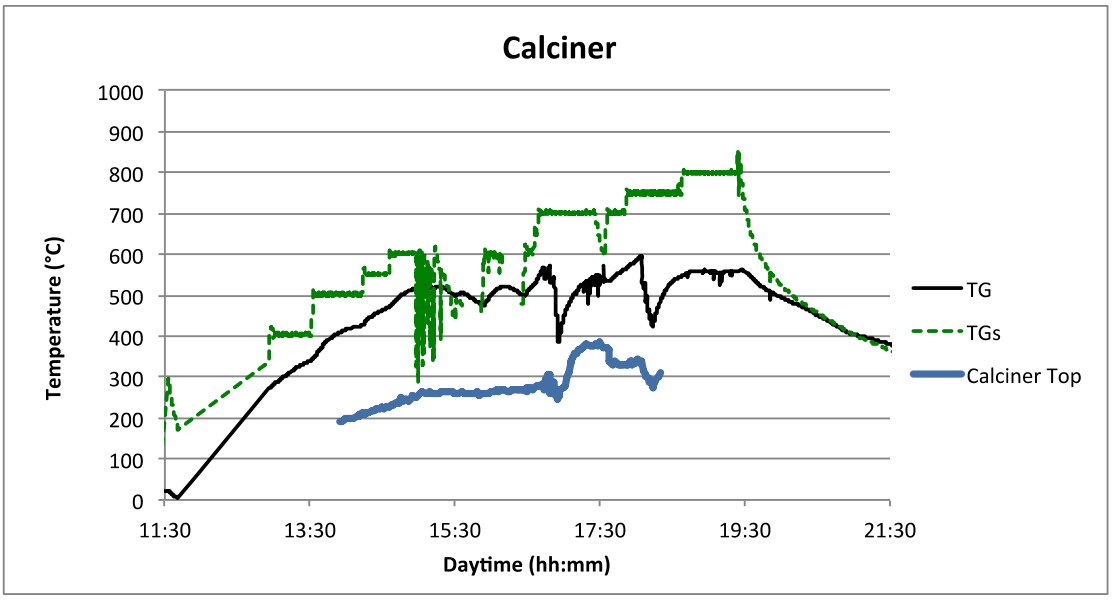

Figure_Apx D-10: Temperatures of the preheating lines and of the calciner. TA–TG are the temperatures measured inside the rig and TAs–TGs are the safety temperatures measured on the electrical furnaces

Although the natural gas combustion temperature was not reached in the calciner, it was proven that we can adequately preheat the gases for calciner and carbonator and to carry out continuous circulation of a hot inert material between the two reactors.

The rig's thermal insulation was improved (mainly the calciner and the connection lines between the two reactors) and in the next test this temperature was reached in order to start the NG combustion (>650°C). By the combustion of NG, silica sand was heated in the calciner to temperatures close to 900°C and the material was circulated between the two reactors and it was demonstrated that the rig can reach the desired temperatures for the calcium looping process (Figure_Apx D-11).

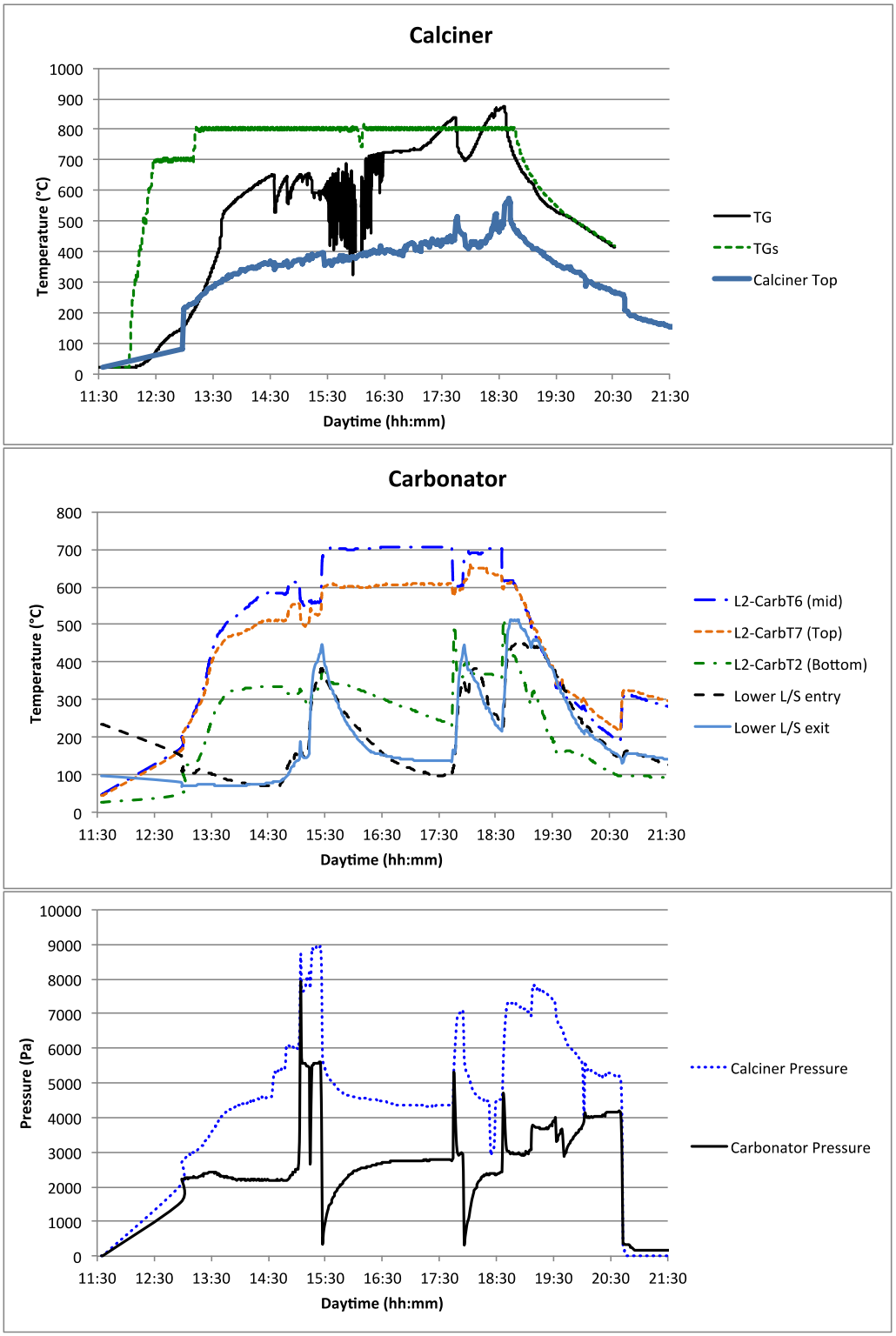

Figure_Apx D-11: First combustion of NG in the fluidised bed of the calciner. The noise in the data in the first chart (TG) was caused by the induction from the electrical heating of the calciner. The problem was solved by earthing the appropriate thermocouple

After additional thermal insulation and fixing some of the issues encountered in the previous run (enabling higher supply of oxygen), another test was performed with silica sand. The calciner was heated by electrical heating to 800°C with fluidising air (65 Ln/min) and added 2 L (3,160 g) of silica sand to the calciner. After the sand was heated up to 650°C, NG (5 Ln/min, 3 kW) was added to the fluidised bed of the calciner and the sand was further heated by its combustion. After reaching almost 900°C in the FB, more sand (2x0.5 L + 0.3 L) was added progressively with care not to stop the combustion process by cooling down the FB too much. The flow of N_2 into the carbonator was increased to 320 Ln/min, which corresponds to a velocity of 2.3 m/s at 650°C. A successful circulation of the hot silica sand was observed and the temperature of 900°C could easily be maintained in the calciner. Afterwards, a first batch of limestone (0.5 L, 620g) was added to the calciner and calcination was observed. Additional 1.5 L of limestone was let to calcine and a first trial of the carbon capture in the carbonator was performed (with initial 15% CO_2) and the conditions in the calciner were switched to oxyfuel conditions (with 21% O_2, 79% CO_2).

Because of a low quantity of limestone and its small size fraction, the efficiency of the CO_2 capture was very low, ca. 15%, but the test was considered as a successful first trial of a newly reconstructed rig (Figure_Apx D-12).

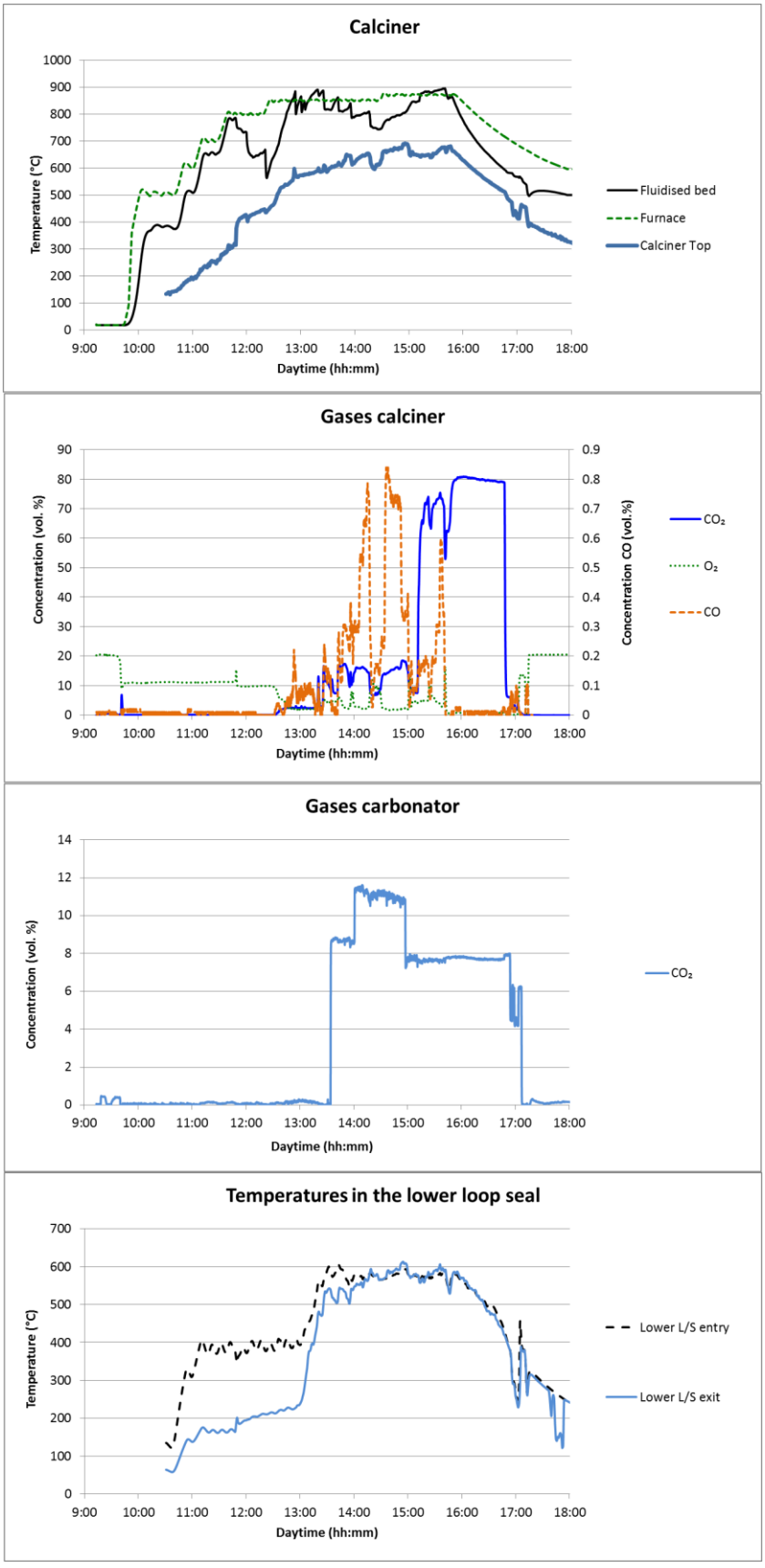

Figure_Apx D-12: First successful trial

Appendix E SUPPLEMENTARY INFORMATION FOR CHAPTERS 6 AND 7

In this appendix supplementary data for the experiments depicted in Chapters 6 and 7 can be found. These figures show the temperatures, pressures and gas compositions in both reactors and complment the results discussed in the aforementioned Chapters. The figures correspond to experiments described, in that order, in the following sections of this thesis: 6.3.1; 6.3.2; 6.3.3 and 7.3.1; 7.3.2; 7.3.3.

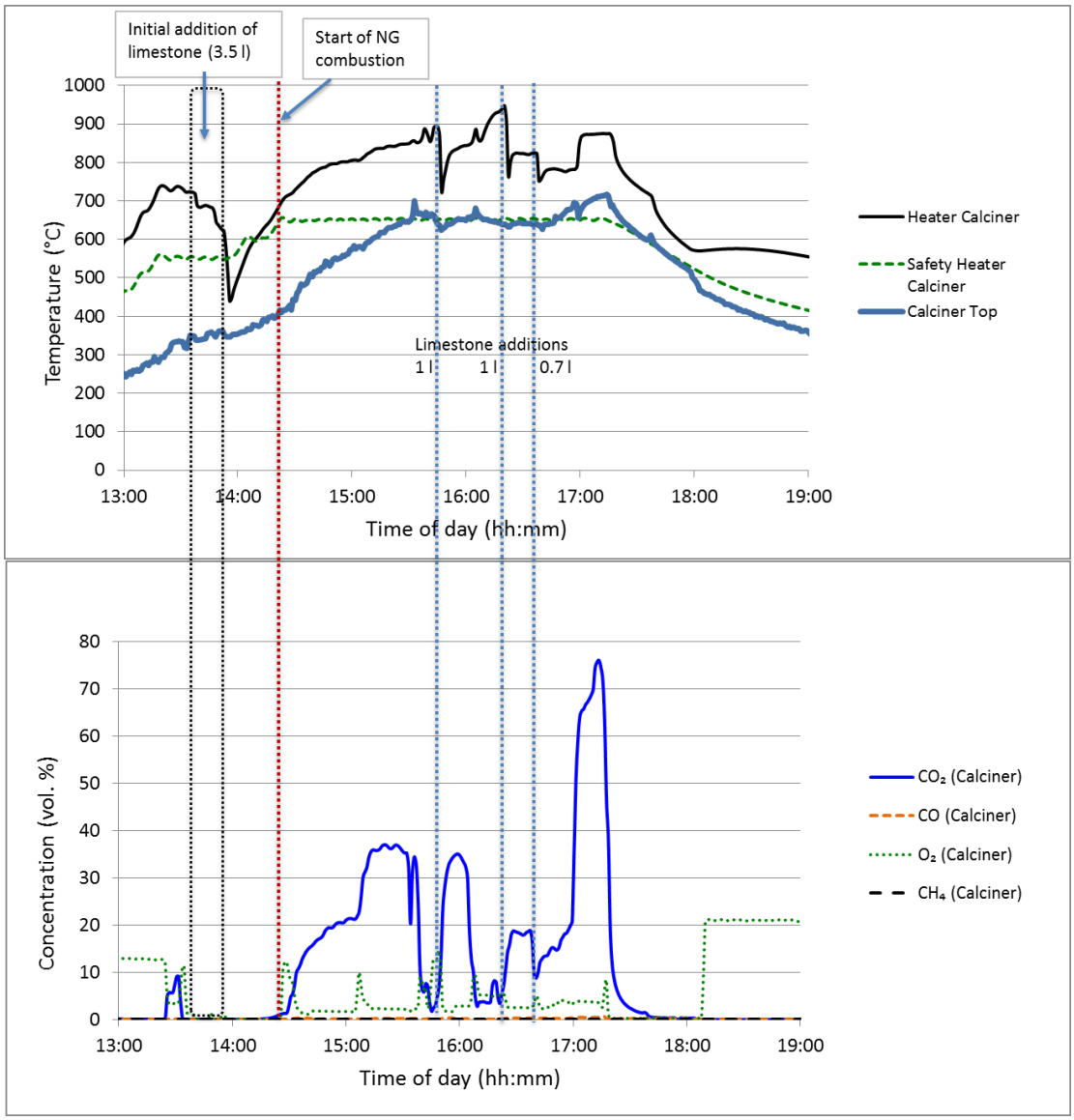

Figure_Apx E-1: Temperature in the fluidised bed and gas concentration at the outlet of the experiment depicted in 6.3.1

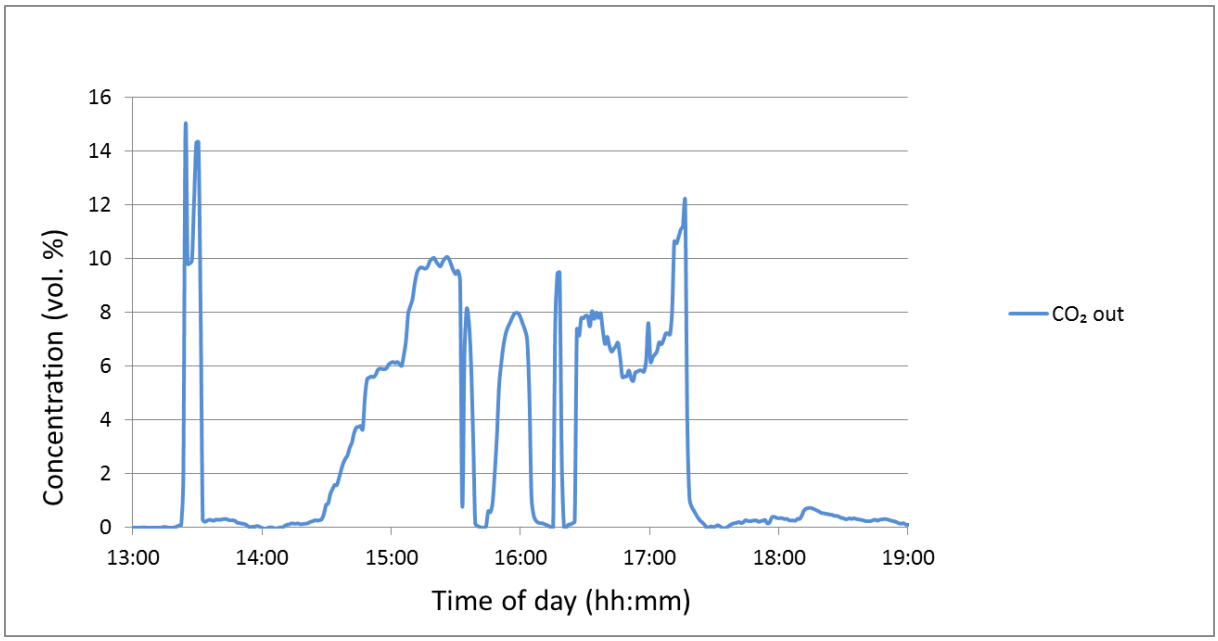

Figure_Apx E-2: CO_2 concentration at the outlet of the carbonator of the experiment depicted in 6.3.1

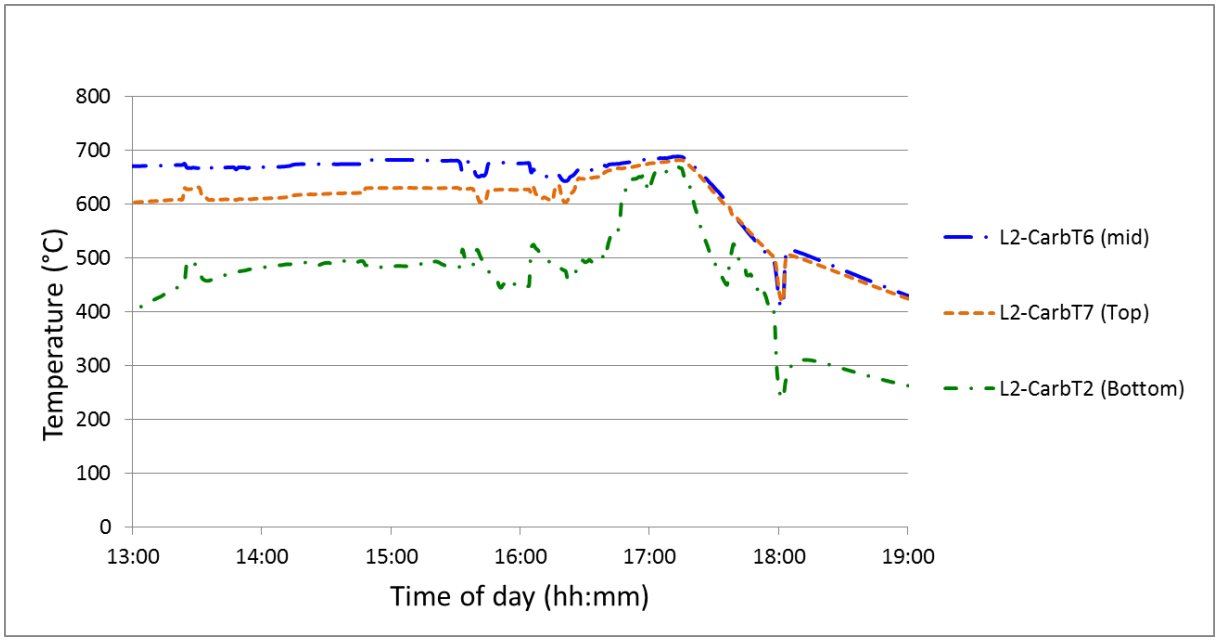

Figure_Apx E-3: Temperatures in the carbonator of the experiment depicted in 6.3.1

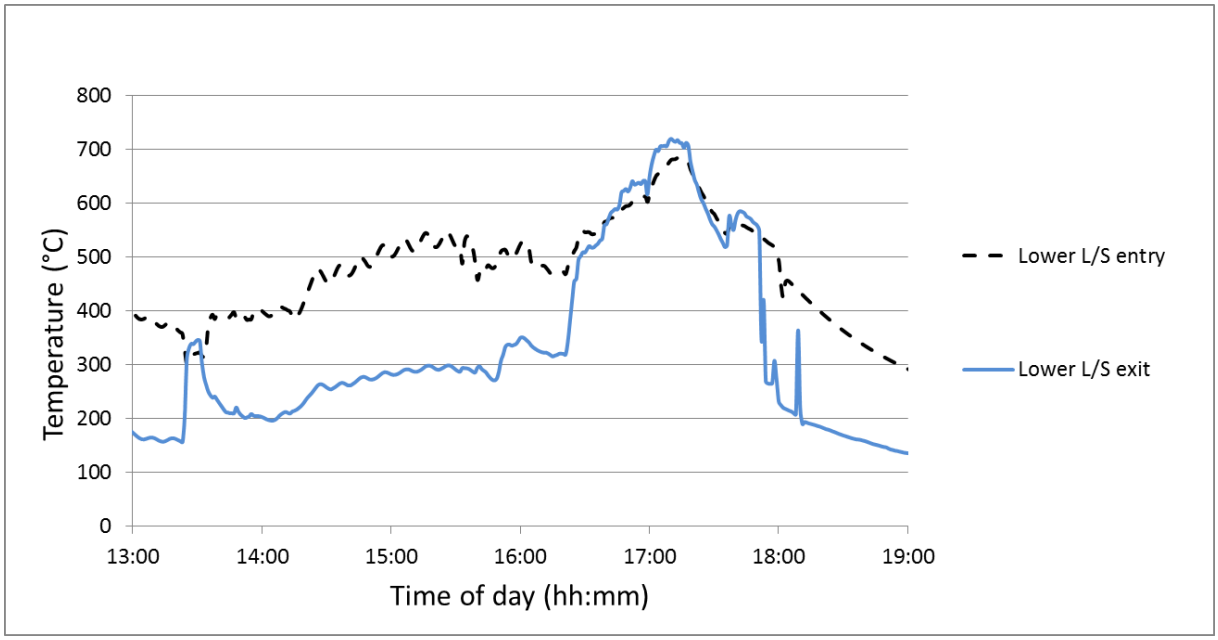

Figure_Apx E-4: Temperatures in the loop-seal of the experiment depicted in 6.3.1

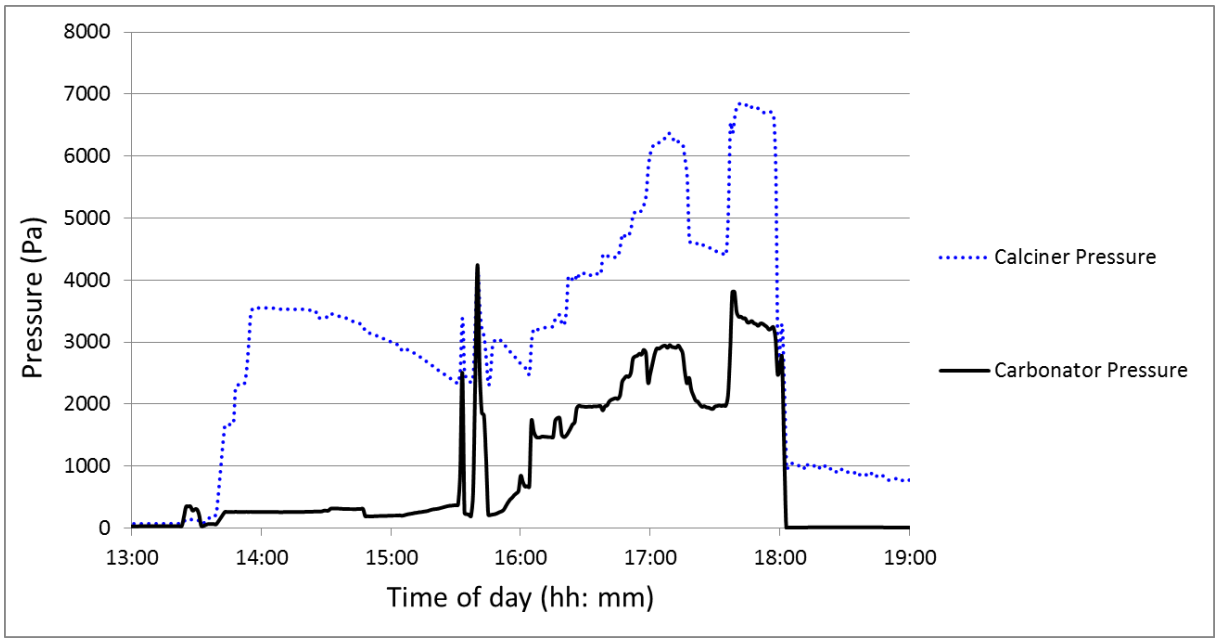

Figure_Apx E-5: Pressure in both fluidised beds of the experiment depicted in 6.3.1

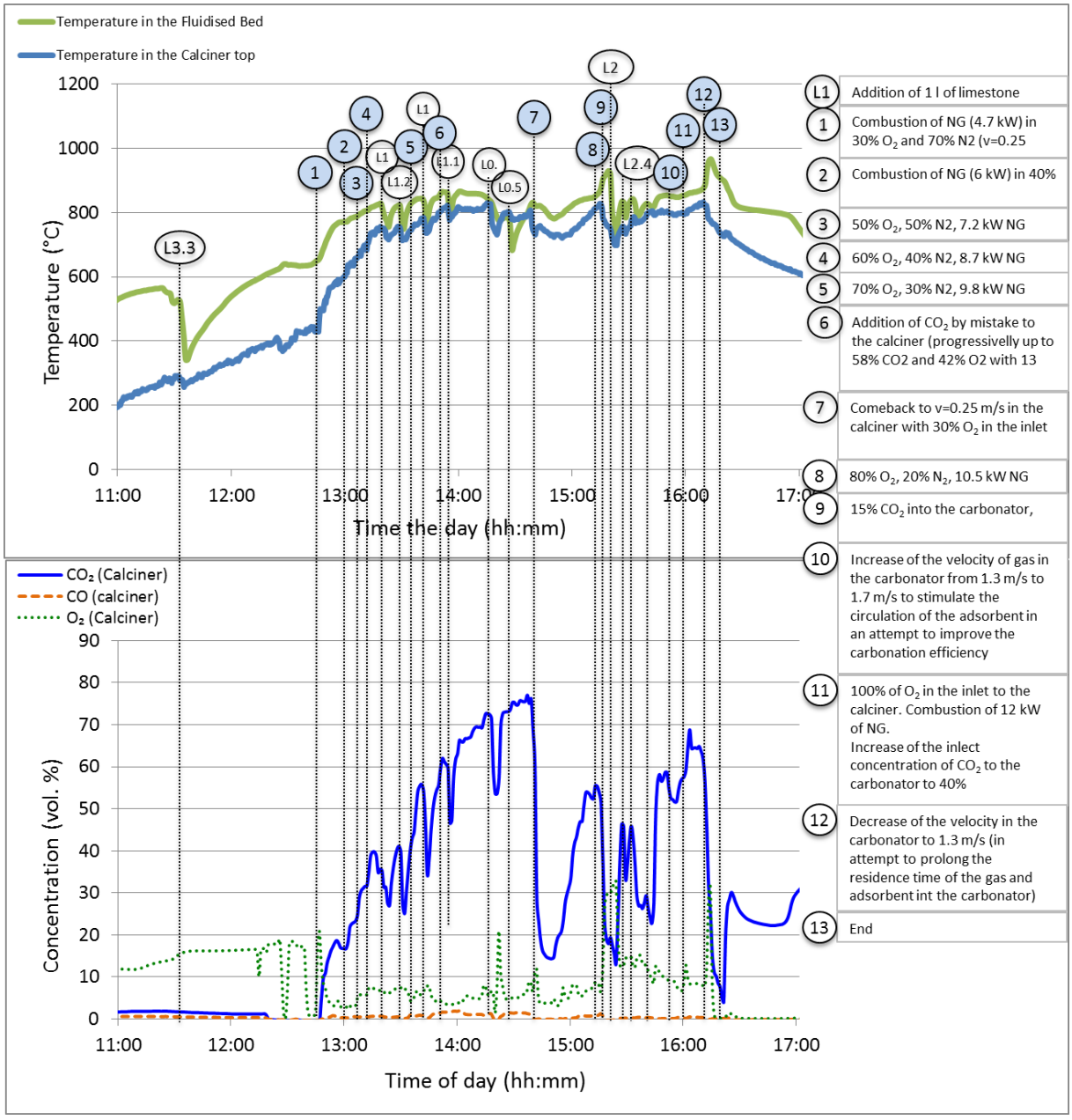

Figure_Apx E-6: Temperature in the fluidised bed and gas concentration at the outlet of the experiment depicted in 6.3.2

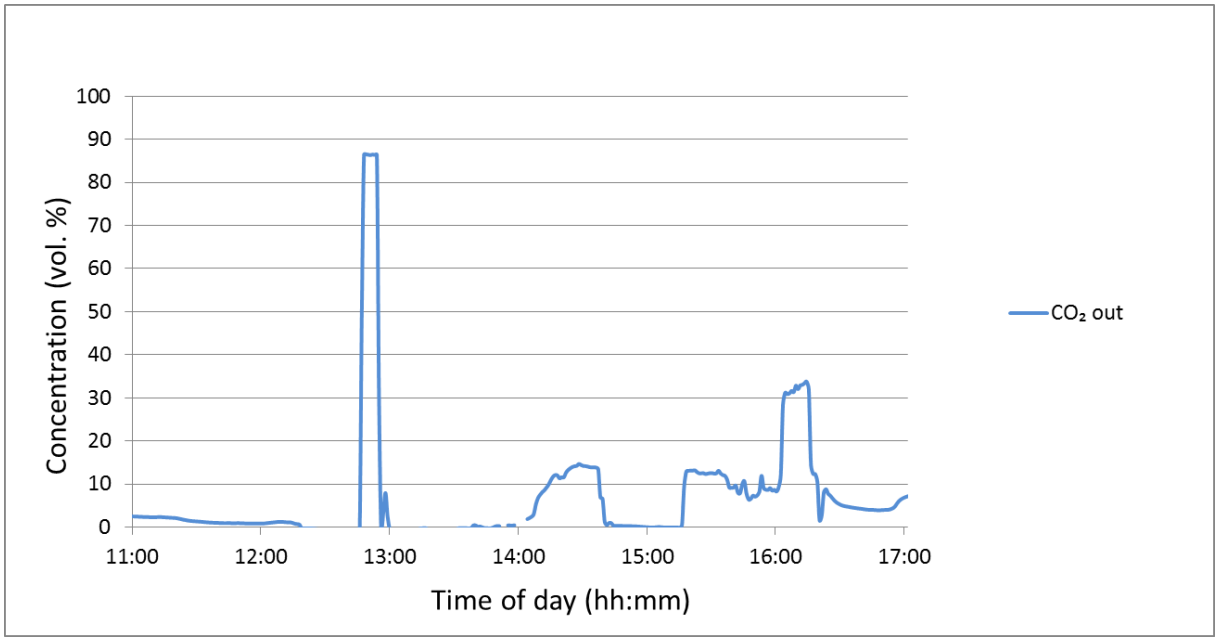

Figure_Apx E-7: CO_2 concentration at the outlet of the carbonator of the experiment depicted in 6.3.2

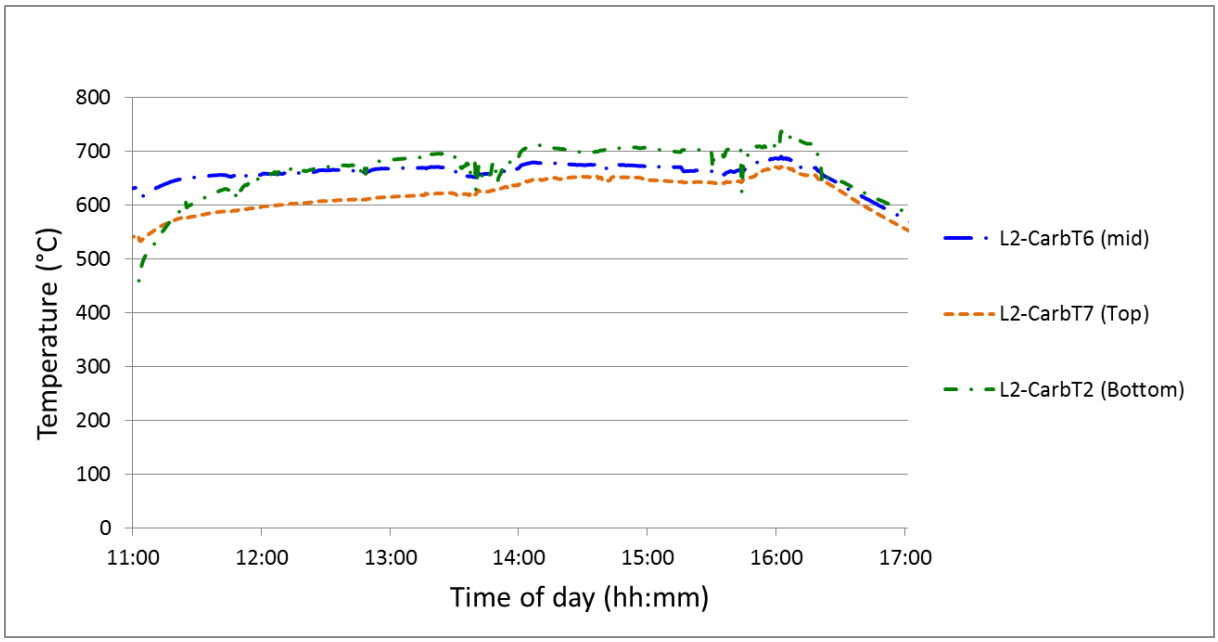

Figure_Apx E-8: Temperatures in the carbonator of the experiment depicted in 6.3.2

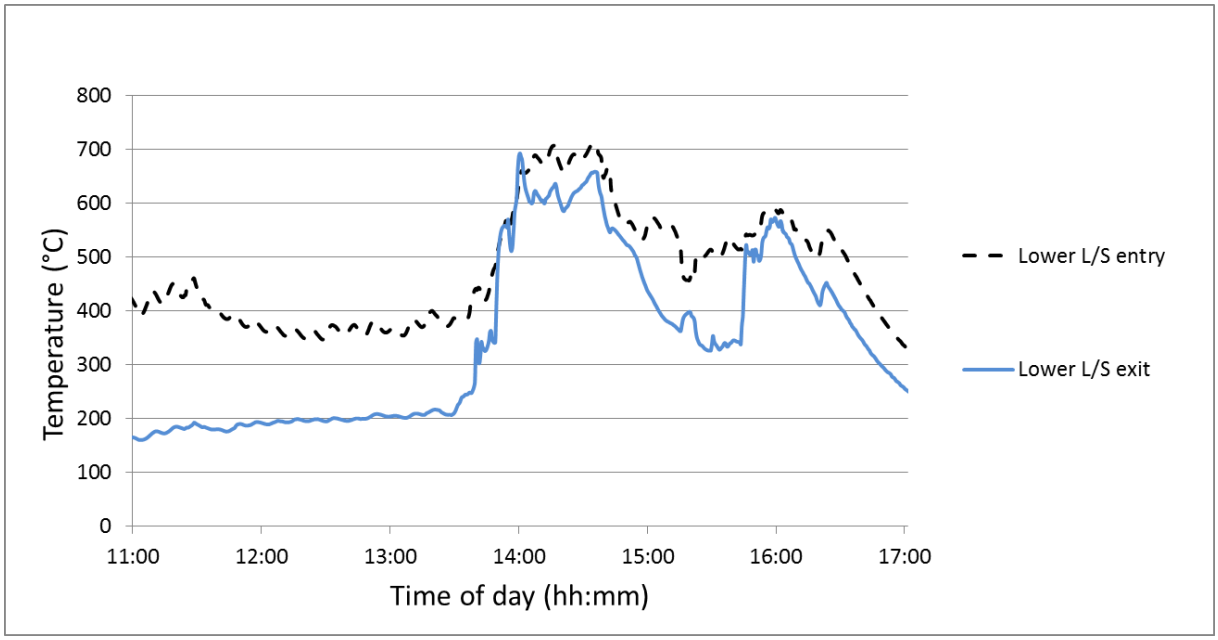

Figure_Apx E-9: Temperatures in the loop-seal of the experiment depicted in 6.3.2

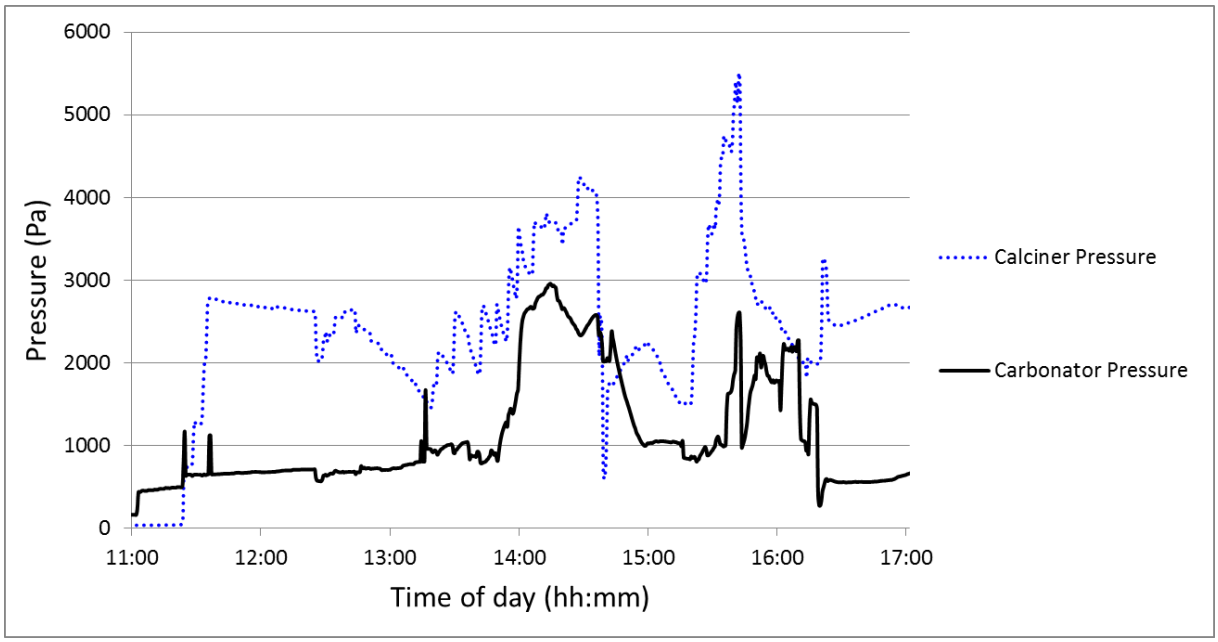

Figure_Apx E-10: Pressure in both fluidised beds of the experiment depicted in 6.3.2

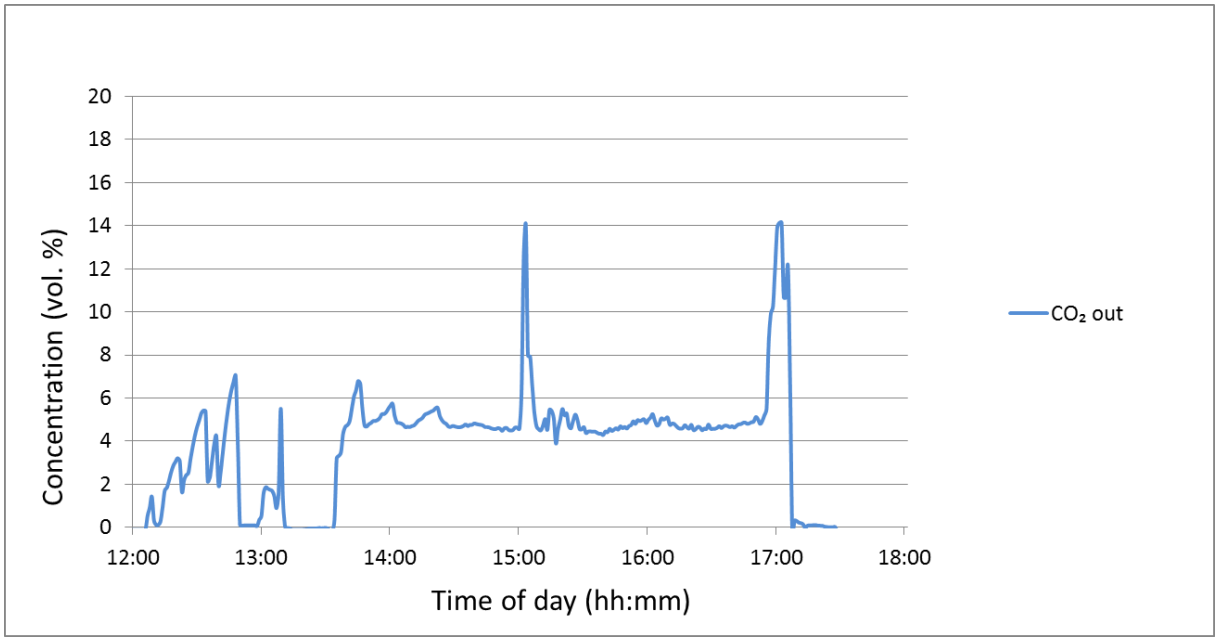

Figure_Apx E-11: CO_2 concentration at the outlet of the carbonator of the experiment depicted in 6.3.3 and 7.3.1

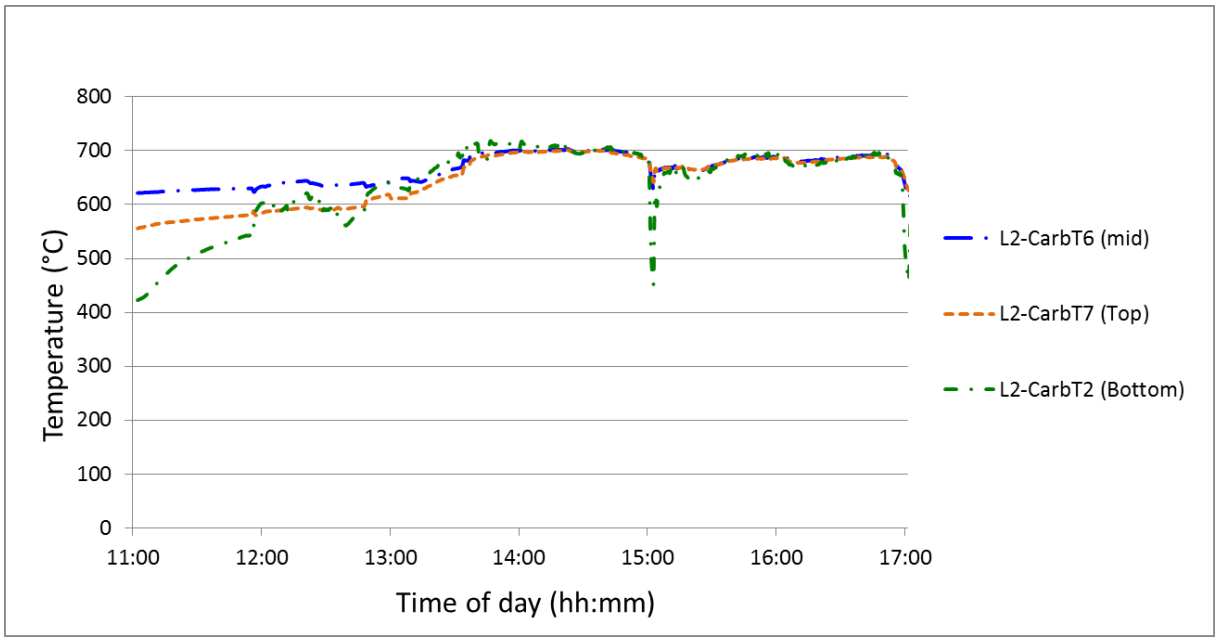

Figure_Apx E-12: Temperatures in the carbonator of the experiment depicted in 6.3.3 and 7.3.1

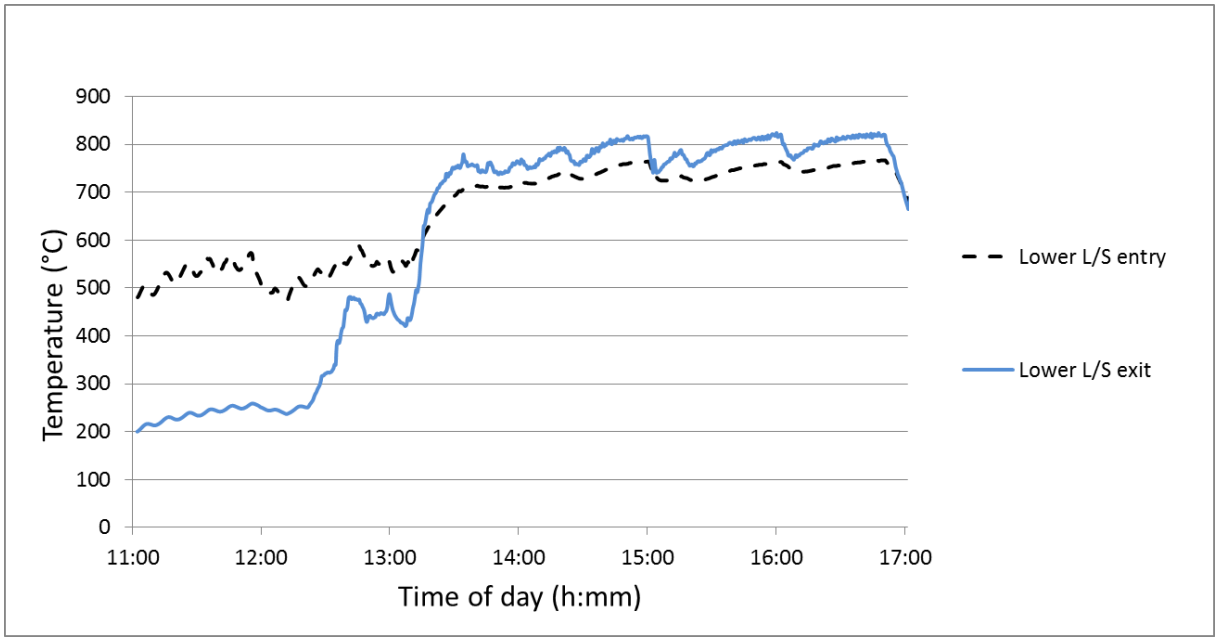

Figure_Apx E-13: Temperatures in the loop-seal of the experiment depicted in 6.3.3 and 7.3.1

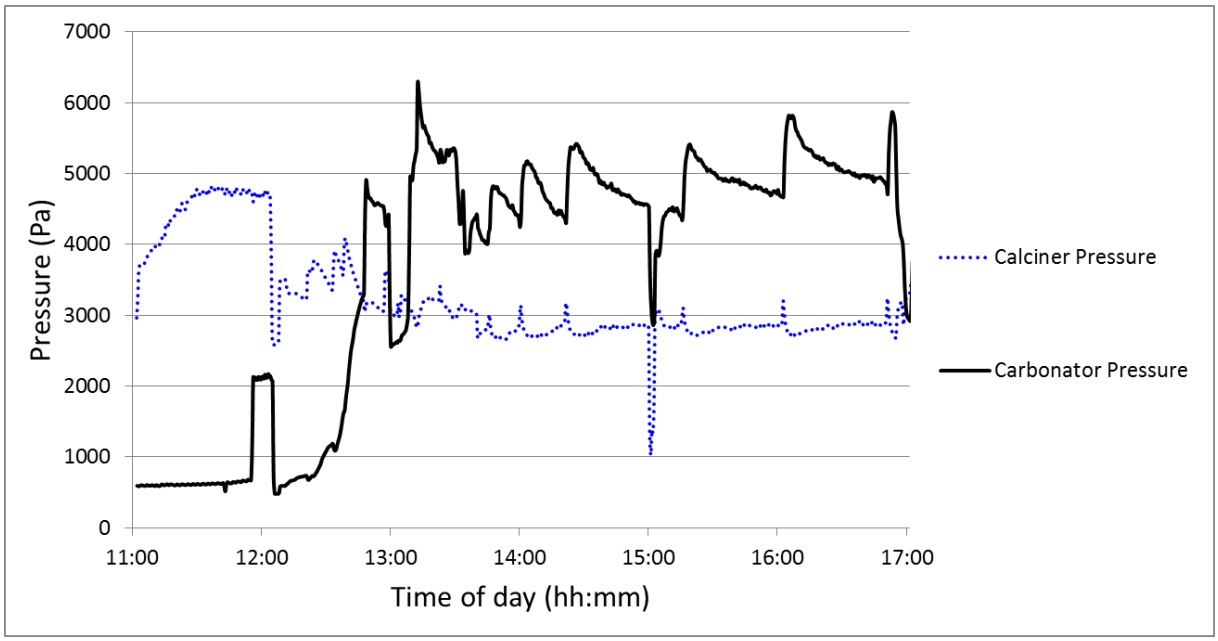

Figure_Apx E-14: Pressure in both fluidised beds of the experiment depicted in 6.3.3 and 7.3.1

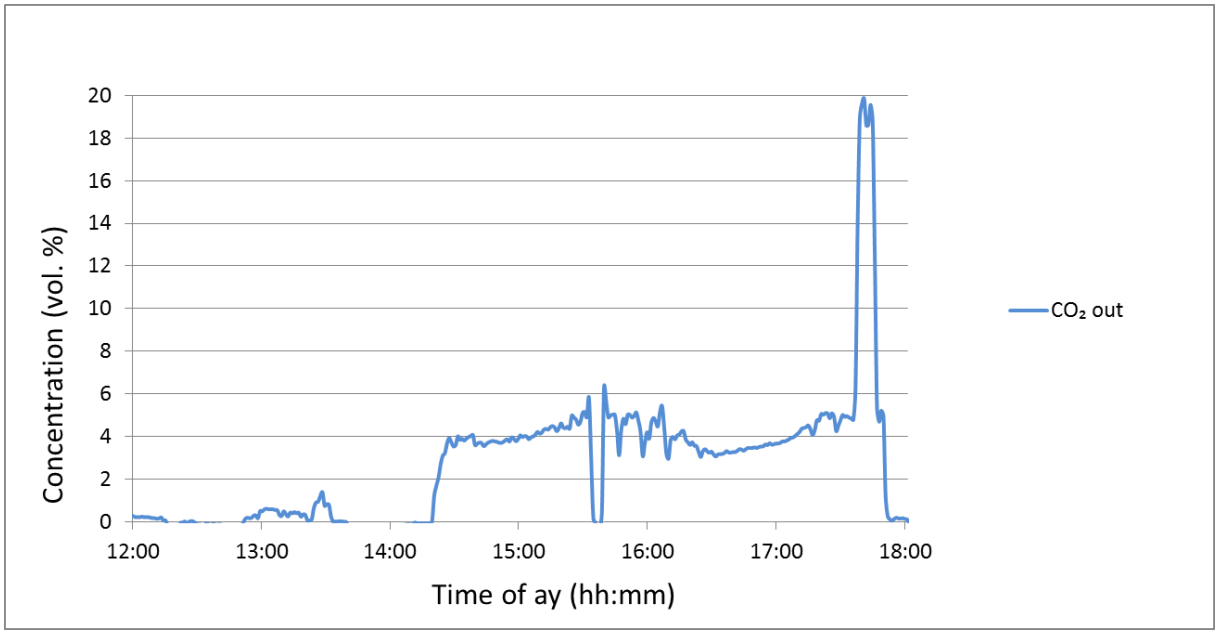

Figure_Apx E-15: CO_2 concentration at the outlet of the carbonator of the experiment depicted in 7.3.2

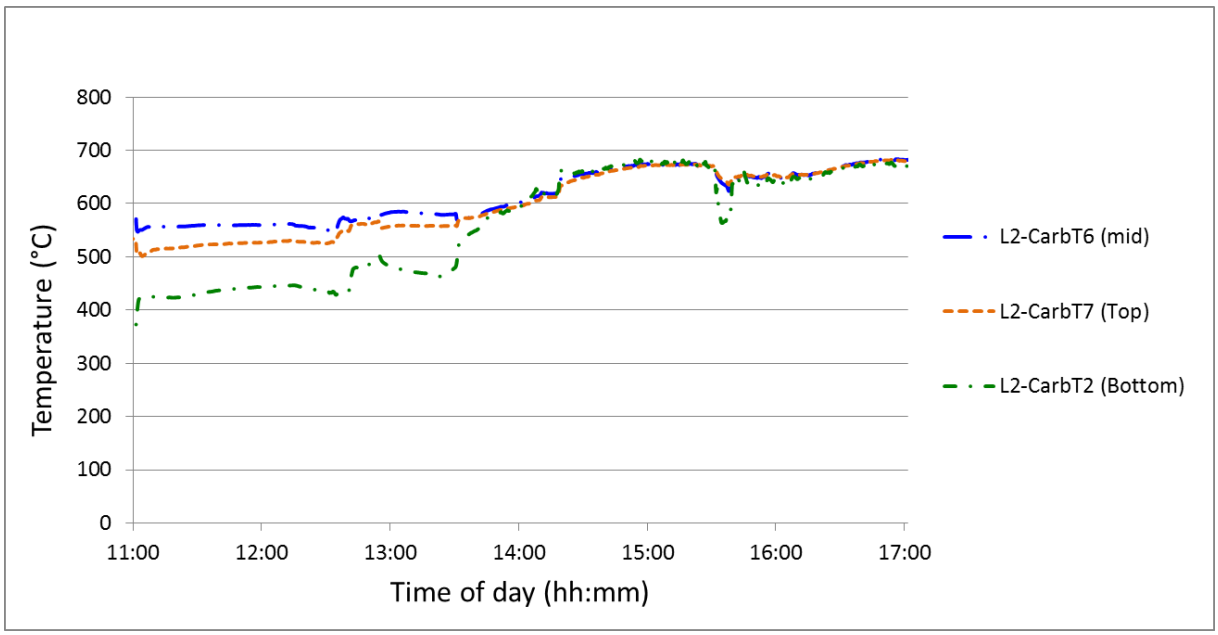

Figure_Apx E-16: Temperatures in the carbonator of the experiment depicted in 7.3.2

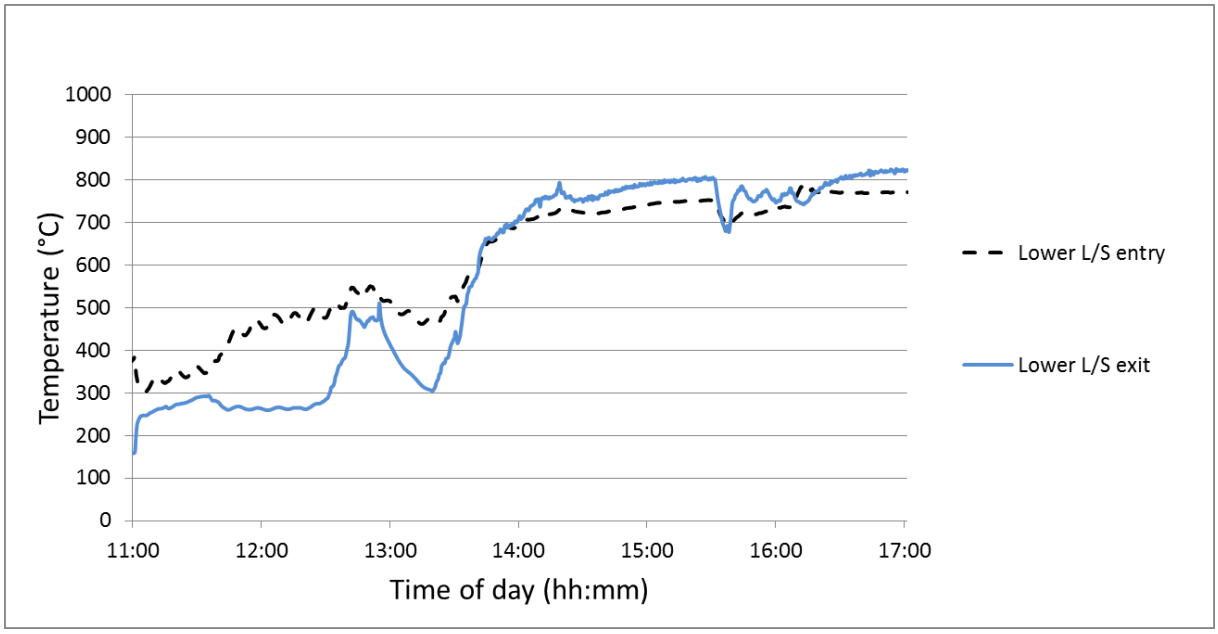

Figure_Apx E-17: Temperatures in the loop-seal of the experiment depicted in 7.3.2

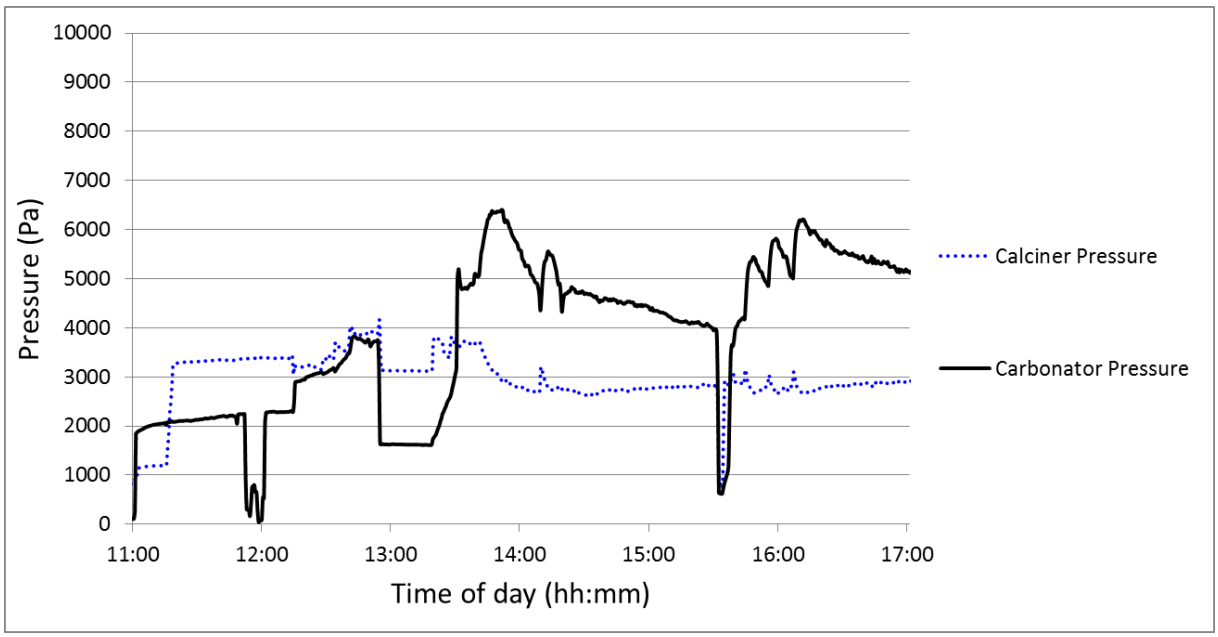

Figure_Apx E-18: Pressure in both fluidised beds of the experiment depicted in 7.3.2

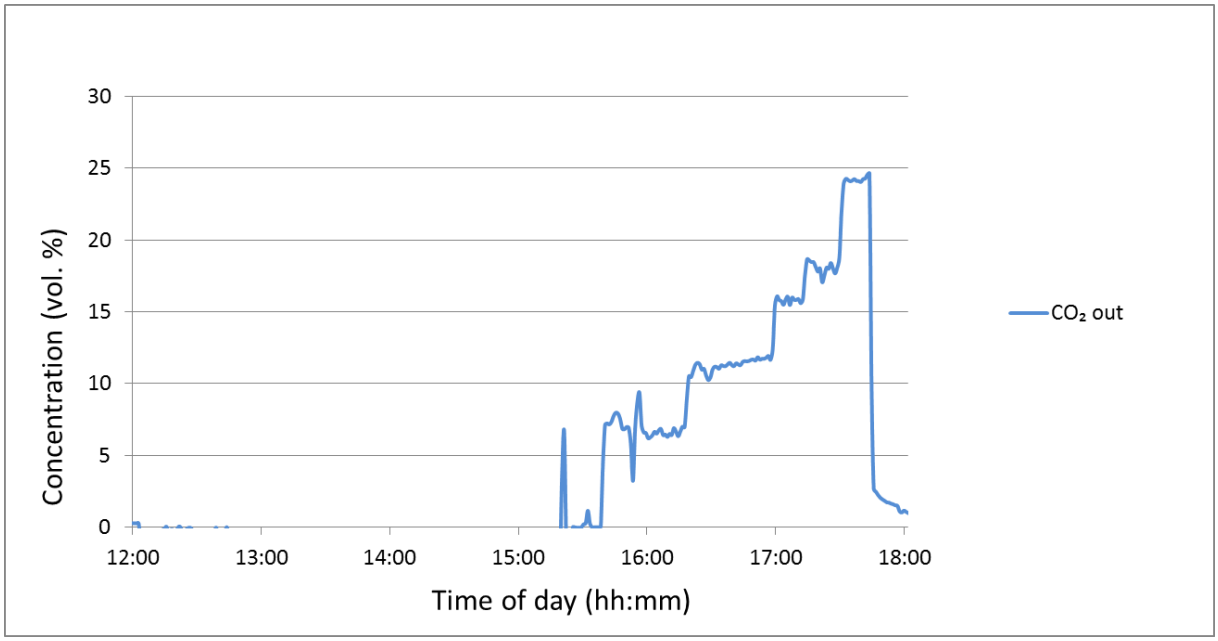

Figure_Apx E-19: CO_2 concentration at the outlet of the carbonator of the experiment depicted in 7.3.3

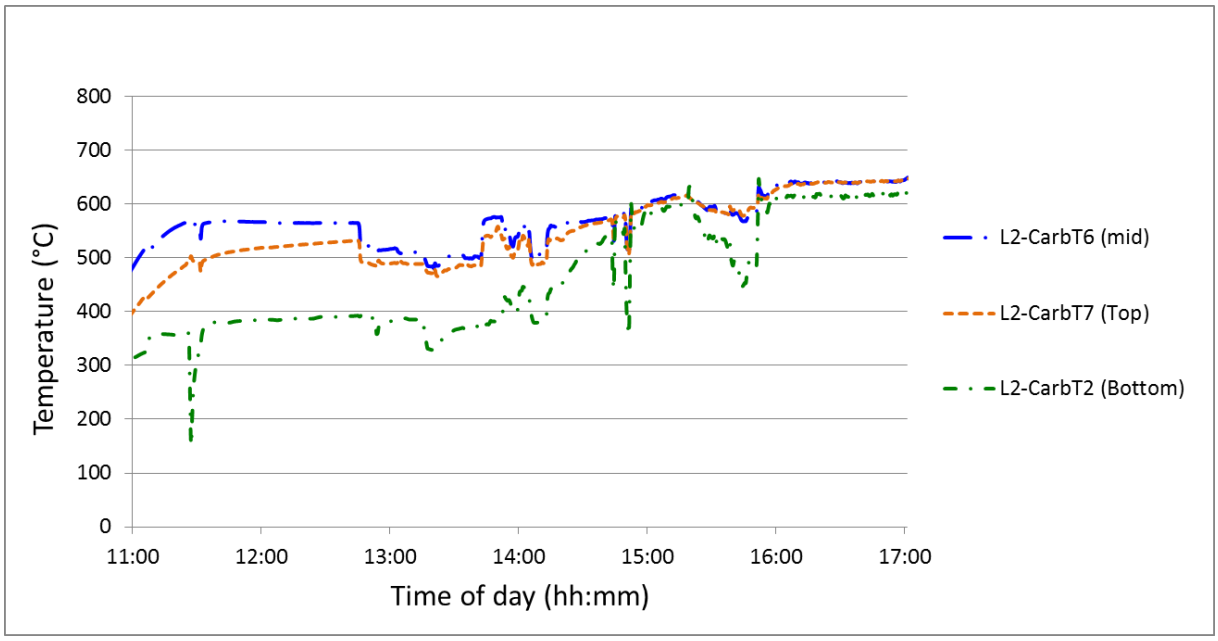

Figure_Apx E-20: Temperatures in the carbonator of the experiment depicted in 7.3.3

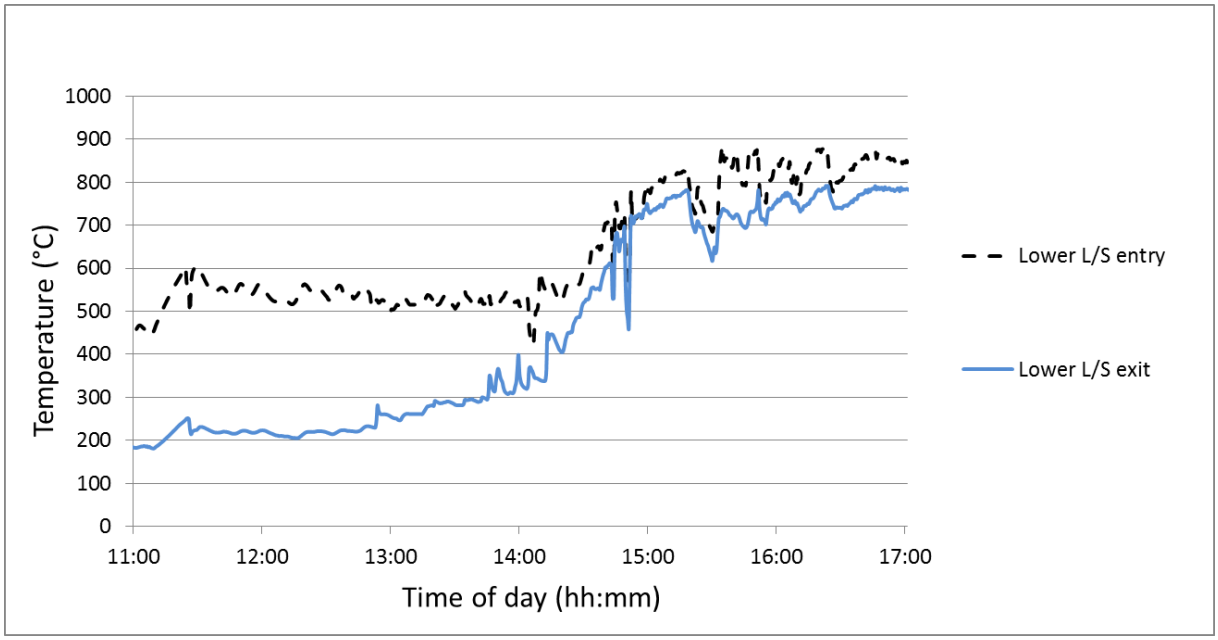

Figure_Apx E-21: Temperatures in the loop-seal of the experiment depicted in 7.3.3

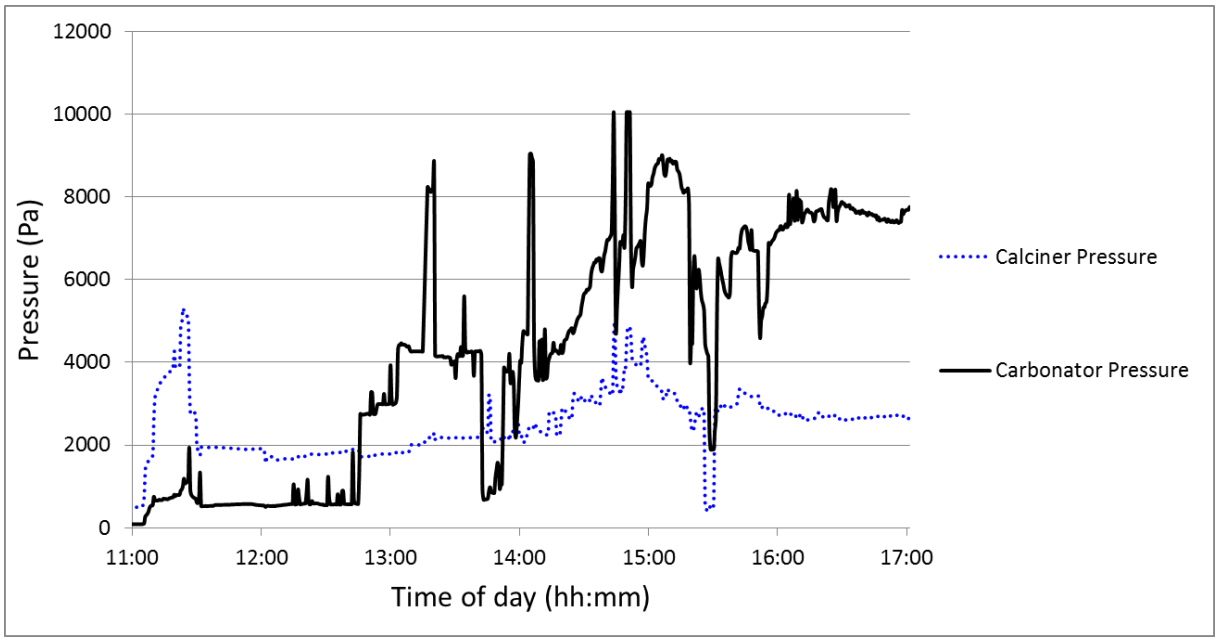

Figure_Apx E-22: Pressure in both fluidised beds of the experiment depicted in 7.3.3